

中央大学博士論文

**Stereodivergent Synthesis of Multisubstituted Pyrrolidines
via Metal-Catalyzed (3+2) Cycloaddition**

古屋 翔平

博士（工学）

中央大学大学院
理工学研究科
応用化学専攻

令和5年度
2024年3月

Contents

Chapter 1	General Introduction	1
1-1.	Utility of Pyrrolidine Derivatives	2
1-2.	Stereodivergent Synthesis of 2,5- <i>cis/trans</i> -Pyrrolidines	4
1-3.	Catalytic Asymmetric 1,3-Dipolar Cycloaddition of Imino Esters	7
1-4.	Outline of the Dissertation	28
1-5.	References	31
Chapter 2	Copper-Catalyzed Asymmetric (3+2) Cycloaddition of Imino Esters with α,β-Unsaturated Sultones	37
2-1.	Introduction	38
2-2.	Results and Discussion	40
2-3.	Conclusion	47
2-4.	Experimental Section	47
2-5.	References	60
Chapter 3	Silver-Catalyzed Asymmetric (3+2) Cycloaddition of Imino Esters with Ylidene-2,3-dioxopyrrolidines	63
3-1.	Introduction	64
3-2.	Results and Discussion	66
3-3.	Conclusion	80
3-4.	Experimental Section	81
3-5.	References	137

Chapter 4	Formal Diastereodivergent Synthesis of 2,5-<i>cis/trans</i>-Pyrrolidines via Asymmetric (3+2) Cycloaddition	141
4-1.	Introduction	142
4-2.	Results and Discussion	144
4-3.	Conclusion	155
4-4.	Experimental Section	155
4-5.	References	187
Chapter 5	Copper-Catalyzed Asymmetric (3+2) Cycloaddition of Imino Lactones with Ylidene-pyrazolones	191
5-1.	Introduction	192
5-2.	Results and Discussion	193
5-3.	Conclusion	199
5-4.	Experimental Section	199
5-5.	References	208
Chapter 6	Conclusion and Perspective	211
	Publication List	214
	Acknowledgement	216

Abbreviation List

Ac	acetyl
AMPA	α -amino-3-hydroxy-5-methyl-4-isoxazolepropionic
Anal.	Analysis
aq.	aqueous
Ar	aryl
Bn	benzyl
Boc	<i>tertiary</i> -butylcarbonyl
br	broad (spectral)
brs	broad singlet
<i>t</i> Bu	<i>tertiary</i> -butyl
BTFM	bis(3,5-trifluoromethylphenyl)
Bz	benzoyl
°C	degrees Celsius
calcd	calculated
cat.	catalytic
Cbz	carbobenzoxy
CCDC	The Cambridge Crystallographic Data Centre
Co.	company
cod	1,5-cyclooctadiene
CPME	cyclopentyl methyl ether
Cy	cyclohexyl
δ	chemical shift in parts per million
d	doublet (spectral)
DA	Diels–Alder
DART	direct analysis in real time
DBU	1,8-diazabicyclo[5.4.0]undec-7-ene
DC	dipolar cycloaddition
decomp.	decomposition
DFT	density functional theory
DIPEA	diisopropylethylamine
DMF	<i>N,N</i> -dimethylformamide
DMSO	dimethylsulfoxide
dr	diastereomeric ratio
DTBM	3,5-di- <i>tert</i> -butyl-4-methoxyphenyl

ee	enantiomeric excess
ent.	enantiomer(s)
equiv.	equivalent(s)
ESI	electrospray ionization
Et	ethyl
EI	electron ionization
EWG	electron withdrawing group(s)
g	gram
h	hour
HCV	hepatitis C virus
<i>Het</i>	Heterocycle(s)
HOMO	highest Occupied Molecular Orbital
HPLC	high-performance liquid chromatography
HRMS	high-resolution mass spectrometry
Hz	hertz (s^{-1})
<i>i</i>	iso
Inc.	incorporated
Int	intermediate(s)
<i>i</i> Pr	iso-propyl
IRC	intrinsic reaction coordinate
<i>J</i>	coupling constant (spectral)
LUMO	Lowest Unoccupied Molecular Orbital
m	multiplet (spectral)
<i>m</i>	meta
MDM2	mouse double minute protein 2
Me	methyl
mg	milligram
MHz	megahertz
min	minutes
mL	milliliter
mm	millimeter
mmol	millimole(s)
mp	melting point
MTBE	methyl <i>tert</i> -butyl ether
<i>n</i>	normal
n. d.	not detected

nm	nanometer(s)
NMDA	N-methyl-D-aspartate
NMR	nuclear magnetic resonance
n. r.	no reaction
MS	molecular sieve
Ns	2-nitrobenzenesulfonyl
<i>o</i>	ortho
<i>p</i>	para
PG	protecting group
Ph	phenyl
PMP	<i>para</i> -methoxyphenyl
ppm	parts per million
<i>i</i> -Pr	<i>iso</i> -propyl
q	quartet (spectral)
quant.	quantitative
R	substituent
ref	reference
rt	room temperature
s	singlet (spectral)
t	triplet (spectral)
<i>t</i>	<i>tertiary (tert)</i>
TBD	1,5,7-Triazabicyclo[4.4.0]dec-5-ene
TBS	<i>tert</i> -butyldimethylsilyl
Tf	trifluoromethane sulfonyl
THF	tetrahydrofuran
tol	tolyl
<i>t_R</i>	retention time
Ts	toluene sulfonyl (tosyl)
TS	transition state
wt	weight

Chapter 1

General Introduction

1-1. Utility of Pyrrolidine Derivatives

A variety of organic compounds are used as biologically active molecules in the fields of pharmaceuticals and natural product chemistry. In general, it is known that the biological activity of these molecules depends not only on their molecular structures but also on their stereochemistry.¹ Therefore, developing the method for the precise preparation of stereoisomer has long been an important research subject in synthetic organic chemistry and medicinal chemistry. Stereodivergent synthesis² that can access multiple stereoisomers including diastereomers from common starting materials has been actively pursued in recent years because it is expected to improve the efficiency of drug discovery (Figure 1-1).

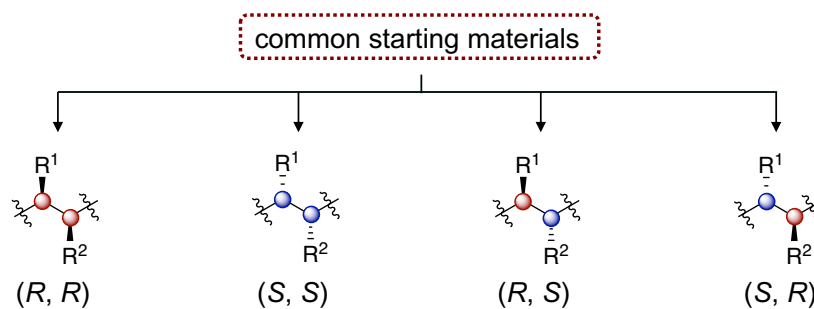


Figure 1-1. Stereodivergent synthesis.

Nitrogen-containing five-membered cyclic compounds, pyrrolidines, are included in the basic skeleton of complex amino acids and in numerous biologically active molecules and asymmetric catalysts.³ Pyrrolidines are rich in structural diversity, and many of them exist with additional cyclic skeletons such as fused- and spirocyclic-structures. The stereochemistry of these pyrrolidines shows that 2,5-*trans* pyrrolidines, whose substituents at the 2- and 5-positions of the pyrrolidine ring have a *trans* relationship, are as common as 2,5-*cis* pyrrolidines (Figure 1-2). For example, kaitocephalin⁴ (glutamate receptor agonist), which was isolated from *Eupenicillium shearii* PF1191, and a pyrrolidine that exhibits anti-HCV (hepatitis C virus) activity⁵ are 2,5-*cis* substituted. (7*S*)-Kaitocephalin in a 2,5-*trans* fashion, which was synthesized in

2016, has been shown to exhibit significantly high α -amino-3-hydroxy-5-methyl-4-isoxazolepropionic (AMPA)-type selectivity, whereas the naturally occurring molecule ((7*R*)-kainocephalin) activates both N-methyl-D-aspartate (NMDA) and AMPA-types.⁶ Furthermore, pyrrolidine derivatives that exhibit influenza neuraminidase inhibitory activity⁷ and MDM2-p53 activity⁸ have the 2,5-*trans* configuration. Therefore, it is strongly desired to develop efficient synthetic methods for the preparation of pyrrolidine derivatives rich in structural and stereodivergency. In particular, the development of stereodivergent synthetic methods for 2,5-*cis/trans* pyrrolidines is an important research issue because it can lead to the efficient creation of new biologically active compounds.

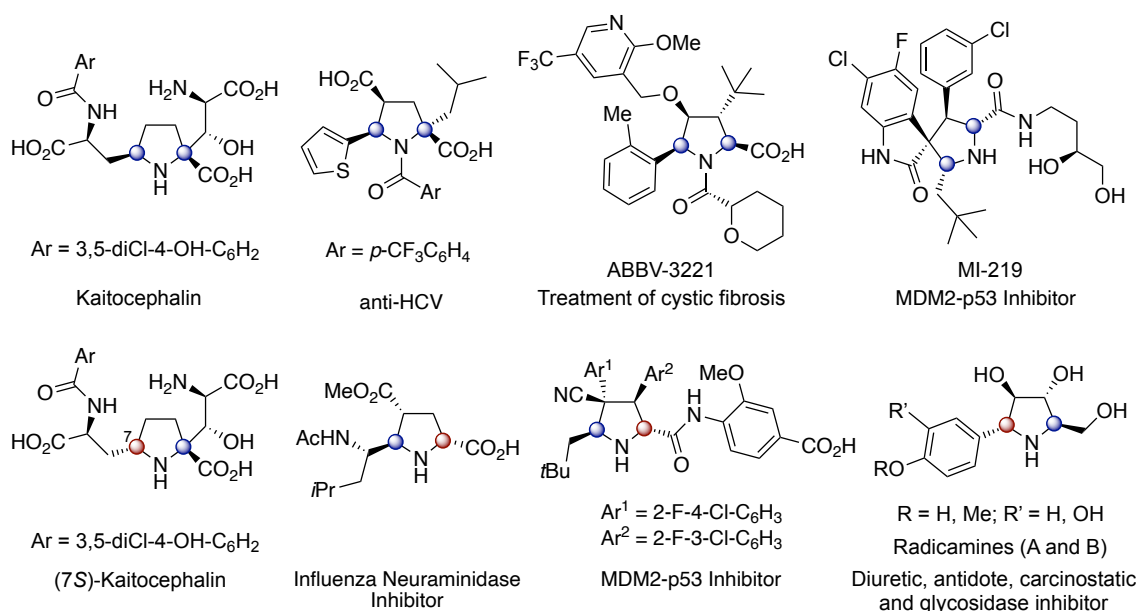
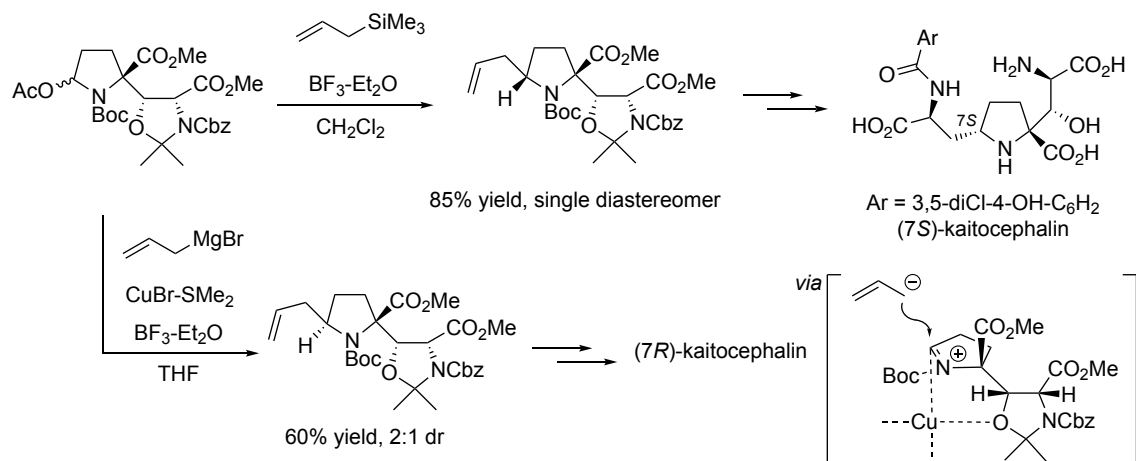


Figure 1-2. Examples of biologically active pyrrolidine with 2,5-*cis/trans* configuration.

1-2. Stereodivergent Synthesis of 2,5-*cis/trans* Pyrrolidines

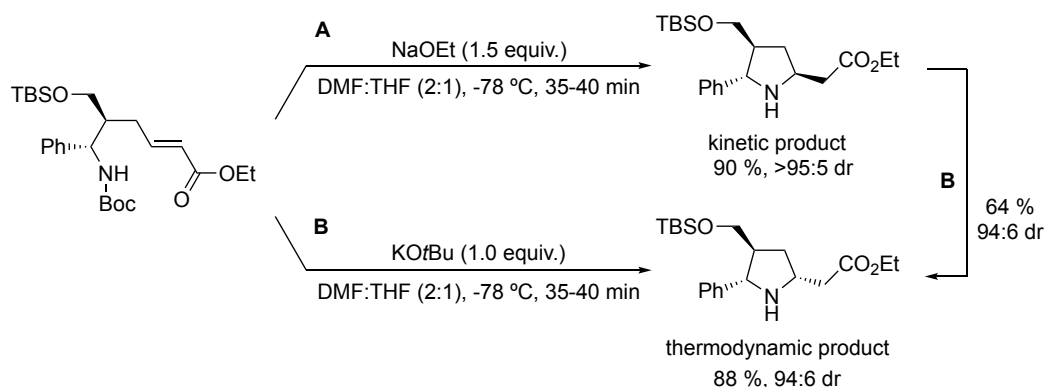
To date, several pioneering studies have been conducted on the stereodivergent synthesis of 2,5-*cis/trans* pyrrolidines. The diastereodivergent synthesis of (7*R*)- and (7*S*)-kaitocephalin described above was achieved using different types of nucleophiles in the allylation reaction (Scheme 1-1).^{6a} Specifically, the allylation reaction of the starting AcO-substituted pyrrolidine proceeded by treatment with allyl trimethyl silane and boron trifluoride diethyl ether complex, affording (7*S*)-pyrrolidine intermediates. In contrast, the diastereomeric (7*R*)-form was afforded as the main product when the same synthetic intermediate was subjected to an allyl copper reagent, which was prepared from an allyl Grignard reagent and a copper dimethyl sulfide bromide complex. It has been proposed that the heterocyclic substituent bonded to the pyrrolidine ring plays the role of an auxiliary group, i.e., the coordination of the oxygen atom of the substituent to the copper center can lead to the (7*R*)-diastereomer. Both intermediates can be converted to kaitocephalin, accomplishing the diastereodivergent synthesis of (7*S*)- and (7*R*)-kaitocephalins.



Scheme 1-1. Diastereodivergent synthesis of (7*R*)- and (7*S*)-kaitocephalin.

The stereodivergent synthesis of 2,5-*cis/trans* pyrrolidines using intramolecular amination reactions, which is one of the typical pyrrolidine synthesis methods, was reported by Scheider and co-workers in 2009 (Scheme 1-2).⁹ This is an example of an

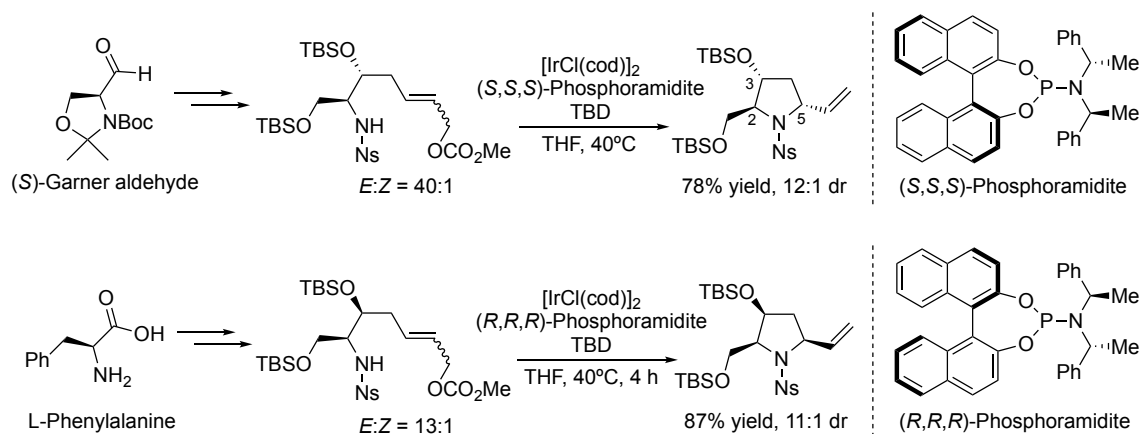
intramolecular aza-Michael addition reaction, which proceeds by the action of a base on a compound that has been prepared by the asymmetric Mannich reaction and subsequent silyl protection. The 2,5-*trans* pyrrolidine is generated with high diastereoselectivity when sodium ethoxide (NaOEt) is used as a base. In contrast, the corresponding 2,5-*cis* configured pyrrolidine is produced when potassium *tert*-butoxide (KOtBu) is used instead of NaOEt. Additionally, the isomerization reaction of the 2,5-*trans* pyrrolidine to the 2,5-*cis* one proceeds under condition **B** using KOtBu. This suggests that the aza-Michael addition giving the pyrrolidine ring is a reversible reaction and the 2,5-*trans* configured pyrrolidine is kinetically generated under condition **A** using NaOEt. Conversely, the 2,5-*cis* pyrrolidine produced by using KOtBu in condition **B** is the thermodynamically favorable product.



Scheme 1-2. Diastereodivergent synthesis using intramolecular aza-Michael addition reaction.

In 2014, Takahata and co-workers reported a method based on iridium-catalyzed stereoselective allylic amination reactions for the diastereodivergent preparation of 2,5-*cis/trans* pyrrolidines (Scheme 1-3).¹⁰ First, the cyclization precursor was prepared from (*S*)-Garner aldehyde with high stereoselectivity. The stereoselective allylic amination to give 2,5-*trans* substituted pyrrolidines took place by the action of an iridium complex and a phosphoramidite-based chiral ligand on this precursor. In contrast, the corresponding 2,5-*cis* substituted pyrrolidines can be obtained from cyclization precursors derived from L-phenylalanine by using the enantiomer of the above-described chiral ligand. The

products can be used as synthetic intermediates of (+)-bulgecinine and (+)-preussin, respectively.

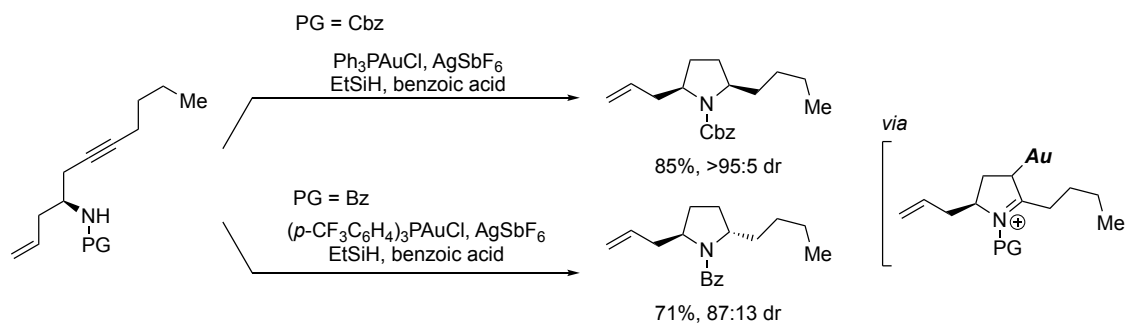


Scheme 1-3. Diastereodivergent synthesis using intramolecular allylic amination reaction.

A diastereodivergent synthetic method using gold-catalyzed intramolecular amination of internal alkynes followed by silane reduction has recently been reported by Fuwa and co-workers (Scheme 1-4).¹¹ The absolute configuration of the constructed stereocenter is determined when the silane reduction of the iminium intermediate takes place, not during the intramolecular amination process. The stereoselectivity was controlled by the protecting group on the amino group and the ligand of the gold catalyst. Specifically, the 2,5-*cis* substituted pyrrolidine was obtained with excellent diastereoselectivity by the intramolecular reaction using the Cbz-protected cyclization precursor. The 2,5-*trans* substituted pyrrolidine was formed as the major product when Bz-protected amino alkynes were applied to the reaction. These 2,5-*cis/trans* pyrrolidines have been used as synthetic intermediates for (+)-monomorine and (+)-indolizidine, respectively.

As described above, these pioneering diastereodivergent syntheses of 2,5-*cis/trans* pyrrolidines have been achieved either by direct introduction of substituents into preconstructed chiral pyrrolidine rings or by intramolecular amination reactions using chiral cyclization precursors as starting materials. Indeed, almost all of these methods

used chiral molecules as starting materials, impacting their efficiency due to the necessity of preparing chiral reaction precursors, which may take several steps. In other words, efficient synthetic methods for the diastereodivergent synthesis of 2,5-*cis/trans* pyrrolidines have rarely been developed. Therefore, the development of new methodologies is desired in organic synthetic chemistry.



Scheme 1-4. Diastereodivergent synthesis using intramolecular amination of internal alkynes and subsequent silane reduction.

1-3. Catalytic Asymmetric 1,3-Dipolar Cycloaddition of Imino Esters

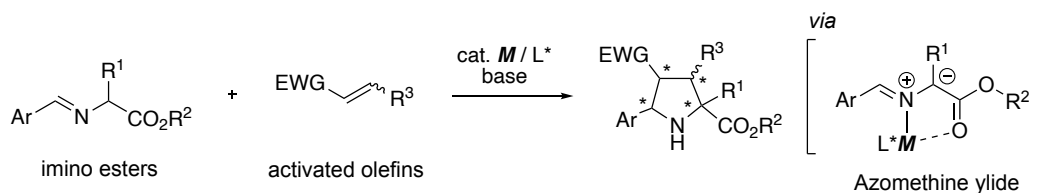
1-3-1. General Background

Along with intramolecular amination, the 1,3-dipolar cycloaddition (1,3-DC) of azomethine ylides with activated alkenes is an efficient synthetic method for the preparation of pyrrolidine derivatives.¹² Azomethine ylides are active species with a cationic nitrogen atom and an adjacent anionic carbon atom. They lead to pyrrolidine rings by (3+2) cycloaddition with activated olefins. Classically, azomethine ylides are known to be generated by the decarboxylation of imines formed by the condensation reaction of *N*-alkylamino acids and aldehydes under high temperatures.^{12c} Lithium azaallyl anions, which are generated by the action of strong bases such as organolithium reagents on imine compounds without active substituents such as carbonyl groups, are also known to give pyrrolidine compounds by the (3+2) cycloaddition reaction.^{12cd,13} In

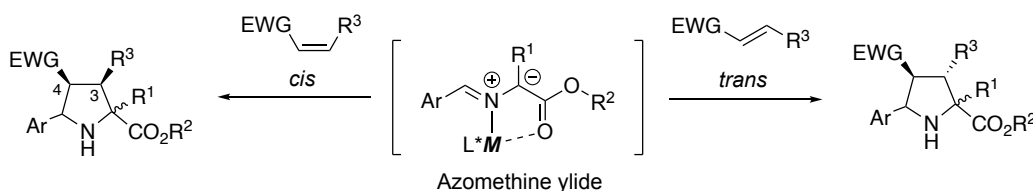
addition, the desilylation of silyl-substituted azomethine ylide precursors with activators such as acids and the thermal ring-opening reaction of aziridines can be used for pyrrolidine synthesis.^{12c,14} However, these classical methods usually require extreme activators such as strong acids, bases, or heat. Therefore, they are not suitable as a methodology for accurately creating multiple stereoisomers.

In contrast, the reaction of imino esters as the azomethine ylide precursors is very promising for the catalytic asymmetric synthesis of pyrrolidines (Figure 1-3a).¹⁵ In this method, the use of a chiral metal complex catalyst as a Lewis acid in combination with a base converts the imino ester to the azomethine ylide complex whose imine and carbonyl groups coordinate to the metal center. The chiral azomethine ylide then undergoes an asymmetric (3+2) cycloaddition reaction with activated olefins, which leads to the stereoselective synthesis of pyrrolidine derivatives. Although this cycloaddition reaction can construct multiple chiral centers in one step, many stereoisomers can be theoretically formed, i.e., if there are four chiral centers, a total of 16 stereoisomers could be obtained. However, the relative configuration of the 3- and 4-positions of the pyrrolidine ring in this cycloaddition reaction reflects the geometric isomerism of the olefin used, giving the corresponding cycloadducts (Figure 1-3b). For example, the relative configuration of the 3- and 4-positions will be *trans* if a *trans*-olefin is used. Thus, there are four accessible diastereoisomers (*endo*, *exo*, *endo'*, *exo'*) in the reaction, with their corresponding enantiomers (Figure 1-3c). The *endo*-adducts refer to a compound in which the carbonyl group at the 2-position is placed *cis* to the aromatic substituent at the 5-position, and the electron-withdrawing substituent at the 4-position is *cis* to these substituents. When the relative configuration of the 2- and 5-positions is *cis* and the substituent at the 4-position is *trans* to that at the 5-position, these adducts are classified as *exo*-diastereomers. In contrast to the above-described 2,5-*cis* cycloadducts, *endo'*/*exo'*-adducts are in the 2,5-*trans* configuration. Namely, the *endo'*-adduct refers to the 4,5-*cis* configuration in 2,5-*trans* adducts, and the *exo'*-adducts refer to the 4,5-*trans* configuration.

(a) Metal complex-catalyzed (3+2) cycloaddition of imino esters

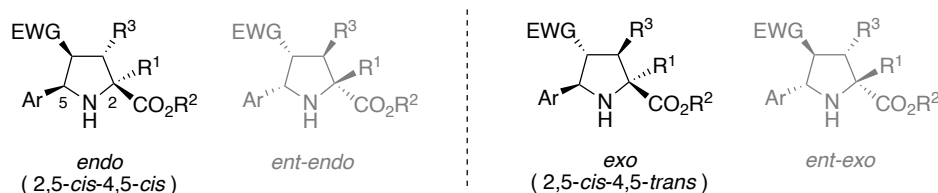


(b) Relationship of olefin and 3,4-relative configuration



(c) Theoretically accessible stereoisomers (*trans*-olefin)

Usual stereochemistry (2,5-*cis*)



Unusual stereochemistry (2,5-*trans*)

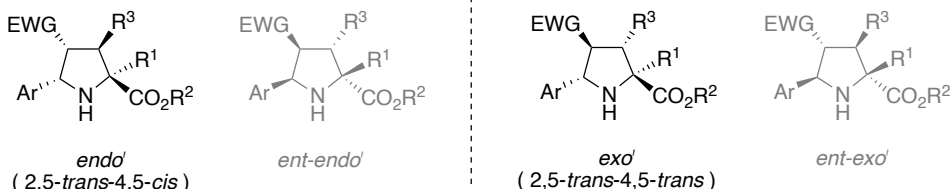


Figure 1-3. Asymmetric 1,3-DC of imino esters and the accessible stereoisomers.

The above-classified stereochemistry of the pyrrolidines is determined by both the reaction mechanism and transition state. This reaction generally constructs the pyrrolidine ring by a concerted cycloaddition, in which two bonds are formed almost simultaneously. The electrons in the HOMO of the azomethine ylide flow into the LUMO of the electron-deficient olefin, forming the two bonds. The reacting azomethine ylide is a bidentate complex of N and O atoms, and the aromatic substituents are *cis* to the carbonyl groups. Therefore, when this azomethine ylide undergoes cycloaddition reactions, the 2,5-*cis* adducts are preferentially formed because their stereochemistry depends on the conformation of the starting materials. When the electron-withdrawing group of the

activated olefins reacts when facing the metal center, the *endo*-form is given, while the *exo*-adducts are formed when the electron-withdrawing group faces the opposite direction. The *endo/exo*-diastereoselectivity depends on the stability of the transition state. Not only the reactivity of the activated olefins but also the catalyst used affect the *endo/exo*-diastereoselectivity. On the other hand, 2,5-*trans* adducts such as *endo'*/*exo'* are rarely formed from this azomethine ylide. To induce such 2,5-*trans* adducts from the *cis*-formed azomethine ylides, it is necessary to go through a stepwise cycloaddition process that switches reaction faces in the middle of the reaction. This is unfavorable for the reaction mechanism compared to the above-described concerted pathway and similar stepwise pathways.

The asymmetric 1,3-DC of imino esters with activated alkenes was first reported by Grigg and co-workers in 1991 using stoichiometric amounts of chiral Co(II) and Mn(II) complex catalysts.¹⁶ Subsequently, in 2002, Zhang, Jorgensen, and co-workers reported the first catalytic asymmetric 1,3-DC reaction.¹⁷ Since then, various teams, including our research group, have developed a variety of catalysts based on their concepts. In particular, copper and silver complexes have been applied frequently in recent years, and chiral bidentate ligands such as P, N-, P, S-, and P, P- have been found to work effectively (Figure 1-4).¹⁵ For example, Zhou and co-workers first reported in 2005 that AgOAc/FcPHOX complexes efficiently catalyze the 1,3-DC of imino esters with dimethyl maleate to give the corresponding *endo*-adducts with high enantioselectivity.¹⁸ The corresponding *endo*-adducts are obtained with high enantioselectivity when *N*-phenylmaleimide, *tert*-butyl acrylate, or dimethyl fumarate are used as activated olefins under the Ag/FcPHOX-catalyzed condition. The copper/Fesulphos complex developed by Carretero and co-workers in the same year has also been shown to be highly catalytically active in this reaction.¹⁹ Other ligands such as ThioClickFerrophos (TCF)²⁰ developed by Fukuzawa and co-workers and 1,3-dihydroimidazolepyridine (DHIPOH)²¹ developed by Deng and co-workers show high stereoselectivity as silver and copper complexes, respectively. TF-BiphamPhos, an asymmetric ligand developed by Wang and co-workers, catalyzes this asymmetric (3+2)

cycloaddition efficiently as both silver and copper complexes.²² In some cases, the axially chiral biaryl diposphine ligands BINAP and Segphos,²³ which are typical asymmetric ligands, and the monodentate phosphine ligand phosphoramidite²⁴ have also been reported to exhibit high stereoselectivity in this reaction.

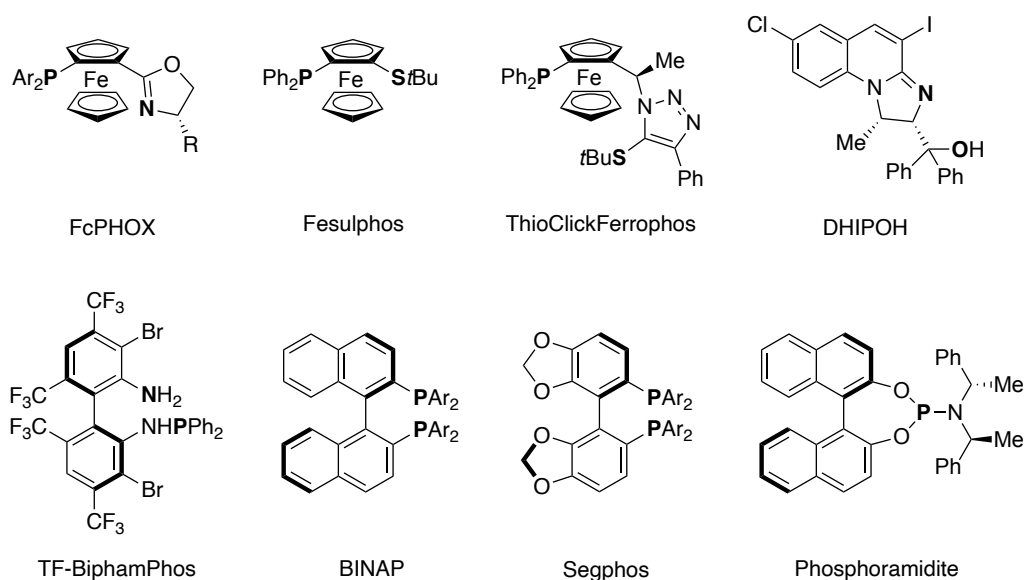


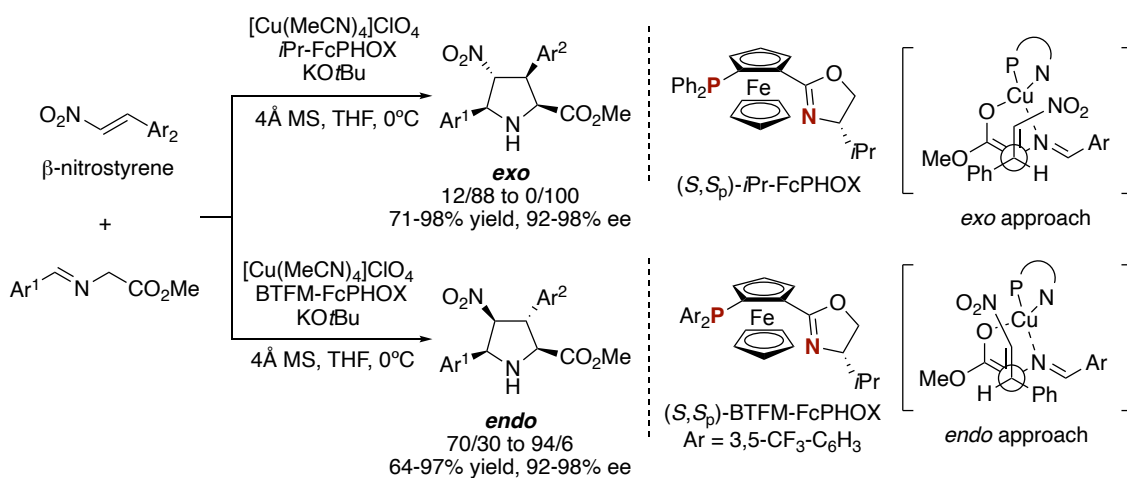
Figure 1-4. Some ligands employed in the copper and silver-catalyzed conditions.

In the Diels-Alder reaction, which is a representative cycloaddition, it has been shown that the *endo*-adduct, which is kinetically favorable, is preferentially formed due to secondary orbital interactions.¹² The contribution of this orbital interaction is small in the 1,3-DC, where steric bulk and electronic properties play a major role. Therefore, the *endo*-adducts are not always preferentially formed in this reaction, and many examples of *exo*-diastereoselectivity indicate these other properties may play a major role. One trend supported by several previous studies is that the diastereoselectivity depends on the nature of the metal center of the catalyst. Specifically, the copper complex-catalyzed reaction often proceeds with *exo*-diastereoselectivity, whereas the silver complex-catalyzed one tends to produce the *endo*-diastereomers. It is usually explained that the interaction between the carbonyl group of the dipole and the silver center stabilizes the transition state for the *endo*-adducts. When the copper complex catalysts are employed, the interactions between the dipole and ligand often affect the stereoselectivity. Based on

the above, representative examples that successfully achieved the *endo/exo*-diastereodivergent synthesis are summarized in this chapter.

1-3-2. *endo/exo*-Diastereodivergent Synthesis

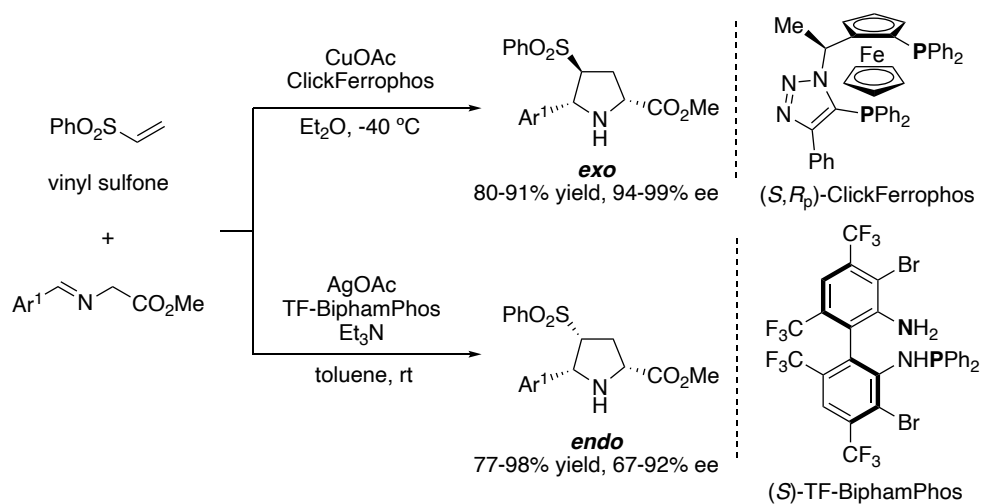
In 2006, Hou and co-workers achieved the pioneering *endo/exo*-diastereodivergent synthesis in the catalytic asymmetric 1,3-DC of imino esters with nitro alkenes (Scheme 1-5).²⁵ When a common copper/FcPHOX complex was used as the catalyst, the *exo*-adducts were produced with high diastereo- and enantioselectivity. In contrast, when an asymmetric ligand with electron-withdrawing substituents CF₃ on the aromatic ring attached to the phosphorus atom was used, the diastereoselectivity switched to give the corresponding *endo*-adducts in a highly enantioselective manner. DFT calculations were used to explain the reversal of diastereoselectivity, and a reasonable transition state was proposed for each. The transition state giving the *exo*-adducts was energetically favored with the nitro group of the active alkene positioned closer to the nitrogen atom on the ligand. On the other hand, a transition state was proposed in which the nitro group was positioned close to the phosphorus atom of the ligand to give the *endo*-adducts. The electrostatic interaction between the copper center and the nitro group of the activated olefins is controlled by an aromatic substituent on the phosphorus atom of the FcPHOX, and the *endo/exo*-diastereoselectivity is successfully achieved. A similar example of the



Scheme 1-5. Ligand-controlled *endo/exo*-diastereodivergent 1,3-DC of nitro olefins.

diastereodivergent synthesis controlled by two types of chiral ligands in the copper complex-catalyzed reaction of imino esters with nitro olefins was achieved by Cossío and co-workers in 2012.²⁶

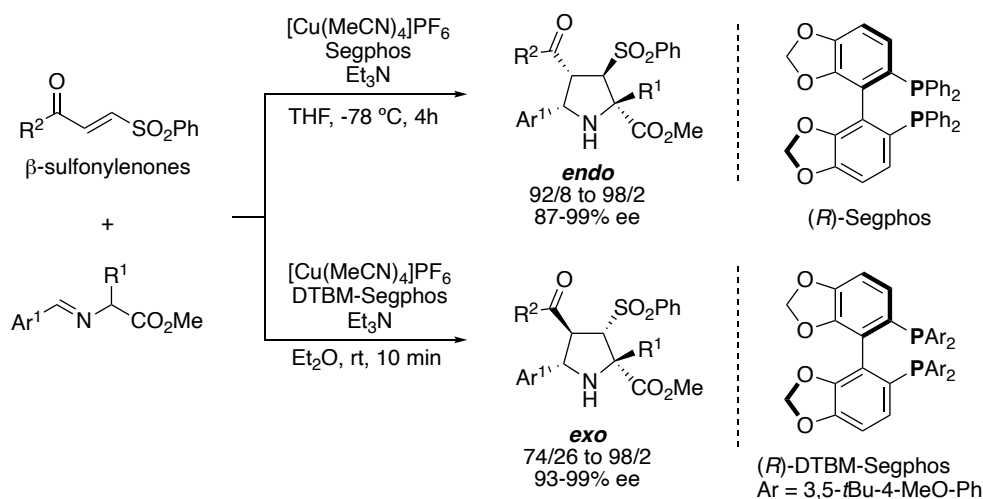
The catalytic asymmetric 1,3-DC of imino esters with vinyl sulfones was reported by Carretero and co-workers in 2006.^{27a} In 2008, our research group showed that an original copper/ClickFerrophos complex catalyst can be used to achieve higher enantioselectivity (Scheme 1-6).^{27b} Although the *exo*-adducts were obtained with high diastereoselectivity in both reports, Wang and co-workers reported in 2009 that their originally developed silver/TF-BiphamPhos gave the corresponding *endo*-adducts with high stereoselectivity.^{27c} This reaction also gave only *endo*-cycloadducts, even when copper salts were employed instead of silver acetate as the metal center. Therefore, its diastereoselectivity is thought to be controlled by the ligand, not the metal center.



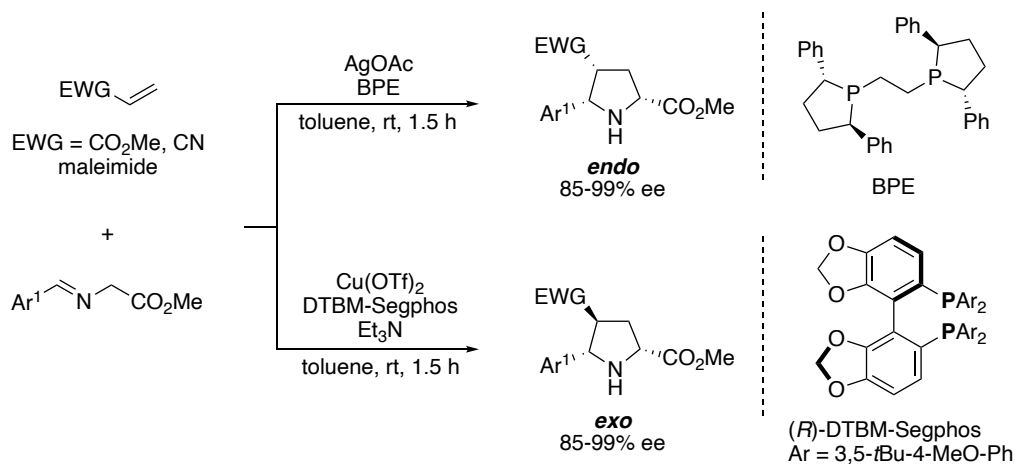
Scheme 1-6. *endo/exo*-Diastereodivergent reaction using vinyl sulfone.

In 2010, Carretero and co-workers reported an *endo/exo*-diastereodivergent copper-catalyzed asymmetric 1,3-DC of imino esters with β -sulfonylenones (Scheme 1-7).²⁸ Two regioisomers could be generated because the activated alkene used here has two types of electron-withdrawing groups, an acetyl group and a sulfonyl group. However, the pyrrolidines with the acetyl group substituted at the 4-position were obtained regioselectively. The diastereoselectivity was controlled by substituents on the

phosphorus atom of the chiral ligand Segphos. When the phenyl group substituted Segphos was employed, the *endo*-adducts were the major diastereomers with high enantioselectivity. DTBM-Segphos, which has bulky and electron-rich substituents, was found to give *exo*-adducts diastereo- and enantioselectively.



Scheme 1-7. *endo/exo*-Diastereodivergent synthesis using β -sulfonylenones.

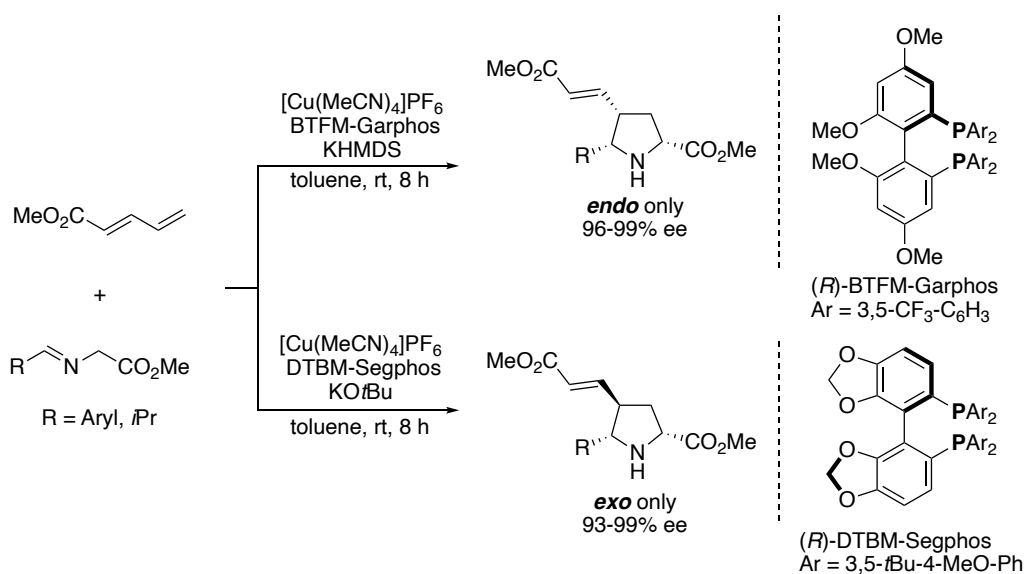


Scheme 1-8. Diastereodivergent synthesis controlled by silver and copper complex catalysts.

In 2012, Martín and co-workers developed an *endo/exo*-diastereodivergent reaction of imino esters with activated olefins such as acrylate, acrylonitrile, and maleimide.²⁹ The proper choice of silver or copper complex catalyst enabled the control of

diastereoselectivity (Scheme 1-8). This report is a typical example of the tendency to use silver complexes to give *endo*-adducts and copper complexes to give *exo*-adducts. Specifically, the use of silver acetate and the chiral ligand BPE gave *endo*-adducts enantioselectively, while the corresponding *exo*-adducts were obtained by using the copper $\text{Cu}(\text{OTf})_2/\text{DTBM-Segphos}$ complex.

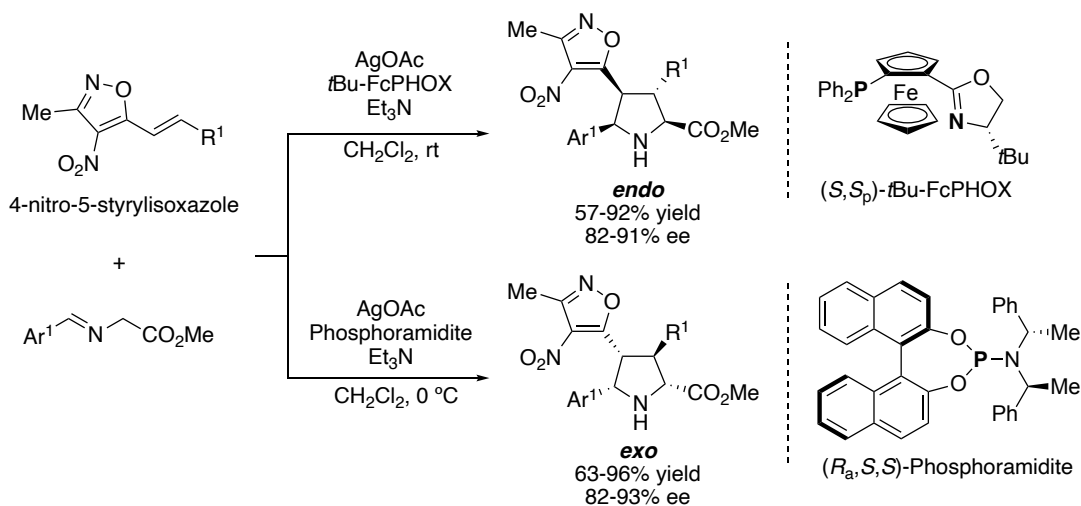
In 2015, Carretero and co-workers achieved *endo/exo*-diastereodivergent synthesis in the asymmetric 1,3-DC using 1,3-conjugated dienes as the activated olefins (Scheme 1-9).³⁰ In this reaction, regioselectivity is controlled under the standard conditions and the cycloaddition reaction takes place at the γ,δ -double bond of the conjugated diene. The *endo*-adducts were selectively obtained by using the biphenyl type of axially chiral diposphine ligand BTFM-Garphos, while *exo*-adducts were produced under conditions using the DTBM-Segphos ligand. Namely, the diastereoselectivity could be completely reversed by the proper choice of the chiral ligand.



Scheme 1-9. Ligand-controlled diastereodivergent synthesis using 1,3-conjugated dienes.

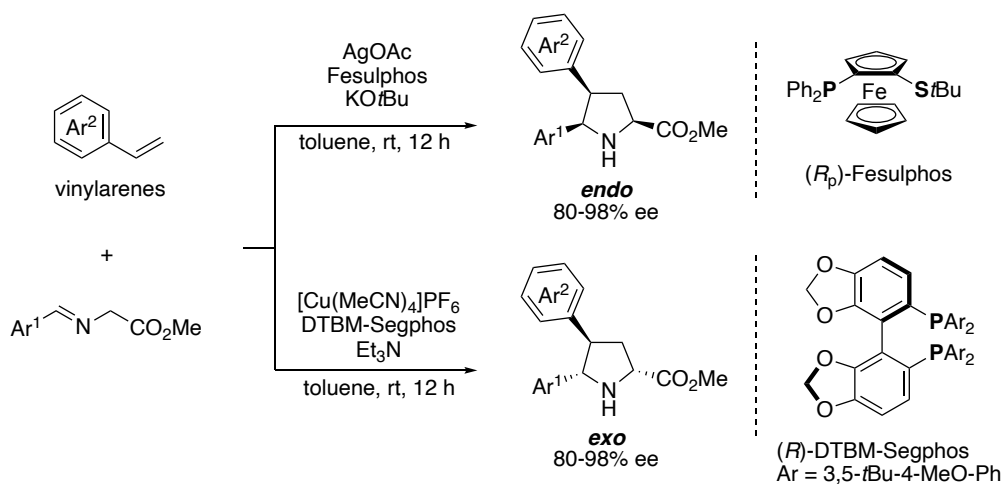
The following year, Wang and co-workers reported the silver-catalyzed *endo/exo*-diastereodivergent reaction of imino esters with nitro isoxazoles (Scheme 1-10).^{31a} The silver/*t*Bu-FcPHOX complex catalyzed this reaction efficiently and gave the corresponding *endo*-cycloadducts in a highly enantioselective manner. On the other hand,

the reaction proceeded with *exo*-diastereoselectivities when a monodentate phosphoramidite ligand was applied to the silver-catalyzed condition. When our original Ag/TCF complex catalyst was used in this asymmetric cycloaddition, the *endo*-diastereomer was produced with high enantioselectivity.^{31b}



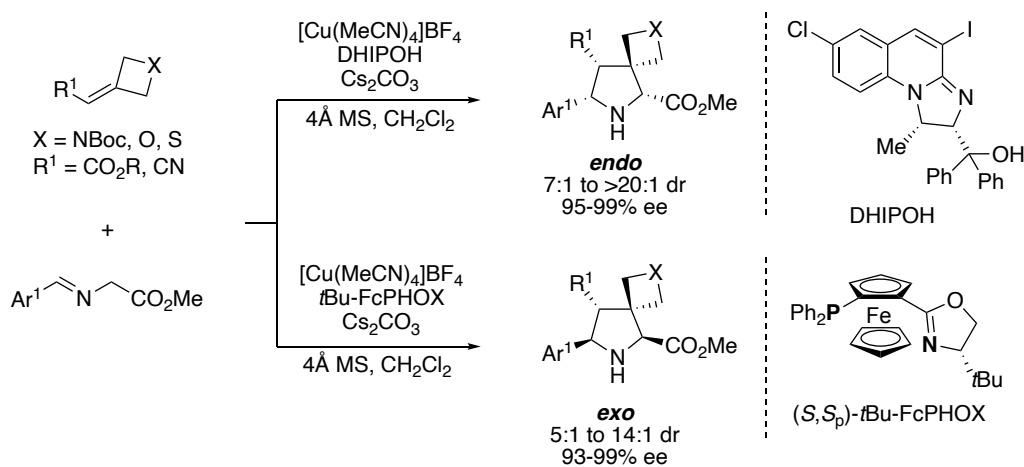
Scheme 1-10. Silver-catalyzed diastereodivergent synthesis in reaction of nitro-substituted isoxazoles.

In 2016, the diastereodivergent synthesis of the asymmetric 1,3-DC using vinyl arenes with nitro groups as active alkenes was reported by Carretero and co-workers (Scheme 1-11).³² The *endo/exo*-diastereoselectivity of the reaction was controlled by the silver and copper complex catalysts, respectively. In other words, the silver/Fesulphos complexes mainly gave *endo*-adducts enantioselectively, while the copper/DTBM-Segphos complexes gave only *exo*-adducts. In addition, it was shown that vinyl heteroarenes with pyridyl, quinolyl, or thiazole moieties could be used in the reaction. The reaction analysis based on theoretical chemical calculations revealed that the electron-withdrawing group attached to the aromatic substituent of the olefins greatly reduced the activation energy.



Scheme 1-11. *endo/exo*-Diastereodivergent reaction of imino esters with nitro-substituted vinyl arenes.

In 2019, Deng and co-workers achieved the diastereodivergent synthesis of spiropyrrolidines via copper complex-catalyzed asymmetric 1,3-DC reactions of imino esters with four-membered exocyclic olefins (Scheme 1-12).³³ The *endo/exo*-diastereoselectivity could be controlled by using an appropriate chiral ligand under the copper-catalyzed condition. Specifically, the *endo*-adducts were enantioselectively given when their originally developed N, O-ligand (DHIPHOH) was used, and the *exo*-adducts were given as the major diastereomer when *t*Bu-FcPHOX was employed.

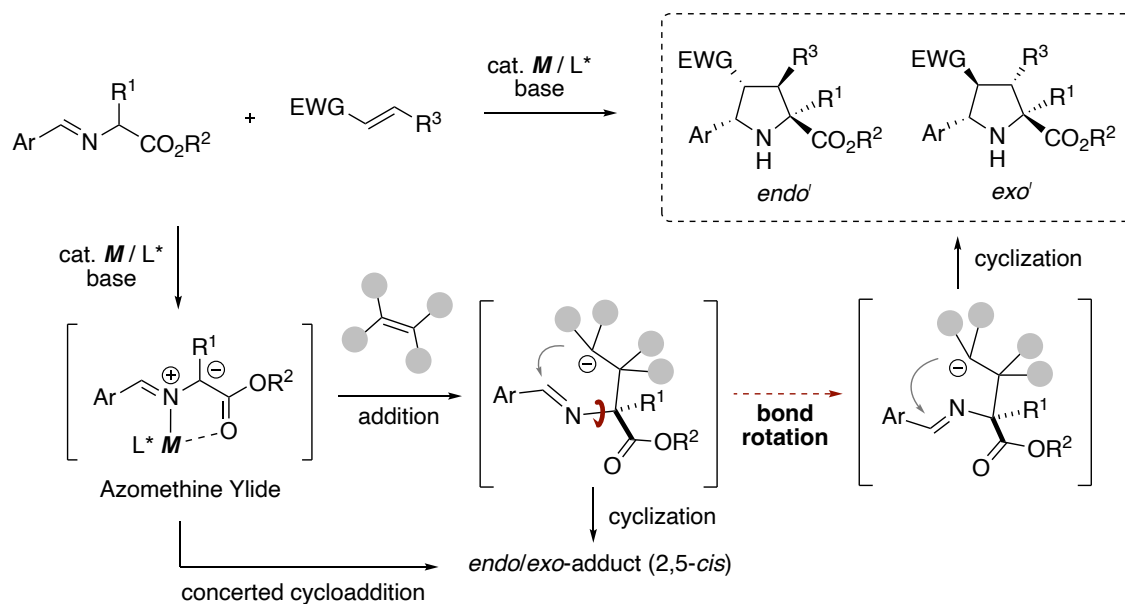


Scheme 1-12. Diastereodivergent synthesis of spiropyrrolidines using four-membered exocyclic olefins.

Sansano and co-workers reported studies on the relationship between *endo/exo*-diastereoselectivity and several dipolarophiles in the reaction using P, P-type chiral ligand Segphos in 2019.³⁴ P, P-Type ligand Segphos usually coordinates in a bidentate fashion to a metal center such as copper and silver to generate the corresponding azomethine ylides, which smoothly react with dipolarophiles. In this case, the dipolarophile does not interact with the metal center, and *exo*-diastereomers are produced. On the other hand, some reactions using the same type of P, P-ligand, DM-Segphos, produce *endo*-diastereomers. This indicates that the *endo*-selective reaction proceeds with the interaction of the metal center and the dipolarophile; DM-Segphos might have behaved as a monodentate ligand. Indeed, DFT calculations revealed that the transition state for *endo*-adducts was more favorable than that for *exo*-adducts in the reaction using DM-Segphos.

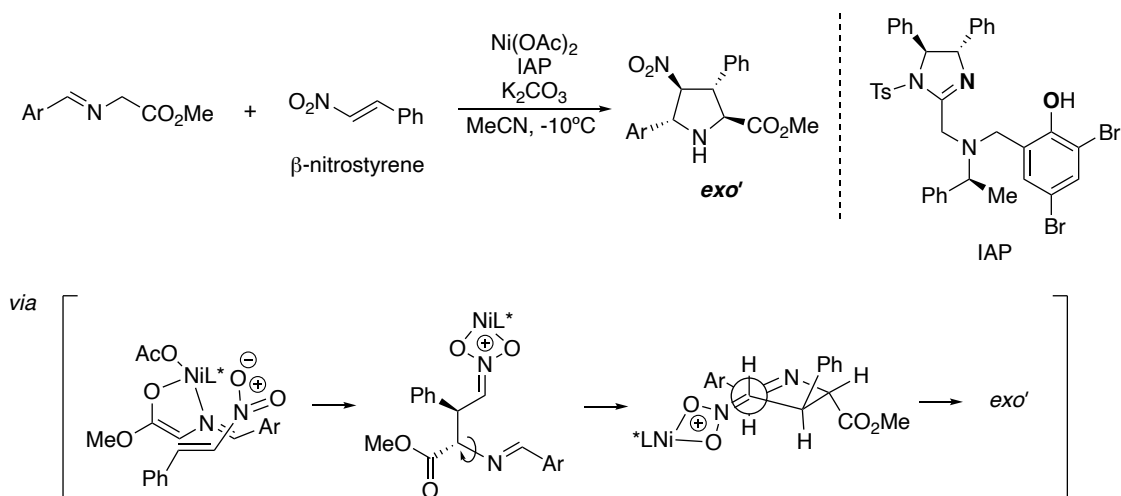
1-3-3. 2,5-*cis/trans*-Diastereodivergent Synthesis Using Imino Esters

As described above, *endo/exo*-diastereodivergent synthesis of pyrrolidine derivatives using asymmetric 1,3-DC has been reported, and numerous methodologies such as metal- and/or ligand-controlled strategies have been developed. However, methodologies for the diastereodivergent syntheses of 2,5-*cis* and 2,5-*trans* adducts (*endo/exo*) have been limited to a few examples.^{12,29} This may be because the 2,5-*trans* adducts are mechanistically difficult stereoisomers to form when using *cis*-type azomethine ylides generated by imino esters with a metal complex catalyst (Scheme 1-13). The cycloaddition reaction generally gives the 2,5-*cis* adducts from *cis*-type azomethine ylides by a concerted mechanism that forms two bonds almost simultaneously and a similar stepwise cycloaddition. In contrast, if the reaction is via stepwise cycloaddition, in which the C–N bond is rotated during the reaction to switch the reaction face of the imine, the 2,5-*trans* adducts can be produced. However, few methods have been established that can lead to this unfavorable reaction pathway, and it is difficult to switch the pathways precisely. Therefore, the 2,5-*cis/trans*-diastereodivergent synthesis has been reported in only a few cases.

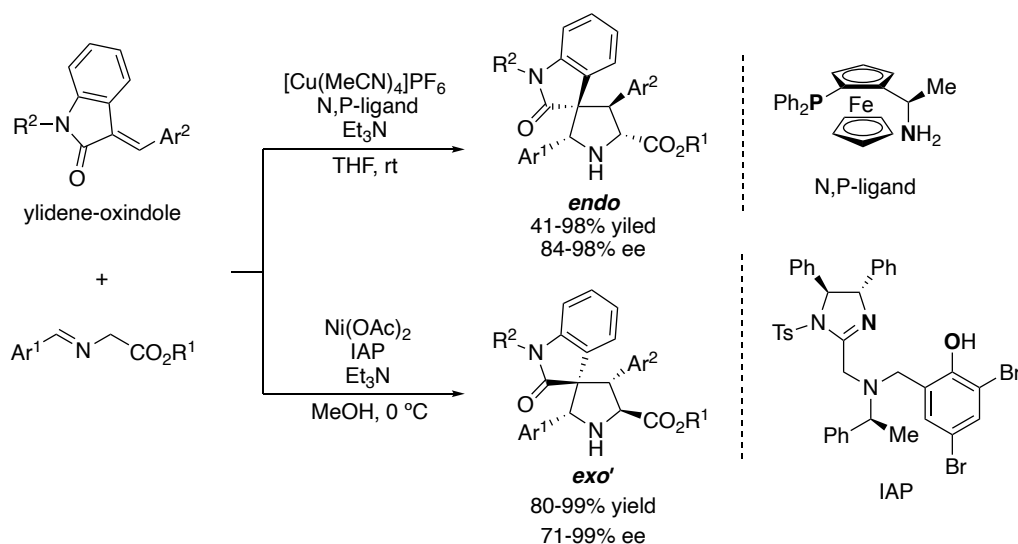


Scheme 1-13. Stepwise addition/cyclization with bond rotation pathway to afford 2,5-*trans* adducts.

In a pioneering study in 2010, Arai and co-workers reported the first synthesis of *exo'*-adducts in the asymmetric 1,3-DC reaction of imino esters with nitro olefins (Scheme 1-14).^{35a,c} In this reaction, which usually proceeds with 2,5-*cis* diastereoselectivity, the diastereoselectivity was switched to the rare 2,5-*trans* when their originally developed nickel/imidazole-aminophenol (IAP) catalyst was used. The mechanism is thought to be the above-described stepwise cycloaddition with bond rotation (Scheme 1-13), rather than the concerted 1,3-DC that is common in this reaction. First, an intermolecular anti-Michael addition reaction takes place from the azomethine ylide generated by the imino ester with a nickel complex catalyst to the nitro olefin. The interaction between the olefin-derived nitro group and the nickel center controls the stereochemistry at the 2- and 3-positions of the forming pyrrolidine ring. The nickel catalyst immediately flips from the imino ester moiety to the anionic nitro group to produce an intermediate. Subsequently, the imino ester-derived C–N bond is rotated and an intramolecular Mannich reaction takes place to give the *exo'*-adducts. If the Mannich reaction occurs without the rotation of the C–N bond after the formation of the intermediate, the *endo*-adducts are generated.



Scheme 1-14. *exo'*-Selective synthesis by nickel complex-catalyzed asymmetric 1,3-DC of imino esters with nitro olefins.

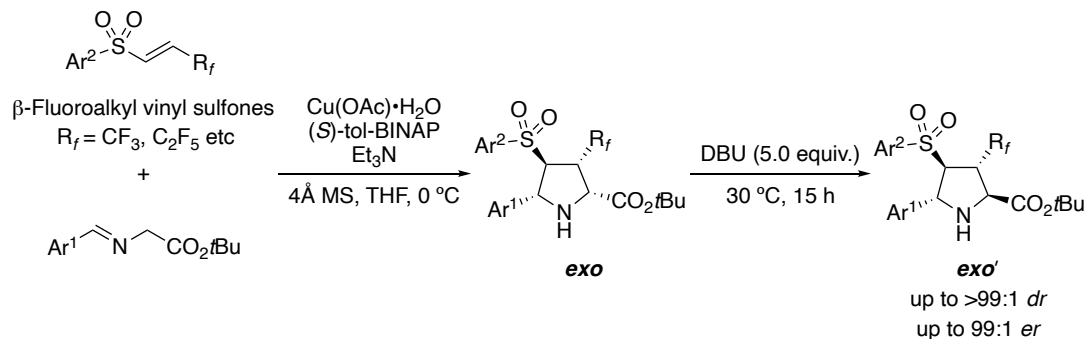


Scheme 1-15. *2,5-cis/trans* Diastereodivergent synthesis of indole-based spiropyrrolidines by catalyst-controlled strategy.

The catalytic asymmetric 1,3-DC of imino esters with ylidene-oxyindoles was first reported by Waldmann and co-workers in 2010, who demonstrated that the *endo*-adducts were obtained with high stereoselectivity when using a copper/ferrocenyl amine complex (Scheme 1-15).^{36a} Wang and co-workers had shown that this reaction proceeds with the same *endo*-diastereo- and enantioselectivity when silver complexes were employed.^{36b} In

contrast, the Ni/IAP complex catalyst developed by Arai and co-workers catalyzed this reaction efficiently and exhibited high *exo'*-diastereoselectivity and enantioselectivity.^{35b} Thus, 2,5-*cis/trans* diastereodivergent synthesis of spiro pyrrolidines, which includes the construction of a quaternary spiro carbon, has been achieved by a catalyst-controlled strategy.

The diastereodivergent synthesis of 2,5-*cis/trans* pyrrolidines can also be achieved by epimerization at the 2-position of the constructed pyrrolidine ring. The first epimerization strategy was developed by Huang and co-workers in 2019 (Scheme 1-16).^{37a} Initially, the *exo*-adducts were synthesized enantioselectively by using a copper/tol-BINAP complex in the asymmetric 1,3-DC of imino esters with β -fluoro alkyl vinyl sulfones. When DBU, an organic base, acted upon the *exo*-adduct obtained here, the stereocenter at the 2-position of the *exo*-adduct was inverted to give the *exo'*-adducts. Namely, the 2,5-*trans* adducts, i.e., *exo'*-adducts, took advantage of the thermodynamic stability of the corresponding *exo*-adducts. This epimerization strategy was successfully extended to the reaction of imino esters with α -fluoro- α,β -allyl ketones.^{37b} Specifically, in the case of Cu/tol-BINAP complexes, the *exo*-selective asymmetric cycloaddition with imino esters and α -fluoro α,β -allyl ketones occurred, yielding pyrrolidines which had fluorine and carbonyl groups substituted at the 4-position. The 2-epimerization of pyrrolidines that have tetrasubstituted carbons at the 4-position was also promoted by the action of DBU, and the *exo/exo'*-diastereodivergent synthesis was accomplished.

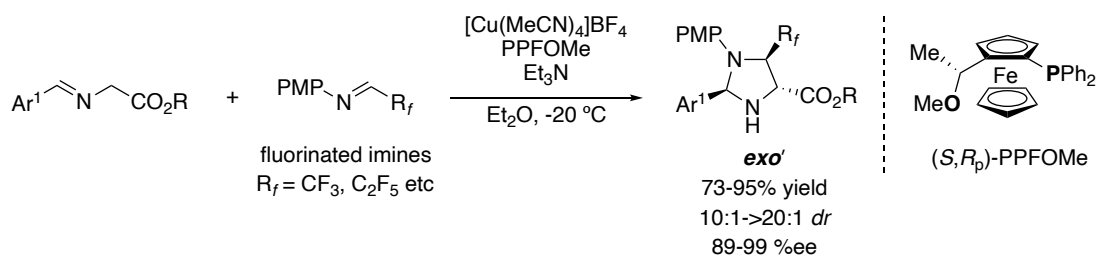


Scheme 1-16. 2,5-*cis* Selective ring formation and subsequent 2-epimerization strategy.

In summary, only two methodologies have been proposed for *2,5-cis/trans* diastereodivergent synthesis in the catalytic asymmetric 1,3-DC using imino esters. One method uses a nickel complex catalyst developed by Arai's group³⁵ and the other uses the epimerization of the initially formed *2,5-cis* adducts achieved by Huang's group.³⁷ Examples of the *2,5-cis/trans* stereodivergent synthesis are limited compared to the *endo/exo*-diastereodivergent synthesis using various methodologies. In other words, although many methodologies have been proposed for stereodivergent synthesis, it is still difficult to achieve *2,5-cis/trans* diastereodivergent synthesis by existing methodologies such as copper- and silver-catalyzed conditions. Therefore, a new and novel strategy is desired for the *2,5-cis/trans* diastereodivergent synthesis using azomethine ylides.

1-3-4. *2,5-trans* Selective Cycloaddition Using Azomethine Ylides

Examples of asymmetric synthesis of both *2,5-cis* and *trans* diastereomers by this reaction are described above. In addition, some reactions are known in which only the *2,5-trans* adduct is selectively obtained, but these are not stereodivergent syntheses. Although it is difficult to decipher the trend for the *2,5-trans* diastereoselectivity from these reactions, they are valuable and pioneering studies.³⁸



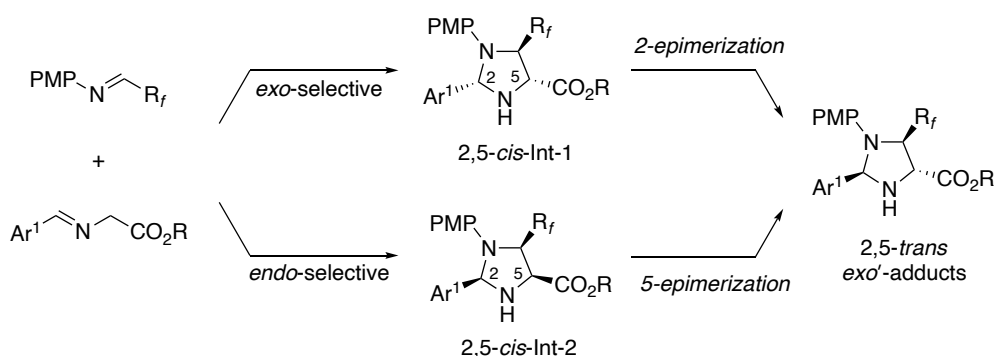
Scheme 1-17. *exo'*-Selective asymmetric 1,3-DC using fluorine-substituted imines.

In 2013, Wang and co-workers reported the asymmetric 1,3-DC reaction of imino esters with fluorine-substituted imines, giving chiral imidazolidines (Scheme 1-17).^{39a} The reaction was found to give the corresponding *exo'*-adducts enantioselectively when the Cu/PPFOMe complex was employed. Although several metals, ligands, and reaction conditions were screened, the diastereoselectivity was never completely switched to *2,5-*

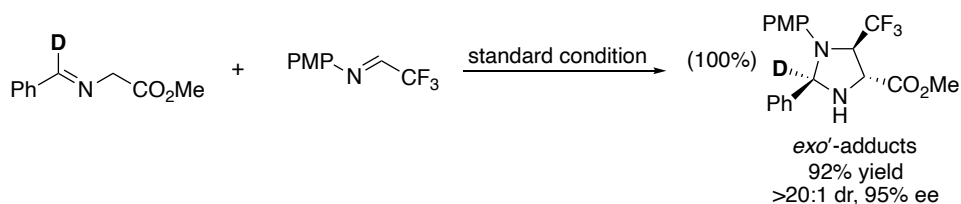
cis. This suggests that the 2,5-*trans* diastereoselectivity may depend highly on the fluorine-substituted imines rather than on the catalyst and conditions.

In 2018, Wang and co-workers reported a study on the mechanism for the rare 2,5-*trans* selectivity observed in the reaction using fluorine-substituted imines.^{39b} First, a reaction mechanism via the epimerization of 2,5-*cis* adducts commonly obtained was considered (Scheme 1-18a). One possible pathway is that the *exo*-selective cycloaddition gives the intermediate 2,5-*cis*-Int-1, which is converted to the corresponding 2,5-*trans* adduct by epimerization of the 2-position. Another route is the *endo*-selective cycloaddition reaction which gives the intermediate 2,5-*cis*-Int-2 and the subsequent epimerization of its 5-position. To validate these possible reaction pathways, corresponding control experiments were carried out. First, the (3+2) cycloaddition reaction was performed using an imino ester whose imine moiety was deuterated as the azomethine ylide precursor to verify whether the 2-epimerization occurs (Scheme 1-18b). The optimal conditions in the presence of methanol as the solvent gave the corresponding 2,5-*trans* adducts with high enantioselectivity. A deuteration ratio of >99% suggested that the 2-epimerization did not occur *in situ*. Next, the reaction pathway involving the epimerization at the 5-position was investigated by using an alanine-derived imino ester in which the hydrogen atom at the α -position was replaced by a methyl group (Scheme 1-18c). If the 2,5-*cis* adduct is formed temporarily as the intermediate, the 2,5-*trans* adduct is never obtained as a product because the tetrasubstituted carbon at the 5-position cannot epimerize. In other words, the *endo*-adduct should be obtained as the product when the common *endo*-selective (3+2) cycloaddition using α -methyl substituted azomethine ylides takes place. However, the *exo'*-adduct was obtained, and its stereochemistry was confirmed by X-ray crystallographic analysis. Therefore, it was clarified that *endo*-selective cycloaddition and subsequent epimerization at the 5-position did not occur.

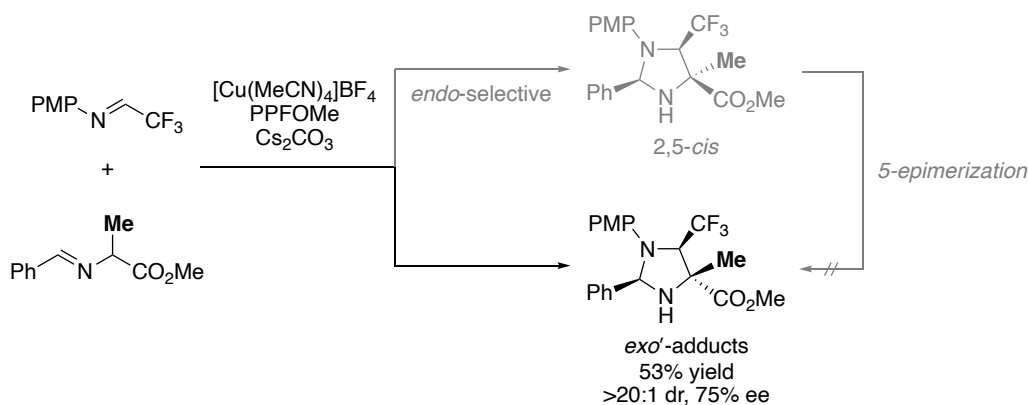
(a) Possible epimerization pathways for the *exo'*-adducts



(b) Investigation of 2-epimerization by using deuterium-labeled imino ester



(c) Investigation of 5-epimerization by using alanine-derived imino ester



Scheme 1-18. 2,5-*cis* Selective cycloaddition and subsequent epimerization pathways.

These control experiments suggest that the 2,5-*trans* diastereoselectivity observed in this reaction is due to a stepwise (3+2) cycloaddition with bond rotation (Figure 1-5). The Mannich reaction initially occurs from azomethine ylide **A** generated by imino esters and the copper catalyst to the *re*-face of fluorine-substituted imines. The stereochemistry is controlled by the Gauche conformation, giving the amphoteric ion intermediate **B**. Next, the copper catalyst coordinating the imino ester moiety switches its coordination to N-PMP to give intermediate **C**, which has a six-membered ring chair configuration. The

C–N bond rotation then takes place to give conformation **D**, and intramolecular cyclization to the *re*-face of the imine moiety results in the formation of the 2,5-*trans* adduct. The chair-configuration intermediate **C** has a hydrogen atom and a methoxy group in the 1,3-diaxial positions, which may contribute to the stabilization of this intermediate. When the hydrogen atom was replaced with an ethyl ester, this intermediate would not be stabilized by 1,3-diaxial interactions and the 2,5-*trans* adduct would not be formed. To test this hypothesis, the 1,3-DC reaction of imino esters with α -CF₃-ketimine esters was investigated, and it was found that *endo*-adducts, not *exo*'-adducts, were obtained. Namely, the six-membered ring intermediate **C** is not formed, and the second cyclization reaction is considered to have immediately occurred after the first bond formation. These results indicate that stabilization of the intermediate plays a key role in the 2,5-*trans* diastereoselectivity; the 1,3-diaxial interaction in the six-membered chair conformation has a significant effect on the rare diastereoselectivity of this imidazolidine formation.

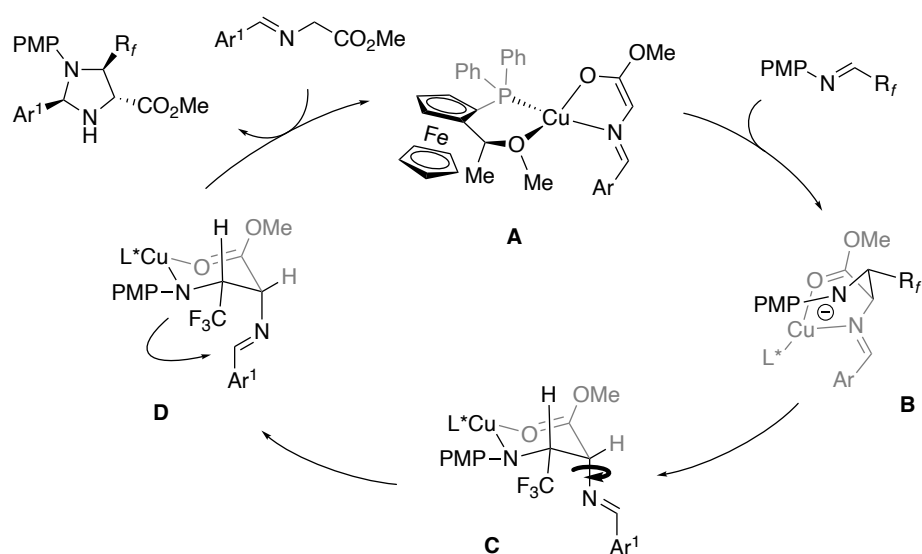
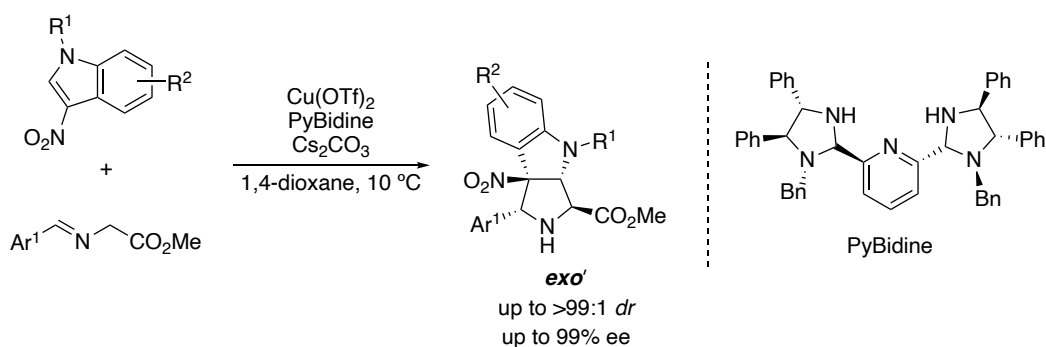


Figure 1-5. Proposed mechanism for the 2,5-*trans* diastereoselective imidazolidine formation by the asymmetric 1,3-DC of imino esters.

Having performed pioneering work on the 2,5-*cis/trans* diastereodivergent synthesis of imino esters by nickel complex catalysts, Arai and co-workers developed the copper-catalyzed asymmetric 1,3-DC reaction of imino esters with nitro indoles in 2014

(Scheme 1-19).⁴⁰ This report is the first example of dearomative asymmetric cycloaddition reactions using indole-derived activated olefins, which had previously been limited as nucleophiles. Interestingly, the reaction was catalyzed by the copper/bis(imidazolidine)pyridine (PyBidine) complex to give the corresponding *exo'*-adducts with high diastereo- and enantioselectivity. Also, the nickel complex catalysts that had been effective for *exo'*-selective reactions were not suitable for controlling the diastereoselectivity. On the other hand, copper/PyBidine complexes are known to give *endo*-adducts stereoselectively in the asymmetric 1,3-DC reaction of imino esters with nitro styrenes.⁴¹ Therefore, this rare diastereoselectivity would be highly dependent on the copper catalyst used and the indole-based nitro olefins.

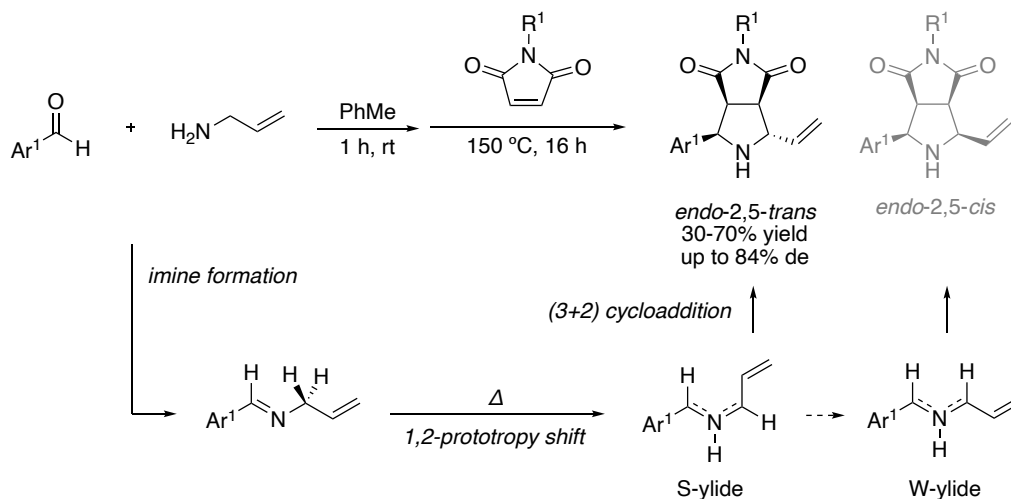


Scheme 1-19. *exo'*-Selective synthesis by asymmetric 1,3-DC using nitro-functionalized electron-deficient indoles.

In recent years, it has been reported that heat-generated azomethine ylides give 2,5-*trans* adducts, which can be considered a classical method. The azomethine ylides derived from imino esters change their conformation during the middle of the cycloaddition, where some azomethine ylides are converted to a favorable conformation for the 2,5-*trans* adducts before the start of bond formation.⁴² However, this method is not suitable for stereodivergent synthesis, including enantiomers, because it requires heating for conformational control.

For example, in 2018, Sansano and co-workers reported that the three-component coupling of an aldehyde, allylamine, and maleimide proceeds with 2,5-*trans*

diastereoselectivity (Scheme 1-20).^{43a} In this reaction, imine formation first takes place, and the resulting imine undergoes a 1,2-hydrogen transfer reaction to generate S-ylides. The generated S-ylide reacts with maleimide which is the dipolarophile to give the 2,5-*trans* pyrrolidines diastereoselectively. If the conformational W-ylide isomers react with the activated olefins, the 2,5-*cis* substituted pyrrolidines are formed. The reaction analysis using DFT calculations indicated the highest activation energy in the transition state of the 1,2-hydrogen transfer reaction, suggesting that it is the rate-limiting step. In addition, the activation energy for the isomerization of S-ylides to W-ylides was estimated to be sufficiently larger than that for the (3+2) cycloaddition reaction. Thus, the cycloaddition of S-ylides with maleimide proceeds preferentially over the isomerization of S-ylides to W-ylides. However, the isomerization could still take place because it has a lower activation energy than the 1,2-hydrogen transfer reaction. In addition, the W-ylide is slightly more thermodynamically stable. These facts suggest that controlling the 2,5-*cis/trans* diastereoselectivity completely would be difficult. It was shown in 2023 that the 2,5-*trans* selectivity is improved by using the same 1,2-hydrogen transfer method when propargyl amine is used instead of allylamine.^{43b}



Scheme 1-20. 2,5-*trans* Selective (3+2) cycloaddition of azomethine ylides generated by the 1,2-hydrogen transfer reaction.

Aly and co-workers reported that azomethine ylides similar to S-ylides are generated not only when using aryl amines and propargyl amines as described above, but also when using amino methyl pyridines and amino acid esters, and that they can be used for the synthesis of 2,5-*trans* adducts.⁴⁴ In particular, when arylidene with an ester moiety and cyano group was applied as the activated alkene, the 2,5-*cis* adducts were kinetically formed and the 2,5-*trans* adducts were thermodynamically obtained. In addition, the kinetic product, the 2,5-*cis* cycloadduct, was readily converted to the 2,5-*trans* conformation under mild conditions. It has been thought that the reverse reaction of the 1,3-DC reaction takes place, in which the regenerated ylide is isomerized and the cycloaddition reaction occurs again.

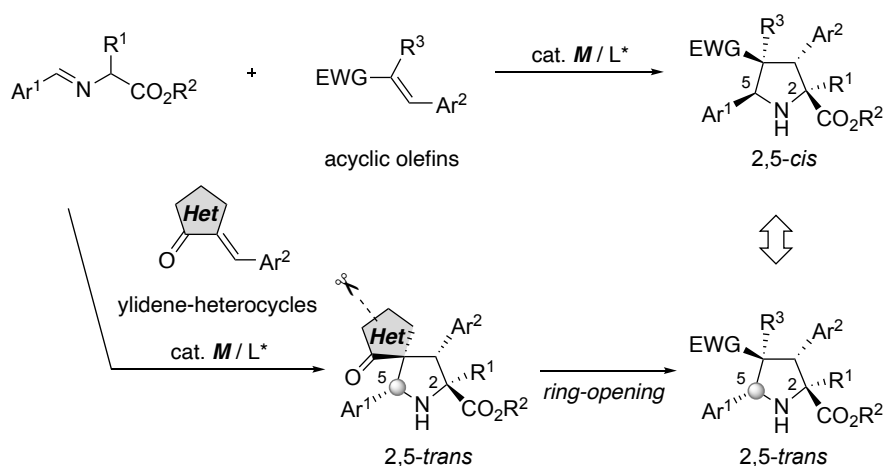
1-4. Outline of the Dissertation

As described in this chapter, despite the potential of both 2,5-*cis/trans* substituted pyrrolidines as biologically active molecules, few methods for efficient diastereodivergent preparation have been developed. Many diastereodivergent syntheses have been developed based on asymmetric 1,3-DC reactions of imino esters with activated olefins, which are efficient synthetic methods for chiral pyrrolidines. However, almost all have featured creating 2,5-*cis* configurations such as *endo/exo* adducts despite the development of many catalytic systems. Indeed, the 2,5-*cis/trans* divergent synthesis is limited to two methods involving epimerization of the 2,5-*cis* adducts found by Huang and co-workers³⁷ and the pioneering work using nickel complexes developed by Arai and co-workers.³⁵ This is due to the fundamental difficulty in synthesizing 2,5-*trans* adducts in the 1,3-DC using imino ester-derived *cis*-formed azomethine ylides. Synthesis of the 2,5-*trans* adducts requires a stepwise addition/cyclization with bond rotation, which is commonly unfavorable to the concerted pathway for giving the corresponding 2,5-*cis* adducts. Therefore, in this study, the author aimed to realize 2,5-*cis/trans* diastereodivergent synthesis using catalytic asymmetric 1,3-DC and to develop a new methodology for the 2,5-*trans* pyrrolidines.

In Chapter 2, the results are described for the asymmetric (3+2) cycloaddition of imino esters with α,β -unsaturated cyclic sulfonic esters. The cyclic sulfonic acid esters (sultones) had only been employed in thermal 1,3-DC reactions with nitrones and nitrile oxides, and their development for the stereoselective synthesis by catalytic reactions had not yet been explored. In this study, catalytic asymmetric (3+2) cycloadditions of imino esters with two types of sultones were investigated. The results showed that the copper complex catalyzed the reaction efficiently and the corresponding sultone-fused pyrrolidines were generated with high enantioselectivity for two types of sultones. Also, the reaction only gave the *exo*-diastereomers (2,5-*cis* adducts).

The research on asymmetric (3+2) cycloaddition of imino esters with ylidene-2,3-dioxypyrrolidines is described in Chapter 3. While previous studies have shown that the common 2,5-*cis* selective reaction proceeded when ylidene-oxindole or ylidene-succinimide was used, this reaction gave the rare *exo'*-adducts (2,5-*trans*). Furthermore, it was found that the corresponding spiropyrrolidines were produced with high enantioselectivity when our original silver/TCF complex catalyst was used. Control experiments suggested that a stepwise addition/cyclization with a bond rotation pathway is responsible for the rare 2,5-*trans* diastereoselectivity, not the 2,5-*cis* selective cycloaddition and subsequent epimerization pathway.

Since it was found that the reaction substrate (activated olefins) frequently governs the 2,5-*cis/trans*-diastereoselectivity, the author envisioned that the formal diastereodivergent synthesis of 2,5-*cis/trans* pyrrolidines could be realized by using different types of activated olefins (Scheme 1-21). The (3+2) cycloaddition of imino esters with acyclic olefins gave the common 2,5-*cis* adducts. In contrast, the (3+2) cycloaddition with ylidene-heterocycles which are easy to ring-open gave the corresponding spiropyrrolidines with 2,5-*trans* diastereoselectivity. Subsequent ring-opening of the heterocyclic moiety led to the 2,5-*trans* pyrrolidines with common substituents. Therefore, the author hypothesized that a series of these reactions could be a new diastereodivergent method to prepare 2,5-*cis/trans* pyrrolidines.



Scheme 1-21. 2,5-*cis/trans* Diastereodivergent synthesis using ylidene-heterocycles.

Based on the above hypothesis, the asymmetric (3+2) cycloaddition of imino lactones with ylidene-isoxazolones and the formal diastereodivergent synthesis of 2,5-*cis/trans* pyrrolidines are described in Chapter 4. The desired cycloaddition using ylidene-isoxazolones⁴¹ was efficiently catalyzed by a chiral silver complex, giving the 2,5-*trans* spiro-pyrrolidines with high enantioselectivity. In addition, the isoxazolone ring was smoothly converted to a ketone group by the Pd/C catalyzed reduction of the weak N–O bond. In contrast, the silver complex-catalyzed asymmetric 1,3-DC of imino lactones with α,β -unsaturated ketones gave the corresponding 2,5-*cis* pyrrolidines with high enantioselectivity. Thus, the formal diastereodivergent synthesis of 2,5-*cis/trans* pyrrolidines was achieved using the isoxazolone ring as a ketone equivalent.

The 2,5-*trans* selective cycloaddition reaction of imino lactones with ylidene-pyrazolones is described in Chapter 5. Pyrazolone is a heterocyclic structure that is similar to the isoxazolone ring described in Chapter 4. The reaction is known to proceed with 2,5-*trans* diastereoselectivity when the organocatalysts are used, but it was found to exhibit similar diastereoselectivity when using metal complex catalysts. Also, the reaction resulted in high enantioselectivity when a common chiral copper complex catalyst was used.

Chapter 6 is a summary of the entire study.

1–5. References

1. Selected review: (a) Brooks, W. H.; Guida, W. C.; Daniel, K. G. *Curr. Top. Med. Chem.* **2011**, *11*, 760–770. (b) Gandhi, K.; Saha, U.; Patel, S. *Curr. Drug Discov. Technol.* **2020**, *17*, 565–573.
2. Selected recent reviews for stereodivergent synthesis: (a) Krautwald, S.; Carreira, E. M. *J. Am. Chem. Soc.* **2017**, *139*, 5627–5639. (b) Lin, L.; Feng, X. *Chem. Eur. J.* **2017**, *23*, 6464–6482. (c) Beletskaya, I. P.; Nájera, C.; Yus, M. *Chem. Rev.* **2018**, *118*, 5080–5200. (d) Nájera, C.; Foubelo, F.; Sansano, J. M.; Yus, M. *Org. Biomol. Chem.* **2020**, *18*, 1232–1278. (e) Huo, X.; Li, G.; Wang, X.; Zhang, W. *Angew. Chem. Int. Ed.* **2022**, *61*, e202210086.
3. (a) Xu, W.-F.; Cheng, X.-C.; Wang, Q.; Fang, H. *Curr. Med. Chem.* **2008**, *15*, 374–385. (b) Vitaku, E.; Smith, D. T.; Njardarson, J. T. *J. Med. Chem.* **2014**, *57*, 10257–10274. (c) Taylor, R. D.; MacCoss, M.; Lawson, A. D. G. *J. Med. Chem.* **2014**, *57*, 5845–5859. (d) Petri, G. L.; Raimondi, M. V.; Spanò, V.; Holl, R.; Barraja, P.; Montalbano, A. *Top. Curr. Chem.* **2021**, *34*, 379–425.
4. Shinya, K.; Kim, Furihata, K.; Hayakawa, Seto, H. *Tetrahedron Lett.* **1997**, *38*, 7079–7078.
5. (a) Burton, G.; Ku, T. W.; Carr, T. J.; Kiesow, T.; Sarisky, R. T.; Lin-Goerke, J.; Hofmann, G. A.; Slater, M. J.; Haigh, D.; Dhanak, D.; Johnson, V. K.; Parry, N. R.; Thommes, P. *Bioorganic Med. Chem. Lett.* **2007**, *17*, 1930–1933. (b) Slater, M. J.; Amphlett, E. M.; Andrews, D. M.; Bravi, G.; Burton, G.; Cheasty, A. G.; Corfield, J. A.; Ellis, M. R.; Fenwick, R. H.; Fernandes, S.; Guidetti, R.; Haigh, D.; Hartley, C. D.; Howes, P. D.; Jackson, D. L.; Jarvest, R. L.; Lovegrove, V. L. H.; Medhurst, K. J.; Parry, N. R.; Price, H.; Shah, P.; Singh, O. M. P.; Stocker, R.; Thommes, P.; Wilkinson, C.; Wonacott, A. *J. Med. Chem.* **2007**, *50*, 897–900.
6. (a) Kawasaki, M.; Shinada, T.; Hamada, M.; Ohfuné, Y. *Org. Lett.* **2005**, *7*, 4165–4167. (b) Yasuo, Y.; Hamada, M.; Kawasaki, M.; Shimamoto, K.; Shigeri, Y.; Akizawa, T.; Konishi, M.; Ohfuné, Y.; Shinada, T. *Org. Biomol. Chem.* **2016**, *14*, 1206–1210.

7. Maring, C. J.; Stoll, V. S.; Zhao, C.; Sun, M.; Krueger, A. C. Stewart, K. D.; Madigan, D. L.; Kati, W. M.; Xu, Y.; Carrick, R. J.; Montgomery, D. A.; Kempf-Grote, A.; Marsh, K. C.; Molla, A.; Steffy, K. R.; Sham, H. L.; Laver, W. G.; Gu, Y.-g.; Kempf, D. J.; Kohlbrenner, W. E. *J. Med. Chem.* **2005**, *48*, 3980–3990.
8. Ding, Q.; Zhang, Z.; Liu, J.-J.; Jiang, N.; Zhang, J.; Ross, T. M.; Chu, X. J.; Bartkovitz, D.; Podlaski, F.; Janson, C.; Tovar, C.; Filipovic, Z. M.; Higgins, B.; Glenn, K.; Packman, K.; Vassilev, L. T.; Graves, B. *J. Med. Chem.* **2013**, *56*, 5979–5983.
9. Enkisch, C.; Schneider, C. *Eur. J. Org. Chem.* **2009**, 5549–5564.
10. Natori, T.; Kikuchi, S.; Kondo, T.; Saito, Y.; Yoshimura, Y. Takahata, H. *Org. Biomol. Chem.* **2014**, *12*, 1983–1994.
11. Nakagawa, H.; Fuwa, H. *Chem. Commun.* **2023**, *59*, 10121–10124.
12. Selected review for 1,3-DC of azomethine ylides: (a) Gothelf, K. V.; Jørgensen, K. A. *Chem. Rev.* **1998**, *98*, 863–910. (b) Hashimoto, T.; Maruoka, K. *Chem. Rev.* **2015**, *115*, 5366–5412. (c) Singh, M. S.; Chowdhury, S.; Koley, S. *Tetrahedron* **2016**, *72*, 1603–1716. (d) Otero-Fraga, J.; Montesinos-Magraner, M.; Mendoza, A. *Synthesis* **2017**, *49*, 802–809.
13. Kauffmann, T.; Berg, H.; Köppelmann, E. *Angew. Chem. Int. Ed. Engl.* **1970**, *9*, 380.
14. Li, J.; Zhao, H.; Zhang, Y. *Synlett* **2015**, *26*, 2745–2750.
15. Selected recent review: (a) Adrio, J.; Carretero, J. C. *Chem. Commun.* **2019**, *55*, 11979–11991. (b) Wei, L.; Chang, X.; Wang, C. J. *Acc. Chem. Res.* **2020**, *53*, 1084–1100. (c) Kumar, S. V.; Guiry, P. J. *Chem. Eur. J.* **2023**, *29*, e202300296.
16. Allway, P.; Grigg, R. *Tetrahedron Lett.* **1991**, *32*, 5817–5820.
17. (a) Longmire, J. M.; Wang, B.; Zhang, X. *J. Am. Chem. Soc.* **2002**, *124*, 13400–13401. (b) Gothelf, A. S.; Gothelf, K. V.; Hazell, R. G.; Jørgensen, K. A. *Angew. Chem. Int. Ed.* **2002**, *41*, 4236–4238.
18. Zheng, W.; Zhou, Y.-G. *Org. Lett.* **2005**, *7*, 5055–5058.
19. Cabrera, S.; Arrayás, R. G.; Carretero, J. C. *J. Am. Chem. Soc.* **2005**, *127*, 16394–16395.
20. (a) Oura, I.; Shimizu, K.; Ogata, K.; Fukuzawa, S.-i. *Org. Lett.* **2010**, *12*, 1752–1755.

- (b) Harada, M.; Kato, S.; Haraguchi, R.; Fukuzawa, S.-i. *Chem. Eur. J.* **2018**, *24*, 2580–2583.
21. Wang, W.-L.; Liu, Y.-Z.; Luo, S.; Yu, X.; Fossey, J. S.; Deng, W.-P. *Chem. Commun.* **2015**, *51*, 9212–9215.
22. (a) Wang, C.-J.; Liang, G.; Xue, Z.-Y.; Gao, F. *J. Am. Chem. Soc.* **2008**, *130*, 17250–17251. (b) Xue, Z.-Y.; Liu, T.-L.; Lu, Z.; Huang, H.; Tao, H.-Y.; Wang, C.-J. *Chem. Commun.* **2010**, *46*, 1727–1729.
23. (a) Nájera, C.; de Gracia Retamosa, M.; Sansano, J. M. *Org. Lett.* **2007**, *9*, 4025–4028. (b) López-Pérez, A.; Adrio, J.; Carretero, J. C. *Angew. Chem. Int. Ed.* **2009**, *48*, 340–343. (c) Yamashita, Y.; Guo, X.-X.; Takashita, R.; Kobayashi, S. *J. Am. Chem. Soc.* **2010**, *132*, 3262–3263. (d) Yamashita, Y.; Imaizumi, T.; Kobayashi, S. *Angew. Chem. Int. Ed.* **2011**, *50*, 4893–4896.
24. (a) Nájera, C.; de Gracia Retamosa, M.; Sansano, J. M. *Angew. Chem. Int. Ed.* **2008**, *47*, 6055–6058. (b) Castelló, L. M.; Nájera, C.; Sansano, J. M.; Larrañaga, O.; de Cózar, A.; Cossío, F. P. *Org. Lett.* **2013**, *15*, 2902–2905.
25. Yan, X.-X.; Peng, Q.; Zhang, Y.; Zhang, K.; Hong, W.; Hou, X.-L.; Wu, Y.-D. *Angew. Chem. Int. Ed.* **2006**, *45*, 1979–1983.
26. Conde, E.; Bello, D.; de Cózar, A.; Sánchez, M.; Vázquez, M. A.; Cossío, F. P. *Chem. Sci.* **2012**, *3*, 1486–1491.
27. (a) Llamas, T.; Arrayás, R.G.; Carretero, J. C. *Org. Lett.* **2006**, *8*, 1795–1798. (b) Fukuzawa, S.-i.; Oki, H. *Org. Lett.* **2008**, *10*, 1747–1750. (c) Liang, G.; Tong, M.-C.; Wang, C.-J. *Adv. Synth. Catal.* **2009**, *351*, 3101–3106.
28. Robles-Machín, R.; González-Esguevillas, M.; Adrio, J.; Carretero, J. C. *J. Org. Chem.* **2010**, *75*, 233–236.
29. Maroto, E. E.; Filippone, S.; Martín-Domenech, A.; Suarez, M.; Martín, N. *J. Am. Chem. Soc.* **2012**, *134*, 12936–12938.
30. González-Esguevillas, M.; Pascual-Escudero, A.; Adrio, J.; Carretero, J. C. *Chem. Eur. J.* **2015**, *21*, 4561–4565.
31. (a) Liu, K.; Xiong, Y.; Wang, Z.-F.; Tao, H.-Y.; Wang, C.-J. *Chem. Commun.* **2016**,

- 52, 9458–9461. (b) Kato, S.; Suzuki, Y.; Suzuki, K.; Haraguchi, R.; Fukuzawa, S.-i. *J. Org. Chem.* **2018**, *83*, 13965–13972.
32. Pascual-Escudero, A.; de Cózar, A.; Cossío, F. P.; Adrio, J. Carretero, J. C. *Angew. Chem. Int. Ed.* **2016**, *55*, 15334–15338.
33. Deng, H.; Jia, R.; Yang, W.-L.; Yu, X.; Deng, W.-P. *Chem. Commun.* **2019**, *55*, 7346–7349.
34. Caleffi, G. S.; Larrañaga, O.; Ferrándiz-Saperas, M.; Costa, P. R. R.; Nájera, C.; de Cózar, A.; Cossío, F. P.; Sansano, J. M. *J. Org. Chem.* **2019**, *84*, 10593–10605.
35. Chiral nickel complex-catalyzed cycloaddition for 2,5-*trans* pyrrolidines: (a) Arai, T.; Yokoyama, N.; Mishiro, A.; Sato, H. *Angew. Chem. Int. Ed.* **2010**, *49*, 7895–7898. (b) Awata, A.; Arai, T. *Chem. Eur. J.* **2012**, *18*, 8278–8282. (c) Arai, T.; Tokumitsu, C.; Miyazaki, T.; Kuwano, S.; Awata, A. *Org. Biomol. Chem.* **2016**, *14*, 1831–1839.
36. (a) Antonchick, A. P.; Gerding-Reimers, C.; Catarinella, M.; Schürmann, M.; Preut, H.; Ziegler, S.; Rauh, D.; Waldmann, H. *Nat. Chem.* **2010**, *2*, 735–740. (b) Liu, T.-L.; Xue, Z.-Y.; Tao, H.-Y.; Wang, C.-J. *Org. Biomol. Chem.* **2011**, *9*, 1980–1986.
37. (a) Cheng, F.; Kalita, S. J.; Zhao, Z.-N.; Yang, X.; Zhao, Y.; Schneider, U.; Shibata, N.; Huang, Y.-Y. *Angew. Chem. Int. Ed.* **2019**, *58*, 16637–16643. (b) Kalita, S. J.; Cheng, F.; Fan, Q.-H.; Shibata, N.; Huang, Y.-Y. *J. Org. Chem.* **2021**, *86*, 8695–8705.
38. Similar examples (2,6-*trans* selective synthesis of piperidine by the formal (3+3) cycloaddition using imino esters): (a) Yang, W.-L.; Li, C.-Y.; Qin, W.-J.; Tang, F.-F.; Yu, X.; Deng, W.-P. *ACS Catal.* **2016**, *6*, 5685–5690. (b) Xiao, L.; Li, B.; Xiao, F.; Fu, C.; Wei, L.; Dang, Y.; Dong, X.-Q.; Wang, C.-J. *Chem. Sci.* **2022**, *13*, 4801–4812. (c) Zhu, B.-K.; Xu, H.; Xiao, L.; Chang, X.; Wei, L.; Teng, Dang, Y.; Dong, X.-Q.; Wang, C.-J. *Chem. Sci.* **2023**, *14*, 4134–4142.
39. (a) Li, Q.-H.; Wei, L.; Chen, X.; Wang, C.-J. *Chem. Commun.* **2013**, *49*, 6277–6279. (b) Wei, L.; Li, Q.-H.; Wang, C.-J. *J. Org. Chem.* **2018**, *83*, 11814–11824.
40. Awata, A.; Arai, T. *Angew. Chem. Int. Ed.* **2014**, *53*, 10462–10465.
41. Arai, T.; Mishiro, A.; Yokoyama, N.; Suzuki, K.; Sato, H. *J. Am. Chem. Soc.* **2010**, *132*, 5338–5339.

42. Gu, Y. G.; Xu, Y.; Krueger, A. C.; Madigan, D.; Sham, H. L. *Tetrahedron Lett.* **2002**, *43*, 955–957.
43. (a) Selva, V.; Selva, E.; Merino, P.; Nájera, C.; Sansano, J. M. *Org. Lett.* **2018**, *20*, 3522–3526. (b) Belabbes, A.; Retamosa, M. G.; Foubelo, F.; Sirvent, A.; Nájera, C.; Yus, M.; Sansano, J. M. *Org. Biomol. Chem.* **2023**, *21*, 1927–1936.
44. (a) Taha, A. G.; Elboray, E. E.; Kobayashi, Y.; Furuta, T.; Abbas-Temirek, H. H.; Aly, M. F. *J. Org. Chem.* **2021**, *86*, 547–558. (b) Radwan, M. F.; Elboray, E. E.; Dardeer, H. M.; Kobayashi, Y.; Furuta, T.; Hamada, S.; Dohi, T.; Aly, M. F. *Chem. Asian J.* **2023**, *18*, e202300215.

Chapter 2

Copper-Catalyzed Asymmetric (3+2) Cycloaddition of Imino Esters with α,β -Unsaturated Sulfones

2-1. Introduction

The asymmetric 1,3-DC of azomethine ylides generated by imino esters and a chiral metal complex catalyst is an efficient method for constructing chiral pyrrolidine rings.¹ Directed toward establishing a new synthetic method for pyrrolidine-containing biologically active compounds,^{2,3} many types of catalyst systems have been reported to control the stereochemistry. In this process, various activated olefins have been employed that have been found to be widely applicable to this reaction. In particular, our research groups have adopted activated olefins bearing a heterocyclic moiety and developed a synthetic method for pyrrolidines containing another heterocycle by this asymmetric cycloaddition.⁴ For example, in 2018, we reported the catalytic asymmetric 1,3-DC of imino esters with benzo[*b*]thiophene-1,1-dioxides to produce sulfone-fused pyrrolidines with high stereoselectivity.^{4a}

As a heterocyclic compound that has potential bioactivity, the author focused on the sultone scaffold (cyclic sulfonic acid esters) which plays an important role in biologically active compounds.⁵ For example, some five- and six-membered sultone derivatives behave as inhibitors of human cytomegalovirus (HCMV), varicella zoster virus (VZV), human immunodeficiency virus (HIV), and bovine viral diarrhea-mucosal disease (BVDV) (Figure 2-1).⁶ Therefore, sultone-containing pyrrolidine compounds are attractive molecules in the field of drug discovery.

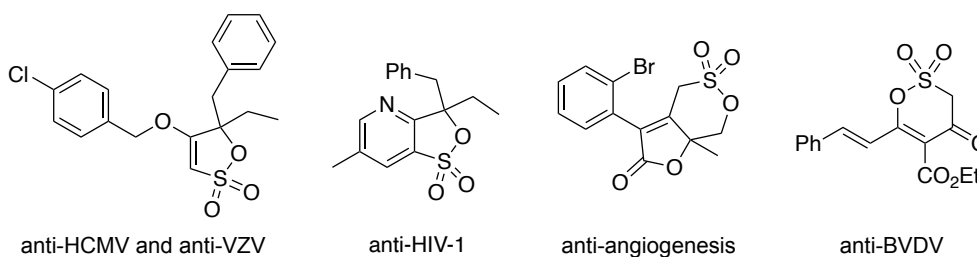


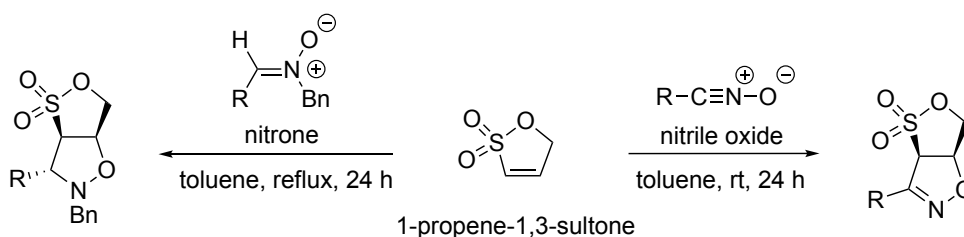
Figure 2-1. Example of biologically active compounds containing sultone moiety.

However, there are few synthetic methods for introducing the sultone moiety by stereoselective cycloaddition. The pioneering work for the synthesis of sultone-fused

compounds by the cycloaddition process was reported by Chan and co-workers in 1997.⁷ They revealed that 1-propene-1,3-sultone behaves as a good dienophile in the thermal Diels-Alder reaction. 1-Propene-1,3-sultone has also been applied in 1,3-DC reactions with nitrile oxides and nitrones and has been shown to work well as a dipolarophile (Figure 2-2a).⁸ However, these reports were conducted using thermal methods, and further studies for the development of catalytic asymmetric synthesis have not been explored.

Based on this background, the author envisioned a catalytic asymmetric 1,3-DC of imino esters with 1-propene-1,3-sultone to afford sulfone-fused pyrrolidines in an optically pure fashion (Figure 2-2b). Additionally, the author examined the reaction using sulfocoumarins (1,2-benzoxathiine-2,2-dioxides) as the dipolarophiles, which had not been applied as activated olefins in the Michael addition and cycloaddition reactions.⁹

(a) Diastereoselective thermal 1,3-DC of 1-propene-1,3-sultone



(b) This work: asymmetric (3+2) cycloaddition of imino esters with α,β -unsaturated sultones

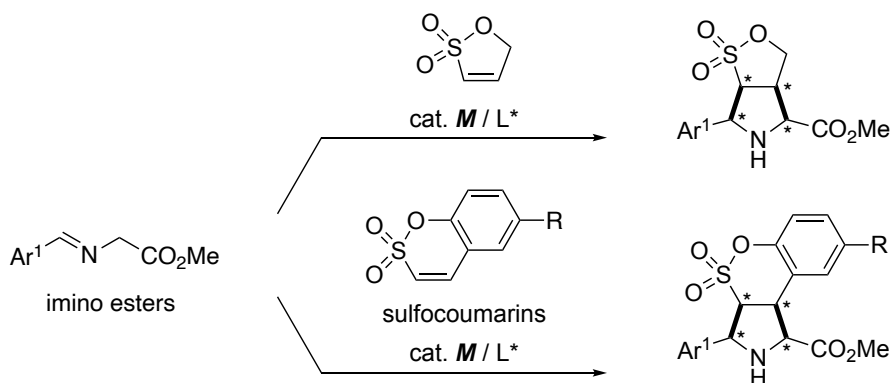
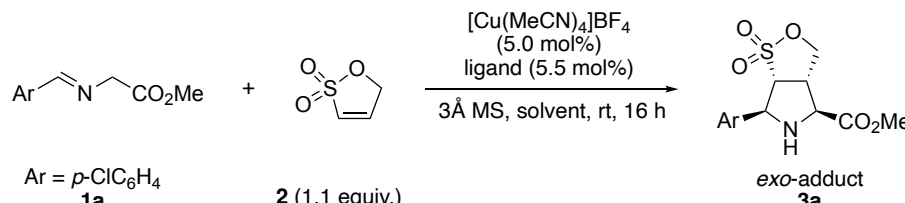


Figure 2-2. (a) previous report of the 1,3-DC of 1-propene-1,3-sultone and (b) this work.

Table 2-1. Initial experiment and optimization of the reaction conditions.^a



entry	ligand	solvent	yield (%) ^b	ee (%) ^c
1 ^d	PPh ₃	THF	>99	-
2	none	THF	26 ^e	-
3 ^f	none	THF	n.r.	-
4 ^g	PPh ₃	THF	33	-
5	L1	THF	85	18
6	L2	THF	99	91
7	L3	THF	87	9
8	L4	THF	99	62
9	L5	THF	96	80
10	L6	THF	70	-9
11	L7	THF	99	45
12	L2	Et ₂ O	96	92
13	L2	toluene	99	95
14	L2	CH ₂ Cl ₂	99	97

[a] Condition: **1a** (0.20 mmol), **2** (0.22 mmol), [Cu(MeCN)₄]BF₄ (0.010 mmol, 5.0 mol%), ligand (0.011 mmol, 5.5 mol%), 3Å MS (100 mg), solvent (1 mL), rt, 16 h. The diastereomeric ratio was determined by crude ¹H NMR. [b] Isolated yield. [c] The enantiomeric excess was determined by chiral HPLC. [d] Et₃N (18 mol %) was added. [e] The diastereomeric ratio was 2:1. [f] Without [Cu(MeCN)₄]BF₄. [g] AgOAc was used instead of [Cu(MeCN)₄]BF₄.

The substrate scope of the asymmetric 1,3-DC of imino esters **1** with 1-propene-1,3-sulfone (**2**) was investigated under the optimized conditions (Table 2-1, entry 14), and a variety of sulfone-fused pyrrolidines were obtained with excellent yield and enantioselectivity as single diastereoisomers. *para*-Bromo, fluoro, and strong electron-withdrawing groups substituted on the imino esters smoothly reacted with 1-propene-1,3-

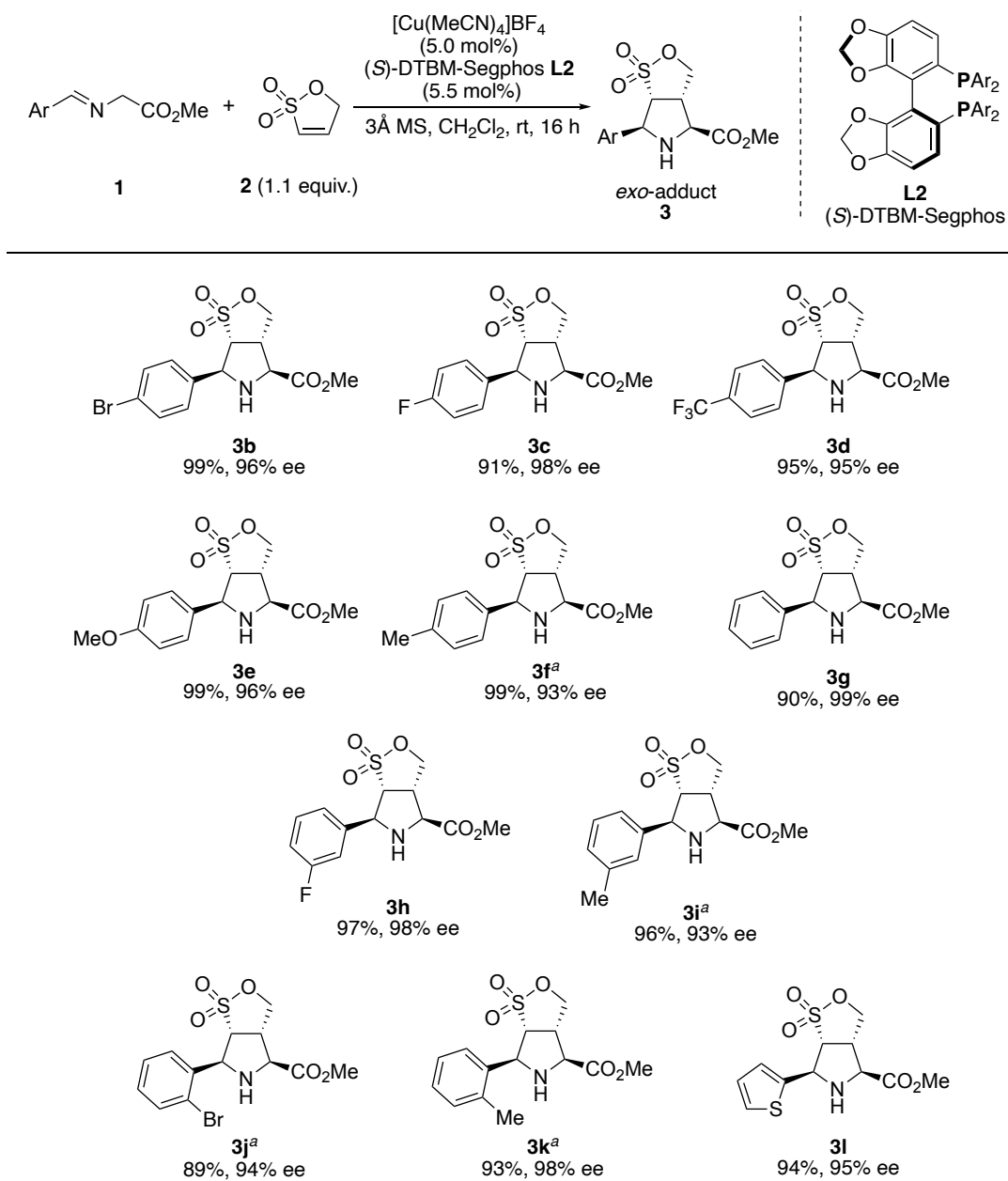
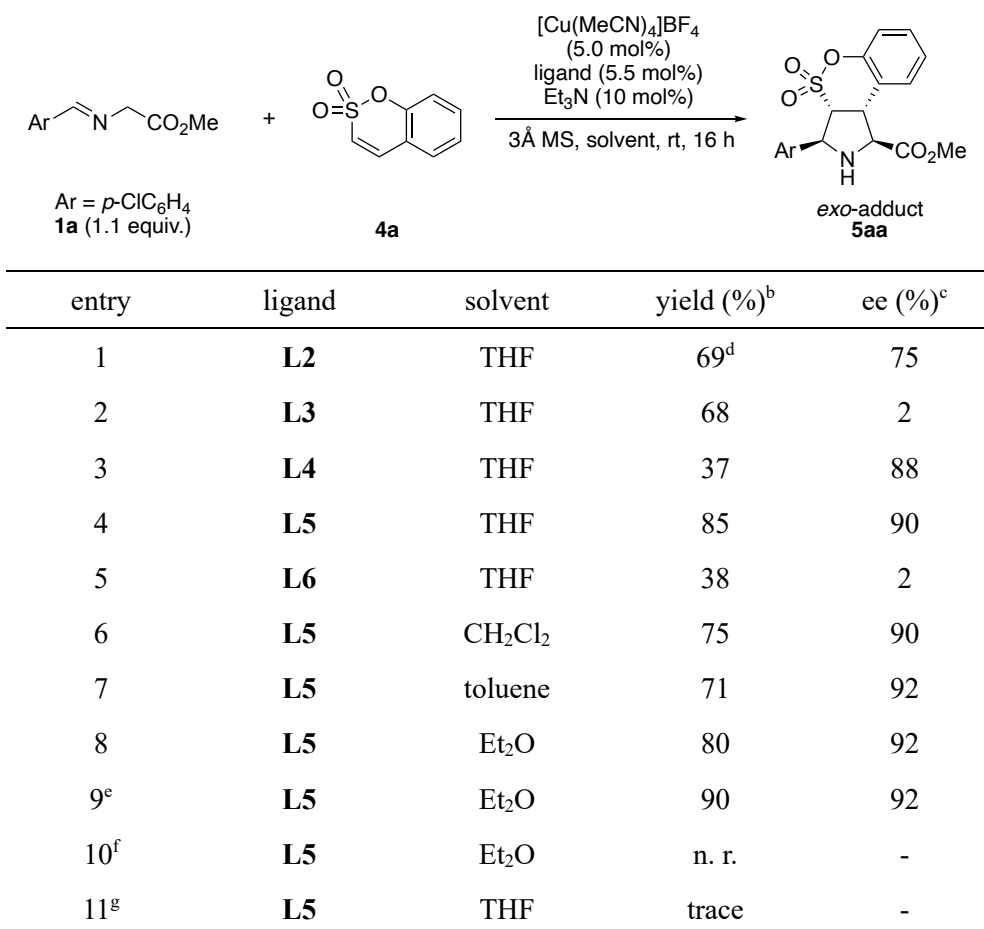


Figure 2-4. Scope of imino esters **1**.

sultone (**2**) to give the corresponding cycloadducts **3b-d**, respectively. The excellent yield and stereoselectivity were also maintained when imino esters bearing electron-donating groups, such as *p*-methoxy and methyl, and no substituents on the aryl groups were used in the reaction (**3e-g**). The reaction of imino esters bearing substituents at the *meta*- and *ortho*-positions also proceeded efficiently under the optimal conditions to give the corresponding cycloadducts **3h-3k** with high yield and enantioselectivity. In addition, a

heteroaryl substrate, such as 2-thiophene, could be applied to the reaction (**31**). Thus, the electronic and steric nature of the aryl groups of imino esters had little effect on the yield of the products, diastereo- and enantioselectivity.

The author next attempted to apply the copper complex-catalyzed system to the reaction of imino esters **1** with sulfocoumarins **4**. As an initial experiment, the reaction of *p*-chloro substituted imino ester **1a** with sulfocoumarin **4a** was carried out in the presence of copper/DTBM-Segphos complex, Et₃N (10 mol%), and 3Å MS (200 mg) in THF at room temperature for 16 h (Table 2-2, entry 1). As a result, the corresponding sulfocoumarin-fused cycloadduct was smoothly formed, however, the yield and stereoselectivity were not satisfactory compared to the reaction of 1-propene-1,3-sultone (**2**). The author screened several ligands under copper-catalyzed conditions to improve the yield and stereoselectivity (Table 2-2, entries 2-6). As shown in entry 4, using (*S*, *S*_p)-*t*Bu-FcPHOX **L5** was most effective in obtaining the product with high yield and enantioselectivity as a single diastereomer. Screening of solvents revealed that Et₂O was suitable for the asymmetric cycloaddition of imino ester **1a** with sulfocoumarins **4a** (entry 8). The reaction proceeded without the addition of a base, such as Et₃N, as well as when 1-propene-1,3-sultone (**2**) was used as the dipolarophile, and the product yield was slightly improved (entry 9). However, no reaction occurred when the reaction temperature was decreased to 0 °C in anticipation of improved enantioselectivity (entry 10). The AgOAc/*t*Bu-FcPHOX complex was unsuitable as a catalyst for the reaction, and the cycloadduct was hardly obtained (entry 11).

Table 2-2. Optimization of reaction of imino esters **1a** with sulfocoumarins **4**.^a

[a] Condition: **1a** (0.22 mmol), **4a** (0.20 mmol), $[\text{Cu}(\text{MeCN})_4]\text{BF}_4$ (5.0 mol%), ligand (5.5 mol%), Et_3N (10 mol%), 3Å MS (200 mg), solvent (1 mL), rt, 16 h. The diastereomeric ratio was determined by crude ^1H NMR. [b] Isolated yield. [c] Determined by chiral HPLC. [d] The diastereomeric ratio was 8:1. [e] Conducted without Et_3N . [f] Conducted at 0 °C. [g] AgOAc was used as the metal salt.

The substrate scope was examined under the optimal conditions catalyzed by the copper/*t*Bu-FcPHOX complex (Table 2-2, entry 9), and a variety of sulfocoumarin-fused pyrrolidines were successfully obtained with high yield, diastereo- and enantioselectivity (Figure 2-5). Imino esters bearing bromo and methoxy groups on the phenyl ring at the *para*-position smoothly reacted with sulfocoumarin **4a** to afford the corresponding cycloadducts **5ba** and **5ea** efficiently. Even when the phenyl group had no substituent, high yield and stereoselectivity resulted (**5ga**, 86% yield, 90% ee). The products **5fa**, **5ia**, and **5ka** were respectively formed while maintaining high yield and stereoselectivity

when a methyl substituent was introduced at *para*-, *meta*-, and *ortho*- positions. A 2-thienyl substituent could also be applied to the reaction without loss of yield, diastereo- and enantioselectivity. Therefore, electronic and steric properties had little effect on the asymmetric cycloaddition as in the case of using 1-propene-1,3-sultone (**2**). A wide scope

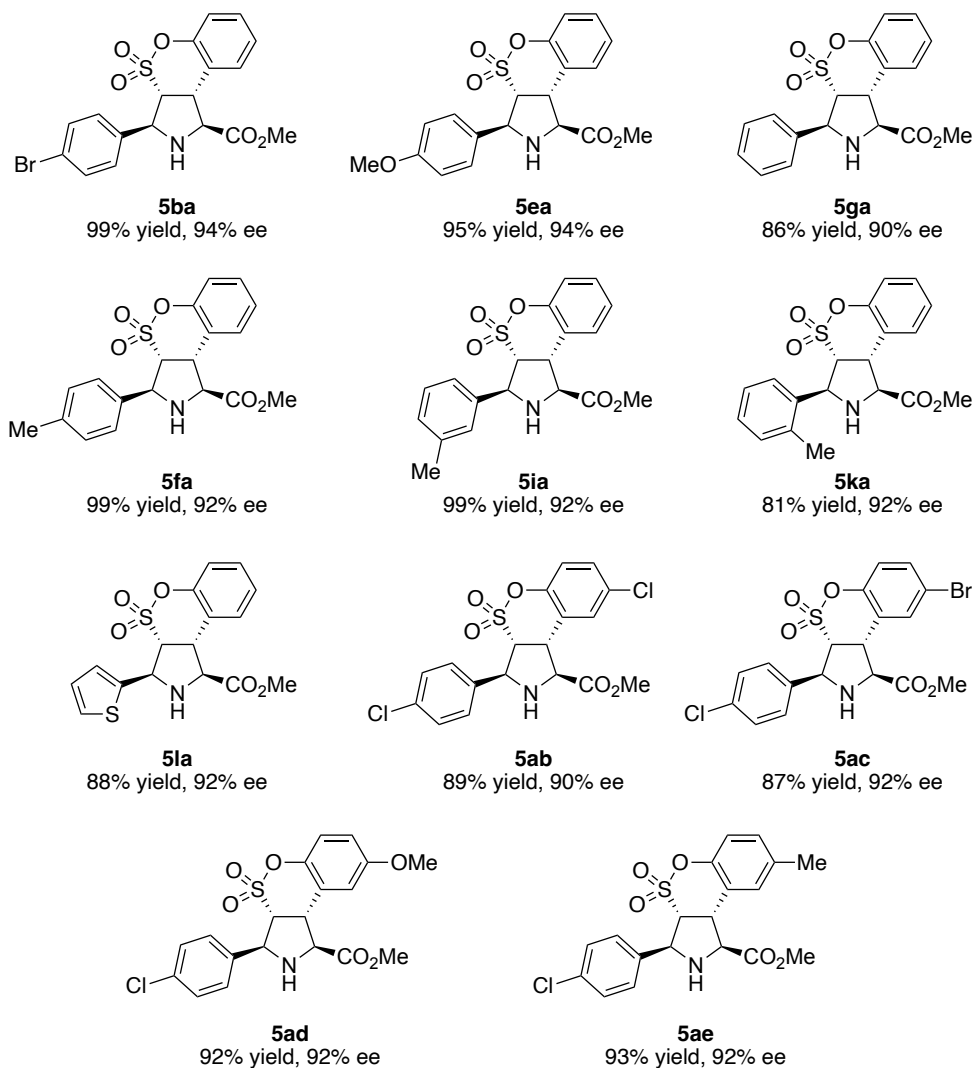
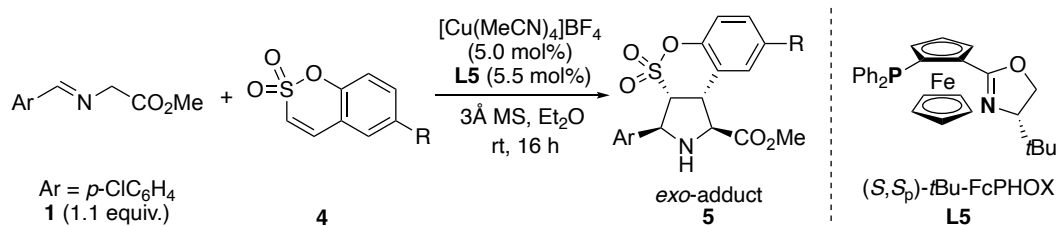


Figure 2-5. Substrate scope of imino ester **1** and sulfocoumarins **4**.

of sulfocoumarins was possible, and the enantioselective synthesis of some sulfocoumarin-fused pyrrolidines containing halogen, methoxy, and methyl substituents (**5ab-5ae**) was highly successful.

The stereochemistry of the sultone-fused pyrrolidines was determined by X-ray crystallographic analysis of the thiophene-substituted product *exo-3I* (Figure 2-6, left). The configuration could be classified as *exo* in that the sulfonyl group is *trans* to the thienyl group and the relative configuration of the methoxycarbonyl group with the thienyl group is *cis*. The *exo*-diastereoselectivity was similar to the previous reports using acyclic vinyl sulfone as the dipolarophile.¹⁰ The absolute configuration depended on the stereochemistry of the ligand, and several stereocenters were determined to be (*3aS*, *4S*, *6S*, *6aS*). The relative and absolute configurations of the sulfocoumarin-fused pyrrolidine were determined by using a single crystal of the thienyl-substituted cycloadduct *exo-5Ia* (Figure 2-6, right). This analysis revealed that the cycloaddition using sulfocoumarin as the activated olefins also proceeded with *exo*-diastereoselectivity as in the case of 1-propene-1,3-sultone (**2**).

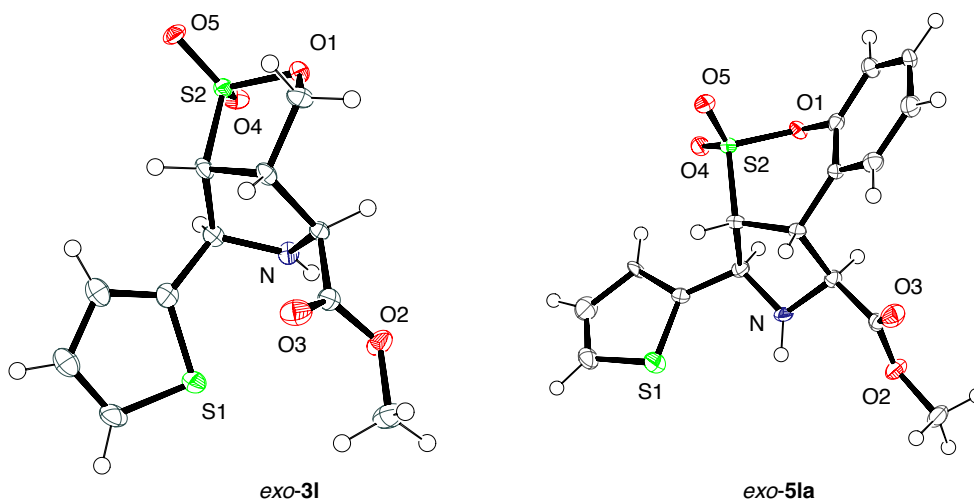


Figure 2-6. ORTEP drawing of the sultone-fused pyrrolidines.

2-3. Conclusion

The author has developed a copper complex-catalyzed asymmetric (3+2) cycloaddition of imino esters **1** with α,β -unsaturated cyclic sultones. The copper/DTBM-Segphos complex smoothly catalyzed the reaction using 1-propene-1,3-sultone (**2**) as the activated olefin to afford the *exo*-diastereomer with excellent enantioselectivity. In addition, the reaction of imino esters **1** with sulfocoumarins **4** proceeded with high yield and stereoselectivity when the copper/*t*Bu-FcPHOX complex was used as the catalyst. These reactions exhibited a wide range of substrate scopes and enabled the synthesis of sultone-fused pyrrolidines with various substituents.

2-4. Experimental Section

The following general information apply to chapter 2 to 5 unless otherwise noted.

General Information. The ^1H NMR spectra were obtained with a Varian Mercury 400 NMR spectrometer at 400 MHz. The ^{13}C NMR spectra were obtained with a Varian Mercury 400 NMR spectrometer 101 MHz. Unless otherwise noted, all NMR measurements were carried out at 25°C. The chemical shifts in the ^1H NMR spectra are recorded relative to $(\text{CH}_3)_4\text{Si}$ (δ 0.00 in CDCl_3) or the solvent peak (δ 1.94 in CD_3CN and δ 2.50 in $\text{DMSO}-d_6$), and the chemical shifts in the ^{13}C NMR are recorded relative to the solvent peak (δ 77.16 in CDCl_3 , δ 1.32 in CD_3CN , and δ 39.52 in $\text{DMSO}-d_6$). The abbreviations s, d, t, q, m, and br signify singlet, doublet, triplet, quartet, multiplet, and broad, respectively. HRMS spectra were measured by JEOL JMS-T100LC AccuTOF. Elemental analyses were performed at A Rabbit Science Japan Co., Ltd. Column chromatography was performed with Fuji Silysia, PSQ60B silica gel. Preparative TLC (PTLC) was carried out using Wakogel[®] B-5F silica gel. Visualization was accomplished with UV light (254 nm). The chiral HPLC analyses were carried out by using a chiral column equipped with a multiwavelength detector.

All reactions were performed with dry glassware under the atmosphere of nitrogen unless otherwise noted. Starting materials, imino esters **1**¹¹ and sulfocoumarins **4**¹² were prepared and identified by reported methods. Racemate products **3** and **5** were synthesized by using PPh₃ as the ligand. 1-propene-1,3-sultone (**2**) and other commercial compounds were used without further purification.

Copper-Catalyzed Asymmetric (3+2) Cycloaddition of Glycine Imino Esters 1 with 1-Propene-1,3-sultone (2). A mixture of [Cu(MeCN)₄]BF₄ (3.2 mg, 10 μmol, 5.0 mol%), (*S*)-DTBM-Segphos **L2** (13.0 mg, 11 μmol, 5.5 mol%) were dissolved in dry CH₂Cl₂ (1.0 mL) at room temperature, and 3Å MS (200 mg) was subsequently added to the mixture. After stirring at the same temperature for 30 min, *p*-chloro phenyl-substituted imino esters **1a** (43.2 mg, 0.20 mmol, 1.0 equiv.) and 1-propene-1,3-sultone (**2**) (26.4 mg, 0.22 mmol, 1.1 equiv.) were added successively. After stirring for 16 h at room temperature, the mixture was diluted with EtOAc (20-30 mL), filtered through a short Celite pad, and concentrated under reduced pressure. ¹H NMR analysis of the crude product showed that the *exo*-diastereomer is the sole product. The residue was purified by PTLC (*n*-hexane/EtOAc = 2/1) to give methyl (3*aS*, 4*S*, 6*S*, 6*aR*)-6-(4-chlorophenyl)hexahydro-[1,2]oxathiol[3,4-*c*]pyrrole-4-carboxylate 1,1-dioxide (**3a**) (66.2 mg, 0.20 mmol, 98% yield, 97% ee) as a colorless solid.

5 mmol Scale Experiment for the Copper-Catalyzed Asymmetric (3+2) Cycloaddition of Imino Esters 1a with Sultone 2. A mixture of [Cu(MeCN)₄]BF₄ (93.2 mg, 0.30 mmol, 5.9 mol%), (*S*)-DTBM-Segphos **L2** (324 mg, 0.324 mmol, 5.5 mol%) were dissolved in dry CH₂Cl₂ (20 mL), and 3Å MS (4.20 g) was subsequently added to the mixture. After stirring at room temperature for 30 min, *p*-chloro phenyl-substituted imino esters **1a** (1.06 g, 5.0 mmol, 1.0 equiv.) and sultone **2** (660 mg, 5.5 mmol, 1.1 equiv.) were added successively. After stirring for 16 h at room temperature, the mixture was diluted with EtOAc (80 mL), filtered through a short Celite pad, and concentrated under reduced pressure. ¹H NMR analysis of the crude product showed that the *exo*-diastereomer is the sole product. The residue was purified by silica gel column chromatography (*n*-

hexane/EtOAc = 2/1) to give methyl (3*aS*, 4*S*, 6*S*, 6*aR*)-6-(4-chlorophenyl)hexahydro-[1,2]oxathiol[3,4-*c*]pyrrole-4-carboxylate 1,1-dioxide (**3a**) (1.65 mg, 4.99 mmol, 99% yield, 98% ee) as a colorless solid.

Methyl (3*aS*, 4*S*, 6*S*, 6*aR*)-6-(4-chlorophenyl)hexahydro-[1,2]oxathiol[3,4-*c*]pyrrole-4-carboxylate 1,1-dioxide (3a). Yield: 98% (66.2 mg, 0.200 mmol, 98% ee); colorless solid; mp 80–82 °C; ¹H NMR (400 MHz, DMSO): δ 7.46 (s, 4H), 4.56 (dd, *J* = 1.8, 10.2 Hz, 1H), 4.46–4.40 (m, 2H), 3.96–3.89 (m, 2H), 3.89–3.64 (m, 1H), 3.70 (s, 3H); ¹³C NMR (100 MHz, CD₃CN): δ 171.2, 139.1, 132.7, 129.2, 128.7, 70.1, 64.7, 64.3, 63.6, 52.3, 47.5; HPLC (Daicel Chiralpak ID-3, *n*-hexane/2-propanol = 70/30, 1.0 mL/min, 220 nm); *t*_R = 14.9 min (minor), 16.5 min (major); [α]_D²⁵ +11.2 (*c* 0.06, MeOH); HRMS (ESI) *m/z*: [M+H]⁺ calcd for C₁₃H₁₅ClNO₅S⁺, 332.0360; found 332.0348.

Methyl (3*aS*, 4*S*, 6*S*, 6*aR*)-6-(4-bromophenyl)hexahydro-[1,2]oxathiol[3,4-*c*]pyrrole-4-carboxylate 1,1-dioxide (3b). Yield: 99% (75.1 mg, 0.200 mmol, 96% ee); colorless solid; mp 104–106 °C; ¹H NMR (400 MHz, CDCl₃): δ 7.43 (d, *J* = 8.4 Hz, 2H), 7.31 (d, *J* = 8.4 Hz, 2H), 4.56 (d, *J* = 6.7 Hz, 1H), 4.45–4.35 (m, 2H), 3.84 (d, *J* = 8.4 Hz, 1H), 3.74 (s, 3H), 3.60–3.42 (m, 2H), 2.56 (br s, 1H); ¹³C NMR (101 MHz, CDCl₃): δ 170.6, 137.8, 132.0, 128.5, 122.5, 69.0, 65.1, 64.1, 63.7, 52.8, 47.8; HPLC (Daicel Chiralpak ID-3, *n*-hexane/2-propanol = 70/30, 1.0 mL/min, 220 nm); *t*_R = 11.0 min (minor), 12.0 min (major); [α]_D²⁵ +4.68 (*c* 0.05, MeOH); HRMS (ESI) *m/z*: [M+Na]⁺ calcd for C₁₃H₁₄BrNNaO₅S⁺, 397.9674; found 397.9657.

Methyl (3*aS*, 4*S*, 6*S*, 6*aR*)-6-(4-fluorophenyl)hexahydro-[1,2]oxathiol[3,4-*c*]pyrrole-4-carboxylate 1,1-dioxide (3c). Yield: 91% (57.1 mg, 0.181 mmol, 98% ee); colorless solid; mp 133–135 °C; ¹H NMR (400 MHz, CD₃CN): δ 7.51–7.47 (m, 2H), 7.15–7.11 (m, 2H), 4.56 (d, *J* = 7.2 Hz, 1H), 4.50 (dd, *J* = 1.7, 10.2 Hz, 1H), 4.44 (dd, *J* = 5.8, 10.2 Hz, 1H), 3.90 (d, *J* = 8.2 Hz, 1H), 3.76 (dd, *J* = 7.2, 9.8 Hz, 1H), 3.73 (s, 3H), 3.69–3.65 (m, 1H), 3.08 (br s, 1H); ¹³C NMR (101 MHz, CD₃CN): δ 171.9, 163.4 (d, *J*_{C-F} = 244 Hz), 136.7 (d, *J*_{C-F} = 3.0 Hz), 130.1 (d, *J*_{C-F} = 8.4 Hz), 116.3 (d, *J* = 21.7 Hz), 70.7, 65.9, 65.3, 64.7, 52.9, 48.8; HPLC (Daicel Chiralpak ID-3, *n*-hexane/2-propanol = 70/30, 1.0

mL/min, 220 nm); t_R = 23.5 min (minor), 24.7 min (major); $[\alpha]_D^{25}$ +18.7 (c 0.05, MeOH); HRMS (ESI) m/z : $[M+H]^+$ calcd for $C_{13}H_{15}FNO_5S^+$, 316.0650; found 316.0658.

Methyl (3a*S*, 4*S*, 6*S*, 6a*R*)-6-(4-(trifluoromethyl)phenyl)hexahydro-[1,2]oxathiolol[3,4-*c*]pyrrole-4-carboxylate 1,1-dioxide (3d). Yield: 95% (69.2 mg, 0.189 mmol, 95% ee); colorless solid; mp 113–115 °C; 1H NMR (400 MHz, CD_3CN): δ 7.70 (d, J = 8.4 Hz, 2H), 7.65 (d, J = 8.4 Hz, 2H), 4.67 (d, J = 6.9 Hz, 1H), 4.52 (dd, J = 1.8, 10.2 Hz, 1H), 4.46 (dd, J = 5.8, 10.2 Hz, 1H), 3.93 (d, J = 8.2 Hz, 1H), 3.80 (dd, J = 6.9, 9.8 Hz, 1H), 3.73 (s, 3H), 3.69–3.62 (m, 1H); ^{13}C NMR (101 MHz, CD_3CN): δ 172.0, 145.6, 130.4 (q, J_{C-F} = 32.2 Hz), 128.7, 126.5 (q, J_{C-F} = 3.9 Hz), 125.4 (q, J_{C-F} = 271.1), 70.9, 65.9, 65.3, 64.7, 52.9, 48.7; HPLC (Daicel Chiralpak ID-3, *n*-hexane/2-propanol = 70/30, 1.0 mL/min, 220 nm); t_R = 7.7 min (minor), 8.5 min (major); $[\alpha]_D^{25}$ –17.8 (c 0.05, MeOH); HRMS (ESI) m/z : $[M+H]^+$ calcd for $C_{14}H_{15}F_3NO_5S^+$, 366.0623; found 366.0629.

Methyl (3a*S*, 4*S*, 6*S*, 6a*R*)-6-(4-methoxyphenyl)hexahydro-[1,2]oxathiolol[3,4-*c*]pyrrole-4-carboxylate 1,1-dioxide (3e). Yield: 99% (65.0 mg, 0.199 mmol, 96% ee); colorless solid; mp 186 °C (decomp.); 1H NMR (400 MHz, $CDCl_3$): δ 7.37 (d, J = 8.6 Hz, 2H), 6.86 (d, J = 8.6 Hz, 2H), 4.57 (d, J = 7.0 Hz, 1H), 4.46–4.43 (m, 2H), 3.85 (d, J = 8.6 Hz, 1H), 3.78 (s, 3H), 3.77 (s, 3H), 3.61 (dd, J = 7.0, 10.0 Hz, 1H), 3.54–3.46 (m, 1H), 2.49 (br s, 1H); ^{13}C NMR (101 MHz, $CDCl_3$): δ 170.8, 159.6, 130.6, 128.0, 114.2, 68.9, 65.3, 64.3, 64.2, 55.3, 52.7, 48.3; HPLC (Daicel Chiralpak ID-3, *n*-hexane/2-propanol = 70/30, 1.0 mL/min, 220 nm); t_R = 17.9 min (minor), 19.4 min (major); $[\alpha]_D^{25}$ +7.44 (c 0.05, $CHCl_3$); HRMS (ESI) m/z : $[M+Na]^+$ calcd for $C_{14}H_{17}NO_6S^+$, 350.0674; found 350.0686.

Methyl (3a*S*, 4*S*, 6*S*, 6a*R*)-6-(4-tolyl)hexahydro-[1,2]oxathiolol[3,4-*c*]pyrrole-4-carboxylate 1,1-dioxide (3f). Yield: 99% (62.3 mg, 0.200 mmol, 93% ee, 1.1 equiv. of **1f** to **2** was used); colorless solid; mp 93–95 °C; 1H NMR (400 MHz, $CDCl_3$): δ 7.35 (d, J = 7.8 Hz, 2H), 7.17 (d, J = 7.8 Hz, 2H), 4.60 (d, J = 6.3 Hz, 1H), 4.49–4.40 (m, 2H), 3.86 (d, J = 8.2 Hz, 1H), 3.77 (s, 3H), 3.68–3.60 (m, 1H), 3.55–3.45 (m, 1H), 2.32 (s, 3H); ^{13}C NMR (101 MHz, $CDCl_3$): δ 170.8, 138.3, 135.6, 129.5, 126.6, 68.9, 65.4, 64.4, 64.3, 52.7,

48.4, 21.0; HPLC (Daicel Chiralpak ID-3, *n*-hexane/2-propanol = 70/30, 1.0 mL/min, 220 nm); t_R = 11.1 min (minor), 12.5 min (major); $[\alpha]_D^{25} +9.30$ (c 0.05, CHCl₃); HRMS (ESI) m/z : $[M+H]^+$ calcd for C₁₄H₁₈NO₅S⁺, 312.0908; found 312.0906.

Methyl (3*aS*, 4*S*, 6*S*, 6*aR*)-6-phenylhexahydro-[1,2]oxathiol[3,4-*c*]pyrrole-4-carboxylate 1,1-dioxide (3*g*). Yield: 90% (53.8 mg, 0.181 mmol, 99% ee); colorless solid; mp 138–140 °C; ¹H NMR (400 MHz, CD₃CN): δ 7.48-7.32 (m, 5H), 4.56 (d, J = 7.2 Hz, 1H), 4.51 (dd, J = 1.7, 10.2 Hz, 1H), 4.44 (dd, J = 5.7, 10.2 Hz, 1H), 3.88 (d, J = 8.4 Hz, 1H), 3.78 (dd, J = 7.2, 9.9 Hz, 1H) 3.73 (s, 3H), 3.67-3.60 (m, 1H), 2.69 (br s, 1H); ¹³C NMR (101 MHz, CD₃CN): δ 172.0, 140.7, 129.7, 129.2, 128.0, 70.7, 66.1, 65.5, 65.4, 52.9, 49.1; HPLC (Daicel Chiralpak IH-3, *n*-hexane/2-propanol = 70/30, 1.0 mL/min, 220 nm); t_R = 30.0 min (minor), 36.3 min (major); $[\alpha]_D^{25} +13.9$ (c 0.04, MeOH); HRMS (ESI) m/z : $[M+H]^+$ calcd for C₁₃H₁₆NO₅S⁺, 298.0744; found 298.0731.

Methyl (3*aS*, 4*S*, 6*S*, 6*aR*)-6-(3-fluorophenyl)hexahydro-[1,2]oxathiol[3,4-*c*]pyrrole-4-carboxylate 1,1-dioxide (3*h*). Yield: 97%, (63.5 mg, 0.201 mmol, 98% ee); colorless solid; mp 128–130 °C; ¹H NMR (400 MHz, CD₃CN): δ 7.43-7.38 (m, 1H), 7.30-7.23 (m, 2H), 7.10-7.06 (m, 1H), 4.61 (d, J = 7.0 Hz, 1H), 4.51 (dd, J = 1.8, 10.2 Hz, 1H), 4.44 (dd, J = 5.7, 10.2 Hz, 1H), 3.91 (d, J = 8.3 Hz, 1H), 3.78 (dd, J = 7.0, 9.7 Hz, 1H), 3.73 (s, 3H), 3.68-3.62 (m, 1H), 3.06 (br s, 1H); ¹³C NMR (101 MHz, CD₃CN): δ 171.9, 163.8 (d, J_{C-F} = 244 Hz), 143.7 (d, J_{C-F} = 7.3 Hz), 131.6 (d, J_{C-F} = 8.4 Hz), 124.0 (d, J_{C-F} = 2.8 Hz), 115.8 (d, J_{C-F} = 21.4 Hz), 114.7 (d, J_{C-F} = 22.8 Hz), 70.8, 65.9, 65.2, 64.7 (d, J = 1.9 Hz), 53.0, 48.7; HPLC (Daicel Chiralpak ID-3, *n*-hexane/2-propanol = 70/30, 1.0 mL/min, 220 nm); t_R = 14.4 min (major), 18.5 min (minor); $[\alpha]_D^{25} +10.8$ (c 0.05, MeOH); HRMS (ESI) m/z : $[M+H]^+$ calcd for C₁₃H₁₅FNO₅S⁺, 316.0664; found 316.0655.

Methyl (3*aS*, 4*S*, 6*S*, 6*aR*)-6-(3-tolyl)hexahydro-[1,2]oxathiol[3,4-*c*]pyrrole-4-carboxylate 1,1-dioxide (3*i*). Yield: 96% (59.8 mg, 0.192 mmol, 93% ee, 1.1 equiv. of **1i** to **2** was used); colorless solid; mp 75–78 °C; ¹H NMR (400 MHz, CD₃CN): δ 7.27-7.22 (m, 3H), 7.15 (d, J = 6.9 Hz, 1H), 4.51-4.46 (m, 2H), 4.43 (dd, J = 5.7, 10.2 Hz, 1H), 3.86 (d, J = 8.3 Hz, 1H), 3.76 (dd, J = 7.1, 9.9 Hz, 1H), 3.73 (s, 3H), 3.64-3.58 (m, 1H), 2.78

(br s, 1H), 2.34 (s, 3H); ^{13}C NMR (101 MHz, CD_3CN): δ 172.1, 140.7, 139.5, 129.8, 129.6, 128.5, 125.0, 70.7, 66.1, 65.5, 65.4, 52.9, 49.2, 21.4; HPLC (Daicel Chiralpak ID-3, *n*-hexane/2-propanol = 70/30, 1.0 mL/min, 220 nm); t_{R} = 26.0 min (minor), 27.8 min (major); $[\alpha]_{\text{D}}^{25}$ +12.4 (*c* 0.04, CHCl_3); HRMS (ESI) m/z : $[\text{M}+\text{H}]^+$ calcd for $\text{C}_{14}\text{H}_{18}\text{NO}_5\text{S}^+$, 312.0906; found 312.0916.

Methyl (3*aS*, 4*S*, 6*S*, 6*aR*)-6-(2-bromophenyl)hexahydro-[1,2]oxathiolol[3,4-*c*]pyrrole-4-carboxylate 1,1-dioxide (3*j*). Yield: 89% (66.8 mg, 0.178 mmol, 94% ee, 1.1 equiv. of **1j** to **2** was used); colorless solid; mp 138–140 °C; ^1H NMR (400 MHz, CD_3CN): δ 7.79 (dd, J = 1.7, 7.8 Hz, 1H), 7.61 (dd, J = 1.1, 7.9 Hz, 1H), 7.41 (dt, J = 1.0, 7.4 Hz, 1H), 7.23 (dt, J = 1.7, 7.6 Hz, 1H), 5.13 (d, J = 3.8 Hz, 1H), 4.55 (d, J = 9.9 Hz, 1H), 4.44 (dd, J = 5.1, 10.1 Hz, 1H), 4.06 (d, J = 8.7 Hz, 1H), 3.86 (dd, J = 3.8, 8.7 Hz, 1H), 3.73 (s, 3H), 3.63-3.57 (m, 1H); ^{13}C NMR (101 MHz, CD_3CN): δ 172.9, 141.2, 133.8, 130.7, 130.3, 128.9, 123.6, 70.5, 67.0, 65.0, 63.8, 52.9, 48.5; HPLC (Daicel Chiralpak ID-3, *n*-hexane/2-propanol = 70/30, 1.0 mL/min, 220 nm); t_{R} = 15.3 min (major), 17.2 min (minor); $[\alpha]_{\text{D}}^{25}$ +36.6 (*c* 0.05, MeOH); HRMS (ESI) m/z : $[\text{M}+\text{H}]^+$ calcd for $\text{C}_{13}\text{H}_{15}\text{BrNO}_5\text{S}^+$, 375.9854; found 375.9839.

Methyl (3*aS*, 4*S*, 6*S*, 6*aR*)-6-(2-tolyl)hexahydro-[1,2]oxathiolol[3,4-*c*]pyrrole-4-carboxylate 1,1-dioxide (3*k*). Yield: 93% (57.8 mg, 0.186 mmol, 98% ee, 1.1 equiv. of **1k** to **2** was used); colorless solid; mp 113–115 °C; ^1H NMR (400 MHz, CD_3CN): δ 7.51-7.49 (m, 1H), 7.26-7.18 (m, 3H), 4.84 (d, J = 6.3 Hz, 1H), 4.55-4.42 (m, 2H), 3.94 (d, J = 8.6 Hz, 1H), 3.86 (dd, J = 6.9, 9.5 Hz, 1H), 3.72 (s, 3H), 3.70-3.65 (m, 1H) 2.43 (s, 3H); ^{13}C NMR (101 MHz, CD_3CN): δ 172.1, 138.6, 137.4, 131.5, 129.0, 128.1, 127.4, 70.7, 66.2, 65.4, 61.6, 52.9, 49.3, 19.5; HPLC (Daicel Chiralpak IH-3, *n*-hexane/2-propanol = 70/30, 1.0 mL/min, 220 nm); t_{R} = 21.0 min (minor), 34.7 min (major); $[\alpha]_{\text{D}}^{25}$ +27.8 (*c* 0.06, CHCl_3); HRMS (ESI) m/z : $[\text{M}+\text{H}]^+$ calcd for $\text{C}_{14}\text{H}_{18}\text{NO}_5\text{S}^+$, 312.0906; found 312.0918.

Methyl (3*aS*, 4*S*, 6*R*, 6*aR*)-6-(2-thienyl)hexahydro-[1,2]oxathiolol[3,4-*c*]pyrrole-4-carboxylate 1,1-dioxide (3*l*). Yield: 94% (56.9 mg, 0.188 mmol, 95% ee); colorless solid;

mp 147–149 °C; ¹H NMR (400 MHz, CD₃CN): δ 7.36 (dd, *J* = 1.2, 5.1 Hz, 1H), 7.11–7.10 (m, 1H), 7.01 (dd, *J* = 3.5, 5.1 Hz, 1H), 4.83 (t, *J* = 6.7 Hz, 1H), 4.48 (dd, *J* = 1.9, 10.2 Hz, 1H), 4.43 (dd, *J* = 5.7, 10.2 Hz, 1H), 3.88 (dd, *J* = 6.9, 7.8 Hz, 1H), 3.81 (dd, *J* = 6.9, 9.8 Hz, 1H), 3.71 (s, 3H), 3.70–3.64 (m, 1H), 3.11 (br s, 1H); ¹³C NMR (100 MHz, CD₃CN): δ 171.8, 144.5, 128.1, 126.6, 126.0, 70.8, 66.2, 65.3, 61.4, 53.0, 48.5; HPLC (Daicel Chiralpak ID-3, *n*-hexane/2-propanol = 70/30, 1.0 mL/min, 220 nm); *t*_R = 15.4 min (major), 17.9 min (major); [α]_D²⁵ –16.9 (*c* 0.03, MeOH); HRMS (DART) *m/z*: [M+H]⁺ calcd for C₁₁H₁₄NO₅S⁺, 304.0313; found 304.0308; CCDC 1993601.

Copper-Catalyzed Asymmetric (3+2) Cycloaddition of Glycine Imino Esters 1 with Sulfocoumarins 4. A mixture of [Cu(MeCN)₄]BF₄ (3.2 mg, 10 μmol, 5.0 mol %), (*S*, *S*_p)-*t*Bu-FcPHOX **L5** (5.5 mg, 11 μmol, 5.5 mol %) were dissolved in dry Et₂O (1.0 mL), and 3 Å MS (200 mg) was subsequently added to the mixture. After stirring at room temperature for 30 min, *p*-chloro phenyl substituted imino esters **1a** (46.4 mg, 0.22 mmol, 1.1 equiv.) and sulfocoumarins **4a** (36.4 mg, 0.20 mmol, 1.0 equiv.) were added successively. After stirring for 16 h at room temperature, the mixture was diluted with EtOAc (20–30 mL), filtered through a short Celite pad, and concentrated under reduced pressure. ¹H NMR analysis of the crude product showed that the *exo*-diastereomer is the sole product. The residue was purified by PTLC (*n*-hexane/EtOAc = 2/1) to give methyl (1*S*, 3*S*, 3*aR*, 9*bR*)-3-(4-chlorophenyl)-2,3,3*a*,9*b*-tetrahydro-1*H*-benzo[5,6][1,2]oxathiino[3,4-*c*]pyrrole-1-carboxylate 4,4-dioxide (**5aa**) (71.0 mg, 0.180 mmol, 90% yield, 92% ee) as a colorless solid.

Methyl (1*S*, 3*S*, 3*aR*, 9*bR*)-3-(4-chlorophenyl)-2,3,3*a*,9*b*-tetrahydro-1*H*-benzo[5,6][1,2]oxathiino[3,4-*c*]pyrrole-1-carboxylate 4,4-dioxide (5aa). Yield: 90% (71.0 mg, 0.180 mmol, 92% ee); colorless solid; mp 110–112 °C; ¹H NMR (400 MHz, CD₃CN): δ 7.56–7.52 (m, 2H), 7.43–7.37 (m, 4H), 7.33–7.28 (m, 1H), 7.18 (dd, *J* = 1.6, 8.2 Hz, 1H), 4.87 (d, *J* = 6.6 Hz, 1H), 4.31 (dd, *J* = 7.7, 9.6 Hz, 1H), 4.20 (dd, *J* = 6.6, 9.6 Hz, 1H), 3.99 (d, *J* = 7.7 Hz, 1H), 3.78 (s, 3H), 3.14 (br s, 1H); ¹³C NMR (101 MHz, CD₃CN): δ 173.1, 151.3, 140.5, 134.2, 130.8, 130.5, 130.1, 129.5, 127.6, 124.7, 120.4,

67.8, 65.9, 63.7, 53.2, 47.2; HPLC (Daicel Chiralpak ID-3, *n*-hexane/2-propanol = 70/30, 1.0 mL/min, 220 nm); t_R = 11.3 min (minor), 18.4 min (major); $[\alpha]_D^{25}$ +2.80 (c 0.06, MeOH); Anal. calcd for C₁₈H₁₆ClNO₅S: C, 54.90; H, 4.10; N, 3.56. found C, 54.91; H, 4.17; N, 3.62%.

Methyl (1S, 3S, 3aR, 9bR)-3-(4-bromophenyl)-2,3,3a,9b-tetrahydro-1H-benzo[5,6][1,2]oxathiino[3,4-c]pyrrole-1-carboxylate 4,4-dioxide (5ba). Yield: 99% (87.0 mg, 0.199 mmol, 94% ee); colorless solid; mp 92–94 °C; ¹H NMR (400 MHz, CD₃CN): δ 7.58–7.52 (m, 2H), 7.50–7.46 (m, 2H), 7.42–7.37 (m, 2H), 7.30 (ddd, J = 1.3, 7.6, 7.6 Hz, 1H), 7.19–7.15 (m, 1H), 4.86 (d, J = 6.4 Hz, 1H), 4.31 (dd, J = 7.6, 9.6 Hz, 1H), 4.20 (dd, J = 6.4, 9.6 Hz, 1H), 3.99 (d, J = 7.6 Hz, 1H), 3.78 (s, 3H), 3.14 (br s, 1H); ¹³C NMR (101 MHz, CD₃CN): δ 173.1, 151.3, 141.0, 132.5, 130.8, 130.5, 130.4, 127.6, 124.6, 122.4, 120.4, 67.8, 65.8, 63.7, 53.2, 47.2; HPLC (Daicel Chiralpak ID-3, *n*-hexane/2-propanol = 70/30, 1.0 mL/min, 220 nm); t_R = 11.6 min (minor), 19.9 min (major); $[\alpha]_D^{25}$ +2.18 (c 0.05, MeOH); Anal. calcd for C₁₈H₁₆BrNO₅S: C, 49.33; H, 3.68; N, 3.20. found C, 49.17; H, 3.67; N, 3.15%.

Methyl (1S, 3S, 3aR, 9bR)-3-phenyl-2,3,3a,9b-tetrahydro-1H-benzo[5,6][1,2]oxathiino[3,4-c]pyrrole-1-carboxylate 4,4-dioxide (5ga). Yield: 86% (61.6 mg, 0.171 mmol, 90% ee); colorless solid; mp 99–101 °C; ¹H NMR (400 MHz, CD₃CN): δ 7.54 (d, J = 7.3 Hz, 2H), 7.46–7.28 (m, 6H), 7.18 (d, J = 8.0 Hz, 1H), 4.86 (d, J = 6.6 Hz, 1H), 4.32 (dd, J = 7.8, 9.7 Hz, 1H), 4.23 (dd, J = 6.6, 9.7 Hz, 1H), 3.98 (d, J = 7.8 Hz, 1H), 3.79 (s, 3H), 2.94 (br s, 1H); ¹³C NMR (101 MHz, CD₃CN): δ 173.1, 151.4, 141.4, 130.8, 130.4, 129.6, 129.2, 128.4, 127.6, 124.9, 120.4, 67.9, 66.0, 64.6, 53.2, 47.5; HPLC (Daicel Chiralpak ID-3, *n*-hexane/2-propanol = 70/30, 1.0 mL/min, 220 nm); t_R = 14.0 min (minor), 20.6 min (major); $[\alpha]_D^{25}$ +8.31 (c 0.04, MeOH); HRMS (ESI) m/z : $[M+H]^+$ calcd for C₁₈H₁₈NO₅S⁺, 360.0900; found 360.0892.

Methyl (1S, 3S, 3aR, 9bR)-3-(4-tolyl)-2,3,3a,9b-tetrahydro-1H-benzo[5,6][1,2]oxathiino[3,4-c]pyrrole-1-carboxylate 4,4-dioxide (5fa). Yield: 99% (74.8 mg, 0.200 mmol, 92% ee); colorless solid; mp 88–92 °C; ¹H NMR (400 MHz,

CD₃CN): δ 7.44–7.37 (m, 4H), 7.30 (ddd, $J = 1.4, 7.6, 7.6$ Hz, 1H), 7.22 (d, $J = 7.8$ Hz, 2H), 7.19–7.16 (m, 1H), 4.80 (d, $J = 6.8$ Hz, 1H), 4.30 (dd, $J = 7.8, 9.8$ Hz, 1H), 4.20 (dd, $J = 6.8, 9.8$ Hz, 1H), 3.95 (d, $J = 7.8$ Hz, 1H), 3.79 (s, 3H), 2.99 (br s, 1H), 2.34 (s, 3H); ¹³C NMR (101 MHz, CD₃CN): δ 173.1, 151.4, 139.0, 138.2, 130.8, 130.4, 130.2, 128.3, 127.6, 125.0, 120.4, 68.0, 66.0, 64.5, 53.2, 47.6, 21.1; HPLC (Daicel Chiralpak ID-3, *n*-hexane/2-propanol = 70/30, 1.0 mL/min, 220 nm); $t_R = 12.4$ min (minor), 20.7 min (major); $[\alpha]_D^{25} +3.29$ (c 0.05, MeOH); HRMS (ESI) m/z : $[M+Na]^+$ calcd for C₁₉H₁₉NNaO₅S⁺, 396.0876; found 396.0871.

Methyl (1*S*, 3*S*, 3*aR*, 9*bR*)-3-(3-tolyl)-2,3,3*a*,9*b*-tetrahydro-1*H*-benzo[5,6][1,2]oxathiino[3,4-*c*]pyrrole-1-carboxylate 4,4-dioxide (5*ia*). Yield: 99% (74.0 mg, 0.198 mmol, 92% ee); colorless solid; mp 119–120 °C; ¹H NMR (400 MHz, CD₃CN): δ 7.41–7.34 (m, 3H), 7.34–7.26 (m, 3H), 7.20–7.14 (m, 2H), 4.80 (d, $J = 6.6$ Hz, 1H), 4.30 (dd, $J = 7.8, 9.8$ Hz, 1H), 4.22 (dd, $J = 6.6, 9.8$ Hz, 1H), 3.96 (d, $J = 7.8$ Hz, 1H), 3.79 (s, 3H), 3.02 (br s, 1H), 2.36 (s, 3H); ¹³C NMR (101 MHz, CD₃CN): δ 173.1, 151.4, 141.2, 139.3, 130.8, 130.4, 129.8, 129.5, 128.9, 127.6, 125.4, 124.9, 120.4, 68.0, 66.0, 64.7, 53.2, 47.6, 21.5; HPLC (Daicel Chiralpak ID-3, *n*-hexane/2-propanol = 70/30, 1.0 mL/min, 220 nm); $t_R = 12.2$ min (minor), 18.1 min (major); $[\alpha]_D^{25} +14.9$ (c 0.04, MeOH); HRMS (ESI) m/z : $[M+Na]^+$ calcd for C₁₉H₁₉NNaO₅S⁺, 396.0876; found 396.0866.

Methyl (1*S*, 3*S*, 3*aR*, 9*bR*)-3-(2-tolyl)-2,3,3*a*,9*b*-tetrahydro-1*H*-benzo[5,6][1,2]oxathiino[3,4-*c*]pyrrole-1-carboxylate 4,4-dioxide (5*ka*). Yield: 81% (60.7 mg, 0.163 mmol, 92% ee); colorless solid; mp 56–59 °C; ¹H NMR (400 MHz, CD₃CN): δ 7.68–7.64 (m, 1H), 7.42–7.36 (m, 2H), 7.32–7.15 (m, 5H), 5.14 (d, $J = 5.8$ Hz, 1H), 4.32 (dd, $J = 8.9, 9.2$ Hz, 1H), 4.22 (dd, $J = 5.8, 9.2$ Hz, 1H), 4.09–4.02 (m, 1H), 3.81 (s, 3H), 3.00 (br s, 1H), 2.44 (s, 3H); ¹³C NMR (101 MHz, CD₃CN): δ 173.5, 151.3, 139.6, 137.2, 131.5, 130.8, 130.4, 128.9, 127.8, 127.5, 127.3, 124.6, 120.3, 67.8, 65.6, 60.5, 53.2, 47.1, 19.5; HPLC (Daicel Chiralpak ID-3, *n*-hexane/2-propanol = 70/30, 1.0 mL/min, 220 nm); $t_R = 15.2$ min (minor), 17.0 min (major); $[\alpha]_D^{25} +68.6$ (c 0.05, MeOH);

HRMS (ESI) m/z : $[M+H]^+$ calcd for $C_{19}H_{20}NO_5S^+$, 374.1057; found 374.1056.

Methyl (1S, 3R, 3aR, 9bR)-3-(2-thienyl)-2,3,3a,9b-tetrahydro-1H-benzo[5,6][1,2]oxathiino[3,4-c]pyrrole-1-carboxylate 4,4-dioxide (5la). Yield: 88% (64.2 mg, 0.176 mmol, 92% ee); colorless solid; mp 144–146 °C; 1H NMR (400 MHz, CD_3CN): δ 7.42–7.37 (m, 2H), 7.36 (dd, J = 1.3, 5.1 Hz, 1H), 7.31 (ddd, J = 1.3, 7.6, 7.6 Hz, 1H), 7.20–7.16 (m, 2H), 7.02 (dd, J = 3.6, 5.1 Hz, 1H), 5.17 (d, J = 6.2 Hz, 1H), 4.35 (dd, J = 7.3, 9.6 Hz, 1H), 4.28 (dd, J = 6.2, 9.6 Hz, 1H), 3.97 (d, J = 7.3 Hz, 1H), 3.76 (s, 3H), 3.33 (br s, 1H); ^{13}C NMR (101 MHz, CD_3CN): δ 172.8, 151.4, 146.0, 130.8, 130.5, 128.2, 127.7, 126.5, 126.2, 124.8, 120.4, 67.8, 66.5, 60.4, 53.2, 47.2; HPLC (Daicel Chiralpak ID-3, *n*-hexane/2-propanol = 70/30, 1.0 mL/min, 220 nm); t_R = 17.9 min (minor), 30.6 min (major); $[\alpha]_D^{25}$ –29.8 (c 0.03, MeOH); Anal. calcd for $C_{16}H_{15}NO_5S_2$: C, 52.59; H, 4.14; N, 3.83. found C, 52.79; H, 3.78; N, 3.75%; CCDC 1993602.

Methyl (1S, 3S, 3aR, 9bR)-8-chloro-3-(4-chlorophenyl)-2,3,3a,9b-tetrahydro-1H-benzo[5,6][1,2]oxathiino[3,4-c]pyrrole-1-carboxylate 4,4-dioxide (5ab). Yield: 89% (76.0 mg, 0.178 mmol, 90% ee); colorless solid; mp 128–130 °C; 1H NMR (400 MHz, DMSO- d_6): δ 7.57–7.43 (m, 6H), 7.37–7.32 (m, 1H), 4.73 (dd, J = 7.3, 7.3 Hz, 1H), 4.56 (dd, J = 7.3, 9.6 Hz, 1H), 4.31 (dd, J = 7.3, 9.6 Hz, 1H), 4.00 (dd, J = 7.3, 7.3 Hz, 1H), 3.95 (dd, J = 7.3, 7.3 Hz, 1H), 3.76 (s, 3H); ^{13}C NMR (101 MHz, DMSO- d_6): δ 171.8, 148.9, 139.6, 132.5, 130.4, 129.49, 129.45, 129.3, 128.3, 126.1, 121.4, 66.5, 63.8, 62.3, 52.4, 45.6; HPLC (Daicel Chiralpak ID-3, *n*-hexane/2-propanol = 70/30, 1.0 mL/min, 220 nm); t_R = 8.96 min (minor), 21.5 min (major); $[\alpha]_D^{25}$ +5.00 (c 0.05, MeOH); Anal. calcd for $C_{18}H_{15}Cl_2NO_5S$: C, 50.48; H, 3.53; N, 3.27. found C, 50.59; H, 3.62; N, 3.18%.

Methyl (1S, 3S, 3aR, 9bR)-8-bromo-3-(4-chlorophenyl)-2,3,3a,9b-tetrahydro-1H-benzo[5,6][1,2]oxathiino[3,4-c]pyrrole-1-carboxylate 4,4-dioxide (5ac). Yield: 87% (81.8 mg, 0.173 mmol, 92% ee); colorless solid; mp 110–114 °C; 1H NMR (400 MHz, CD_3CN): δ 7.61 (d, J = 2.3 Hz, 1H), 7.55–7.49 (m, 3H), 7.42–7.36 (m, 2H), 7.10 (d, J = 8.7 Hz, 1H), 4.83 (dd, J = 6.8, 7.2 Hz, 1H), 4.29 (dd, J = 7.4, 9.6 Hz, 1H), 4.21 (dd, J = 6.8, 9.6 Hz, 1H), 3.99 (dd, J = 7.4, 7.4 Hz, 1H), 3.78 (s, 3H), 3.14 (dd, J = 7.2, 7.4 Hz,

1H); ¹³C NMR (101 MHz, CD₃CN): δ 172.8, 150.6, 140.1, 134.3, 133.7, 133.3, 130.1, 129.5, 127.2, 122.4, 119.7, 67.6, 65.5, 63.8, 53.2, 46.7; HPLC (Daicel Chiralpak ID-3, *n*-hexane/2-propanol = 70/30, 1.0 mL/min, 220 nm); *t*_R = 9.73 min (minor), 26.3 min (major); [α]_D²⁵ -4.11 (c 0.04, MeOH); Anal. calcd for C₁₈H₁₅BrClNO₅S: C, 45.73; H, 3.20; N, 2.96. found C, 45.94; H, 3.23; N, 3.01%.

Methyl (1*S*, 3*S*, 3*aR*, 9*bR*)-3-(4-chlorophenyl)-8-methoxy-2,3,3*a*,9*b*-tetrahydro-1*H*-benzo[5,6][1,2]oxathiino[3,4-*c*]pyrrole-1-carboxylate 4,4-dioxide (5*ad*). Yield: 92% (78.3 mg, 0.185 mmol, 92% ee); colorless solid; mp 154–158 °C; ¹H NMR (400 MHz, DMSO-*d*₆): δ 7.5 (d, *J* = 8.5 Hz, 2H), 7.5 (d, *J* = 8.5 Hz, 2H), 7.21 (d, *J* = 9.0 Hz, 1H), 6.97 (dd, *J* = 3.0, 9.0 Hz, 1H), 6.89 (d, *J* = 3.0 Hz, 1H), 4.73 (dd, *J* = 7.1, 7.5 Hz, 1H), 4.47 (dd, *J* = 7.1, 9.6 Hz, 1H), 4.25 (dd, *J* = 7.5, 9.6 Hz, 1H), 3.98 (dd, *J* = 7.5, 7.5 Hz, 1H), 3.92 (dd, *J* = 7.5, 7.5 Hz, 1H), 3.76 (s, 3H), 3.75 (s, 3H); ¹³C NMR (101 MHz, DMSO-*d*₆): δ 172.0, 157.0, 143.7, 139.9, 132.4, 129.4, 128.3, 124.7, 120.4, 114.6, 114.1, 66.6, 63.9, 62.2, 55.6, 52.4, 46.0; HPLC (Daicel Chiralpak ID-3, *n*-hexane/2-propanol = 70/30, 1.0 mL/min, 220 nm); *t*_R = 14.9 min (minor), 34.4 min (major); [α]_D²⁵ +7.61 (c 0.04, MeOH); HRMS (ESI) *m/z*: [M+Na]⁺ calcd for C₁₉H₁₈ClNNaO₆S⁺, 446.0436; found 446.0442.

Methyl (1*S*, 3*S*, 3*aR*, 9*bR*)-3-(4-chlorophenyl)-8-methyl-2,3,3*a*,9*b*-tetrahydro-1*H*-benzo[5,6][1,2]oxathiino[3,4-*c*]pyrrole-1-carboxylate 4,4-dioxide (5*ae*). Yield: 93% (75.8 mg, 0.186 mmol, 92% ee); colorless solid; mp 135–137 °C; ¹H NMR (400 MHz, DMSO-*d*₆): δ 7.55 (d, *J* = 8.5 Hz, 2H), 7.45 (d, *J* = 8.5 Hz, 2H), 7.23–7.18 (m, 1H), 7.16–7.11 (m, 2H), 4.75 (dd, *J* = 7.0, 7.0 Hz, 1H), 4.50 (dd, *J* = 7.0, 9.5 Hz, 1H), 4.24 (dd, *J* = 7.4, 9.5 Hz, 1H), 4.00 (m, 1H), 3.91 (dd, *J* = 7.4, 7.4 Hz, 1H), 3.77 (s, 3H), 2.30 (s, 3H); ¹³C NMR (101 MHz, DMSO-*d*₆): δ 172.2, 148.0, 140.0, 136.0, 132.4, 129.8, 129.7, 129.4, 128.3, 123.2, 119.2, 66.6, 64.1, 62.1, 52.4, 45.9, 20.5; HPLC (Daicel Chiralpak ID-3, *n*-hexane/2-propanol = 70/30, 1.0 mL/min, 220 nm); *t*_R = 10.9 min (minor), 34.1 min (major); [α]_D²⁵ +7.06 (c 0.05, MeOH); Anal. calcd for C₁₉H₁₈ClNO₅S: C, 55.95; H, 4.45; N, 3.43. found C, 56.08; H, 4.43; N, 3.40%.

X-ray Crystallographic Analysis. The crystallographic data of *exo-31* and *exo-51a* were summarized in Table S2-1. Single crystals of *exo-31* and *exo-51a* were prepared from CH₂Cl₂/MeCN co-solvent by vapor diffusion technique using *n*-hexane as the anti-solvent. A suitable single crystal was selected and mounted on the glass fiber and transferred to the goniometer of a Rigaku VariMax Saturn CCD diffractometer with graphite-monochromated Mo K α radiation ($\lambda = 71.073$ pm). Yadokari-XG 2009 program was used as a graphical interface. The structure was solved and refined by SIR-2004 by SHELX-97 programs. The refinement was performed anisotropically for all non-hydrogen atoms. Hydrogen atoms were placed using AFIX instructions. The crystallographic data of *exo-31* and *exo-51a* were summarized in Table S2-1.

Table S2-1. Crystal data and structure refinements for *exo-3l* and *exo-5la*.

Compound	<i>exo-3l</i>	<i>exo-5la</i>
CCDC	1993601	1993602
Empirical formula	C ₁₁ H ₁₃ NO ₅ S ₂	C ₁₆ H ₁₅ NO ₅ S ₂
Formula weight	303.35	365.42
Crystal system	orthorhombic	orthorhombic
Space group	P 2ac 2ab	P 2ac 2ab
a, Å	6.043(2)	8.5122(15)
b, Å	7.662(2)	9.4305(15)
c, Å	27.127(8)	20.019(4)
α, °	90	90
β, °	90	90
γ, °	90	90
Volume, Å ³	1256.0(7)	1607.0(5)
Z	4	4
Temperature, K	93	93
2θ range for data collection, °	6.908 to 54.954	6.284 to 54.932
σ _{calcd} , g cm ⁻³	1.604	1.510
μ, mm ⁻¹	0.440	0.358
F(000)	632	760
Crystal size, mm ³	0.240 × 0.200 × 0.050	0.250 × 0.160 × 0.070
Crystal color, habit	colorless, prism	colorless, block
Radiation	MoKα	MoKα
Reflections collected	8075	13161
Independent	2619	3665
Index ranges	-7 ≤ h ≤ 7, -9 ≤ k ≤ 9, -31 ≤ l ≤ 35	-11 ≤ h ≤ 11, -12 ≤ k ≤ 10, -24 ≤ l ≤ 25
Flack	-0.06(6)	-0.01(4)
Absolute configuration	ad	ad
Data/restraints/parameters	2619/0/172	3665/0/217
Final R indexes [<i>I</i> > 2σ(<i>I</i>)]	R1 = 0.0574, wR2 = 0.1470	R1 = 0.0461, wR2 = 0.1136
Final R indexes [all data]	R1 = 0.0675, wR2 = 0.1577	R1 = 0.0535, wR2 = 0.1241
Goodness-of-fit on <i>F</i> ²	1.050	1.047
Largest peak/deepest hole, e Å ⁻³	0.479/-0.692	0.464/-0.611

2–5. References

1. Selected review: (a) Adrio, J. Carretero, J. C. *Chem. Commun.* **2014**, *50*, 12434–12446. (b) Hashimoto, T.; Maruoka, K. *Chem. Rev.* **2015**, *115*, 5366–5412. (c) Döndas, H. A.; de Gracia Retamosa, M.; Sansano, J. M. *Synthesis*, **2017**, *49*, 2819–2851.
2. Selected review: (a) Morphy, R.; Rankovic, Z. *J. Med. Chem.* **2005**, *48*, 6523–6543. (b) Meunier, B. *Acc. Chem. Res.* **2008**, *41*, 69–77. (c) Raj, R.; Land, K. M.; Kumar, V. *RSC Adv.* **2015**, *5*, 82676–82698.
3. Selected examples of 1,3-DC for molecular hybridization: (a) Sigh, D.; Devi, N.; Kumar, V.; Malakar, C. C.; Mehra, S.; Rawal, R. K.; Kaith, B. S.; Singh, V. *RSC Adv.* **2016**, *6*, 88066–88076. (b) Liu, X.-L.; Feng, T.-T.; Jiang, W.-D.; Yang, C.; Tian, M.-Y.; Jiang, Y.; Lin, B.; Zhao, Z.; Zhou, Y. *Tetrahedron Lett.* **2016**, *57*, 4411–4416. (c) Lin, B.; Zhang, W.-H.; Wang, D.-D.; Gong, Y.; Wei, Q.-D.; Liu, X.-L.; Feng, T.-T.; Zhou, Y.; Yuan, W.-C. *Tetrahedron* **2017**, *73*, 5176–5188.
4. (a) Harada, M.; Kato, S.; Haraguchi, R.; Fukuzawa, S.-i. *Chem. Eur. J.* **2018**, *24*, 2580–2583. (b) Kato, S.; Suzuki, Y.; Suzuki, K.; Haraguchi, R.; Fukuzawa, S.-i. *J. Org. Chem.* **2018**, *83*, 13965–13972.
5. Selected review: Mondal, S. *Chem. Rev.* **2012**, *112*, 5339–5355.
6. (a) de Castro, S.; Peromingo, M. T.; Naesens, L.; Andrei, G.; Snoeck, R.; Balzarini, J.; Velázquez, S. J.; Camarasa, M.-J. *J. Med. Chem.* **2008**, *51*, 5823–5832. (b) Castro, S. D.; García-Aparicio, C.; Andrei, G.; Snoeck, R.; Balzarini, J.; Camarasa, M.-J.; Velázquez, S. *J. Med. Chem.* **2009**, *52*, 1582–1591. (c) de Castro, S.; Familiar, O.; Andrei, G.; Snoeck, R.; Balzarini, J.; Camarasa, M.-J.; Velázquez, S. *ChemMedChem.* **2011**, *6*, 686–697. (d) Xu, H.-W.; Zhao, L.-J.; Liu, H.-F.; Zhao, D.; Luo, J.; Xie, X.-P.; Liu, W.-S.; Zheng, J.-X.; Dai, G.-F.; Liu, H.-M.; Liu, L.-H.; Liang, Y.-B. *Bioorg. Med. Chem. Lett.* **2014**, *24*, 2388–2391.
7. Lee, A. W.; Chan, W. H.; Jiang, L. S.; Poon, K. W. *Chem. Commun.* **1997**, 611–612.
8. (a) Zhang, H.; Chan, W. H.; Lee, A. W. M.; Wong, W. Y. *Tetrahedron Lett.* **2003**, *44*, 395–397. (b) Tian, L.; Xu, G.-Y.; Ye, Y.; Liu, L.-Z. *J. Heterocycl. Chem.* **2003**, *40*,

- 1071–1074. (c) Zhang, H.-K.; Chan, W.-H.; Lee, A. W. M.; Wong, W.-Y.; Xia, P.-F. *Tetrahedron: Asymmetry* **2005**, *16*, 761–771. (d) Zhang, H.-K.; Chan, W.-H.; Lee, A. W. M.; Wong, W.-Y. *J. Heterocycl. Chem.* **2008**, *45*, 957–962. (e) Yoshimura, A.; Nguyen, K. C.; Rohde, G. T.; Postnikov, P. S.; Yusubov, M. S.; Zhdankin, V. V. *J. Org. Chem.* **2017**, *82*, 11742–11751.
9. (a) Tars, K.; Vullo, D.; Kazaks, A.; Leitans, J.; Lend, A.; Grandane, A.; Zalubovskis, R.; Scozzafava, A.; Supuran, C. *J. Med. Chem.* **2013**, *56*, 293–300. (b) Tanc, M.; Carta, F.; Bozdog, M.; Scozzafava, A.; Supuran, C. T. *Bioorg. Med. Chem.* **2013**, *21*, 4502–4510. (c) Tanc, M.; Carta, F.; Scozzafava, A.; Supuran, C. T. *Org. Biomol. Chem.* **2015**, *13*, 77–80.
10. (a) Llamas, T.; Arrayás, R. G.; Carretero, J. C. *Org. Lett.* **2006**, *8*, 1795–1798. (b) Llamas, T.; Arrayás, R. G.; Carretero, J. C. *Synthesis* **2007**, 950–956. (c) Liang, G.; Tong, M.-C.; Wang, C.-J. *Adv. Synth. Catal.* **2009**, *351*, 3101–3106.
11. (a) Grigg, R.; Gunaratne, H. Q. N.; Kemp, J. *J. Chem. Soc., Perkin Trans. 1*, **1984**, 41–46. (b) Longmire, J. M.; Wang, B.; Zhang, X. *J. Am. Chem. Soc.* **2002**, *124*, 13400–13401. (c) Grigg, R.; Cooper, D. M.; Holloway, S.; McDonald, S.; Millington, E.; Sarker, M. A. B. *Tetrahedron* **2005**, *61*, 8677–8685.
12. (a) Grandane, A.; Belyakov, S.; Trapencieris, P.; Zalubovskis, R. *Tetrahedron*, **2012**, *68*, 5541–5546. (b) Nocentini, A.; Carta, F.; Tanc, M.; Selleri, S.; Supran, C. T.; Bazzicalupi, C.; Gratteri, P. *Chem. Eur. J.* **2018**, *24*, 7840–7844.

Chapter 3

Silver-Catalyzed Asymmetric (3+2) Cycloaddition of Imino Esters with Ylidene-2,3-dioxopyrrolidines

3-1. Introduction

Spirocyclic pyrrolidines are among the most important units that are present in numerous naturally occurring alkaloids, drugs, and pharmaceutically active compounds (Figure 3-1).¹ Therefore, the structurally and stereochemically diverse preparation of these molecules would have the potential to aid in drug discovery.

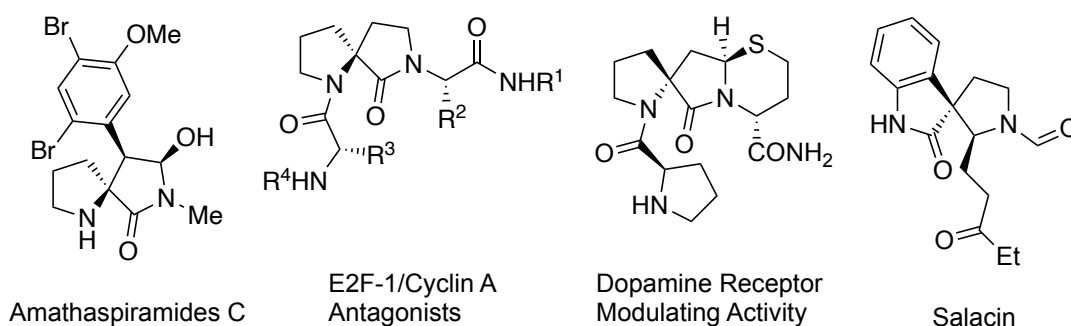


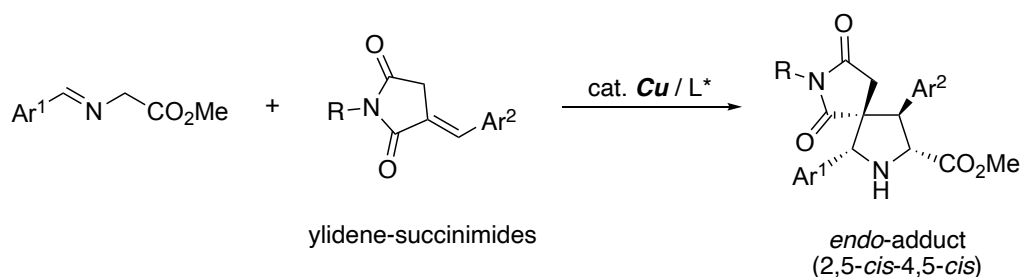
Figure 3-1. Examples of biologically active compounds containing spiropyrrolidines.

This has prompted many research groups to develop efficient synthetic methodologies to construct the scaffold by using intramolecular cyclization² and intermolecular 1,3-DC.³ Among them, the catalytic asymmetric 1,3-DC of azomethine ylides with a variety of electron-deficient alkene dipolarophiles has been a robust synthetic tool for the construction of structurally diverse pyrrolidine derivatives with access to spirocyclic pyrrolidines with chiral quaternary centers.⁴ However, this method is not suitable for the stereodivergent preparation of spiropyrrolidines; 2,5-*cis* configurations such as *endo*- and *exo*-adducts are usually formed, and 2,5-*trans* configurations such as *endo'*- and *exo'*-adducts are difficult to obtain.⁵ Indeed, a variety of exocyclic alkenes such as 2-oxoindolin-3-ylidenes,⁶ 2-alkylidene-cycloketones,⁷ and α -methylene- γ -butyrolactones⁸ have been proposed as dipolarophiles to construct chiral spirocyclic pyrrolidine skeletons for azomethine ylides, but most of them afforded 2,5-*cis* cycloadducts. For example, Deng and co-workers revealed that the chiral copper-catalyzed (3+2) cycloaddition of azomethine ylides with α -alkylidene succinimides⁹ and its sulfur analog thiazolidinediones provided spirocyclic pyrrolidines as *endo*-

diastereomers (Figure 3-2a). On the other hand, the *exo'*-selective construction of spiropyrrolidines is limited to a single example developed by Arai and co-workers, which is a nickel complex-catalyzed reaction of imino esters with 2-oxoindolin-3-ylidenes.^{6c}

In this study, the author focused on 4-ylidene-2,3-dioxopyrrolidines, which are good Michael acceptors in the organocatalyzed asymmetric hetero-DA reactions and Michael addition/cyclization reactions.¹⁰ However, examples for the spirocyclic construction are limited; the synthesis of spirooxyindoles by the (3+2) cycloaddition reaction of 4-ylidene-2,3-dioxopyrrolidines with *N*-2,2,2-trifluoroethylisatin ketimines is the only example.¹¹ Thus, the author envisioned that asymmetric (3+2) cycloaddition of imino esters with 4-ylidene-2,3-dioxopyrrolidines would provide a new method for the construction of spiropyrrolidines (Figure 3-2b). The reaction was catalyzed by a chiral silver complex and proceeded with an unusual *exo'*-diastereoselectivity. In addition, a chiral ligand TCF developed by our groups¹² was the most efficient for enantioselective preparation of the cycloadducts.

(a) Previous report: *endo*-selective reaction using ylidene-succinimides



(b) This work: *exo'*-selective reaction using ylidene-2,3-dioxopyrrolidines

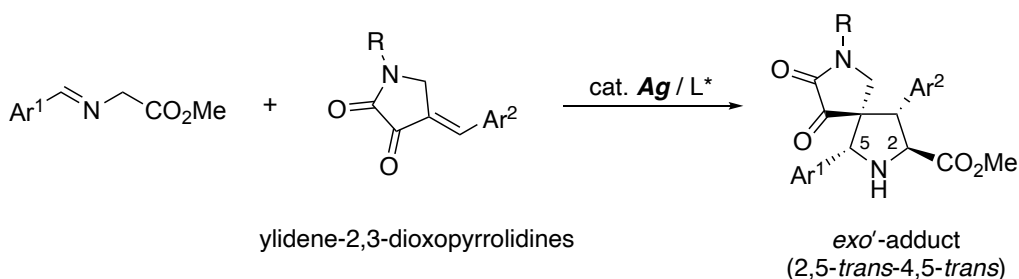
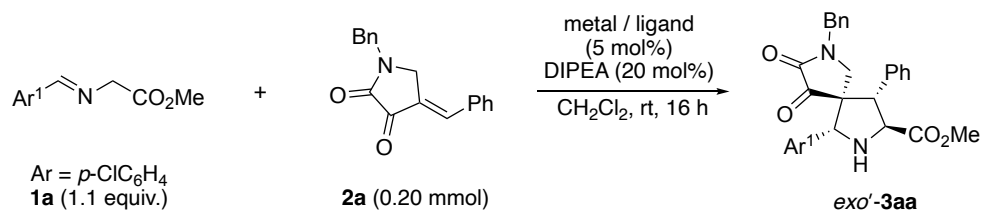


Figure 3-2. (a) Previous report on construction of spiropyrrolidines and (b) this work.

3-2. Results and Discussion

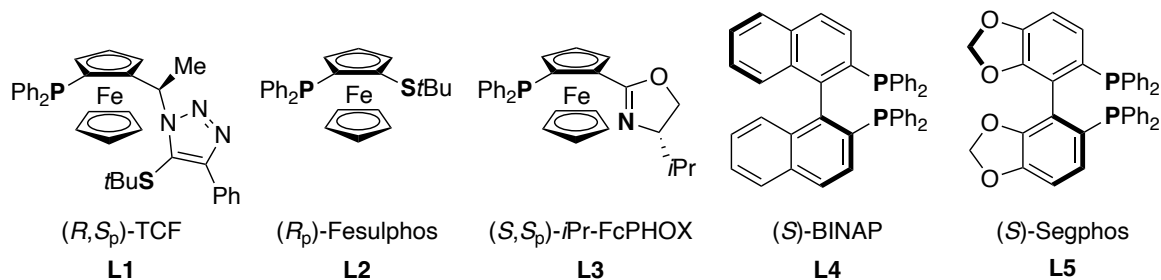
The author first carried out the reaction of *p*-chloro phenyl-substituted imino ester **1a** with ylidene-2,3-dioxopyrrolidine **2a** in CH₂Cl₂ at room temperature for 16 h in the presence of silver acetate (AgOAc, 5.0 mol%), (*R*, *S*_p)-TCF **L1** (5.0 mol%), and diisopropylethylamine (DIPEA, 20 mol%). The (3+2) cycloaddition smoothly yielded the corresponding spiropyrrolidines with high diastereo- and enantioselectivity (Table 3-1, entry 1). The major product could be isolated by column chromatography and was determined to be the *exo'*-diastereomer, which is rarely obtained in the (3+2) cycloaddition of imino esters (details of stereochemistry are shown in Figure 3-6 below). On the other hand, there were two other diastereomers in addition to the major cycloadduct. However, they were difficult to isolate and purify by column chromatography, and their structures could not be determined.

The author next conducted screening of silver and copper complexes that are frequently applied to the cycloaddition reaction.^{4,5} The ligands employed in this study are shown in Figure 3-3. Several ferrocene-based ligands such as Fesulphos **L2** and FcPHOX **L3**, were not effective under the silver-catalyzed condition and decreased the diastereo- and enantioselectivity (Table 3-1, entries 2, 3). The reaction using BINAP **L4** and Segphos **L5** as the ligands also resulted in high yield, but with lower stereoselectivity than when TCF **L1** was used. When [Cu(MeCN)₄]BF₄ was applied to the reaction as the metal salt, the diastereoselectivity increased (entries 6-10). However, none of the ligands were effective for the reaction, giving the *exo'*-adducts with low to moderate enantioselectivity. Therefore, it was revealed that our original AgOAc/TCF complex was superior in the *exo'*-diastereo- and enantioselective cycloaddition of imino ester **1a** with ylidene-2,3-dioxopyrrolidine **2a**. Subsequently, the author carried out further examinations using the AgOAc/TCF complex.

Table 3-1. Screening of chiral silver and copper complexes.^a

entry	metal / ligand	yield (%) ^b	dr (%) ^c	ee (%) ^d
1	AgOAc / L1	70	80	82
2	AgOAc / L2	88 ^e	34	-11
3	AgOAc / L3	87 ^e	64	40
4	AgOAc / L4	80 ^e	32	-9
5	AgOAc / L5	99 ^e	33	10
6	[Cu(MeCN) ₄]BF ₄ / L1	63	92	-16
7	[Cu(MeCN) ₄]BF ₄ / L2	76	96	3
8	[Cu(MeCN) ₄]BF ₄ / L3	71	90	-56
9	[Cu(MeCN) ₄]BF ₄ / L4	62	64	13
10	[Cu(MeCN) ₄]BF ₄ / L5	88	90	20

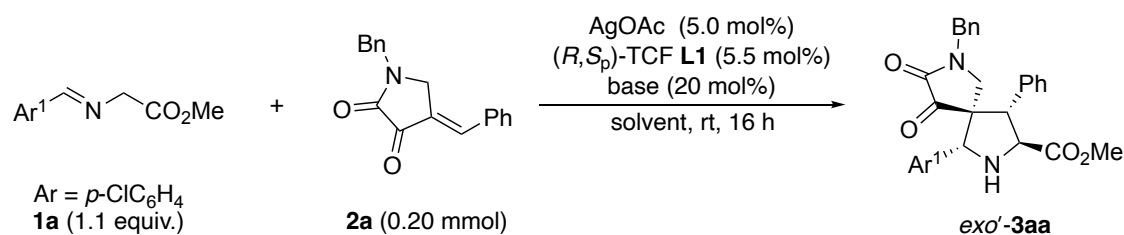
[a] Condition: **1a** (0.22 mmol), **2a** (0.20 mmol), metal salt (5.0 mol%), ligand (5.5 mol%), DIPEA (20 mol%), CH₂Cl₂ (1 mL), rt, 16 h. [b] Isolated yield. [c] Determined by crude ¹H NMR. [d] Determined by chiral HPLC. [e] Combined yield.

**Figure 3-3.** Chiral ligands employed in this study.

The reaction conditions were optimized and the results are shown in Table 3-2. It was revealed that the silver/TCF complex-catalyzed reaction of imino ester **1a** with ylidene-2,3-dioxopyrrolidines **2a** proceeded with excellent yield, diastereo- and

enantioselectivity in the presence of AgOCOCF₃ as the metal salt and Et₃N as the base in THF at 0 °C (entry 1). The enantioselectivity when the reaction was carried out at 0 °C was 96% ee, whereas at room temperature it decreased to 90% ee (entry 2). AgOCOCF₃ was the most suitable for giving the desired product with a high yield, with other silver salts such as AgOTf, AgF, and AgOAc giving the cycloadducts in moderate to good yield

Table 3-2. Optimization of the reaction conditions^a



entry	base	solvent	yield (%) ^b	dr (%) ^c	ee (%) ^d
1 ^{ef}	Et ₃ N	THF	91	>99	96
2 ^f	Et ₃ N	THF	85	>99	90
3 ^g	Et ₃ N	THF	60	97	94
4 ^h	Et ₃ N	THF	65	98	90
5	Et ₃ N	THF	79	97	96
6	none	THF	70	97	90
7	K ₂ CO ₃	THF	68	96	86
8	DBU	THF	42	75	22
9	DIPEA	THF	77	88	90
10	DIPEA	Et ₂ O	52	79	90
11	DIPEA	MTBE	61	87	92
12	DIPEA	toluene	46	84	86
13	DIPEA	CH ₂ Cl ₂	70	80	82

[a] Condition: **1a** (0.22 mmol), **2a** (0.20 mmol), metal salt (5.0 mol%), ligand (5.5 mol%), DIPEA (20 mol%), CH₂Cl₂ (1 mL), rt, 16 h. [b] Isolated yield. [c] Determined by crude ¹H NMR. [d] Determined by chiral HPLC. [e] Conducted at 0°C. [f] AgOCOCF₃ was used instead of AgOAc. [g] AgOTf was used instead of AgOAc. [h] AgF was used instead of AgOAc.

(entry 2-5). Although the addition of base was not always required for the reaction, the product **3aa** was obtained in high yield and excellent enantioselectivity when Et₃N was used as the additive (entries 5-7). The yield and stereoselectivity of the product were decreased when DBU was added to the reaction (entry 8). THF was selected as the most suitable solvent because other solvents such as Et₂O, MTBE, toluene, and CH₂Cl₂ resulted in low yield (entries 9-13).

The scope of imino esters **1** under the optimal reaction conditions was investigated next, and the results are summarized in Figure 3-4. It was revealed that a wide range of imino esters **1** was applicable for the stereoselective (3+2) cycloaddition. When *para*-fluoro- and bromo-substituted imino esters **1b** and **1c** were applied to the reaction, the corresponding spiropyrrolidines **3ba** and **3ca** were obtained with excellent yield and enantioselectivity. *meta*-Chloro-substituted imino ester **1d** also gave the cycloadduct **3da** as a single diastereomer, but the yield was moderate. Imino esters **1e** and **1f** bearing methyl groups at the *para*- and *meta*-positions successfully gave the corresponding products **3ea** and **3fa** with excellent yield and stereoselectivity, and an *ortho*-substituent could also be applied to the reaction with slightly lower values. Although the strong electron-withdrawing CF₃ group gave a moderate yield and diastereoselectivity, the high enantioselectivity was maintained. The strong electron-donating methoxy group was successfully applied to the reaction, giving the product **3ia** with excellent stereoselectivity. The phenyl group with no substituent smoothly reacted with 2,3-dioxopyrrolidine **2a**, and a thienyl group could also be used in the stereoselective (3+2) cycloaddition.

Additionally, the optimal reaction conditions could be applied to a wide range of ylidene-2,3-dioxopyrrolidines **2** for the asymmetric reaction (Figure 3-5). For example, when 2,3-dioxopyrrolidines with *para*-substituted aryl groups were used, the corresponding spiropyrrolidines **3ab**, **3ac**, **3ad**, and **3ae** were obtained with excellent enantioselectivity. Substituents at the *meta*-position maintained excellent enantioselectivity, but the diastereoselectivity was slightly decreased. An *ortho*-methyl

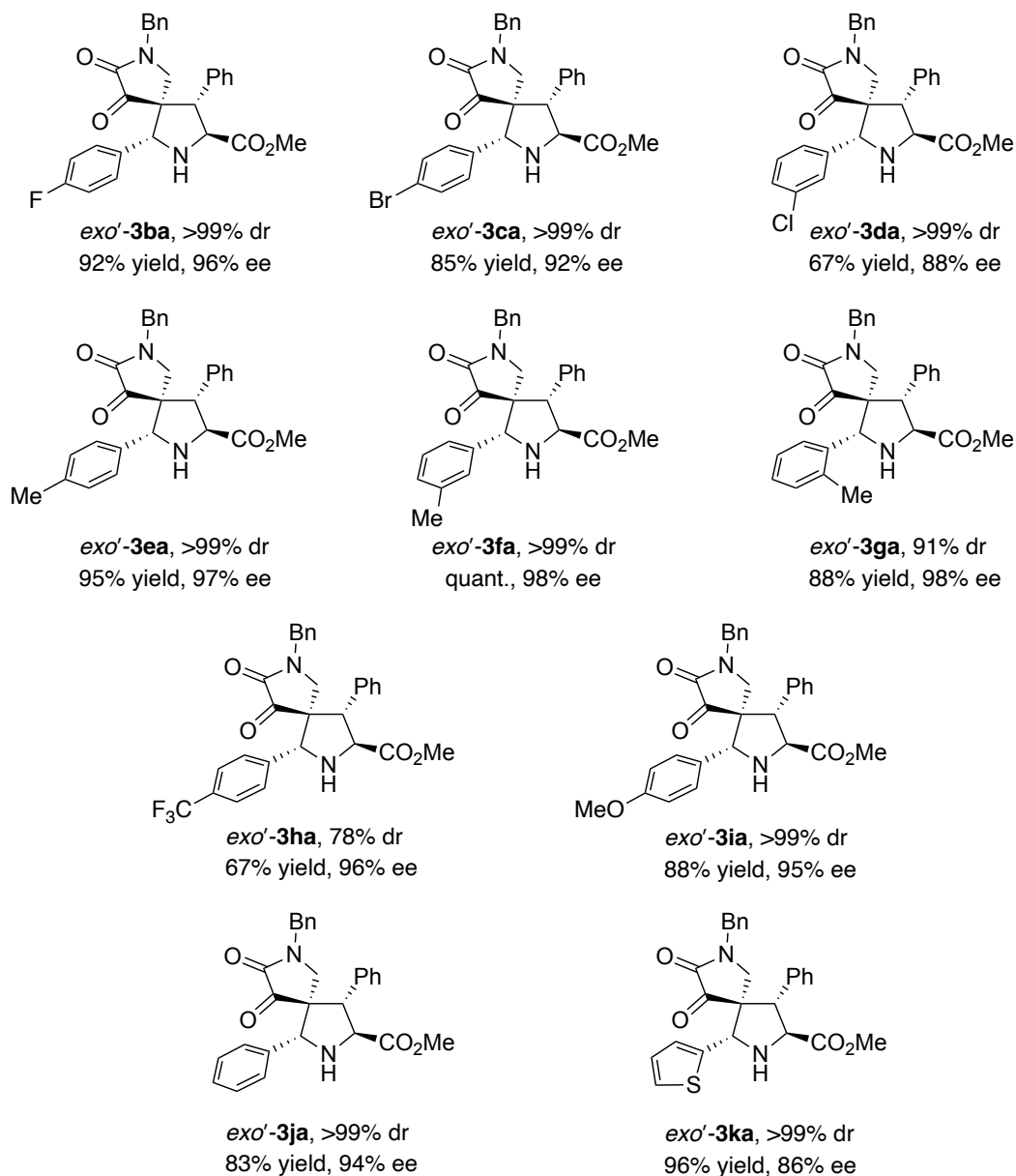
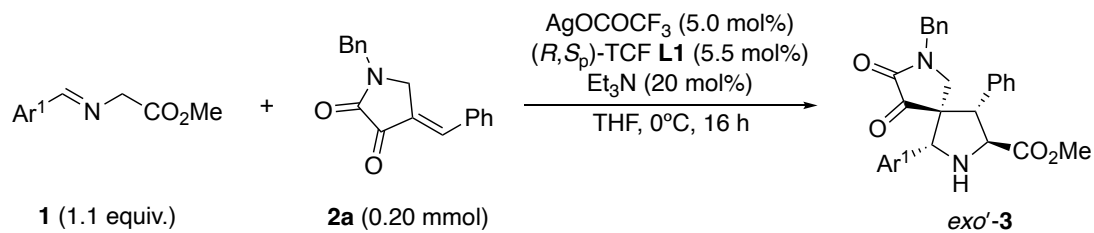


Figure 3-4. Scope of imino esters **1**.

group slightly decreased the stereoselectivity to give the cycloadducts **3ah**. 2,3-Dioxopyrrolidines bearing a 2-thienyl group efficiently reacted with imino esters **1a**, giving the products **3ai** with excellent enantioselectivity. These results indicated that the substituent of the 2,3-dioxopyrrolidines **2** had some influence on the reaction, but they could be applied with high enantioselectivity.

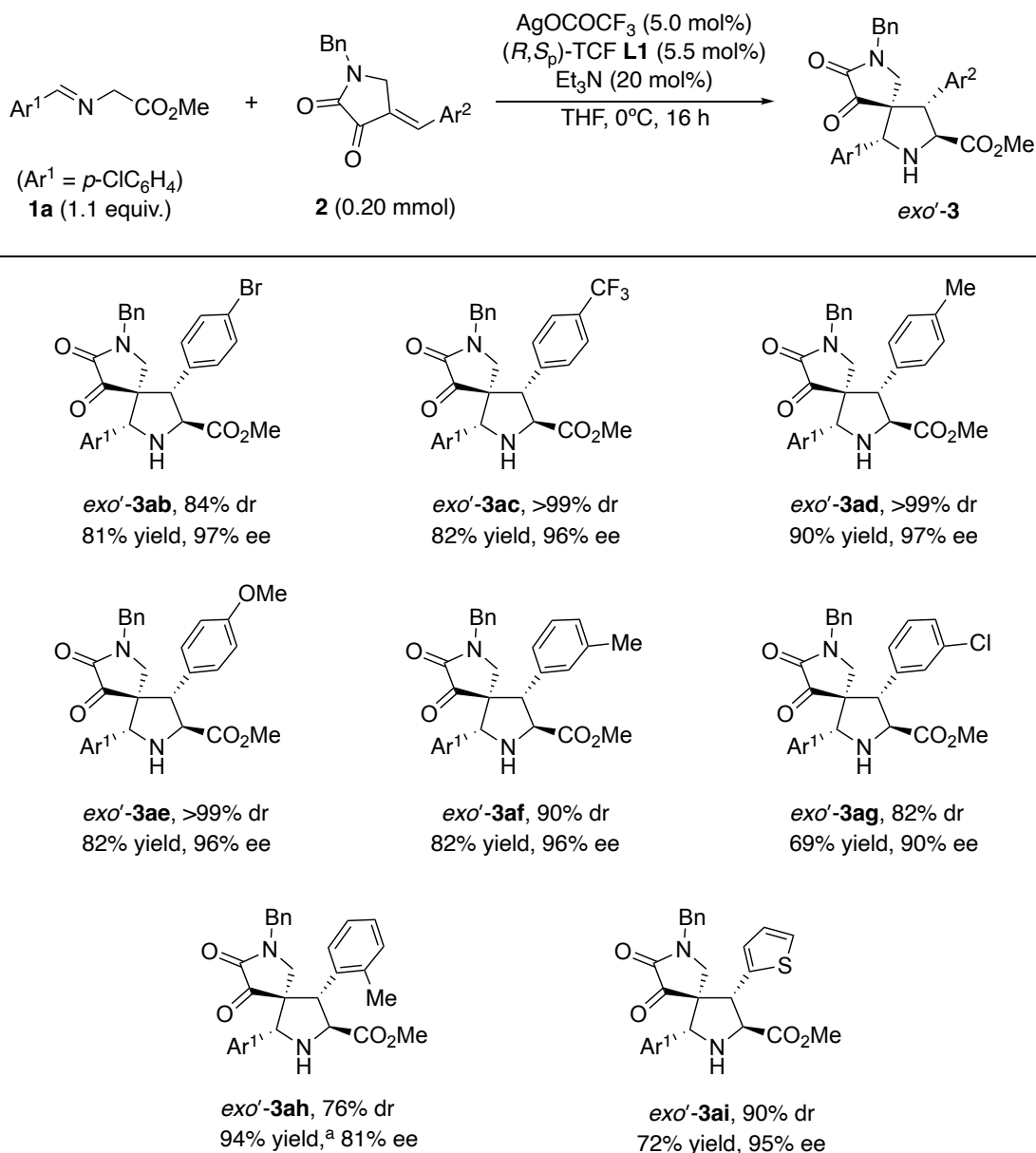
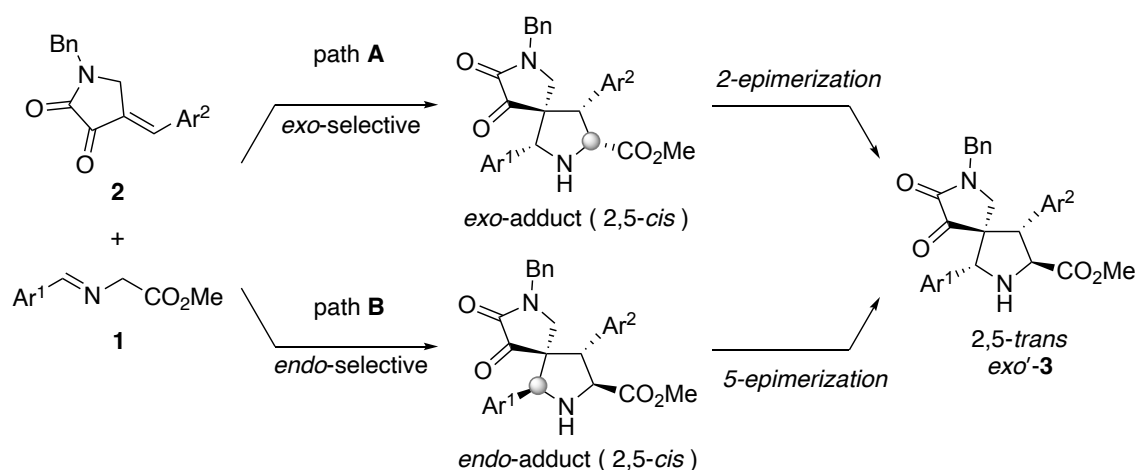


Figure 3-5. Scope of ylidene-2,3-dioxopyrrolidines **2**. [a] Combined yields are shown.

The metal complex-catalyzed (3+2) cycloaddition of imino esters **1** with activated olefins generally proceeds with *exo*- or *endo*-diastereoselectivity (2,5-*cis* configuration).^{4,5} On the other hand, the formation of 2,5-*trans* diastereomers such as *exo'*-adducts is unusual and has been limited to a few examples.^{6c,13} The author was interested in the unexpected stereochemical outcome and engaged in experiments to elucidate details of this diastereoselectivity. With the previous reports in mind, *exo'*-cycloadducts might be formed via base-promoted epimerization of the first generated 2,5-*cis* pyrrolidines (Scheme 3-1).^{13e,14} According to this viewpoint, two reaction pathways are possible. One is the epimerization of the 2-position of the pyrrolidine ring after the formation of *exo*-cycloadducts by the 1,3-DC of imino esters **1** with 2,3-dioxopyrrolidines **2** (path A). Another is the *endo*-selective formation and subsequent 5-epimerization of the pyrrolidine ring (path B).

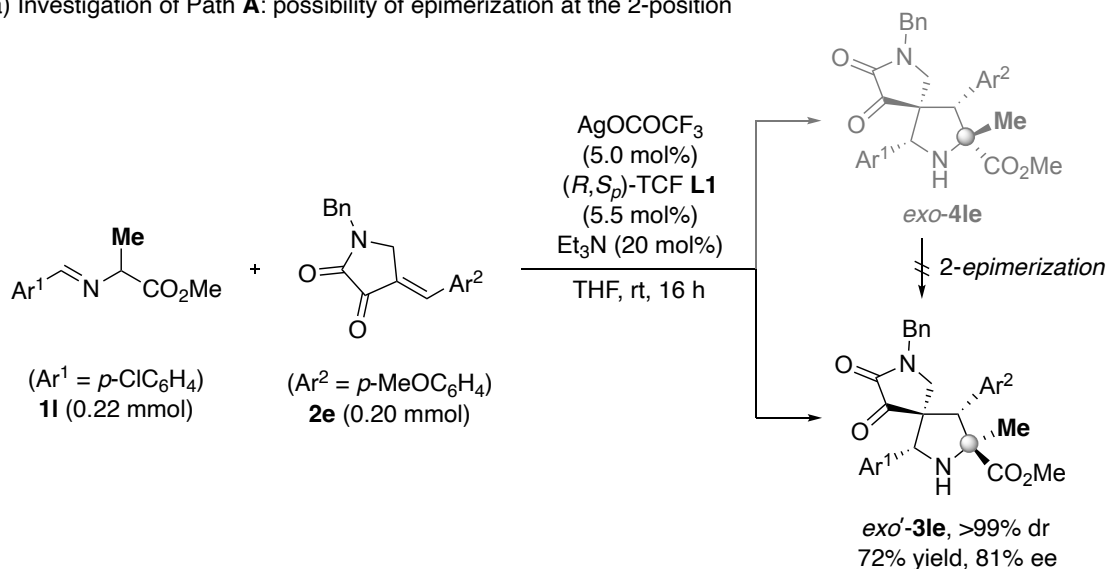


Scheme 3-1. Possible epimerization pathways to afford *exo'*-cycloadducts.

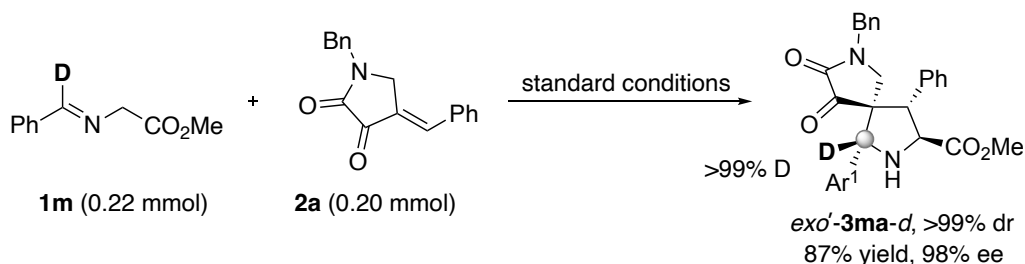
To investigate the possibility of the 2,5-*trans* pyrrolidines being generated by the 2-epimerization after the first formed *exo*-cycloadducts, an initial control experiment was conducted with the α -methyl-substituted imino esters **11** derived from (\pm)-alanine as the azomethine ylide precursor (Scheme 3-2a). In this case, if the *exo*-**41e** (2,5-*cis* configuration) was generated as the intermediate via reaction pathway A, no epimerization at the 2-position would take place because this stereocenter is a quaternary carbon. As a result of the experiment, α -methyl-substituted imino ester **11** reacted with

2,3-dioxopyrrolidines **2e** at room temperature, yielding *exo'*-cycloadducts as a single diastereomer. The racemic products *rac*-**3le** synthesized by using PPh₃ as the ligand were suitable for the preparation of a single crystal containing solvent THF, and the stereochemistry (2,5-*trans* configuration) could be determined by X-ray crystallographic analysis (Figure 3-6, right). This result indicated that *exo'*-adducts were not generated via *exo*-cycloadducts, ruling out the epimerization pathway A in Scheme 3-1.

(a) Investigation of Path A: possibility of epimerization at the 2-position



(b) Investigation of Path B: possibility of epimerization at the 5-position



Scheme 3-2. Control experiment for epimerization pathways.

A deuterium-labeled experiment was performed to investigate the possibility of the proposed *endo*-selective (3+2) cycloaddition and subsequent epimerization at the 5-position of the cycloadducts (Scheme 3-2b). Deuterium-labeled imino ester **1m-d** reacted with 2,3-dioxopyrrolidine **2a** under the optimized conditions, giving the corresponding *exo'*-**3ma-d** as a single diastereomer with high yield and excellent enantioselectivity. This control experiment gave 2,5-*trans* spiro pyrrolidine *exo'*-**3ma-d** with >99% deuterium

ratio as a single stereoisomer. Thus, it was unlikely that 5-epimerization took place under the reaction conditions, and reaction pathway B in Scheme 3-1 was not reasonable for the mechanism for 2,5-*trans* stereochemistry.

A single crystal of chiral spiropyrrolidine *exo'*-**3ae** was suitable for the X-ray crystallographic analysis (Figure 3-6, left). The absolute configuration of several chiral centers could be determined; the 2, 3, 4, and 5-positions of the pyrrolidine ring were *S*, *S*, *R*, and *R*, respectively. In general, the stereochemistry of the 2-position depends on the chirality of the ligand used, and this is consistent with previous reports using (*R*, *S*)-TCF.¹² Therefore, the point of interest is the stereochemistry of the 5-position, in which the aryl group is placed *trans* to the methoxy carbonyl group at the 2-position (2,5-*trans* configuration). As described above, the 2,5-*trans* configuration was also confirmed when α -methyl substituted imino ester **II** was used (Figure 3-6, right).

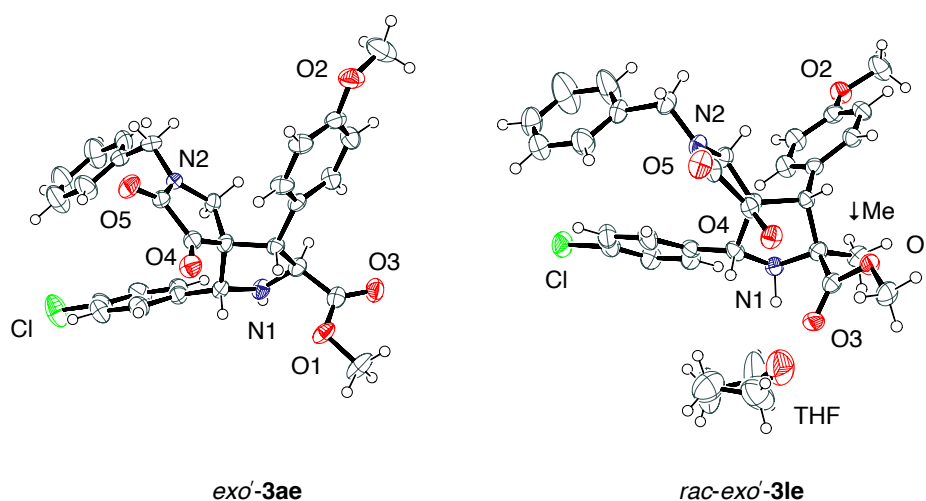


Figure 3-6. ORTEP drawing of 2,5-*trans* spiropyrrolidines.

Based on the results of the control experiments, X-ray analysis, and previous reports,^{6c,12} the author proposed a plausible reaction mechanism (Figure 3-7). The unusual stereochemistry of the 2,5-*trans* diastereomer is accessible by a stepwise addition/cyclization with bond rotation instead of a common concerted 1,3-DC. First, Michael addition of azomethine ylides **A** generated by a silver catalyst to ylidene-2,3-

dioxopyrrolidines **2** takes place. The nucleophilic addition proceeds from the *si*-face of azomethine ylides **A** to the *si*-face of the 2,3-dioxopyrrolidine **2** in an anti-selective manner, and would be controlled by the interaction between the oxygen functionality of 2,3-dioxopyrrolidine **2** and the silver center (Figure 3-7, B). Although a strained intermediate giving the *endo*-adduct is generated temporarily, it is smoothly converted to intermediate **C** whose 2,3-dioxo functionality coordinates to the silver center. Before the subsequent intramolecular Mannich reaction, the C–N single bond rotates to provide the most stable transition state **D** for giving the *exo'*-adducts. Finally, the silver catalyst is regenerated as soon as the Mannich reaction takes place and affords the desired *exo'*-adducts. The metal-catalyzed stepwise (3+2) cycloaddition of azomethine ylides with electron-deficient olefins for the *exo'*-cycloadduct have been limited to only a few examples using chiral nickel- or copper-complex catalysts.^{6c,12} Therefore, this is the first example of a silver-catalyzed *exo'*-selective asymmetric (3+2) cycloaddition.

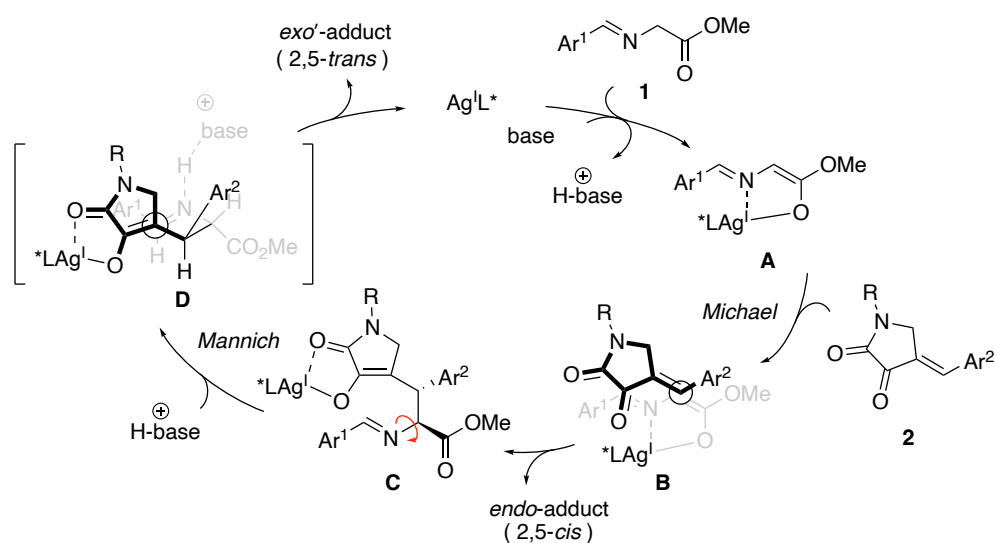


Figure 3-7. Postulated mechanism for *exo'*-selective asymmetric (3+2) cycloaddition of imino esters **1** with ylidene-2,3-dioxopyrrolidines **2**.

To gain insight into the stereochemistry at the 5-position of the pyrrolidine ring, DFT calculations of the intramolecular Mannich reaction were performed based on the possible reaction mechanism shown in Figure 3-7.¹⁵ The AgOAc/PPh₃ complex was selected as the catalyst in this computational study because the 2,5-*trans* selective reaction also proceeded under this condition.

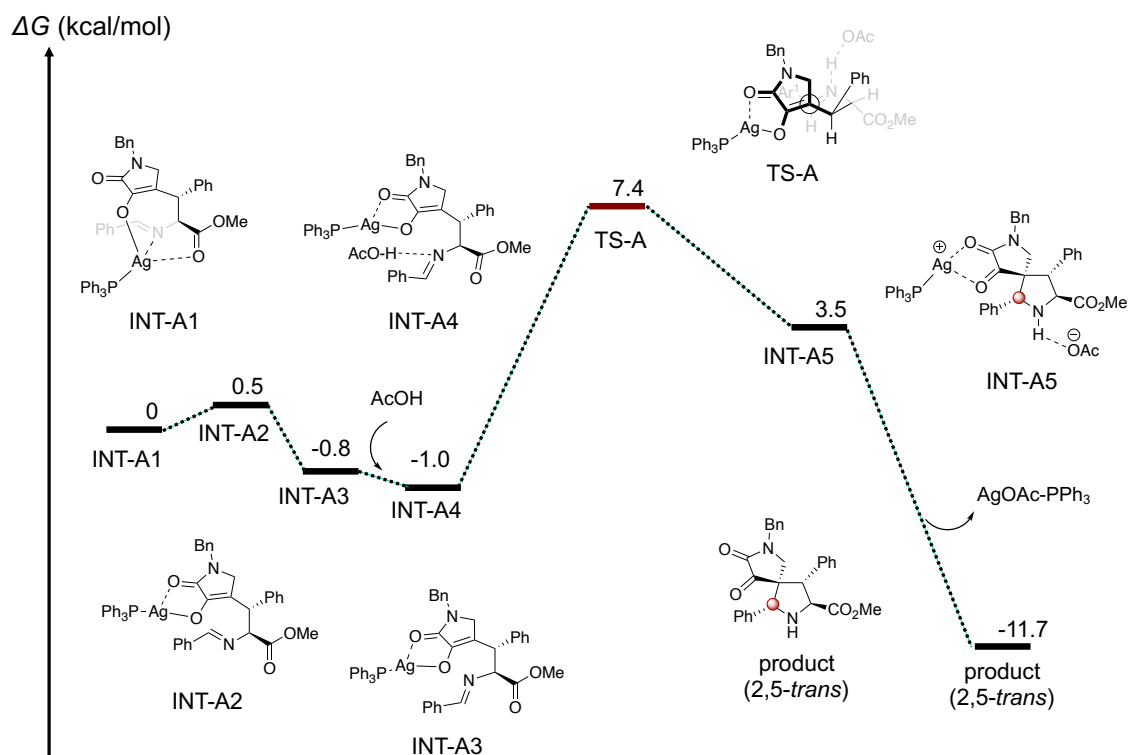


Figure 3-8. The postulated mechanism for the Mannich reaction giving the *exo'*-(2,5-*trans*) adducts under the AgOAc/PPh₃-catalyzed condition (route A). The DFT calculations were carried out at B3PW91/LanL2DZ(Ag)+6-31G*(other atoms) with gd3bj level of theory.

Firstly, the Michael adducts **INT-A1** produced by the Michael addition reaction, the intermediate **INT-A2** whose diketone moiety coordinated to the silver center and the intermediate **INT-A3**, which is produced by the C–N bond rotation of the intermediate **INT-A2** were calculated (Figure 3-8, route A). As a result, it was found that there was little energy difference between each intermediate **INT-A1-3**. Although transition states should exist between each intermediate, they were not calculated due to occurring more

easily than Mannich cyclization in general. The Mannich reaction is proposed to proceed by the action of acetic acid present as a conjugate acid on this intermediate **INT-A3**, and the Gibbs activation energy of the transition state **TS-A** was calculated to be 8.4 kcal/mol.

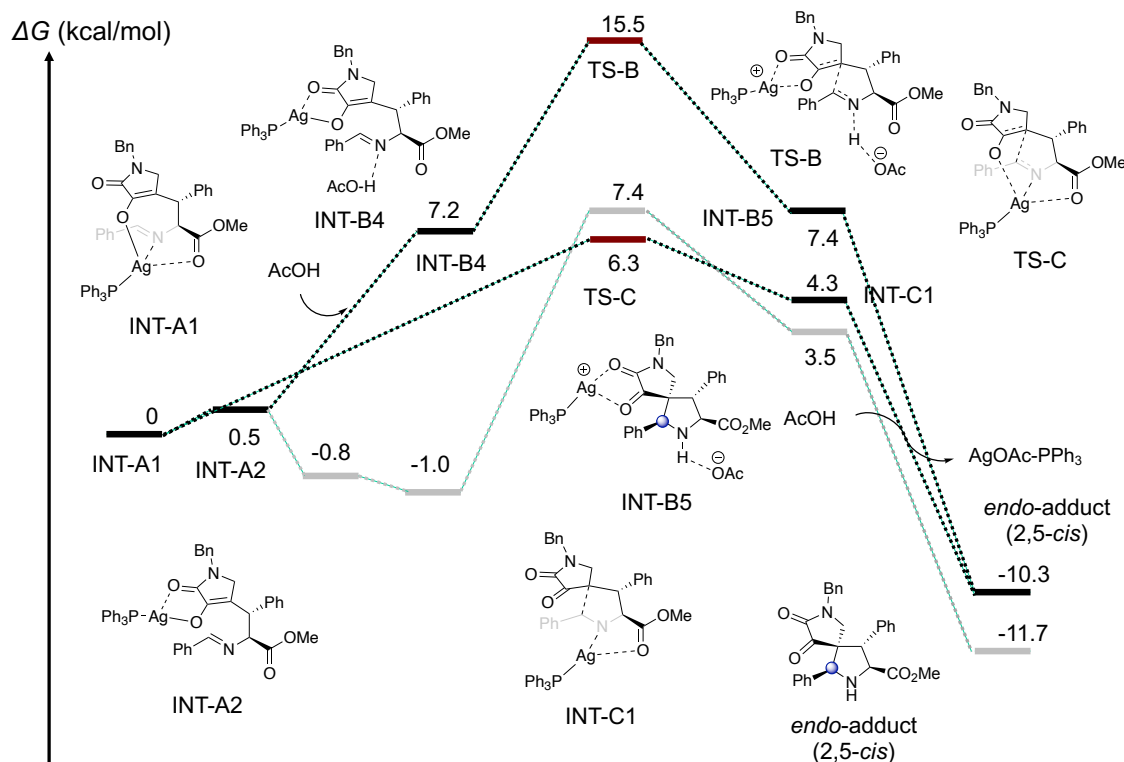


Figure 3-9. The possible mechanism for the Mannich reaction giving the *endo*-(2,5-*cis*) adducts under the AgOAc/PPh₃-catalyzed condition (route B and C). The DFT calculations were carried out at B3PW91/LanL2DZ(Ag)+6-31G*(other atoms) with gd3bj level of theory.

The mechanism for the Mannich reaction which gives *endo*-(2,5-*cis*) adducts was next examined (Figure 3-9, route B). The stability of the intermediate **INT-B4**, in which acetic acid acts on the imine moiety of the intermediate **INT-A2**, was calculated to be 7.2 kcal/mol, indicating that it is unstable compared to the corresponding **INT-A4** ($\Delta G = -1.0$ kcal/mol). The Gibbs activation energy of the transition state **TS-B**, in which the Mannich reaction occurs via the intermediate **INT-B4**, was calculated to be 8.3 kcal/mol. In other words, the formation of intermediate **INT-B4** is thermodynamically unfavorable, and the activation energy of the C–C bond formation process is larger than that of **TS-A**.

Therefore, the formation of the *endo*-adduct by this route B is unacceptable.

However, the *endo*-adduct can be formed by the intramolecular direct Mannich reaction of the Michael adduct **INT-A1** (Figure 3-9, route C). The transition state **TS-C**, where the Mannich reaction occurs directly from the intermediate **INT-A1**, was calculated to be 6.3 kcal/mol, which is slightly lower than the $\Delta G = 7.4$ kcal/mol for the **TS-A** when the *exo'*-adduct is formed. This suggests that the Mannich reaction from the intermediate **INT-A1** via the transition state **TS-C** is kinetically advantageous. Thus, although the formation of the intermediates **INT-A2-4** for leading to the 2,5-*trans* adduct is possible to be thermodynamically favored, it cannot be concluded that the pathway for the 2,5-*trans* adduct is more favorable than that for the 2,5-*cis* adduct only by the result of this calculation study.

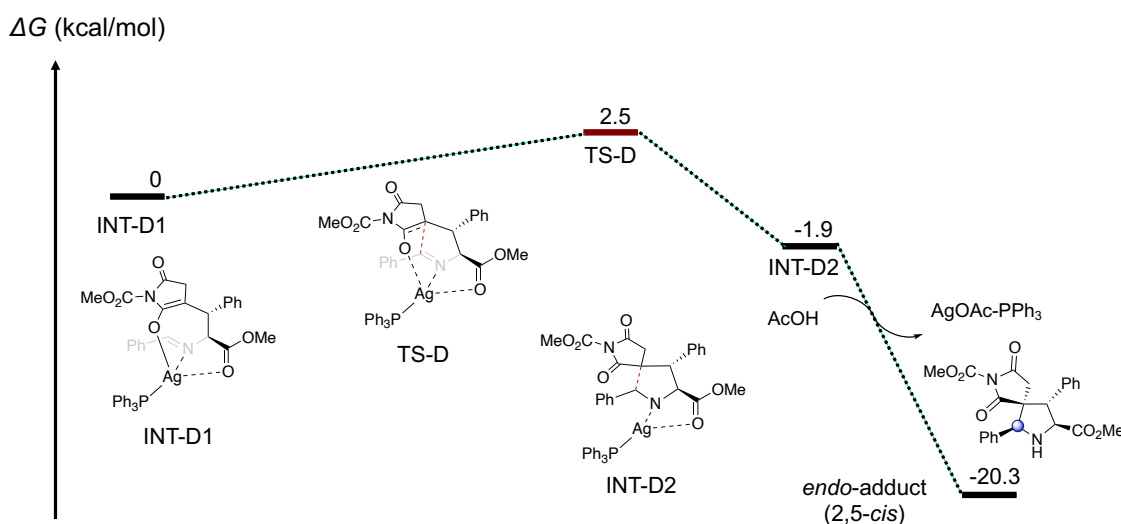


Figure 3-10. The mechanism for the Mannich reaction giving the *endo*-(2,5-*cis*) adducts under the AgOAc/PPh₃-catalyzed condition (route D). The DFT calculations were carried out at B3PW91/LanL2DZ(Ag)+6-31G*(other atoms) with gd3bj level of theory.

On the other hand, the (3+2) cycloaddition using ylidene-succinimides whose structures are similar to ylidene-2,3-dioxopyrrolidines has been reported to afford *endo*-diastereomers (Figure 3-2a).⁹ We also reported that the silver-catalyzed reaction of imino esters with ylidene-succinimides proceeds with the same *endo*-selectivities.¹⁶ Based on the results, the DFT calculation of the reaction using N-CO₂Me-substituted ylidene-

succinimides as the activated olefins was also performed for comparison with the reaction using ylidene-2,3-dioxopyrrolidines.

First, the reaction pathway for the formation of the *endo*-adduct by the Mannich reaction directly from the Michael adduct **INT-D1** was calculated (Figure 3-10, route D). As a result, the activation energy of the transition state **TS-D** was estimated to be $\Delta G = 2.5$ kcal/mol, which is lower than that of the reaction using ylidene-2,3-dioxopyrrolidines (**TS-C**).

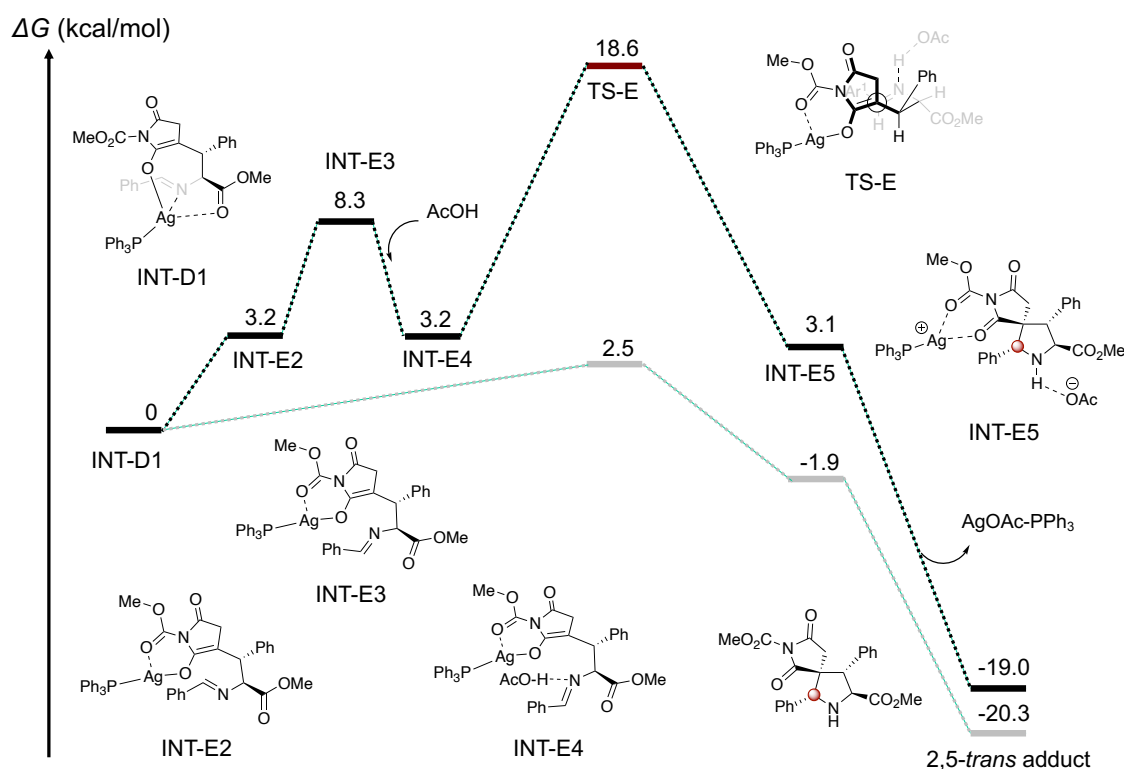


Figure 3-11. The mechanism for the Mannich reaction giving the *exo'*-(2,5-*trans*) adducts under the AgOAc/PPh₃-catalyzed condition (route E). The DFT calculations were carried out at B3PW91/LanL2DZ(Ag)+6-31G*(other atoms) with gd3bj level of theory.

The author next analyzed the reaction pathway similar to that shown in Figure 3-8 for giving the 2,5-*trans* adduct via the further intermediates (Figure 3-11). After the Michael adduct **INT-D1** was generated, intermediate **INT-E2** would be formed by the silver catalyst flip to the succinimide moiety. The energy of the intermediate **INT-E2** was calculated to be $\Delta G = 3.2$ kcal/mol and that of the intermediate **INT-E3**, in which the

C–N bond derived from the imino ester is rotated, was calculated to be $\Delta G = 8.3$ kcal/mol. The intermediate **INT-E4**, in which acetic acid acts on the intermediate **INT-E3**, was calculated to be $\Delta G = 3.2$ kcal/mol, and the activation energy of the Mannich reaction from this intermediate **INT-E4** as a starting material was calculated to be 15.4 kcal/mol (**TS-E**). Therefore, the formation of the intermediates **INT-E2-4** is thermodynamically unfavorable in the reaction using ylidene-succinimides, and a very high activation energy of the transition state **TS-E** is required compared to **TS-D** giving *endo*-adduct. These results supported that the silver complex catalyzed (3+2) cycloaddition using ylidene-succinimide as the activated olefins proceed with high *endo*-diastereoselectivity, not giving 2,5-*trans* adducts.

Thus, the above computational studies suggest that the formation of thermodynamically stable intermediates before the Mannich reaction and the activation energy which is equivalent to kinetically favorable *cis*-selective cyclization would be needed to obtain pyrrolidines with a 2,5-*trans* configuration. However, further calculation studies that consider the solvent effect and applying chiral ligand, are necessary because it could not be concluded that the 2,5-*trans* selective Mannich reaction is more favorable than the 2,5-*cis* selective one in the reaction using ylidene-2,3-dioxopyrrolidines.

3–3. Conclusion

In conclusion, the author developed a catalytic asymmetric (3+2) cycloaddition of imino esters with ylidene-2,3-dioxopyrrolidines. The reaction proceeded with unusual 2,5-*trans* diastereoselectivities, and the 2,5-*trans* cycloadducts were obtained with excellent enantioselectivity when our original Ag/TCF complex was used. Additionally, a wide range of imino esters and ylidene-2,3-dioxopyrrolidines could be applied to the reaction, giving various spiroyrrolidines with high yield and excellent stereoselectivity. Control experiments suggested that the 2,5-diastereoselectivity was not due to a common 2,5-*cis* selective cycloaddition and subsequent epimerization, i.e., a stepwise Michael addition/Mannich reaction was proposed as a reasonable pathway.

3–4. Experimental Section

The general information was described in the Experimental Section of Chapter 2.

Unless otherwise stated, all reactions were carried out with oven-dried glassware under the atmosphere of nitrogen. Starting materials, ylidene-2,3-dioxopyrrolidines **2** were prepared and identified by reported methods.¹⁷ Racemic products of **3** were prepared using PPh₃ (5.5 mol%) as the ligand. All other chemical reagents used commercial grade and used as received.

Silver-Catalyzed *exo'*-Selective Asymmetric (3+2) Cycloaddition of Imino Esters **1 with Ylidene-2,3-dioxopyrrolidines **2**.** A mixture of AgOCOCF₃ (2.2 mg, 10 μmol, 5.0 mol%) and (*R*, *S_p*)-ThioClickFerrophos **L1** (6.9 mg, 11 μmol, 5.5 mol%) were dissolved in dry THF (1.0 mL) at room temperature and stirred for 30 minutes at the same temperature. After the reaction mixture was cooled to 0°C, to the mixture were added *p*-chloro phenyl imino esters **1a** (46.4 mg, 0.22 mmol, 1.10 equiv.), ylidene-2,3-dioxopyrrolidines **2a** (55.5 mg, 0.20 mmol, 1.0 equiv.), and Et₃N (5.6 μL, 40 μmol, 20 mol%). After stirring for 16 h at 0°C, the mixture was diluted with 30 mL EtOAc, filtered through a short Celite pad, and concentrated under reduced pressure. ¹H NMR analysis of the crude mixture showed that the *exo'*-adduct is the sole product. The residue was purified by silica gel column chromatography (20 g, toluene/EtOAc/acetone = 10/1/1) to give methyl (1*R*, 3*S*, 4*S*, 5*R*)-7-benzyl-1-(4-chlorophenyl)-8,9-dioxo-4-phenyl-2,7-diazaspiro[4.4]nonane-3-carboxylate (*exo'*-**3aa**) (89.0 mg, 0.182, 91% yield, >99% dr, 96% ee) as a pale yellow solid.

2 mmol Scale Preparation of methyl (1*R*, 3*S*, 4*S*, 5*R*)-7-benzyl-1-(4-chlorophenyl)-8,9-dioxo-4-phenyl-2,7-diazaspiro[4.4]nonane-3-carboxylate (*exo'*-3aa**).** A mixture of AgOCOCF₃ (22.1 mg, 0.01 mmol, 5.0 mol%) and (*R*, *S_p*)-ThioClickFerrophos **L1** (69.3 mg, 0.11 mmol, 5.5 mol%) were dissolved in dry THF (10.0 mL) at room temperature and stirred for 30 minutes at the same temperature. After the reaction mixture was cooled to 0°C, to the mixture were added imino esters **1a** (466 mg, 2.20 mmol, 1.10 equiv.),

ylidene-2,3-dioxopyrrolidine **2a** (555 mg, 2.00 mmol, 1.00 equiv.), and Et₃N (55.4 μL, 0.397 mmol, 19.9 mol%). After stirring for 16 h at 0°C, the mixture was diluted with 60 mL EtOAc, filtered through a short Celite pad, and concentrated under reduced pressure. ¹H NMR analysis of the crude mixture showed that the *exo'*-adduct is the sole product. The residue was purified by silica gel column chromatography (50 g, toluene/EtOAc/acetone = 10/1/1) to give methyl (1*R*, 3*S*, 4*S*, 5*R*)-7-benzyl-1-(4-chlorophenyl)-8,9-dioxo-4-phenyl-2,7-diazaspiro[4.4]nonane-3-carboxylate (*exo'*-**3aa**) (889 mg, 1.82 mmol, 90.8% yield, >99% dr, 96% ee) as a pale yellow solid.

Control Experiment: Reaction of α -Methyl-substituted Imino Ester 1l with Ylidene-2,3-dioxopyrrolidine 2e. A mixture of AgOCOCF₃ (2.2 mg, 10 μmol, 5.0 mol%) and (*R*, *S_p*)-ThioClickFerrophos **L1** (6.9 mg, 11 μmol, 5.5 mol%) were dissolved in dry THF (1.0 mL) at room temperature. After stirring for 30 minutes at the same temperature, to the mixture were successively added α -substituted imino esters **1l** (49.6 mg, 0.22 mmol, 1.10 equiv.), ylidene-2,3-dioxopyrrolidines **2e** (61.5 mg, 0.20 mmol, 1.0 equiv.), and Et₃N (5.6 μL, 40 μmol, 20 mol%). After stirring for 16 h at room temperature, the mixture was diluted with 30 mL EtOAc, filtered through a short Celite pad, and concentrated under reduced pressure. ¹H NMR analysis of the crude mixture showed that the *exo'*-adduct is the sole product. The residue was purified by silica gel column chromatography (20 g, toluene/EtOAc/acetone = 10/1/1) to give methyl (1*R*, 3*S*, 4*S*, 5*R*)-7-benzyl-1-(4-chlorophenyl)-4-(4-methoxyphenyl)-3-methyl-8,9-dioxo-2,7-diazaspiro[4.4]nonane-3-carboxylate (*exo'*-**3le**) (77.0 mg, 0.145 mmol, 72.2%, > 99% dr, 81% ee) as a pale yellow solid.

Control Experiment: Reaction of Deuterium-labeled Imino Ester 1m with Ylidene-2,3-dioxopyrrolidine 2a. A mixture of AgOCOCF₃ (2.2 mg, 10 μmol, 5.0 mol%) and (*R*, *S_p*)-ThioClickFerrophos **L1** (6.9 mg, 11 μmol, 5.5 mol%) were dissolved in dry THF (1.0 mL) at room temperature and stirred for 30 minutes at the same temperature. After the reaction mixture was cooled to 0°C, to the mixture were added deuterium-labeled imino esters **1m-d** (39.2 mg, 0.22 mmol, 1.10 equiv.), ylidene-2,3-dioxopyrrolidines **2a** (55.5

mg, 0.20 mmol, 1.0 equiv.), and Et₃N (5.6 μL, 40 μmol, 20 mol%). After stirring for 16 h at 0°C, the mixture was diluted with 30 mL EtOAc, filtered through a short Celite pad, and concentrated under reduced pressure. ¹H NMR analysis of the crude mixture showed that the *exo'*-adduct is the sole product. The residue was purified by silica gel column chromatography (20 g, toluene/EtOAc/acetone = 10/1/1) to give methyl (1*R*, 3*S*, 4*S*, 5*R*)-7-benzyl-8,9-dioxo-1,4-diphenyl-2,7-diazaspiro[4.4]nonane-3-carboxylate-1-*d* (*exo'*-**3ma-d**) (79.2 mg, 0.174 mmol, 86.9%, >99% dr, 98% ee) as a pale yellow solid.

Methyl (1*R*, 3*S*, 4*S*, 5*R*)-7-benzyl-1-(4-chlorophenyl)-8,9-dioxo-4-phenyl-2,7-diazaspiro[4.4]nonane-3-carboxylate (*exo'*-3aa**).** (89.0 mg, 90.9%, >99% dr, 96% ee); pale yellow solid; mp 147–149 °C; ¹H NMR (400 MHz, CDCl₃): δ 7.27–7.30 (m, 3H), 7.21–7.23 (m, 1H), 7.10–7.16 (m, 8H), 6.52–6.57 (m, 2H), 4.95 (s, 1H), 4.32–4.38 (m, 3H), 3.92 (d, 1H, *J* = 14.6 Hz), 3.70 (s, 3H), 3.16 (s, 2H); ¹³C NMR (101 MHz, CDCl₃): δ 202.4, 174.6, 158.8, 134.89, 134.86, 134.3, 133.6, 129.2, 129.0, 128.9, 128.3, 127.9, 127.8, 127.73, 127.70, 69.3, 59.8, 58.1, 56.8, 52.9, 48.2, 43.7; HPLC (Daicel Chiralpak IH-3, *n*-hexane/2-propanol = 70/30, 1.0 mL/min, 254 nm); *t*_R = 24.0 min (minor), 37.7 min (major); [α]_D²⁵ 26.92 (*c* 0.06, CHCl₃); HRMS (ESI) *m/z*: [M+Na]⁺ Calcd for C₂₈H₂₅³⁵ClN₂NaO₄⁺, 511.1395; found 511.1375.

Methyl (1*R*, 3*S*, 4*S*, 5*R*)-7-benzyl-1-(4-fluorophenyl)-8,9-dioxo-4-phenyl-2,7-diazaspiro[4.4]nonane-3-carboxylate (*exo'*-3ba**).** (87.4 mg, 92.4%, >99% dr, 96% ee); pale yellow solid; mp 145–150 °C; ¹H NMR (400 MHz, CDCl₃): δ 7.27–7.30 (m, 3H), 7.09–7.22 (m, 7 H), 6.84–6.89 (m, 2H), 6.56 (m, 2H), 4.97 (s, 1H), 4.42 (d, 1H, *J* = 8.8 Hz), 4.33 (d, 1H, *J* = 8.8 Hz), 4.29 (d, 1H, *J* = 14.6 Hz), 3.96 (d, 1H, *J* = 14.6 Hz), 3.71 (s, 3H), 3.23 (d, 1H, *J* = 11.9 Hz), 3.18 (d, 1H, *J* = 11.9 Hz); ¹³C NMR (101 MHz, CDCl₃): δ 202.4, 174.6, 162.6 (d, *J*_{C-F} = 247 Hz), 158.8, 135.0, 133.7, 131.9 (d, *J*_{C-F} = 3.1 Hz), 129.2, 128.9, 128.3, 128.0 (d, *J*_{C-F} = 8.2 Hz), 127.9, 127.8, 127.7, 115.7 (d, *J*_{C-F} = 21.5 Hz), 69.3, 59.8, 58.28+58.27 (rotamer), 56.7, 52.9, 48.2, 43.7; HPLC (Daicel Chiralpak IH-3, *n*-hexane/2-propanol = 70/30, 1.0 mL/min, 254 nm); *t*_R = 25.5 min (minor), 38.4 min (major); [α]_D²⁵ 59.61 (*c* 0.06, CHCl₃); HRMS (ESI) *m/z*: [M+Na]⁺ Calcd for

C₂₈H₂₅FN₂NaO₄⁺, 495.1691; found 495.1679.

Methyl (1R, 3S, 4S, 5R)-7-benzyl-1-(4-bromophenyl)-8,9-dioxo-4-phenyl-2,7-diazaspiro[4.4]nonane-3-carboxylate (exo'-3ca). (90.2 mg, 84.5%, >99% dr, 92% ee); pale yellow solid; mp 145–147 °C; ¹H NMR (400 MHz, CDCl₃): δ 7.28–7.33 (m, 5H), 7.22–7.23 (m, 1H), 7.13–7.17 (m, 4H), 7.08–7.13 (m, 2H), 6.56 (d, 2H, *J* = 7.0 Hz), 4.96 (s, 1H), 4.47 (d, 1H, *J* = 8.9 Hz), 4.35 (d, 1H, *J* = 14.6 Hz), 4.33 (d, 1H, *J* = 8.9 Hz), 3.93 (d, 1H, *J* = 14.6 Hz), 3.71 (s, 3H), 3.25 (d, 1H, *J* = 12.0 Hz), 3.21 (d, 1H, *J* = 12.0 Hz); ¹³C NMR (101 MHz, CDCl₃): δ 202.3, 174.6, 158.8, 135.4, 134.9, 133.6, 132.0, 129.2, 129.0, 128.4, 128.1, 128.0, 127.8, 127.7, 122.6, 69.3, 59.8, 58.1, 56.9, 53.0, 48.2, 43.7; HPLC (Daicel Chiralpak IH-3, *n*-hexane/2-propanol = 70/30, 1.0 mL/min, 254 nm); *t*_R = 26.7 min (minor), 40.8 min (major); [α]_D²⁵ 38.64 (*c* 0.05, CHCl₃); HRMS (ESI) *m/z*: [M+H]⁺ Calcd for C₂₈H₂₆⁷⁹BrN₂O₄⁺, 533.1070; found 533.1068.

Methyl (1R, 3S, 4S, 5R)-7-benzyl-1-(3-chlorophenyl)-8,9-dioxo-4-phenyl-2,7-diazaspiro[4.4]nonane-3-carboxylate (exo'-3da). (66.0 mg, 67.4%, >99% dr, 88% ee); pale yellow solid; mp 157–160 °C; ¹H NMR (400 MHz, CDCl₃): δ 7.35 (s, 1H), 7.27–7.30 (m, 3H), 7.09–7.22 (m, 7H), 6.95 (d, 1H, *J* = 7.7 Hz), 6.55 (m, 2H), 4.98 (s, 1H), 4.35 (d, 1H, *J* = 8.9 Hz), 4.31 (d, 1H, *J* = 8.9 Hz), 4.24 (d, 1H, *J* = 14.7 Hz), 4.02 (d, 1H, *J* = 14.7 Hz), 3.69 (s, 3H), 3.16 (s, 2H); ¹³C NMR (101 MHz, CDCl₃): δ 202.3, 174.5, 158.8, 138.8, 134.9, 134.8, 133.7, 130.1, 129.2, 128.9, 128.8, 128.4, 128.0, 127.8, 127.7, 126.6, 124.8, 69.1, 59.8, 58.1, 57.1, 52.9, 48.2, 43.8; HPLC (Daicel Chiralpak IC-3, *n*-hexane/EtOAc = 70/30, 1.0 mL/min, 254 nm); *t*_R = 9.3 min (minor), 10.5 min (major); [α]_D²⁵ 91.00 (*c* 0.06, CHCl₃); HRMS (ESI) *m/z*: [M+H]⁺ Calcd for C₂₈H₂₆³⁵ClN₂O₄⁺, 489.1576; found 489.1581.

Methyl (1R, 3S, 4R, 5R)-7-benzyl-8,9-dioxo-4-phenyl-1-(*p*-tolyl)-2,7-diazaspiro[4.4]nonane-3-carboxylate (exo'-3ea). (89.2 mg, 95.2%, >99% dr, 97% ee); pale yellow solid; mp 70–73 °C; ¹H NMR (400 MHz, CDCl₃): δ 7.25–7.30 (m, 2H), 7.02–7.18 (m, 10H), 6.51 (d, 2H, *J* = 7.5 Hz), 4.98 (s, 1H), 4.42 (d, 1H, *J* = 8.8 Hz), 4.34 (d, 1H, *J* = 8.8 Hz), 4.12 (s, 2H), 3.70 (s, 3H), 3.30 (d, 1H, *J* = 11.8 Hz), 3.17 (d, 1H, *J* = 11.8

Hz), 2.33 (s, 3H); ^{13}C NMR (101 MHz, CDCl_3): δ 202.6, 174.7, 159.0, 138.1, 135.2, 133.7, 133.2, 129.5, 129.1, 128.7, 128.2, 127.8, 127.62, 127.60, 126.3, 69.8, 59.9, 58.4, 56.9, 52.8, 48.1, 43.9, 21.3; HPLC (Daicel Chiralpak IH-3, *n*-hexane/2-propanol = 70/30, 1.0 mL/min, 254 nm); t_{R} = 28.1 min (minor), 32.3 min (major); $[\alpha]_{\text{D}}^{25}$ 32.25 (*c* 0.05, CHCl_3); HRMS (ESI) m/z : $[\text{M}+\text{Na}]^+$ calcd for $\text{C}_{29}\text{H}_{28}\text{N}_2\text{NaO}_4^+$, 491.1941; found 491.1930.

Methyl (1*R*, 3*S*, 4*S*, 5*R*)-7-benzyl-8,9-dioxo-4-phenyl-1-(*m*-tolyl)-2,7-diazaspiro[4.4]nonane-3-carboxylate (exo'-3*fa*). (93.7 mg, 99.9%, >99% dr, 98% ee); pale yellow solid; mp 66–68 °C; ^1H NMR (400 MHz, CDCl_3): δ 7.26–7.29 (m, 3H), 7.05–7.21 (m, 9H), 6.52 (d, 2H, J = 7.0 Hz), 5.02 (s, 1H), 4.66 (d, 1H, J = 8.9 Hz), 4.33 (d, 1H, J = 8.9 Hz), 4.16 (d, 1H, J = 14.7 Hz), 4.09 (d, 1H, J = 14.7 Hz), 3.74 (s, 3H), 3.42 (d, 1H, J = 12.1 Hz), 3.29 (d, 1H, J = 12.1 Hz), 2.27 (s, 3H); ^{13}C NMR (101 MHz, CDCl_3): δ 202.6, 174.7, 159.1, 138.5, 136.4, 135.2, 133.8, 129.4, 129.1, 128.8, 128.7, 128.2, 127.8, 127.7, 127.6, 127.0, 123.6, 69.9, 59.9, 58.3, 57.0, 52.8, 48.1, 44.0, 21.6; HPLC (Daicel Chiralpak AD-H, *n*-hexane/2-propanol = 70/30, 1.0 mL/min, 254 nm); t_{R} = 10.8 min (major), 14.0 min (minor); $[\alpha]_{\text{D}}^{25}$ 26.35 (*c* 0.05, CHCl_3); HRMS (ESI) m/z : $[\text{M}+\text{Na}]^+$ Calcd for $\text{C}_{29}\text{H}_{28}\text{N}_2\text{NaO}_4^+$, 491.1941; found 491.1942.

Methyl (1*R*, 3*S*, 4*S*, 5*R*)-7-benzyl-8,9-dioxo-4-phenyl-1-(*o*-tolyl)-2,7-diazaspiro[4.4]nonane-3-carboxylate (exo'-3*ga*). (82.1 mg, 87.6%, 91% dr, 98% ee); Pale yellow solid; mp 55–57 °C; ^1H NMR (400 MHz, CDCl_3): δ 7.68–7.72 (m, 1H), 7.05–7.30 (m, 11H), 6.57 (d, 2H, J = 7.5 Hz), 5.15 (s, 1H), 4.36 (d, 1H, J = 7.7 Hz), 4.30 (d, 1H, J = 7.7 Hz), 4.17 (d, 1H, J = 14.8 Hz), 4.00 (d, 1H, J = 14.8 Hz), 3.73 (s, 3H), 3.37 (d, 1H, J = 11.8 Hz), 3.05 (d, 1H, J = 11.8 Hz), 2.11 (s, 3H); ^{13}C NMR (101 MHz, CDCl_3): δ 202.6, 174.7, 158.9, 136.4, 136.1, 134.8, 133.8, 131.2, 129.1, 128.9, 128.3, 128.2, 128.0, 127.8, 127.7, 127.5, 125.9, 65.8, 61.1, 58.5, 57.0, 52.8, 48.2, 44.4, 19.9; HPLC (Daicel Chiralpak IC-3, *n*-hexane/EtOAc = 70/30, 1.0 mL/min, 254 nm); t_{R} = 9.40 min (minor), 12.3 min (major); $[\alpha]_{\text{D}}^{25}$ 43.49 (*c* 0.06, CHCl_3); HRMS (ESI) m/z : $[\text{M}+\text{Na}]^+$ Calcd for $\text{C}_{29}\text{H}_{28}\text{N}_2\text{NaO}_4^+$, 491.1941; found 491.1921.

Methyl (1R, 3S, 4S, 5R)-7-benzyl-8,9-dioxo-4-phenyl-1-(4-(trifluoromethyl)phenyl)-2,7-diazaspiro[4.4]nonane-3-carboxylate (exo'-3ha). (70.4 mg, 67.4%, 78% dr, 96% ee); pale yellow solid; mp 166–169 °C; ¹H NMR (400 MHz, CDCl₃): δ 7.44–7.49 (m, 2H), 7.33–7.37 (m, 2H), 7.28–7.31 (m, 3H), 7.13–7.19 (m, 3H), 7.05–7.11 (m, 2H), 6.54 (d, 2H, *J* = 7.0 Hz), 5.05 (s, 1H), 4.44 (d, 1H, *J* = 9.0 Hz), 4.33 (d, 1H, *J* = 9.0 Hz), 4.28 (d, 1H, *J* = 14.6 Hz), 3.95 (d, 1H, *J* = 14.6 Hz), 3.71 (s, 3H), 3.22 (d, 1H, *J* = 12.0 Hz), 3.16 (d, 1H, *J* = 12.0 Hz); ¹³C NMR (101 MHz, CDCl₃): δ 202.2, 174.5, 158.7, 140.6 (q, *J*_{C-F} = 1.2 Hz), 134.6, 133.5, 130.7 (q, *J*_{C-F} = 32.6 Hz), 129.2, 128.9, 128.5, 128.0, 127.8, 127.7, 126.9, 125.7 (q, *J*_{C-F} = 3.6 Hz), 123.9 (q, *J*_{C-F} = 273 Hz), 69.2, 59.7, 58.1, 57.2, 53.0, 48.2, 43.6; HPLC (Daicel Chiralpak IH-3, *n*-hexane/2-propanol = 70/30, 1.0 mL/min, 254 nm); *t*_R = 16.4 min (minor), 28.5 min (major); [α]_D²⁵ 38.27 (*c* 0.06, CHCl₃); HRMS (ESI) *m/z*: [M+Na]⁺ Calcd for C₂₉H₂₅F₃N₂NaO₄⁺, 545.1659; found 545.1658.

Methyl (1R, 3S, 4S, 5R)-7-benzyl-1-(4-methoxyphenyl)-8,9-dioxo-4-phenyl-2,7-diazaspiro[4.4]nonane-3-carboxylate (exo'-3ia). (85.2 mg, 87.9%, >99% dr, 95% ee); pale yellow solid; mp 99–102 °C; ¹H NMR (400 MHz, CDCl₃): δ 7.26–7.27 (m, 3H), 7.06–7.20 (m, 7H), 6.74 (d, 2H, *J* = 8.8 Hz), 6.51 (d, 2H, *J* = 7.5 Hz), 4.95 (s, 1H), 4.31–4.36 (m, 2H), 4.20 (d, 1H, *J* = 14.8 Hz), 4.07 (d, 1H, *J* = 14.8 Hz), 3.80 (s, 3H), 3.70 (s, 3H), 3.25 (d, 1H, *J* = 11.8 Hz), 3.14 (d, 1H, *J* = 11.8 Hz); ¹³C NMR (101 MHz, CDCl₃): δ 202.7, 174.8, 159.6, 159.0, 135.3, 133.8, 129.1, 128.8, 128.2, 128.1, 127.8, 127.7, 127.6, 127.5, 114.1, 69.7, 59.8, 58.5, 56.7, 55.3, 52.8, 48.1, 43.9; HPLC (Daicel Chiralpak IH-3, *n*-hexane/2-propanol = 70/30, 1.0 mL/min, 250 nm); *t*_R = 40.5 min (minor), 51.0 min (major); [α]_D²⁵ 36.41 (*c* 0.06, CHCl₃); HRMS (ESI) *m/z*: [M+Na]⁺ Calcd for C₂₉H₂₈N₂NaO₅⁺, 507.1890; found 507.1889.

Methyl (1R, 3S, 4S, 5R)-7-benzyl-8,9-dioxo-1,4-diphenyl-2,7-diazaspiro[4.4]nonane-3-carboxylate (exo'-3ja). (75.1 mg, 82.6%, >99% dr, 94% ee); pale yellow solid; mp 126–130 °C; ¹H NMR (400 MHz, CDCl₃): δ 7.25–7.28 (m, 8H), 7.11–7.20 (m, 3H), 7.04–7.10 (m, 2H), 6.49 (d, 2H, *J* = 7.0 Hz), 5.03 (s, 1H), 4.44 (d, 1H, *J* = 8.8 Hz), 4.35 (d, 1H, *J* = 8.8 Hz), 4.13 (d, 1H, *J* = 14.7 Hz), 4.07 (d, 1H, *J* = 14.7 Hz), 3.71 (s, 3H), 3.27 (d, 1H, *J*

= 11.9 Hz), 3.18 (d, 1H, $J = 11.9$ Hz); ^{13}C NMR (101 MHz, CDCl_3): δ 202.5, 174.7, 159.0, 136.4, 135.1, 133.7, 129.1, 128.9, 128.8, 128.6, 128.2, 127.8, 127.7, 127.6, 126.5, 69.9, 59.9, 58.4, 56.9, 52.9, 48.1, 43.9; HPLC (Daicel Chiralpak IC-3, *n*-hexane/EtOAc = 70/30, 1.0 mL/min, 254 nm); $t_{\text{R}} = 13.8$ min (minor), 15.2 min (major); $[\alpha]_{\text{D}}^{25}$ 66.07 (c 0.06, CHCl_3); HRMS (ESI) m/z : $[\text{M}+\text{Na}]^+$ Calcd for $\text{C}_{28}\text{H}_{26}\text{N}_2\text{NaO}_4^+$, 477.1785; found 477.1787.

Methyl (1S, 3S, 4S, 5R)-7-benzyl-8,9-dioxo-4-phenyl-1-(thiophen-2-yl)-2,7-diazaspiro[4.4]nonane-3-carboxylate (exo'-3ka). (88.3 mg, 95.9%, >99% dr, 86% ee); pale yellow solid; mp 70–72 °C; ^1H NMR (400 MHz, CDCl_3): δ 7.10–7.28 (m, 9H), 6.91 (dd, 1H, $J = 5.0, 3.6$ Hz), 6.80 (m, 1H), 6.60 (d, 2H, $J = 7.3$ Hz), 5.25 (s, 1H), 4.34 (d, 1H, $J = 9.0$ Hz), 4.22–4.28 (m, 2H), 4.18 (d, 1H, $J = 14.8$ Hz), 3.68 (s, 3H), 3.47 (d, 1H, $J = 11.8$ Hz), 3.19 (d, 1H, $J = 11.8$ Hz); ^{13}C NMR (101 MHz, CDCl_3): δ 201.9, 174.3, 158.9, 140.3, 134.6, 133.8, 129.2, 128.9, 128.3, 127.78, 127.75, 127.7, 127.5, 125.0, 124.6, 66.2, 59.8, 58.5, 56.6, 52.9, 48.2, 44.1; HPLC (Daicel Chiralpak IC-3, *n*-hexane/EtOAc = 70/30, 1.0 mL/min, 254 nm); $t_{\text{R}} = 16.8$ min (minor), 19.3 min (major); $[\alpha]_{\text{D}}^{25}$ 37.27 (c 0.07, CHCl_3); HRMS (ESI) m/z : $[\text{M}+\text{Na}]^+$ Calcd for $\text{C}_{26}\text{H}_{24}\text{N}_2\text{NaO}_4\text{S}^+$, 483.1349; found 483.1353.

Methyl (1R, 3S, 4S, 5R)-7-benzyl-4-(4-bromophenyl)-1-(4-chlorophenyl)-8,9-dioxo-2,7-diazaspiro[4.4]nonane-3-carboxylate (exo'-3ab). (91.9 mg, 80.9%, 84% dr, 97% ee); pale yellow solid; mp 93–96 °C; ^1H NMR (400 MHz, CDCl_3): δ 7.34–7.39 (m, 2H), 7.25–7.27 (m, 1H), 7.12–7.20 (m, 6H), 6.95–7.00 (m, 2H), 6.59 (d, 2H, $J = 7.0$ Hz), 4.95 (s, 1H), 4.30 (d, 1H, $J = 8.9$ Hz), 4.24 (d, 1H, $J = 8.9$ Hz), 4.20 (d, 1H, $J = 14.7$ Hz), 4.15 (d, 1H, $J = 14.7$ Hz), 3.70 (s, 3H), 3.20 (d, 1H, $J = 12.0$ Hz), 3.13 (d, 1H, $J = 12.0$ Hz); ^{13}C NMR (101 MHz, CDCl_3): δ 202.2, 174.2, 158.6, 134.6, 134.4, 133.8, 133.5, 132.4, 129.4, 129.1, 129.0, 128.1, 127.82, 127.77, 122.5, 69.2, 59.8, 57.9, 56.4, 53.0, 48.3, 43.5; HPLC (Daicel Chiralpak AD-H, *n*-hexane/2-propanol = 70/30, 1.0 mL/min, 254 nm); $t_{\text{R}} = 18.9$ min (major), 26.9 min (minor); $[\alpha]_{\text{D}}^{25}$ 22.80 (c 0.06, CHCl_3); HRMS (ESI) m/z : $[\text{M}+\text{H}]^+$ Calcd for $\text{C}_{28}\text{H}_{25}^{79}\text{Br}^{35}\text{ClN}_2\text{O}_4^+$, 567.0681; found 567.0657.

Methyl (1R, 3S, 4S, 5R)-7-benzyl-1-(4-chlorophenyl)-8,9-dioxo-4-(4-(trifluoromethyl)phenyl)-2,7-diazaspiro[4.4]nonane-3-carboxylate (exo'-3ac). (91.2 mg, 81.9%, >99% dr, 96% ee); pale yellow solid; mp 104–107 °C; ¹H NMR (400 MHz, CDCl₃): δ 7.49–7.54 (m, 2H), 7.22–7.25 (m, 2H), 7.12–7.19 (m, 7H), 6.61 (d, 2H, *J* = 7.0 Hz), 4.96 (s, 1H), 4.45 (d, 1H, *J* = 8.9 Hz), 4.34 (d, 1H, *J* = 8.9 Hz), 4.19 (d, 1H, *J* = 14.4 Hz), 4.11 (d, 1H, *J* = 14.4 Hz), 3.72 (s, 3H), 3.29 (d, 1H, *J* = 12.2 Hz), 3.12 (d, 1H, *J* = 12.2 Hz); ¹³C NMR (101 MHz, CDCl₃): δ 201.9, 174.1, 158.5, 139.0 (q, *J*_{C-F} = 1.3 Hz), 134.5, 134.4, 133.5, 130.5 (q, *J*_{C-F} = 32.8 Hz), 129.1, 129.0, 128.3, 128.2, 127.9, 127.8, 126.2 (q, *J*_{C-F} = 3.8 Hz), 123.8 (d, *J*_{C-F} = 272 Hz), 69.4, 59.9, 57.9, 56.2, 53.0, 48.3, 43.4; HPLC (Daicel Chiralpak IC-3, *n*-hexane/EtOAc = 70/30, 1.0 mL/min, 254 nm); *t*_R = 7.15 min (major), 7.73 min (minor); [α]_D²⁵ 48.18 (*c* 0.05, CHCl₃); HRMS (ESI) *m/z*: [M+H]⁺ Calcd for C₂₉H₂₅³⁵ClF₃N₂O₄⁺, 557.1449; found 557.1428.

Methyl (1R, 3S, 4S, 5R)-7-benzyl-1-(4-chlorophenyl)-8,9-dioxo-4-(*p*-tolyl)-2,7-diazaspiro[4.4]nonane-3-carboxylate (exo'-3ad). (91.0 mg, 90.4%, >99% dr, 97% ee); pale yellow solid; mp 88–92 °C; ¹H NMR (400 MHz, CDCl₃): δ 7.21–7.25 (m, 1H), 7.11–7.15 (m, 6H), 7.04–7.10 (m, 2H), 6.99–7.04 (m, 2H), 6.57 (d, 2H, *J* = 7.2 Hz), 4.96 (s, 1H), 4.39 (d, 1H, *J* = 8.9 Hz), 4.35 (d, 1H, *J* = 14.6 Hz), 4.29 (d, 1H, *J* = 8.9 Hz), 3.96 (d, 1H, *J* = 14.6 Hz), 3.70 (s, 3H), 3.21 (s, 2H), 2.33 (s, 3H); ¹³C NMR (101 MHz, CDCl₃): δ 202.5, 174.6, 158.8, 138.0, 134.9, 134.3, 133.6, 131.7, 129.9, 129.0, 128.9, 127.9, 127.77, 127.75, 127.6, 69.2, 59.8, 58.1, 56.7, 52.9, 48.2, 43.7, 21.2; HPLC (Daicel Chiralpak IH-3, *n*-hexane/2-propanol = 70/30, 1.0 mL/min, 250 nm); *t*_R = 23.1 min (minor), 28.1 min (minor); [α]_D²⁵ 41.5 (*c* 0.07, CDCl₃); HRMS (ESI) *m/z*: [M+Na]⁺ calcd for C₂₉H₂₇³⁵ClN₂NaO₄⁺, 525.1552; found 525.1541.

Methyl (1R, 3S, 4S, 5R)-7-benzyl-1-(4-chlorophenyl)-4-(4-methoxyphenyl)-8,9-dioxo-2,7-diazaspiro[4.4]nonane-3-carboxylate (exo'-3ae). (85.0 mg, 81.9%, >99% dr, 96% ee); pale yellow solid; mp 80–83 °C; ¹H NMR (400 MHz, CDCl₃): δ 7.12–7.21 (m, 7H), 7.03–7.09 (m, 2H), 6.75–6.82 (m, 2H), 6.57 (d, 2H, *J* = 7.1 Hz), 4.98 (s, 1H), 4.40 (d, 1H, *J* = 8.9 Hz), 4.32 (d, 1H, *J* = 14.6 Hz), 4.27 (d, 1H, *J* = 8.9 Hz), 4.02 (d, 1H, *J* = 14.6 Hz),

3.81 (s, 3H), 3.71 (s, 3H), 3.24 (s, 2H); ^{13}C NMR (101 MHz, CDCl_3): δ 202.6, 174.6, 159.3, 158.8, 135.0, 134.2, 133.7, 129.0, 128.9 (two peaks overlapped), 127.9, 127.8, 127.7, 126.6, 114.5, 69.1, 60.0, 58.3, 56.6, 55.3, 52.9, 48.2, 43.6; HPLC (Daicel Chiralpak AD-H, *n*-hexane/2-propanol = 70/30, 1.0 mL/min, 254 nm); t_{R} = 17.8 min (major), 27.7 min (minor); $[\alpha]_{\text{D}}^{25}$ 40.05 (*c* 0.06, CHCl_3); HRMS (ESI) m/z : $[\text{M}+\text{Na}]^+$ Calcd for $\text{C}_{29}\text{H}_{27}^{35}\text{ClN}_2\text{NaO}_5^+$, 541.1501; found 541.1496.

Methyl (1R, 3S, 4S, 5R)-7-benzyl-1-(4-chlorophenyl)-8,9-dioxo-4-(*m*-tolyl)-2,7-diazaspiro[4.4]nonane-3-carboxylate (*exo'*-3af). (82.8 mg, 82.3%, 90% dr, 96% ee); pale yellow solid; mp 69–72 °C; ^1H NMR (400 MHz, CDCl_3): δ 7.07–7.25 (m, 9H), 6.91–6.95 (m, 2H), 6.56 (d, 2H, J = 7.1 Hz), 4.93 (s, 1H), 4.38 (d, 1H, J = 8.7 Hz), 4.32 (d, 1H, J = 14.4 Hz), 4.30 (d, 1H, J = 8.7 Hz), 3.98 (d, 1H, J = 14.4 Hz), 3.71 (s, 3H), 3.20 (s, 2H), 2.28 (s, 3H); ^{13}C NMR (101 MHz, CDCl_3): δ 202.4, 174.7, 158.8, 138.9, 134.9, 134.8, 134.3, 133.7, 129.2, 129.01, 128.98, 128.9, 128.5, 127.9, 127.8, 127.7, 124.8, 69.4, 59.9, 58.1, 56.8, 52.9, 48.2, 43.7, 21.6; HPLC (Daicel Chiralpak IC-3, *n*-hexane/EtOAc = 70/30, 1.0 mL/min, 254 nm); t_{R} = 9.96 min (minor), 12.8 min (major); $[\alpha]_{\text{D}}^{25}$ 27.41 (*c* 0.07, CHCl_3); HRMS (ESI) m/z : $[\text{M}+\text{Na}]^+$ Calcd for $\text{C}_{29}\text{H}_{27}^{35}\text{ClN}_2\text{NaO}_4^+$, 525.1552; found 525.1527.

Methyl (1R, 3S, 4S, 5R)-7-benzyl-4-(3-chlorophenyl)-1-(4-chlorophenyl)-8,9-dioxo-2,7-diazaspiro[4.4]nonane-3-carboxylate (*exo'*-3ag). (69.0 mg, 68.7%, 82% dr, 90% ee); pale yellow solid; mp 76–80 °C; ^1H NMR (400 MHz, CDCl_3): δ 7.10–7.27 (m, 10H), 6.97 (d, 1H, J = 7.6 Hz), 6.60 (d, 2H, J = 7.1 Hz), 4.90 (s, 1H), 4.28–4.31 (m, 3H), 4.04 (d, 1H, J = 14.6 Hz), 3.71 (s, 3H), 3.20 (d, 1H, J = 11.9 Hz), 3.11 (d, 1H, J = 11.9 Hz); ^{13}C NMR (101 MHz, CDCl_3): δ 202.1, 174.2, 158.6, 137.2, 135.1, 134.6, 134.5, 133.6, 130.5, 129.1, 129.0, 128.7, 128.1, 127.8, 127.8 (two peaks overlapped), 126.3, 69.4, 59.9, 57.9, 56.2, 53.0, 48.3, 43.6; HPLC (Daicel Chiralpak IC-3, *n*-hexane/EtOAc = 70/30, 1.0 mL/min, 254 nm); t_{R} = 9.7 min (minor), 10.9 min (major); $[\alpha]_{\text{D}}^{25}$ 22.43 (*c* 0.05, CHCl_3); HRMS (ESI) m/z : $[\text{M}+\text{H}]^+$ Calcd for $\text{C}_{28}\text{H}_{25}^{35}\text{Cl}_2\text{N}_2\text{O}_4^+$, 523.1186; found 523.1166.

Methyl (1R, 3S, 4S, 5R)-7-benzyl-1-(4-chlorophenyl)-8,9-dioxo-4-(*o*-tolyl)-2,7-

diazaspiro[4.4]nonane-3-carboxylate (exo'-3ah). (94.4 mg, 93.8%, 76% dr, 81% ee); pale yellow solid; mp 70–73 °C; ¹H NMR (400 MHz, CDCl₃): δ 7.09–7.28 (m, 11H), 6.62 (d, 2H, *J* = 7.0 Hz), 4.78 (s, 1H), 4.62 (d, 1H, *J* = 6.6 Hz), 4.41 (d, 1H, *J* = 14.6 Hz), 4.14 (d, 1H, *J* = 6.6 Hz), 3.85 (d, 1H, *J* = 14.6 Hz), 3.75 (s, 3H), 3.33 (d, 1H, *J* = 11.9 Hz), 3.19 (d, 1H, *J* = 11.9 Hz), 2.21 (s, 3H); ¹³C NMR (101 MHz, CDCl₃): δ 202.6, 174.8, 158.6, 137.1, 135.2, 134.6, 134.4, 133.6, 131.5, 129.0, 128.9, 128.1, 127.99, 127.97, 127.94, 127.89, 126.3, 77.6, 64.1, 57.7, 52.9, 51.3, 48.3, 44.4, 20.2; HPLC (Daicel Chiralpak IC-3, *n*-hexane/EtOAc = 70/30, 1.0 mL/min, 254 nm); *t*_R = 9.30 min (minor), 9.92 min (major); [α]_D²⁵ 13.65 (*c* 0.05, CHCl₃); HRMS (ESI) *m/z*: [M+Na]⁺ calcd for C₂₉H₂₇³⁵ClN₂NaO₄⁺, 525.1552; found 525.1529.

Methyl (1R, 3S, 4S, 5R)-7-benzyl-1-(4-chlorophenyl)-8,9-dioxo-4-(thiophen-2-yl)-2,7-diazaspiro[4.4]nonane-3-carboxylate (exo'-3ai). (71.7 mg, 72.4%, 90% dr, 95% ee); pale yellow solid; mp 158–160 °C; ¹H NMR (400 MHz, CDCl₃): δ 7.22–7.24 (m, 1H), 7.10–7.19 (m, 7H), 6.92 (dd, 1H, *J* = 5.1, 3.6 Hz), 6.84–6.87 (m, 1H), 6.63 (d, 2H, *J* = 7.0 Hz), 4.93 (s, 1H), 4.54 (dd, 1H, *J* = 9.0, 0.8 Hz), 4.48 (d, 1H, *J* = 14.6 Hz), 4.25 (d, 1H, *J* = 9.0 Hz), 4.00 (d, 1H, *J* = 14.6 Hz), 3.75 (s, 3H), 3.25 (d, 1H, *J* = 11.8 Hz), 3.20 (d, 1H, *J* = 11.8 Hz); ¹³C NMR (101 MHz, CDCl₃): δ 201.8, 174.0, 158.8, 138.0, 134.6, 134.4, 133.6, 129.0, 128.9, 128.0, 127.8, 127.7, 127.5, 126.3, 125.2, 68.6, 61.8, 58.2, 53.1, 52.4, 48.3, 43.8; HPLC (Daicel Chiralpak AD-H, *n*-hexane/2-propanol = 70/30, 1.0 mL/min, 254 nm); *t*_R = 17.1 min (major), 27.7 min (minor); [α]_D²⁵ 29.25 (*c* 0.05, CHCl₃); HRMS (ESI) *m/z*: [M+Na]⁺ Calcd for C₂₆H₂₃³⁵ClN₂NaO₄S⁺, 517.0959; found 517.0985.

Methyl (1R, 3S, 4S, 5R)-7-benzyl-1-(4-chlorophenyl)-4-(4-methoxyphenyl)-3-methyl-8,9-dioxo-2,7-diazaspiro[4.4]nonane-3-carboxylate (exo'-3le). (77.0 mg, 0.145 mmol, 72.2%, > 99% dr, 81% ee); pale yellow solid; mp 84–87 °C; ¹H NMR (400 MHz, CDCl₃): δ 7.12–7.21 (m, 9H), 6.77–6.80 (m, 4H), 4.65 (s, 1H), 4.29 (d, 1H, *J* = 14.3 Hz), 4.08 (s, 1H), 4.06 (d, 1H, *J* = 14.3 Hz), 3.86 (s, 3H), 3.80 (s, 3H), 3.17 (d, 1H, *J* = 11.8 Hz), 3.01 (d, 1H, *J* = 11.8 Hz), 1.24 (s, 3H); ¹³C NMR (101 MHz, CDCl₃): δ 202.6, 177.2, 159.1, 158.8, 135.9, 134.1, 133.8, 131.5, 128.9, 128.9, 128.3, 128.3, 128.2, 127.9, 114.1, 67.7,

67.3, 58.2, 57.4, 55.3, 53.0, 48.5, 46.6, 24.5; HPLC (Daicel Chiralpak AD-H, *n*-hexane/2-propanol = 70/30, 1.0 mL/min, 254 nm); t_R = 37.0 min (minor), 57.2 min (major); $[\alpha]_D^{25}$ 13.38 (*c* 0.06, CHCl₃); HRMS (ESI) m/z : [M+H]⁺ Calcd for C₃₀H₃₀³⁵ClN₂O₅⁺, 533.1838; found 533.1841.

Methyl (1R, 3S, 4S, 5R)-7-benzyl-8,9-dioxo-1,4-diphenyl-2,7-diazaspiro[4.4]nonane-3-carboxylate-1-d (exo'-3ma-d). (79.2 mg, 0.174 mmol, 86.9%, >99% dr, 98% ee); Pale yellow solid; mp 73–76 °C; ¹H NMR (400 MHz, CDCl₃): δ 7.26–7.28 (m, 6H), 7.05–7.19 (m, 7H), 6.49 (d, 2H, *J* = 7.1 Hz), 4.50 (d, 1H, *J* = 8.7 Hz), 4.34 (d, 1H, *J* = 8.7 Hz), 4.13 (d, 1H, *J* = 14.9 Hz), 4.07 (d, 1H, *J* = 14.9 Hz), 3.72 (s, 3H), 3.31 (d, 1H, *J* = 12.0 Hz), 3.21 (d, 1H, *J* = 12.0 Hz); ¹³C NMR (101 MHz, CDCl₃): δ 202.5, 174.6, 159.0, 136.2, 135.0, 133.7, 129.1, 128.9, 128.8, 128.6, 128.3, 127.8, 127.7, 127.5, 126.4, 70.6, 59.9, 58.3, 56.9, 52.9, 48.1, 43.9; HPLC (Daicel Chiralpak IC-3, *n*-hexane/EtOAc = 70/30, 1.0 mL/min, 254 nm); t_R = 12.3 min (minor), 13.3 min (major); $[\alpha]_D^{25}$ 33.80 (*c* 0.06, CHCl₃); HRMS (ESI) m/z : [M+H]⁺ Calcd for C₂₈H₂₆³⁵ClN₂O₄⁺, 456.2028; found 456.2009.

X-ray Crystallographic Analysis. The crystallographic data of *exo'*-**3ae** and *rac-exo'*-**3le** were summarized in Table S3-1. Single crystals of *exo'*-**3ae** were prepared from CH₂Cl₂/MeCN co-solvent by antisolvent addition technique using *n*-hexane as an antisolvent and single crystals of *rac-exo'*-**3le** were prepared from tetrahydrofuran by vapor diffusion technique using ethanol as an antisolvent. A suitable single crystal was respectively selected and mounted on the glass fiber and transferred to the goniometer of a Rigaku VariMax Saturn CCD diffractometer with graphite-monochromated MoK α radiation ($\lambda = 71.073$ pm). Yadokari-XG 2009 program was used as a graphical interface. The structure was solved and refined by SIR-2004 by SHELX-97 programs. The refinement was performed anisotropically for all non-hydrogen atoms. Hydrogen atoms were placed using AFIX instructions.

In the case of *rac-exo'*-**3le**, *CrystalStructure* crystallographic software package was used as a graphical interface. The structure was solved and refined by SHELXS Version 2014/5 and SHELXL Version 2016/6. The difference Fourier maps has suggested that the voids of each crystal were occupied by tetrahydrofuran molecules, which could not be appropriate because of heavy disorders. The electron density associated with the solvent molecule was removed by SQUEEZE routine of PLATON.

Table S3-1. Crystal data and structure refinements for *exo'*-**3ae** and *rac-exo'*-**3le**.

Compound	<i>exo'</i> - 3ae	<i>rac-exo'</i> - 3le
CCDC	2125423	2125424
Empirical formula	C ₂₉ H ₂₇ ClN ₂ O ₅	C ₃₄ H ₃₇ ClN ₂ O ₆
Formula weight	518.97	605.13
Crystal system	orthorhombic	monoclinic
Space group	P 2ac 2ab	-I 2ya
a, Å	8.665(18)	22.549(9)
b, Å	9.860(2)	22.549(9)
c, Å	29.967(6)	33.331(13)
α, °	90	90
β, °	90	93.82(2)
γ, °	90	90
Volume, Å ³	2560.5(9)	6277(4)
Z	4	8
Temperature, K	93(2)	93
2θ range for data collection, °	6.826 to 54.950	6.100 to 54.846
σ _{calcd} , g cm ⁻³	1.346	1.281
μ, mm ⁻¹	0.192	0.169
F(000)	1088	2560.00
Crystal size, mm ³	0.150 × 0.140 × 0.100	0.223 × 0.127 × 0.103
Crystal color, habit	colorless, block	colorless, block
Radiation	MoKα	MoKα
Reflections collected	20971	24474
Independent	5832	7102
Index ranges	-11 ≤ h ≤ 11, -12 ≤ k ≤ 12, -35 ≤ l ≤ 38	-29 ≤ h ≤ 28, -9 ≤ k ≤ 10, -40 ≤ l ≤ 42
Flack	0.09(5)	-
Absolute configuration	ad	-
Data/restraints/parameters	5832/0/334	7102/0/395
Final R indexes [<i>I</i> > 2σ(<i>I</i>)]	R1 = 0.0667, wR2 = 0.1529	R1 = 0.0848, wR2 = 0.1550
Final R indexes [all data]	R1 = 0.0910, wR2 = 0.1696	R1 = 0.1198, wR2 = 0.1715
Goodness-of-fit on <i>F</i> ²	1.024	1.000
Largest peak/deepest hole, e Å ⁻³	0.330/-0.337	0.748/-0.593

Computational Study. The molecular geometries for the transition states (TS) and the intermediates (INT) were calculated with the Gaussian 16 software package. The stationary points and the harmonic vibrational frequencies were calculated at B3PW91/LanL2DZ(Ag)+6-31G* level of theory to estimate the Gibbs free energy. All Gibbs free energy values were calculated at 298.15 K, and all transition structures were optimized without constraints. Transition structures show only one negative eigenvalue in their diagonalized force constant matrices, and their associated eigenvectors were confirmed to correspond to the motion along the reaction coordinate. The intrinsic reaction coordinate (IRC) routes were calculated in both directions toward the corresponding minima for each transition-state structure. When the IRC calculations failed to reach the energy minima on the potential energy surface, geometry optimizations were carried out as a continuation of the IRC path.

Table S3-2. Total electronic energies (E, in a.u.), thermal correction to Gibbs free energy (TCGFE, in a.u.), and number of imaginary frequencies (NIMAG) in the Mannich reaction of the Michael adduct formed by the (3+2) cycloaddition of 2,3-dioxopyrrolidine **2** with azomethine ylide derived from imino ester **1** and AgOAc/PPh₃ complex. ^a

Structure	E (a.u.)	TCGFE (a.u.)	NIMAG (ν) ^b
INT-A1	-2674.02359268	0.659966	0
INT-A2	-2674.02133364	0.658504	0
INT-A3	-2674.02652407	0.661554	0
INT-A4	-2903.05853616	0.714692	0
TS-A	-2903.04989357	0.719373	1 (-336.42)
INT-A5	-2903.05880482	0.722152	0
product (2,5- <i>trans</i>)	-1492.67502243	0.426970	0
INT-B4	-2903.05100039	0.720137	0
TS-B	-2903.03829860	0.720745	1 (-122.03)
INT-B5	-2903.05251132	0.722058	0
product (2,5- <i>cis</i>)	-1492.67142254	0.425662	0
TS-C	-2674.01290641	0.659279	1 (-348.59)
INT-C1	-2674.01802458	0.661298	0

^[a] Computed at B3PW91/LanL2DZ(Ag)+6-31G*(other atoms) with gd3bj level of theory. ^[b] The number in parentheses shows the imaginary frequency ν (cm⁻¹).

Table S3-3. Total electronic energies (E, in a.u.), thermal correction to Gibbs free energy (TCGFE, in a.u.), and number of imaginary frequencies (NIMAG) in the Mannich reaction of the Michael adduct formed by the (3+2) cycloaddition using N-CO₂Me-substituted ylidene-succinimide as the activated olefin.^a

Structure	E (a.u.)	TCGFE (a.u.)	NIMAG (ν) ^b
INT-D1	-2631.53904573	0.597027	0
TS-D	-2631.53599266	0.598001	1 (-316.30)
INT-D2	-2631.54321324	0.598097	0
product (<i>endo</i>)	-1450.20082262	0.360674	0
INT-E2	-2631.53067129	0.593800	0
INT-E3	-2631.52545236	0.596672	0
INT-E4	-2860.57048183	0.654942	0
TS-E	-2860.54599304	0.655019	1 (-142.54)
INT-E5	-2860.57400451	0.658226	0
product (<i>2,5-trans</i>)	-1450.19873118	0.360632	0

^[a] Computed at B3PW91/LanL2DZ(Ag)+6-31G*(other atoms) with gd3bj level of theory. ^[b] The number in parentheses shows the imaginary frequency ν (cm⁻¹).

INT-A1

Center Number	Atomic Number	Atomic Type	Coordinates (Angstroms)		
			X	Y	Z
1	47	0	1.104359	0.950080	-0.004707
2	15	0	3.220859	-0.037761	0.556928
3	6	0	4.162538	0.653938	1.958145
4	6	0	3.486320	0.784603	3.179662
5	6	0	5.499335	1.050351	1.861769
6	6	0	4.147769	1.292456	4.293499
7	1	0	2.444034	0.480205	3.254180
8	6	0	6.156122	1.569137	2.979303
9	1	0	6.028284	0.952692	0.917786
10	6	0	5.484484	1.688219	4.194971
11	1	0	3.619076	1.384890	5.238695
12	1	0	7.195745	1.876618	2.897540
13	1	0	5.998283	2.090285	5.064388
14	6	0	4.406650	-0.022804	-0.832463
15	6	0	5.287030	-1.079531	-1.089145
16	6	0	4.402250	1.089581	-1.683341
17	6	0	6.152664	-1.021060	-2.180766

18	1	0	5.278024	-1.957933	-0.450831
19	6	0	5.270707	1.149258	-2.771446
20	1	0	3.703091	1.902961	-1.496523
21	6	0	6.146104	0.091423	-3.023583
22	1	0	6.827089	-1.850622	-2.378083
23	1	0	5.254917	2.014473	-3.429174
24	1	0	6.815438	0.130690	-3.879113
25	6	0	3.017625	-1.789179	1.007513
26	6	0	1.836523	-2.442661	0.640499
27	6	0	4.010334	-2.483333	1.716098
28	6	0	1.656448	-3.788123	0.958299
29	1	0	1.029101	-1.895954	0.164848
30	6	0	3.830838	-3.829775	2.021433
31	1	0	4.909491	-1.965657	2.042857
32	6	0	2.655256	-4.483346	1.637596
33	1	0	0.714746	-4.261757	0.697817
34	1	0	4.599879	-4.365962	2.572373
35	1	0	2.511854	-5.530730	1.892650
36	6	0	-2.289711	1.689911	-0.048952
37	6	0	-1.462487	2.227048	-1.330079
38	1	0	-1.596144	1.826134	0.790775
39	1	0	-2.171849	2.418921	-2.143367
40	6	0	-3.746477	-0.476699	-0.657706
41	1	0	-3.949060	-0.274252	-1.724850
42	1	0	-4.672658	-0.241772	-0.110832
43	6	0	-3.493790	2.568322	0.175691
44	6	0	-3.590305	3.329011	1.344940
45	6	0	-4.525448	2.657812	-0.766036
46	6	0	-4.689811	4.156450	1.572553
47	1	0	-2.795168	3.264870	2.084900
48	6	0	-5.627291	3.480553	-0.542744
49	1	0	-4.468596	2.081946	-1.687132
50	6	0	-5.713090	4.235167	0.628323
51	1	0	-4.747412	4.738018	2.489520
52	1	0	-6.420277	3.533634	-1.284743
53	1	0	-6.572074	4.877971	0.803034
54	7	0	-3.395413	-1.875244	-0.487216
55	6	0	-1.644003	-0.663952	0.418423
56	6	0	-2.208118	-2.052301	0.183406
57	8	0	-1.727488	-3.135621	0.498327
58	6	0	-4.338476	-2.942469	-0.709091
59	1	0	-4.671939	-2.935793	-1.755942
60	1	0	-3.783347	-3.872475	-0.537856
61	6	0	-5.535438	-2.860504	0.212025
62	6	0	-6.836780	-2.921115	-0.289359
63	6	0	-5.344303	-2.708511	1.590378
64	6	0	-7.935177	-2.839381	0.568977
65	1	0	-6.993688	-3.029204	-1.361313
66	6	0	-6.437522	-2.622425	2.448593
67	1	0	-4.332512	-2.654802	1.985343
68	6	0	-7.737416	-2.688378	1.940486
69	1	0	-8.943312	-2.885710	0.164190
70	1	0	-6.276115	-2.503485	3.517171
71	1	0	-8.590099	-2.618748	2.611223

72	7	0	-0.451184	1.284135	-1.687617
73	6	0	-2.549215	0.238222	-0.115862
74	8	0	-0.534879	-0.453806	1.000878
75	6	0	-0.865611	0.202990	-2.258651
76	6	0	0.037159	-0.920202	-2.523046
77	6	0	-0.473639	-2.223147	-2.556228
78	6	0	1.416272	-0.718173	-2.687989
79	6	0	0.386255	-3.310086	-2.693735
80	1	0	-1.539899	-2.383561	-2.421197
81	6	0	2.268931	-1.802424	-2.856723
82	1	0	1.809076	0.294093	-2.696098
83	6	0	1.757415	-3.102188	-2.841431
84	1	0	-0.015518	-4.319124	-2.668887
85	1	0	3.333098	-1.633074	-2.987506
86	1	0	2.428641	-3.951099	-2.941431
87	1	0	-1.898692	0.104129	-2.606939
88	8	0	0.172365	3.550434	-0.164619
89	8	0	-1.461511	4.592562	-1.314515
90	6	0	-0.807080	3.510587	-0.889045
91	6	0	-0.998781	5.845545	-0.796723
92	1	0	0.040062	6.019019	-1.089416
93	1	0	-1.655524	6.598656	-1.231735
94	1	0	-1.075892	5.850464	0.293658

INT-A2

Center Number	Atomic Number	Atomic Type	Coordinates (Angstroms)		
			X	Y	Z
1	47	0	-1.301725	-0.213764	0.628229
2	15	0	-3.650637	-0.044159	0.483544
3	6	0	-4.477731	0.547587	1.998909
4	6	0	-3.832298	1.540012	2.747539
5	6	0	-5.730337	0.076295	2.406874
6	6	0	-4.442553	2.067140	3.882959
7	1	0	-2.850700	1.895136	2.439577
8	6	0	-6.334134	0.600107	3.549721
9	1	0	-6.228041	-0.705742	1.839464
10	6	0	-5.694002	1.597197	4.286096
11	1	0	-3.936193	2.836872	4.459319
12	1	0	-7.305060	0.226675	3.865279
13	1	0	-6.165519	2.002432	5.177604
14	6	0	-4.487530	-1.620788	0.119031
15	6	0	-5.327796	-1.811265	-0.980411
16	6	0	-4.201895	-2.702207	0.965273
17	6	0	-5.872540	-3.071234	-1.234712
18	1	0	-5.546918	-0.982616	-1.647144
19	6	0	-4.757811	-3.953281	0.718210
20	1	0	-3.529012	-2.564165	1.809197
21	6	0	-5.590500	-4.142064	-0.388196
22	1	0	-6.515064	-3.213948	-2.099790
23	1	0	-4.528138	-4.785684	1.378004

24	1	0	-6.011564	-5.123143	-0.591168
25	6	0	-4.186188	1.138700	-0.791491
26	6	0	-3.219696	1.697937	-1.634778
27	6	0	-5.529255	1.520356	-0.917759
28	6	0	-3.602790	2.610775	-2.617839
29	1	0	-2.171032	1.439774	-1.509962
30	6	0	-5.906280	2.427955	-1.903566
31	1	0	-6.275666	1.115556	-0.238574
32	6	0	-4.942459	2.969804	-2.758613
33	1	0	-2.847264	3.048033	-3.265302
34	1	0	-6.948737	2.720428	-2.000134
35	1	0	-5.237402	3.683047	-3.524181
36	6	0	3.698972	-1.236117	0.572022
37	6	0	3.737612	-2.267604	-0.639229
38	1	0	3.115527	-1.742652	1.347466
39	1	0	4.315327	-1.813175	-1.458800
40	6	0	3.446088	1.083213	-0.701963
41	1	0	3.916323	0.717400	-1.630076
42	1	0	4.176407	1.738084	-0.204927
43	6	0	5.094592	-0.981322	1.094584
44	6	0	5.402413	-1.286261	2.424324
45	6	0	6.107900	-0.461727	0.279639
46	6	0	6.682009	-1.066411	2.933356
47	1	0	4.627927	-1.707074	3.061084
48	6	0	7.387967	-0.238554	0.783088
49	1	0	5.905317	-0.243428	-0.765798
50	6	0	7.680080	-0.538540	2.114277
51	1	0	6.899482	-1.311495	3.970221
52	1	0	8.160249	0.165416	0.132755
53	1	0	8.678881	-0.366568	2.507761
54	7	0	2.243798	1.830863	-1.036478
55	6	0	1.594592	0.133125	0.387969
56	6	0	1.151255	1.331348	-0.402118
57	8	0	-0.005908	1.767859	-0.488734
58	6	0	2.263524	3.095540	-1.726284
59	1	0	2.736241	2.974403	-2.710024
60	1	0	1.213830	3.365913	-1.892162
61	6	0	2.972493	4.180903	-0.945242
62	6	0	3.832134	5.075110	-1.586385
63	6	0	2.768566	4.304272	0.433210
64	6	0	4.473244	6.085139	-0.867363
65	1	0	4.006599	4.978152	-2.656646
66	6	0	3.411381	5.307616	1.154605
67	1	0	2.110250	3.603766	0.941445
68	6	0	4.264653	6.203065	0.506158
69	1	0	5.142579	6.772279	-1.379162
70	1	0	3.248656	5.389376	2.226388
71	1	0	4.768691	6.983431	1.070564
72	7	0	2.389355	-2.571403	-1.014302
73	6	0	2.942209	-0.021354	0.177924
74	8	0	0.769011	-0.572232	1.078231
75	6	0	1.858421	-1.732672	-1.819916
76	6	0	0.426384	-1.711323	-2.123862
77	6	0	-0.065988	-0.758392	-3.024000

78	6	0	-0.470320	-2.582436	-1.485349
79	6	0	-1.427394	-0.691720	-3.310361
80	1	0	0.626030	-0.058784	-3.488568
81	6	0	-1.829343	-2.521661	-1.780984
82	1	0	-0.074845	-3.289729	-0.762597
83	6	0	-2.309467	-1.578821	-2.695695
84	1	0	-1.802673	0.055500	-4.004463
85	1	0	-2.522968	-3.199163	-1.291414
86	1	0	-3.371826	-1.527798	-2.913789
87	1	0	2.454455	-0.960355	-2.332594
88	8	0	4.087230	-4.243231	0.723977
89	8	0	5.637951	-3.657723	-0.806113
90	6	0	4.466030	-3.506485	-0.157604
91	6	0	6.465090	-4.719666	-0.325242
92	1	0	5.955698	-5.681461	-0.432570
93	1	0	7.366343	-4.689868	-0.938565
94	1	0	6.710282	-4.556859	0.728082

INT-A3

Center Number	Atomic Number	Atomic Type	Coordinates (Angstroms)		
			X	Y	Z
1	47	0	1.401566	-0.559071	-1.541246
2	15	0	3.301892	0.154165	-0.318139
3	6	0	2.979620	-0.156733	1.446785
4	6	0	2.413831	-1.390296	1.795215
5	6	0	3.186822	0.816789	2.429204
6	6	0	2.052259	-1.641566	3.115019
7	1	0	2.202245	-2.137543	1.035781
8	6	0	2.817185	0.560401	3.748700
9	1	0	3.600515	1.784338	2.161044
10	6	0	2.245552	-0.663905	4.091906
11	1	0	1.579698	-2.587190	3.364715
12	1	0	2.950818	1.330852	4.503235
13	1	0	1.929873	-0.847672	5.115342
14	6	0	3.590119	1.948211	-0.427871
15	6	0	4.843162	2.505983	-0.144194
16	6	0	2.508375	2.779625	-0.746946
17	6	0	5.009170	3.889464	-0.164225
18	1	0	5.685465	1.859295	0.088209
19	6	0	2.681197	4.163340	-0.757322
20	1	0	1.539364	2.354981	-1.004484
21	6	0	3.926942	4.719408	-0.464291
22	1	0	5.983569	4.319440	0.053401
23	1	0	1.840336	4.804015	-1.010126
24	1	0	4.058886	5.798355	-0.480649
25	6	0	4.925590	-0.595345	-0.658390
26	6	0	5.354683	-0.671141	-1.989977
27	6	0	5.751659	-1.069960	0.365215
28	6	0	6.605023	-1.203309	-2.292077
29	1	0	4.707470	-0.312291	-2.787771

30	6	0	7.000419	-1.611138	0.057507
31	1	0	5.416241	-1.019748	1.397497
32	6	0	7.429370	-1.675575	-1.267820
33	1	0	6.933747	-1.257602	-3.326585
34	1	0	7.637348	-1.982590	0.856176
35	1	0	8.402156	-2.098386	-1.504972
36	6	0	-2.943407	-2.410755	-0.493625
37	6	0	-1.895851	-2.992460	0.547296
38	6	0	-0.827954	-1.094222	1.371178
39	1	0	-2.840077	-3.046626	-1.378315
40	1	0	-2.375210	-3.877638	0.988111
41	1	0	-0.161681	-1.088996	0.503780
42	6	0	-2.591591	-1.010491	-0.873413
43	6	0	-3.276359	0.204511	-0.320643
44	1	0	-3.344516	0.168446	0.777009
45	1	0	-4.293317	0.356753	-0.708031
46	6	0	-0.646461	-3.529724	-0.157095
47	7	0	-1.658782	-2.039712	1.598972
48	6	0	-0.722071	0.088407	2.230931
49	6	0	-0.023762	1.198128	1.743976
50	6	0	-1.350649	0.168161	3.481381
51	6	0	0.051206	2.373203	2.486697
52	1	0	0.445352	1.143735	0.766344
53	6	0	-1.266977	1.336980	4.229717
54	1	0	-1.896294	-0.697748	3.845534
55	6	0	-0.567449	2.443715	3.734011
56	1	0	0.596990	3.226004	2.090762
57	1	0	-1.750327	1.393157	5.202218
58	1	0	-0.507885	3.356677	4.321844
59	6	0	-4.372638	-2.518119	-0.006056
60	6	0	-5.390092	-2.715501	-0.947240
61	6	0	-4.725096	-2.371230	1.340044
62	6	0	-6.727234	-2.768001	-0.558111
63	1	0	-5.126065	-2.823977	-1.997607
64	6	0	-6.063092	-2.426996	1.732896
65	1	0	-3.941738	-2.204610	2.075257
66	6	0	-7.069173	-2.623791	0.787503
67	1	0	-7.502046	-2.924303	-1.304961
68	1	0	-6.318926	-2.312318	2.783810
69	1	0	-8.111061	-2.665299	1.095414
70	7	0	-2.404049	1.295236	-0.717381
71	6	0	-1.456798	-0.641474	-1.533984
72	6	0	-1.314473	0.846561	-1.386721
73	8	0	-0.333073	1.524295	-1.732130
74	8	0	-0.524095	-1.372986	-2.069640
75	6	0	-2.577595	2.648136	-0.254348
76	1	0	-2.555801	2.668380	0.843780
77	1	0	-1.701627	3.204168	-0.608327
78	6	0	-3.853883	3.275754	-0.762636
79	6	0	-4.693136	3.983159	0.099928
80	6	0	-4.208059	3.158568	-2.111006
81	6	0	-5.864626	4.575521	-0.375012
82	1	0	-4.431322	4.065120	1.153325
83	6	0	-5.377900	3.745069	-2.587709

84	1	0	-3.563215	2.595152	-2.781813
85	6	0	-6.209846	4.457505	-1.720547
86	1	0	-6.511223	5.120132	0.308744
87	1	0	-5.643526	3.645196	-3.637317
88	1	0	-7.124840	4.912039	-2.091956
89	8	0	-0.979688	-4.324268	-1.181504
90	8	0	0.501481	-3.362213	0.204170
91	6	0	0.112338	-4.783726	-1.980553
92	1	0	0.820000	-5.356815	-1.375171
93	1	0	-0.334091	-5.412101	-2.751861
94	1	0	0.615450	-3.923035	-2.428826

INT-A4

Center Number	Atomic Number	Atomic Type	Coordinates (Angstroms)		
			X	Y	Z
1	6	0	2.738400	1.558353	-0.884879
2	6	0	2.726722	2.379146	0.445706
3	6	0	0.485908	1.939328	1.152334
4	1	0	1.854925	1.892152	-1.443081
5	1	0	3.699606	2.289505	0.935184
6	1	0	0.092295	2.565494	0.351829
7	6	0	2.497598	0.111644	-0.593732
8	6	0	3.473787	-0.916991	-0.112038
9	1	0	3.962540	-0.638000	0.832481
10	1	0	4.254452	-1.166434	-0.843957
11	6	0	2.505419	3.841717	0.114555
12	7	0	1.743118	1.818313	1.366774
13	1	0	2.423877	1.295323	2.742380
14	6	0	-0.481657	1.228958	1.995957
15	6	0	-1.762694	1.756119	2.196607
16	6	0	-0.142812	-0.006304	2.570194
17	6	0	-2.683558	1.077781	2.991101
18	1	0	-2.036726	2.697473	1.728997
19	6	0	-1.070183	-0.688182	3.353116
20	1	0	0.838634	-0.433819	2.386573
21	6	0	-2.336987	-0.140897	3.575626
22	1	0	-3.676307	1.493409	3.140873
23	1	0	-0.802377	-1.649987	3.782668
24	1	0	-3.056662	-0.668017	4.197276
25	6	0	3.968951	1.876844	-1.699461
26	6	0	3.842372	2.475944	-2.956352
27	6	0	5.254693	1.601410	-1.217521
28	6	0	4.968416	2.787474	-3.718860
29	1	0	2.848078	2.697145	-3.338558
30	6	0	6.382522	1.907889	-1.975640
31	1	0	5.379441	1.144687	-0.238349
32	6	0	6.243375	2.503200	-3.230675
33	1	0	4.848633	3.251812	-4.694858
34	1	0	7.372220	1.682247	-1.585929
35	1	0	7.123059	2.743390	-3.822549

36	7	0	2.635597	-2.082830	0.141900
37	6	0	1.234150	-0.408971	-0.586865
38	6	0	1.334490	-1.803177	-0.055357
39	8	0	0.368731	-2.560686	0.196915
40	8	0	0.096177	0.132184	-0.855779
41	6	0	3.133016	-3.275635	0.783180
42	1	0	3.510802	-3.018595	1.780139
43	1	0	2.266944	-3.933962	0.917055
44	6	0	4.202973	-3.959013	-0.034877
45	6	0	5.360995	-4.445527	0.575175
46	6	0	4.045497	-4.121078	-1.415750
47	6	0	6.342734	-5.094245	-0.175979
48	1	0	5.496968	-4.310471	1.646571
49	6	0	5.025276	-4.762763	-2.169690
50	1	0	3.152051	-3.728924	-1.896674
51	6	0	6.177508	-5.253887	-1.551206
52	1	0	7.240069	-5.466239	0.312705
53	1	0	4.891808	-4.878791	-3.242568
54	1	0	6.943501	-5.752468	-2.139902
55	8	0	3.576317	4.583275	0.430997
56	8	0	1.504260	4.296545	-0.405373
57	6	0	3.502722	5.964070	0.061877
58	1	0	4.451868	6.399534	0.374732
59	1	0	3.372522	6.058229	-1.019672
60	1	0	2.666645	6.450757	0.571529
61	47	0	-1.557791	-1.292611	-0.002996
62	15	0	-3.709610	-0.405145	-0.479334
63	6	0	-4.232502	-0.780077	-2.188942
64	6	0	-4.149271	-2.108570	-2.625096
65	6	0	-4.727707	0.201467	-3.053778
66	6	0	-4.574287	-2.454210	-3.905109
67	1	0	-3.744129	-2.869695	-1.961227
68	6	0	-5.144669	-0.146566	-4.338715
69	1	0	-4.777445	1.236577	-2.727140
70	6	0	-5.072360	-1.472679	-4.764592
71	1	0	-4.504893	-3.486870	-4.236804
72	1	0	-5.523016	0.621876	-5.008132
73	1	0	-5.394413	-1.740742	-5.767503
74	6	0	-3.578623	1.413317	-0.459555
75	6	0	-4.535737	2.242214	0.132025
76	6	0	-2.429259	1.973186	-1.038761
77	6	0	-4.346744	3.625190	0.144231
78	1	0	-5.417083	1.812517	0.599377
79	6	0	-2.253936	3.354869	-1.035554
80	1	0	-1.646100	1.332620	-1.440156
81	6	0	-3.209629	4.182802	-0.441359
82	1	0	-5.087773	4.265204	0.616840
83	1	0	-1.351908	3.781512	-1.466358
84	1	0	-3.059762	5.259293	-0.423233
85	6	0	-5.184075	-0.817754	0.507269
86	6	0	-5.006304	-1.419428	1.756729
87	6	0	-6.479736	-0.556972	0.041878
88	6	0	-6.110565	-1.732318	2.548491
89	1	0	-3.999956	-1.641575	2.099955

90	6	0	-7.581839	-0.872045	0.833403
91	1	0	-6.623800	-0.117350	-0.941868
92	6	0	-7.398305	-1.455139	2.089477
93	1	0	-5.965371	-2.201033	3.518472
94	1	0	-8.585161	-0.668419	0.468012
95	1	0	-8.260055	-1.703470	2.703691
96	6	0	3.247382	-0.084253	3.858507
97	6	0	3.948795	-0.278514	5.179259
98	1	0	3.274955	0.001316	5.996585
99	1	0	4.251925	-1.320379	5.293478
100	1	0	4.823272	0.377457	5.242450
101	8	0	2.926418	1.179224	3.636925
102	8	0	3.000546	-1.000436	3.085146

TS-A

Center Number	Atomic Number	Atomic Type	Coordinates (Angstroms)		
			X	Y	Z
1	6	0	-2.537946	2.007318	0.429898
2	6	0	-2.723680	2.571777	-1.058148
3	6	0	-1.153697	0.935912	-1.506924
4	1	0	-1.753702	2.594292	0.923932
5	1	0	-3.777045	2.749650	-1.272945
6	1	0	-0.383200	1.583501	-1.087945
7	6	0	-2.008491	0.602250	0.333862
8	6	0	-2.925116	-0.576746	0.162455
9	1	0	-3.356421	-0.684007	-0.839776
10	1	0	-3.760215	-0.553043	0.872588
11	6	0	-1.979556	3.887230	-1.131012
12	7	0	-2.231750	1.596856	-1.996067
13	1	0	-3.032368	1.036453	-2.367609
14	6	0	-0.630666	-0.298981	-2.100883
15	6	0	0.751136	-0.525284	-1.995997
16	6	0	-1.443362	-1.263100	-2.712857
17	6	0	1.318157	-1.696317	-2.485590
18	1	0	1.377910	0.241104	-1.553536
19	6	0	-0.869514	-2.440921	-3.189021
20	1	0	-2.524160	-1.137739	-2.789207
21	6	0	0.504425	-2.663997	-3.077948
22	1	0	2.393166	-1.842613	-2.418343
23	1	0	-1.509668	-3.188007	-3.651352
24	1	0	0.939889	-3.584502	-3.459592
25	6	0	-3.800749	2.118505	1.252646
26	6	0	-3.726080	2.561658	2.575906
27	6	0	-5.044310	1.736020	0.732755
28	6	0	-4.869205	2.623568	3.372916
29	1	0	-2.761654	2.855846	2.985949
30	6	0	-6.185413	1.794607	1.530388
31	1	0	-5.121429	1.384798	-0.296233
32	6	0	-6.103900	2.237920	2.851597
33	1	0	-4.794045	2.972805	4.399928

34	1	0	-7.143103	1.491025	1.114762
35	1	0	-6.997053	2.283293	3.469745
36	7	0	-2.076070	-1.728531	0.447435
37	6	0	-0.813645	0.133843	0.938160
38	6	0	-0.872344	-1.384971	0.888844
39	8	0	0.069679	-2.147593	1.205933
40	8	0	0.211209	0.736517	1.317919
41	6	0	-2.535489	-3.081238	0.175203
42	1	0	-2.736375	-3.153351	-0.898692
43	1	0	-1.711021	-3.751740	0.431220
44	6	0	-3.783760	-3.391338	0.963399
45	6	0	-5.038589	-3.256475	0.361892
46	6	0	-3.696271	-3.754109	2.311138
47	6	0	-6.195288	-3.488072	1.107665
48	1	0	-5.097939	-2.944679	-0.680865
49	6	0	-4.852703	-3.986563	3.053461
50	1	0	-2.717858	-3.850314	2.778664
51	6	0	-6.105737	-3.853366	2.451037
52	1	0	-7.168984	-3.378914	0.636155
53	1	0	-4.777875	-4.271096	4.100242
54	1	0	-7.008819	-4.032939	3.029477
55	8	0	-2.736994	4.871673	-0.624641
56	8	0	-0.842576	4.048736	-1.524346
57	6	0	-2.112190	6.155299	-0.533317
58	1	0	-2.864646	6.814129	-0.099676
59	1	0	-1.228597	6.103859	0.109428
60	1	0	-1.816800	6.506477	-1.525700
61	47	0	1.991303	-0.991139	1.139740
62	15	0	4.100217	-0.166073	0.443821
63	6	0	5.131711	0.738410	1.637733
64	6	0	5.330580	0.175810	2.904757
65	6	0	5.746166	1.952507	1.311466
66	6	0	6.150636	0.814278	3.831474
67	1	0	4.839427	-0.759777	3.164051
68	6	0	6.560456	2.592557	2.245318
69	1	0	5.579780	2.398666	0.334592
70	6	0	6.765804	2.023982	3.502553
71	1	0	6.301469	0.374075	4.813500
72	1	0	7.032236	3.537799	1.989908
73	1	0	7.398524	2.526416	4.229417
74	6	0	3.677162	1.043511	-0.848125
75	6	0	4.094477	0.898742	-2.174337
76	6	0	2.767424	2.058762	-0.507890
77	6	0	3.598524	1.759864	-3.154848
78	1	0	4.782767	0.104043	-2.447311
79	6	0	2.281348	2.917294	-1.488407
80	1	0	2.398481	2.142756	0.511767
81	6	0	2.690737	2.761281	-2.815604
82	1	0	3.908731	1.630798	-4.188389
83	1	0	1.543938	3.671889	-1.234012
84	1	0	2.280291	3.410238	-3.584136
85	6	0	5.222845	-1.357049	-0.348122
86	6	0	4.712382	-2.595670	-0.752623
87	6	0	6.565781	-1.044238	-0.593384

88	6	0	5.532007	-3.507301	-1.416522
89	1	0	3.674750	-2.845332	-0.540227
90	6	0	7.383741	-1.959905	-1.251380
91	1	0	6.968840	-0.089201	-0.266516
92	6	0	6.866852	-3.188940	-1.667474
93	1	0	5.129941	-4.467277	-1.729055
94	1	0	8.425979	-1.715311	-1.438799
95	1	0	7.507887	-3.901332	-2.180010
96	6	0	-5.201893	-0.545215	-2.473078
97	6	0	-6.722214	-0.647896	-2.552633
98	1	0	-7.150094	0.214398	-3.071871
99	1	0	-7.025948	-1.578057	-3.041329
100	1	0	-7.124006	-0.658075	-1.530326
101	8	0	-4.711551	0.626389	-2.424851
102	8	0	-4.540263	-1.612709	-2.403632

INT-A5

Center Number	Atomic Number	Atomic Type	Coordinates (Angstroms)		
			X	Y	Z
1	6	0	2.437194	-1.912186	0.747254
2	6	0	2.788667	-2.735694	-0.535302
3	6	0	1.241141	-1.159536	-1.191745
4	1	0	1.594765	-2.408128	1.243114
5	1	0	3.861491	-2.875367	-0.664336
6	1	0	0.412197	-1.789187	-0.845397
7	6	0	1.874533	-0.593612	0.189375
8	6	0	2.850285	0.551324	-0.059226
9	1	0	3.322544	0.548938	-1.045053
10	1	0	3.647819	0.572859	0.688417
11	6	0	2.111765	-4.094050	-0.512412
12	7	0	2.277516	-2.006768	-1.699723
13	1	0	3.082535	-1.477621	-2.075848
14	6	0	0.679428	-0.109746	-2.102830
15	6	0	-0.704459	0.104515	-2.064499
16	6	0	1.470460	0.698695	-2.925995
17	6	0	-1.295299	1.120583	-2.811442
18	1	0	-1.322206	-0.553315	-1.462111
19	6	0	0.876770	1.721008	-3.668441
20	1	0	2.552446	0.574757	-2.979145
21	6	0	-0.500313	1.942016	-3.611753
22	1	0	-2.374655	1.250487	-2.784265
23	1	0	1.505268	2.346955	-4.297183
24	1	0	-0.951336	2.738369	-4.199268
25	6	0	3.559304	-1.757076	1.740347
26	6	0	3.281967	-1.831235	3.109220
27	6	0	4.872686	-1.489735	1.327722
28	6	0	4.290162	-1.640032	4.054415
29	1	0	2.264265	-2.039412	3.434822
30	6	0	5.878858	-1.297296	2.272591
31	1	0	5.103737	-1.408604	0.265241

32	6	0	5.593423	-1.371135	3.637180
33	1	0	4.057056	-1.702898	5.114691
34	1	0	6.891033	-1.083704	1.937931
35	1	0	6.382195	-1.220172	4.370070
36	7	0	2.036725	1.760702	0.080087
37	6	0	0.744244	0.054985	0.886609
38	6	0	0.848127	1.550228	0.615199
39	8	0	-0.052779	2.390390	0.853914
40	8	0	-0.218544	-0.442575	1.453162
41	6	0	2.551284	3.041878	-0.379963
42	1	0	2.790649	2.927780	-1.442206
43	1	0	1.745467	3.770948	-0.263193
44	6	0	3.784178	3.423853	0.402226
45	6	0	5.052132	3.197582	-0.140071
46	6	0	3.662695	3.943637	1.694920
47	6	0	6.190446	3.495880	0.610159
48	1	0	5.134098	2.760895	-1.135255
49	6	0	4.801140	4.240612	2.441599
50	1	0	2.673104	4.111512	2.116592
51	6	0	6.068263	4.016246	1.898582
52	1	0	7.175029	3.315278	0.185861
53	1	0	4.701400	4.645756	3.445616
54	1	0	6.957243	4.245481	2.481236
55	8	0	2.894686	-5.041999	-1.040475
56	8	0	0.983766	-4.310714	-0.107194
57	6	0	2.307585	-6.340139	-1.157993
58	1	0	3.086054	-6.974341	-1.582817
59	1	0	1.998743	-6.710706	-0.176512
60	1	0	1.437855	-6.303591	-1.820235
61	47	0	-2.029932	1.393405	0.846233
62	15	0	-4.060911	0.260865	0.386701
63	6	0	-5.033396	-0.332099	1.803215
64	6	0	-5.245695	0.540260	2.877994
65	6	0	-5.592637	-1.614667	1.825983
66	6	0	-6.025410	0.138517	3.959411
67	1	0	-4.797204	1.531545	2.867328
68	6	0	-6.366657	-2.015355	2.914469
69	1	0	-5.414036	-2.298862	1.000815
70	6	0	-6.585799	-1.140338	3.978653
71	1	0	-6.186894	0.818306	4.791638
72	1	0	-6.795128	-3.013970	2.931551
73	1	0	-7.186372	-1.456832	4.827268
74	6	0	-3.568177	-1.227404	-0.533506
75	6	0	-3.946744	-1.436427	-1.863144
76	6	0	-2.645123	-2.092370	0.076704
77	6	0	-3.395660	-2.499876	-2.579456
78	1	0	-4.646697	-0.760779	-2.346110
79	6	0	-2.099992	-3.151620	-0.641747
80	1	0	-2.313668	-1.909960	1.095620
81	6	0	-2.470271	-3.349001	-1.974941
82	1	0	-3.675302	-2.647822	-3.619068
83	1	0	-1.349658	-3.788406	-0.182950
84	1	0	-2.017464	-4.155479	-2.544933
85	6	0	-5.241959	1.136962	-0.680638

86	6	0	-4.802013	2.248872	-1.407421
87	6	0	-6.563006	0.692904	-0.819035
88	6	0	-5.670074	2.901538	-2.281468
89	1	0	-3.780948	2.604164	-1.284553
90	6	0	-7.429413	1.350935	-1.688728
91	1	0	-6.911451	-0.161964	-0.245404
92	6	0	-6.982880	2.451755	-2.423316
93	1	0	-5.322546	3.763374	-2.844677
94	1	0	-8.454505	1.005430	-1.793046
95	1	0	-7.661573	2.962959	-3.100855
96	6	0	5.309083	0.156517	-2.324092
97	6	0	6.825560	0.334988	-2.361575
98	1	0	7.324826	-0.601917	-2.625605
99	1	0	7.111723	1.129109	-3.057315
100	1	0	7.167013	0.622984	-1.357897
101	8	0	4.873438	-0.975120	-1.958318
102	8	0	4.592365	1.157599	-2.600726

product (2,5-trans)

Center Number	Atomic Number	Atomic Type	Coordinates (Angstroms)		
			X	Y	Z
1	6	0	0.526185	1.438373	0.283877
2	6	0	1.346439	1.860201	-0.962345
3	6	0	2.377426	-0.020120	0.038960
4	1	0	0.985707	1.913229	1.157763
5	1	0	0.733569	1.899806	-1.864711
6	1	0	2.888893	0.492576	0.866017
7	6	0	0.875832	-0.068794	0.426418
8	6	0	0.036193	-0.998957	-0.456416
9	1	0	0.668288	-1.642115	-1.083148
10	1	0	-0.654912	-0.451869	-1.106995
11	6	0	1.938517	3.252713	-0.817157
12	7	0	2.410535	0.861506	-1.129157
13	1	0	2.226467	0.316460	-1.967885
14	6	0	3.058271	-1.342402	-0.213075
15	6	0	2.815275	-2.447926	0.611742
16	6	0	3.972842	-1.483632	-1.263287
17	6	0	3.446423	-3.666816	0.377844
18	1	0	2.137631	-2.367737	1.456400
19	6	0	4.607018	-2.704029	-1.498281
20	1	0	4.210458	-0.625741	-1.885524
21	6	0	4.341597	-3.802445	-0.683549
22	1	0	3.238256	-4.510838	1.030235
23	1	0	5.314761	-2.791037	-2.318847
24	1	0	4.833132	-4.754195	-0.867193
25	6	0	-0.945688	1.762623	0.302806
26	6	0	-1.563825	1.964234	1.543961
27	6	0	-1.735214	1.828464	-0.850293
28	6	0	-2.929618	2.221410	1.631210
29	1	0	-0.964903	1.919627	2.450785

30	6	0	-3.101116	2.088858	-0.766848
31	1	0	-1.292040	1.688960	-1.832535
32	6	0	-3.702498	2.287630	0.473268
33	1	0	-3.387122	2.373474	2.605377
34	1	0	-3.695784	2.126949	-1.674760
35	1	0	-4.768231	2.490121	0.536308
36	7	0	-0.724672	-1.816044	0.470234
37	6	0	0.587109	-0.516698	1.840291
38	6	0	-0.498525	-1.594556	1.790401
39	8	0	-1.043488	-2.135049	2.738955
40	8	0	1.091729	-0.081674	2.848989
41	6	0	-1.734232	-2.737514	-0.007343
42	1	0	-1.294487	-3.354560	-0.800770
43	1	0	-1.985568	-3.386062	0.837139
44	6	0	-2.959346	-2.013575	-0.512628
45	6	0	-3.212469	-1.891136	-1.880228
46	6	0	-3.846875	-1.436504	0.401867
47	6	0	-4.345823	-1.213959	-2.333165
48	1	0	-2.525513	-2.339031	-2.596372
49	6	0	-4.981257	-0.768337	-0.048196
50	1	0	-3.641303	-1.515542	1.466674
51	6	0	-5.235602	-0.658104	-1.416169
52	1	0	-4.536291	-1.129455	-3.400239
53	1	0	-5.668369	-0.330057	0.670482
54	1	0	-6.123868	-0.137528	-1.765370
55	8	0	1.755028	4.158099	-1.600933
56	8	0	2.700494	3.351716	0.281985
57	6	0	3.350580	4.612056	0.476956
58	1	0	2.610626	5.413088	0.553243
59	1	0	3.908216	4.510786	1.407937
60	1	0	4.025529	4.821378	-0.357235

INT-B4

Center Number	Atomic Number	Atomic Type	Coordinates (Angstroms)		
			X	Y	Z
1	47	0	1.859960	-0.268404	-1.821985
2	15	0	3.528593	0.512126	-0.331230
3	6	0	4.764790	-0.671447	0.286094
4	6	0	5.430101	-1.468840	-0.654987
5	6	0	5.023031	-0.851529	1.647689
6	6	0	6.351697	-2.425969	-0.239417
7	1	0	5.213134	-1.346045	-1.714299
8	6	0	5.937988	-1.819399	2.062821
9	1	0	4.495047	-0.250588	2.382096
10	6	0	6.602769	-2.607005	1.123180
11	1	0	6.864083	-3.039696	-0.975703
12	1	0	6.127937	-1.960121	3.123974
13	1	0	7.312010	-3.363096	1.449730
14	6	0	2.660618	1.159360	1.133508
15	6	0	3.257333	2.108119	1.974514

16	6	0	1.357122	0.726290	1.394928
17	6	0	2.556762	2.600581	3.073549
18	1	0	4.258630	2.472694	1.758038
19	6	0	0.654949	1.220341	2.492182
20	1	0	0.883806	0.011580	0.729249
21	6	0	1.257363	2.156573	3.332384
22	1	0	3.020700	3.339841	3.721692
23	1	0	-0.365102	0.897423	2.681128
24	1	0	0.705767	2.550934	4.182096
25	6	0	4.477575	1.947189	-0.925126
26	6	0	3.750014	2.962040	-1.565157
27	6	0	5.857805	2.076805	-0.747663
28	6	0	4.409644	4.102806	-2.013943
29	1	0	2.674615	2.855777	-1.700052
30	6	0	6.512308	3.219836	-1.209661
31	1	0	6.419950	1.289669	-0.252104
32	6	0	5.790066	4.232801	-1.839584
33	1	0	3.844991	4.889946	-2.506723
34	1	0	7.586420	3.317888	-1.073467
35	1	0	6.301535	5.122514	-2.197930
36	6	0	-2.839214	-1.751768	-1.173828
37	6	0	-2.895939	-2.660013	0.112780
38	6	0	-1.325326	-1.839440	1.780466
39	1	0	-2.284421	-2.329069	-1.920907
40	1	0	-3.950616	-2.929279	0.259067
41	6	0	-2.110487	-0.454417	-1.014682
42	6	0	-2.641214	0.732650	-0.268487
43	1	0	-2.721583	0.561260	0.810484
44	1	0	-3.626226	1.058832	-0.628158
45	6	0	-2.230611	-4.017265	-0.121555
46	6	0	-4.228454	-1.499597	-1.730578
47	6	0	-4.453262	-1.626331	-3.104278
48	6	0	-5.281987	-1.072660	-0.913022
49	6	0	-5.703020	-1.338843	-3.651981
50	1	0	-3.637134	-1.950901	-3.745863
51	6	0	-6.531963	-0.781693	-1.458022
52	1	0	-5.130100	-0.952276	0.157861
53	6	0	-6.747819	-0.914482	-2.830173
54	1	0	-5.861019	-1.449446	-4.722138
55	1	0	-7.336879	-0.447621	-0.807614
56	1	0	-7.723001	-0.690125	-3.255146
57	7	0	-1.648109	1.765845	-0.511673
58	6	0	-0.944381	-0.119664	-1.645126
59	6	0	-0.623027	1.307826	-1.268082
60	8	0	0.407796	1.933131	-1.559630
61	8	0	-0.157341	-0.822053	-2.405492
62	6	0	-1.610917	2.996379	0.244283
63	1	0	-1.270001	2.799035	1.269468
64	1	0	-0.857759	3.632449	-0.233827
65	6	0	-2.960725	3.666719	0.281158
66	6	0	-3.556796	3.990161	1.501203
67	6	0	-3.644564	3.950970	-0.906310
68	6	0	-4.810733	4.603337	1.538658
69	1	0	-3.039310	3.746290	2.426508

70	6	0	-4.898785	4.554695	-0.872729
71	1	0	-3.191048	3.680009	-1.857437
72	6	0	-5.485293	4.885459	0.351799
73	1	0	-5.262998	4.852561	2.495778
74	1	0	-5.422635	4.765410	-1.801818
75	1	0	-6.464883	5.356199	0.378104
76	1	0	-1.283375	-1.260899	2.707534
77	6	0	-0.017021	-2.337709	1.337912
78	6	0	0.963360	-2.446152	2.340394
79	6	0	0.334743	-2.640455	0.015206
80	6	0	2.248039	-2.881593	2.040490
81	1	0	0.707356	-2.171999	3.361345
82	6	0	1.627180	-3.070889	-0.283052
83	1	0	-0.348735	-2.479467	-0.807778
84	6	0	2.584799	-3.198845	0.723666
85	1	0	2.995194	-2.955000	2.825346
86	1	0	1.879382	-3.298785	-1.315474
87	1	0	3.595575	-3.515752	0.483118
88	8	0	-2.036915	-4.511611	-1.210267
89	8	0	-1.969579	-4.641087	1.035599
90	6	0	-1.310917	-5.905144	0.914377
91	1	0	-1.186847	-6.266777	1.935290
92	1	0	-1.916633	-6.599509	0.326187
93	1	0	-0.338040	-5.771068	0.432763
94	7	0	-2.513886	-1.970432	1.324246
95	1	0	-3.618941	-1.153839	2.132139
96	6	0	-3.864745	0.470447	3.187091
97	8	0	-2.663891	0.711870	3.253771
98	8	0	-4.368073	-0.597268	2.590181
99	6	0	-4.924107	1.383214	3.743841
100	1	0	-5.368054	1.946553	2.914855
101	1	0	-5.721828	0.808341	4.222383
102	1	0	-4.480495	2.086813	4.450277

TS-B

Center Number	Atomic Number	Atomic Type	Coordinates (Angstroms)		
			X	Y	Z
1	47	0	1.771422	-1.323910	-0.317316
2	15	0	3.975219	-0.598035	0.208310
3	6	0	3.916274	1.199397	0.502031
4	6	0	2.851671	1.685929	1.275268
5	6	0	4.843696	2.091127	-0.045139
6	6	0	2.726644	3.052555	1.508098
7	1	0	2.090482	1.008192	1.651439
8	6	0	4.710529	3.461330	0.186754
9	1	0	5.658965	1.723665	-0.661728
10	6	0	3.656136	3.942229	0.964279
11	1	0	1.882516	3.422198	2.083580
12	1	0	5.429303	4.152084	-0.246820
13	1	0	3.550138	5.010471	1.135477

14	6	0	5.302793	-0.867928	-1.008061
15	6	0	6.653734	-0.751775	-0.655584
16	6	0	4.957559	-1.196672	-2.323443
17	6	0	7.644050	-0.939534	-1.617152
18	1	0	6.927723	-0.524405	0.371522
19	6	0	5.949950	-1.380753	-3.285156
20	1	0	3.909670	-1.319262	-2.585731
21	6	0	7.293347	-1.248308	-2.933294
22	1	0	8.690794	-0.849750	-1.338562
23	1	0	5.674417	-1.636955	-4.304730
24	1	0	8.068062	-1.396868	-3.680896
25	6	0	4.653863	-1.284967	1.754883
26	6	0	4.565416	-2.668585	1.955147
27	6	0	5.272808	-0.482905	2.719509
28	6	0	5.106634	-3.245713	3.100668
29	1	0	4.067242	-3.290999	1.214485
30	6	0	5.806185	-1.063886	3.870148
31	1	0	5.328898	0.592662	2.576010
32	6	0	5.727528	-2.443282	4.060411
33	1	0	5.034056	-4.319632	3.250511
34	1	0	6.280993	-0.435672	4.619393
35	1	0	6.141235	-2.892927	4.959207
36	6	0	-2.511092	1.604872	1.126861
37	6	0	-2.754084	2.757739	0.067578
38	6	0	-2.003448	1.181993	-1.601594
39	1	0	-1.609509	1.876964	1.684712
40	1	0	-3.732155	3.217003	0.256722
41	6	0	-2.228560	0.305223	0.439782
42	6	0	-3.262592	-0.736480	0.104078
43	1	0	-3.964459	-0.431652	-0.676471
44	1	0	-3.836361	-1.047927	0.985920
45	6	0	-1.771898	3.907655	0.247635
46	6	0	-3.670046	1.501976	2.096730
47	6	0	-3.425150	1.477499	3.472018
48	6	0	-4.989904	1.390595	1.637836
49	6	0	-4.475770	1.342882	4.380366
50	1	0	-2.402066	1.566933	3.831457
51	6	0	-6.038485	1.253431	2.545694
52	1	0	-5.206340	1.399988	0.569165
53	6	0	-5.786881	1.228765	3.918784
54	1	0	-4.268776	1.329939	5.447839
55	1	0	-7.056431	1.163422	2.174502
56	1	0	-6.607842	1.122917	4.623683
57	7	0	-2.464076	-1.859831	-0.389600
58	6	0	-0.974495	-0.328443	0.467829
59	6	0	-1.155213	-1.664218	-0.228557
60	8	0	-0.221121	-2.410360	-0.599997
61	8	0	0.148554	0.077099	0.841442
62	6	0	-3.066495	-2.919906	-1.184357
63	1	0	-3.327039	-2.502306	-2.164148
64	1	0	-2.303121	-3.693108	-1.311870
65	6	0	-4.304578	-3.454456	-0.511791
66	6	0	-5.565484	-3.126463	-1.014696
67	6	0	-4.206962	-4.232975	0.646163

68	6	0	-6.718157	-3.577031	-0.369962
69	1	0	-5.630733	-2.500555	-1.901173
70	6	0	-5.356907	-4.682158	1.291693
71	1	0	-3.224543	-4.480038	1.044637
72	6	0	-6.616275	-4.354324	0.783331
73	1	0	-7.695678	-3.314015	-0.766519
74	1	0	-5.273046	-5.287062	2.191281
75	1	0	-7.514001	-4.702727	1.288078
76	1	0	-2.533336	0.446998	-2.217583
77	6	0	-0.558145	1.222120	-1.848798
78	6	0	-0.059837	0.200959	-2.680420
79	6	0	0.351024	2.163273	-1.346074
80	6	0	1.288009	0.145216	-3.025977
81	1	0	-0.747516	-0.547220	-3.066407
82	6	0	1.691137	2.129001	-1.718403
83	1	0	0.034966	2.923565	-0.647822
84	6	0	2.167994	1.126514	-2.559611
85	1	0	1.639853	-0.645375	-3.684623
86	1	0	2.372381	2.878512	-1.329304
87	1	0	3.217910	1.106088	-2.838764
88	8	0	-1.090240	4.098059	1.234641
89	8	0	-1.796160	4.732177	-0.805538
90	6	0	-0.934395	5.870044	-0.719978
91	1	0	-1.094579	6.424411	-1.644700
92	1	0	-1.191313	6.481013	0.149694
93	1	0	0.109114	5.550516	-0.640813
94	7	0	-2.830977	2.189145	-1.251746
95	1	0	-3.829012	1.922100	-1.482158
96	6	0	-5.424100	0.359892	-2.463531
97	8	0	-4.451372	-0.368153	-2.793295
98	8	0	-5.354277	1.386340	-1.713861
99	6	0	-6.818875	-0.019874	-2.948214
100	1	0	-7.404772	-0.389311	-2.097086
101	1	0	-7.338464	0.862445	-3.335624
102	1	0	-6.775344	-0.795989	-3.717008

INT-B5

Center Number	Atomic Number	Atomic Type	Coordinates (Angstroms)		
			X	Y	Z
1	47	0	1.716579	-1.505205	-0.233028
2	15	0	3.875328	-0.604942	0.219566
3	6	0	3.817250	1.213501	0.234499
4	6	0	2.749308	1.822311	0.907579
5	6	0	4.781508	2.001445	-0.401661
6	6	0	2.658279	3.210336	0.961840
7	1	0	1.967023	1.220000	1.360560
8	6	0	4.681892	3.392426	-0.352521
9	1	0	5.601083	1.535533	-0.941089
10	6	0	3.626108	3.995854	0.332232
11	1	0	1.809780	3.665700	1.463937

12	1	0	5.429522	4.002663	-0.852965
13	1	0	3.551801	5.080088	0.365827
14	6	0	5.210412	-1.059865	-0.930594
15	6	0	6.557351	-0.956165	-0.560306
16	6	0	4.878151	-1.509247	-2.213436
17	6	0	7.558253	-1.280612	-1.473588
18	1	0	6.819865	-0.630516	0.442937
19	6	0	5.881215	-1.829065	-3.126810
20	1	0	3.832354	-1.614675	-2.490095
21	6	0	7.221782	-1.711942	-2.758287
22	1	0	8.601893	-1.200419	-1.180991
23	1	0	5.615776	-2.177686	-4.121284
24	1	0	8.004479	-1.966452	-3.468000
25	6	0	4.532849	-1.052870	1.859514
26	6	0	4.458824	-2.394240	2.256487
27	6	0	5.123612	-0.109993	2.707205
28	6	0	4.985354	-2.791178	3.482419
29	1	0	3.984456	-3.125920	1.605295
30	6	0	5.642106	-0.510246	3.938958
31	1	0	5.169797	0.933802	2.409473
32	6	0	5.577180	-1.848429	4.326069
33	1	0	4.924249	-3.833139	3.784972
34	1	0	6.094540	0.227078	4.596958
35	1	0	5.979148	-2.156670	5.287585
36	6	0	-2.463505	1.669095	1.114733
37	6	0	-2.514587	2.904308	0.177220
38	6	0	-1.957686	1.121386	-1.292660
39	1	0	-1.604206	1.779568	1.783021
40	1	0	-3.430702	3.482088	0.349614
41	6	0	-2.186989	0.475718	0.180223
42	6	0	-3.263113	-0.612879	0.047244
43	1	0	-4.006761	-0.371556	-0.711992
44	1	0	-3.751192	-0.835512	0.999697
45	6	0	-1.378600	3.877750	0.488031
46	6	0	-3.708805	1.515065	1.953230
47	6	0	-3.602524	1.312696	3.331745
48	6	0	-4.982413	1.546826	1.365816
49	6	0	-4.743310	1.142717	4.118517
50	1	0	-2.616381	1.291777	3.791978
51	6	0	-6.119787	1.374628	2.151246
52	1	0	-5.088560	1.671612	0.287533
53	6	0	-6.006206	1.172511	3.528792
54	1	0	-4.643238	0.989467	5.190455
55	1	0	-7.099599	1.392311	1.680356
56	1	0	-6.897183	1.038309	4.137346
57	7	0	-2.495259	-1.788570	-0.390851
58	6	0	-0.989284	-0.335748	0.520787
59	6	0	-1.204818	-1.712544	-0.102066
60	8	0	-0.301826	-2.552440	-0.312022
61	8	0	0.030393	-0.035177	1.115580
62	6	0	-3.143334	-2.868936	-1.124640
63	1	0	-3.415992	-2.461804	-2.105451
64	1	0	-2.404225	-3.666439	-1.239864
65	6	0	-4.378732	-3.335843	-0.398030

66	6	0	-5.637023	-2.906592	-0.827416
67	6	0	-4.274625	-4.145321	0.737479
68	6	0	-6.782141	-3.287786	-0.127715
69	1	0	-5.701436	-2.260798	-1.700336
70	6	0	-5.418461	-4.525773	1.436528
71	1	0	-3.293273	-4.474454	1.074961
72	6	0	-6.675071	-4.095962	1.004041
73	1	0	-7.757977	-2.947316	-0.464713
74	1	0	-5.331427	-5.156380	2.317901
75	1	0	-7.567703	-4.390200	1.550505
76	1	0	-2.583715	0.539634	-1.983403
77	6	0	-0.533411	1.050473	-1.799696
78	6	0	-0.108296	-0.122500	-2.440974
79	6	0	0.371778	2.107113	-1.691348
80	6	0	1.201275	-0.253893	-2.910306
81	1	0	-0.820727	-0.926172	-2.608632
82	6	0	1.676811	1.985792	-2.164341
83	1	0	0.044401	3.045738	-1.263761
84	6	0	2.104049	0.803414	-2.764086
85	1	0	1.494362	-1.163080	-3.432004
86	1	0	2.368144	2.816209	-2.054401
87	1	0	3.123785	0.715638	-3.129233
88	8	0	-0.591335	3.785500	1.410726
89	8	0	-1.370387	4.901712	-0.375709
90	6	0	-0.345655	5.875407	-0.175098
91	1	0	-0.512679	6.635543	-0.938695
92	1	0	-0.415438	6.309626	0.826432
93	1	0	0.641439	5.419716	-0.301630
94	7	0	-2.518269	2.446991	-1.202093
95	1	0	-3.491134	2.351838	-1.526352
96	6	0	-5.183662	0.461683	-2.689111
97	8	0	-4.317483	-0.448878	-2.826775
98	8	0	-5.077637	1.471261	-1.931605
99	6	0	-6.495829	0.320571	-3.459157
100	1	0	-7.293863	0.043366	-2.758003
101	1	0	-6.779733	1.280299	-3.903181
102	1	0	-6.423863	-0.446777	-4.234914

product (2,5-*cis*)

Center Number	Atomic Number	Atomic Type	Coordinates (Angstroms)		
			X	Y	Z
1	6	0	0.731973	0.826659	0.177315
2	6	0	1.114455	1.628305	-1.072959
3	6	0	1.965333	-0.621102	-1.287924
4	1	0	1.593367	0.846174	0.856038
5	1	0	0.230139	1.845437	-1.685554
6	6	0	0.675588	-0.605189	-0.398405
7	6	0	-0.584496	-0.870574	-1.237785
8	1	0	-0.366207	-0.927805	-2.312145
9	1	0	-1.344974	-0.094809	-1.089543

10	6	0	1.749811	2.952891	-0.674703
11	6	0	-0.488278	1.274071	0.942520
12	6	0	-0.602750	0.904627	2.289816
13	6	0	-1.526041	2.015854	0.366732
14	6	0	-1.727416	1.252618	3.033651
15	1	0	0.199835	0.339258	2.755378
16	6	0	-2.649836	2.370601	1.111379
17	1	0	-1.465530	2.337379	-0.668800
18	6	0	-2.755884	1.989336	2.446484
19	1	0	-1.794571	0.953242	4.076476
20	1	0	-3.445521	2.941316	0.640300
21	1	0	-3.632038	2.266957	3.027074
22	7	0	-1.101515	-2.144586	-0.769008
23	6	0	0.625565	-1.666724	0.682069
24	6	0	-0.503837	-2.643385	0.348046
25	8	0	-0.826436	-3.635999	0.977733
26	8	0	1.297360	-1.718882	1.682106
27	6	0	-2.376252	-2.636501	-1.249228
28	1	0	-2.318625	-2.795309	-2.333285
29	1	0	-2.532175	-3.606783	-0.766715
30	6	0	-3.489686	-1.669903	-0.914079
31	6	0	-4.265167	-1.085860	-1.916426
32	6	0	-3.721396	-1.319793	0.421021
33	6	0	-5.269642	-0.171374	-1.593141
34	1	0	-4.083884	-1.347057	-2.957535
35	6	0	-4.721173	-0.408494	0.744784
36	1	0	-3.111783	-1.760204	1.206362
37	6	0	-5.499179	0.167665	-0.261310
38	1	0	-5.868729	0.275925	-2.382442
39	1	0	-4.888690	-0.142503	1.784246
40	1	0	-6.279384	0.880507	-0.006463
41	1	0	1.791838	-1.302530	-2.130774
42	6	0	3.215325	-1.082764	-0.572521
43	6	0	3.488679	-2.451327	-0.496590
44	6	0	4.087096	-0.176690	0.032601
45	6	0	4.608787	-2.914975	0.187889
46	1	0	2.813364	-3.164484	-0.968883
47	6	0	5.207018	-0.639920	0.722132
48	1	0	3.889833	0.888056	-0.048448
49	6	0	5.470663	-2.006828	0.803651
50	1	0	4.807062	-3.982318	0.242822
51	1	0	5.877449	0.073196	1.195599
52	1	0	6.345360	-2.364242	1.341300
53	8	0	2.730540	3.070972	0.023875
54	8	0	1.062720	3.989952	-1.184192
55	6	0	1.544582	5.287862	-0.813199
56	1	0	0.877808	5.997633	-1.302856
57	1	0	1.506847	5.406613	0.272759
58	1	0	2.573892	5.422102	-1.155601
59	7	0	2.057196	0.763144	-1.765839
60	1	0	1.999033	0.841485	-2.772483

TS-C

Center Number	Atomic Number	Atomic Type	Coordinates (Angstroms)		
			X	Y	Z
1	47	0	1.384257	1.093834	-0.220854
2	15	0	3.385534	-0.064688	0.356050
3	6	0	4.927489	0.902373	0.447780
4	6	0	4.872892	2.166300	1.049196
5	6	0	6.147602	0.418714	-0.037452
6	6	0	6.030897	2.929054	1.181534
7	1	0	3.920247	2.552167	1.406351
8	6	0	7.303256	1.189511	0.087168
9	1	0	6.191163	-0.555828	-0.516338
10	6	0	7.247601	2.441728	0.699980
11	1	0	5.981761	3.908380	1.650412
12	1	0	8.247648	0.810613	-0.295437
13	1	0	8.149387	3.041124	0.795342
14	6	0	3.718823	-1.326988	-0.923052
15	6	0	4.155710	-2.617918	-0.607265
16	6	0	3.492509	-0.982578	-2.262037
17	6	0	4.375531	-3.548477	-1.623664
18	1	0	4.311657	-2.898867	0.430494
19	6	0	3.720934	-1.909915	-3.273982
20	1	0	3.110902	0.006730	-2.506355
21	6	0	4.161506	-3.195803	-2.956033
22	1	0	4.707342	-4.552422	-1.370760
23	1	0	3.529134	-1.637507	-4.308249
24	1	0	4.323003	-3.925848	-3.745036
25	6	0	3.339357	-1.024504	1.902033
26	6	0	2.117967	-1.599476	2.278057
27	6	0	4.490225	-1.261697	2.664321
28	6	0	2.059253	-2.428774	3.396518
29	1	0	1.203829	-1.382317	1.730969
30	6	0	4.420054	-2.081090	3.790082
31	1	0	5.435593	-0.806632	2.380828
32	6	0	3.207229	-2.671573	4.151861
33	1	0	1.106201	-2.871593	3.672055
34	1	0	5.313628	-2.259401	4.383348
35	1	0	3.157023	-3.313435	5.028081
36	6	0	-2.221033	1.968578	0.032006
37	6	0	-1.204788	2.494412	-1.117621
38	6	0	-1.216360	0.386506	-1.786898
39	1	0	-1.735921	2.193776	0.989737
40	1	0	-1.832853	2.871597	-1.938193
41	6	0	-2.277858	0.466350	-0.077555
42	6	0	-3.509693	-0.376680	-0.306186
43	1	0	-3.794363	-0.457502	-1.366840
44	1	0	-4.388790	-0.008014	0.239711
45	6	0	-0.411478	3.646146	-0.562553
46	7	0	-0.376752	1.402485	-1.523698
47	6	0	-3.553651	2.660336	-0.014302
48	6	0	-4.013042	3.384069	1.090035
49	6	0	-4.373329	2.586774	-1.148015

50	6	0	-5.255860	4.017038	1.068105
51	1	0	-3.387960	3.446039	1.978578
52	6	0	-5.616793	3.213688	-1.175446
53	1	0	-4.037270	2.030661	-2.020811
54	6	0	-6.063316	3.933362	-0.065723
55	1	0	-5.594143	4.573402	1.938904
56	1	0	-6.239171	3.140271	-2.064015
57	1	0	-7.033423	4.423259	-0.085573
58	7	0	-3.113331	-1.688756	0.183423
59	6	0	-1.416877	-0.270667	0.788001
60	6	0	-1.923546	-1.700474	0.847777
61	8	0	-1.390519	-2.659877	1.392147
62	8	0	-0.385131	0.126247	1.356018
63	6	0	-3.917625	-2.863825	-0.034233
64	1	0	-4.033230	-3.033609	-1.113705
65	1	0	-3.344502	-3.702285	0.377705
66	6	0	-5.272214	-2.755495	0.625968
67	6	0	-6.447227	-2.953928	-0.100450
68	6	0	-5.359511	-2.435466	1.985797
69	6	0	-7.693914	-2.843879	0.519086
70	1	0	-6.387461	-3.193498	-1.160660
71	6	0	-6.600772	-2.321027	2.606137
72	1	0	-4.445226	-2.272888	2.552469
73	6	0	-7.773098	-2.525730	1.873745
74	1	0	-8.601386	-2.999504	-0.059248
75	1	0	-6.655981	-2.071879	3.663022
76	1	0	-8.742127	-2.434210	2.357830
77	1	0	-2.134569	0.651710	-2.334891
78	6	0	-0.787248	-0.985255	-2.143266
79	6	0	-1.499711	-1.658195	-3.146370
80	6	0	0.244678	-1.670452	-1.492561
81	6	0	-1.175959	-2.965768	-3.503631
82	1	0	-2.309782	-1.141617	-3.658590
83	6	0	0.574927	-2.973233	-1.845703
84	1	0	0.777544	-1.192883	-0.678159
85	6	0	-0.132160	-3.626781	-2.854900
86	1	0	-1.737051	-3.466989	-4.288775
87	1	0	1.380065	-3.478455	-1.320597
88	1	0	0.123012	-4.647708	-3.128030
89	8	0	0.685999	3.562682	-0.036312
90	8	0	-1.089951	4.794632	-0.647022
91	6	0	-0.475242	5.933101	-0.034504
92	1	0	-1.179822	6.752853	-0.175025
93	1	0	-0.306305	5.746604	1.029524
94	1	0	0.479704	6.155863	-0.518075

INT-C1

Center Number	Atomic Number	Atomic Type	Coordinates (Angstroms)		
			X	Y	Z
1	47	0	1.384362	1.072124	-0.306852
2	15	0	3.387577	-0.008089	0.353304
3	6	0	4.899245	1.010308	0.378631
4	6	0	4.807629	2.302429	0.912121
5	6	0	6.129719	0.541674	-0.094847
6	6	0	5.941014	3.108372	0.990468
7	1	0	3.845665	2.676364	1.256868
8	6	0	7.260429	1.355138	-0.023659
9	1	0	6.200402	-0.454259	-0.524087
10	6	0	7.168831	2.635718	0.522584
11	1	0	5.863516	4.109771	1.405821
12	1	0	8.213148	0.987749	-0.396762
13	1	0	8.051009	3.268597	0.575781
14	6	0	3.751045	-1.325449	-0.858021
15	6	0	4.221363	-2.587551	-0.481930
16	6	0	3.516080	-1.049777	-2.211588
17	6	0	4.464050	-3.559453	-1.453683
18	1	0	4.385447	-2.815362	0.567572
19	6	0	3.769612	-2.016890	-3.178637
20	1	0	3.105724	-0.084855	-2.502030
21	6	0	4.242944	-3.274709	-2.800861
22	1	0	4.821291	-4.541689	-1.154305
23	1	0	3.568882	-1.798817	-4.223883
24	1	0	4.424297	-4.036389	-3.554958
25	6	0	3.384022	-0.870461	1.957265
26	6	0	2.169938	-1.387912	2.426417
27	6	0	4.560786	-1.082750	2.686912
28	6	0	2.140066	-2.136495	3.601597
29	1	0	1.239578	-1.189131	1.902042
30	6	0	4.522566	-1.821150	3.868593
31	1	0	5.501890	-0.668664	2.334679
32	6	0	3.314534	-2.355201	4.322424
33	1	0	1.191090	-2.535697	3.948636
34	1	0	5.437160	-1.979703	4.434729
35	1	0	3.288871	-2.933456	5.242763
36	6	0	-2.330828	1.838751	-0.052301
37	6	0	-1.251553	2.463033	-1.052289
38	6	0	-1.265923	0.325018	-1.654843
39	1	0	-1.990899	2.035899	0.970144
40	1	0	-1.821225	2.907529	-1.887735
41	6	0	-2.192352	0.321226	-0.297385
42	6	0	-3.432828	-0.556300	-0.477470
43	1	0	-3.665432	-0.733384	-1.536084
44	1	0	-4.324074	-0.127238	-0.004844
45	6	0	-0.522462	3.590562	-0.365171
46	7	0	-0.387473	1.409178	-1.479383
47	6	0	-3.718011	2.389899	-0.209465
48	6	0	-4.387128	2.934787	0.890627
49	6	0	-4.388656	2.347668	-1.439515

50	6	0	-5.688595	3.423003	0.772873
51	1	0	-3.879283	2.972055	1.852331
52	6	0	-5.689098	2.830458	-1.563196
53	1	0	-3.890117	1.928610	-2.310546
54	6	0	-6.345448	3.371107	-0.455851
55	1	0	-6.189807	3.840814	1.642599
56	1	0	-6.192384	2.784669	-2.526010
57	1	0	-7.360563	3.747862	-0.551547
58	7	0	-3.079504	-1.817776	0.159162
59	6	0	-1.456056	-0.342667	0.804955
60	6	0	-1.987909	-1.758627	0.964145
61	8	0	-1.536469	-2.642113	1.681651
62	8	0	-0.549185	0.132292	1.474433
63	6	0	-3.931818	-2.978917	0.059661
64	1	0	-4.042666	-3.252252	-0.997753
65	1	0	-3.403939	-3.791146	0.570370
66	6	0	-5.284489	-2.727186	0.684130
67	6	0	-6.452384	-2.766632	-0.078539
68	6	0	-5.368359	-2.406434	2.044274
69	6	0	-7.691575	-2.496446	0.505802
70	1	0	-6.392855	-3.006362	-1.138605
71	6	0	-6.602014	-2.133344	2.629091
72	1	0	-4.458436	-2.370476	2.639658
73	6	0	-7.768096	-2.177693	1.860358
74	1	0	-8.594028	-2.528593	-0.099582
75	1	0	-6.656310	-1.886301	3.686448
76	1	0	-8.730824	-1.962585	2.317006
77	1	0	-2.047536	0.552440	-2.410612
78	6	0	-0.657331	-0.989156	-2.072430
79	6	0	-0.974995	-1.502688	-3.334378
80	6	0	0.210665	-1.730248	-1.261816
81	6	0	-0.440778	-2.712358	-3.779517
82	1	0	-1.644094	-0.937088	-3.980535
83	6	0	0.741388	-2.942049	-1.693929
84	1	0	0.482509	-1.369719	-0.276008
85	6	0	0.420051	-3.437712	-2.956308
86	1	0	-0.697304	-3.085545	-4.768306
87	1	0	1.414170	-3.491971	-1.042522
88	1	0	0.840828	-4.380828	-3.295882
89	8	0	0.590479	3.531929	0.126836
90	8	0	-1.281183	4.694296	-0.308275
91	6	0	-0.723825	5.799712	0.407729
92	1	0	-1.481051	6.583140	0.367537
93	1	0	-0.515321	5.517152	1.443484
94	1	0	0.202879	6.133682	-0.067153

INT-D1

Center Number	Atomic Number	Atomic Type	Coordinates (Angstroms)		
			X	Y	Z
1	47	0	-0.317503	-0.815567	-0.323635
2	15	0	-2.625657	-0.784558	0.277274
3	6	0	-3.451096	-2.404636	0.393462
4	6	0	-2.679991	-3.512261	0.766857
5	6	0	-4.817924	-2.567483	0.134669
6	6	0	-3.275468	-4.764929	0.903498
7	1	0	-1.611636	-3.393265	0.934855
8	6	0	-5.408524	-3.823220	0.264497
9	1	0	-5.414791	-1.714439	-0.178120
10	6	0	-4.639571	-4.921463	0.653702
11	1	0	-2.670993	-5.620636	1.192658
12	1	0	-6.469253	-3.944642	0.059776
13	1	0	-5.101717	-5.900378	0.752511
14	6	0	-3.628389	0.114267	-0.957684
15	6	0	-4.397497	1.233752	-0.628321
16	6	0	-3.580343	-0.323519	-2.288909
17	6	0	-5.118851	1.902026	-1.619674
18	1	0	-4.428016	1.585767	0.398611
19	6	0	-4.304845	0.340675	-3.273816
20	1	0	-2.970977	-1.186614	-2.550874
21	6	0	-5.076211	1.457859	-2.940509
22	1	0	-5.712334	2.773792	-1.355927
23	1	0	-4.260286	-0.004876	-4.303337
24	1	0	-5.635162	1.982260	-3.711198
25	6	0	-2.971820	0.073300	1.842404
26	6	0	-2.097732	1.098997	2.226596
27	6	0	-4.100222	-0.218894	2.620195
28	6	0	-2.370518	1.842903	3.374446
29	1	0	-1.192376	1.311507	1.662267
30	6	0	-4.358207	0.521849	3.771582
31	1	0	-4.769398	-1.025251	2.332483
32	6	0	-3.497213	1.557238	4.145282
33	1	0	-1.682729	2.634585	3.655772
34	1	0	-5.230222	0.289613	4.378131
35	1	0	-3.702413	2.133078	5.044637
36	6	0	3.085934	-0.861005	0.188254
37	6	0	2.581217	-1.348838	-1.285967
38	6	0	1.839992	0.690744	-1.968818
39	1	0	2.311100	-1.243507	0.863360
40	1	0	3.435912	-1.286478	-1.969904
41	6	0	3.077527	0.608121	0.321923
42	6	0	4.187403	1.591373	0.167302
43	1	0	4.602169	1.693699	-0.848139
44	1	0	5.049560	1.413597	0.826892
45	6	0	2.143634	-2.778837	-1.129095
46	7	0	1.488133	-0.526917	-1.680223
47	6	0	4.386351	-1.545593	0.516897
48	6	0	4.444092	-2.458774	1.574598
49	6	0	5.548536	-1.312950	-0.227910

50	6	0	5.631207	-3.121952	1.885056
51	1	0	3.547179	-2.645669	2.161667
52	6	0	6.737594	-1.971028	0.079034
53	1	0	5.525719	-0.612517	-1.059623
54	6	0	6.783307	-2.880200	1.137120
55	1	0	5.655927	-3.825952	2.713435
56	1	0	7.630338	-1.774527	-0.509703
57	1	0	7.710534	-3.394431	1.376745
58	6	0	1.944770	1.233179	0.836287
59	8	0	0.833905	0.756815	1.146189
60	1	0	2.886806	0.926337	-2.184818
61	6	0	0.890225	1.786709	-2.149693
62	6	0	1.366438	3.104102	-2.102659
63	6	0	-0.487509	1.569560	-2.309175
64	6	0	0.482980	4.178830	-2.160848
65	1	0	2.431809	3.288881	-1.989646
66	6	0	-1.369578	2.640678	-2.372889
67	1	0	-0.864002	0.555260	-2.405831
68	6	0	-0.887190	3.949722	-2.286099
69	1	0	0.868814	5.191943	-2.095512
70	1	0	-2.432423	2.453623	-2.491272
71	1	0	-1.579048	4.787521	-2.325697
72	8	0	1.106516	-3.114789	-0.580657
73	8	0	3.053192	-3.643543	-1.581737
74	6	0	2.788927	-5.025591	-1.315885
75	1	0	3.635046	-5.568311	-1.736963
76	1	0	2.722927	-5.192736	-0.237533
77	1	0	1.853870	-5.333533	-1.791220
78	6	0	3.558511	2.925326	0.547054
79	7	0	2.232242	2.663419	0.939438
80	8	0	4.112090	4.002981	0.529893
81	6	0	1.271141	3.602225	1.318829
82	8	0	1.566798	4.817786	0.842475
83	8	0	0.288470	3.352690	1.982472
84	6	0	0.634825	5.837562	1.196814
85	1	0	1.045776	6.757198	0.778601
86	1	0	-0.347699	5.621336	0.767018
87	1	0	0.543609	5.917796	2.283592

TS-D

Center Number	Atomic Number	Atomic Type	Coordinates (Angstroms)		
			X	Y	Z
1	47	0	-0.414260	-1.038877	-0.460515
2	15	0	-2.693342	-0.742739	0.163509
3	6	0	-3.787485	-2.166404	-0.141245
4	6	0	-3.249064	-3.452629	-0.012265
5	6	0	-5.137939	-2.009404	-0.476221
6	6	0	-4.059800	-4.571147	-0.197596
7	1	0	-2.193198	-3.574184	0.221365
8	6	0	-5.943543	-3.130313	-0.669280

9	1	0	-5.553577	-1.011745	-0.592383
10	6	0	-5.406839	-4.411091	-0.525915
11	1	0	-3.636411	-5.567083	-0.097081
12	1	0	-6.990488	-3.003708	-0.933093
13	1	0	-6.036456	-5.283909	-0.678837
14	6	0	-3.437894	0.600230	-0.828612
15	6	0	-4.143684	1.660394	-0.251713
16	6	0	-3.259331	0.563641	-2.218581
17	6	0	-4.674936	2.666982	-1.060361
18	1	0	-4.272061	1.703121	0.825956
19	6	0	-3.798284	1.563037	-3.022450
20	1	0	-2.683299	-0.243316	-2.667410
21	6	0	-4.507231	2.618618	-2.443819
22	1	0	-5.219033	3.490463	-0.604555
23	1	0	-3.647773	1.529837	-4.098119
24	1	0	-4.917239	3.406357	-3.070638
25	6	0	-3.006140	-0.241742	1.883468
26	6	0	-2.114513	0.672708	2.461019
27	6	0	-4.119589	-0.689522	2.604589
28	6	0	-2.355613	1.152223	3.746934
29	1	0	-1.226299	1.004243	1.929619
30	6	0	-4.343957	-0.216237	3.896851
31	1	0	-4.806021	-1.405839	2.161765
32	6	0	-3.466735	0.709096	4.466051
33	1	0	-1.660384	1.866980	4.177730
34	1	0	-5.205402	-0.570121	4.457934
35	1	0	-3.647032	1.078437	5.472744
36	6	0	3.056165	-1.014975	0.206731
37	6	0	2.477450	-1.591491	-1.193620
38	6	0	2.012884	0.513075	-1.688182
39	1	0	2.357411	-1.374703	0.970982
40	1	0	3.324810	-1.629361	-1.894692
41	6	0	2.925364	0.480766	0.165227
42	6	0	4.037688	1.486743	0.149720
43	1	0	4.491045	1.666334	-0.834303
44	1	0	4.863560	1.241921	0.831737
45	6	0	1.985063	-2.992784	-0.957697
46	7	0	1.445668	-0.704636	-1.618568
47	6	0	4.425876	-1.548152	0.513031
48	6	0	4.637646	-2.328845	1.654128
49	6	0	5.513222	-1.300870	-0.334845
50	6	0	5.898846	-2.848904	1.944741
51	1	0	3.801684	-2.526432	2.322374
52	6	0	6.775478	-1.816223	-0.049134
53	1	0	5.371971	-0.699622	-1.230340
54	6	0	6.973371	-2.594204	1.092886
55	1	0	6.041820	-3.451423	2.838542
56	1	0	7.606603	-1.610710	-0.719408
57	1	0	7.957977	-2.996700	1.316743
58	6	0	1.837123	1.043787	0.907046
59	8	0	0.805866	0.488936	1.281162
60	1	0	3.017013	0.559539	-2.140116
61	6	0	1.278992	1.778850	-1.899016
62	6	0	1.998479	2.885951	-2.375736

63	6	0	-0.071468	1.963475	-1.578567
64	6	0	1.392047	4.129975	-2.524263
65	1	0	3.050154	2.767965	-2.628768
66	6	0	-0.686997	3.200872	-1.735149
67	1	0	-0.654670	1.133524	-1.197095
68	6	0	0.043196	4.291886	-2.207393
69	1	0	1.976262	4.974163	-2.880621
70	1	0	-1.738993	3.304937	-1.483180
71	1	0	-0.433475	5.262258	-2.323463
72	8	0	0.891745	-3.280252	-0.495258
73	8	0	2.916472	-3.905780	-1.240936
74	6	0	2.587572	-5.260710	-0.916518
75	1	0	3.468776	-5.844129	-1.183117
76	1	0	2.373168	-5.352152	0.151597
77	1	0	1.717010	-5.588739	-1.490892
78	6	0	3.390496	2.779077	0.621231
79	7	0	2.085329	2.453119	1.055544
80	8	0	3.907853	3.870069	0.663900
81	6	0	1.081322	3.353535	1.444754
82	8	0	1.290794	4.555067	0.910406
83	8	0	0.144359	3.062666	2.154255
84	6	0	0.306281	5.535763	1.233705
85	1	0	0.644862	6.449729	0.745406
86	1	0	-0.670434	5.230777	0.848193
87	1	0	0.243637	5.676318	2.316350

INT-D2

Center Number	Atomic Number	Atomic Type	Coordinates (Angstroms)		
			X	Y	Z
1	47	0	-0.494432	-1.125018	-0.542986
2	15	0	-2.732075	-0.723598	0.126236
3	6	0	-3.921557	-2.064185	-0.197731
4	6	0	-3.484606	-3.384284	-0.029656
5	6	0	-5.243704	-1.813949	-0.583063
6	6	0	-4.369418	-4.442852	-0.225526
7	1	0	-2.449842	-3.579108	0.245181
8	6	0	-6.123397	-2.876119	-0.786985
9	1	0	-5.580055	-0.790790	-0.729188
10	6	0	-5.688998	-4.189909	-0.604268
11	1	0	-4.025105	-5.465280	-0.093924
12	1	0	-7.148204	-2.677392	-1.090323
13	1	0	-6.376104	-5.016620	-0.765588
14	6	0	-3.382616	0.696131	-0.822240
15	6	0	-4.121805	1.723410	-0.226735
16	6	0	-3.098112	0.753585	-2.193037
17	6	0	-4.580825	2.790972	-1.000100
18	1	0	-4.330191	1.693831	0.839090
19	6	0	-3.567087	1.813029	-2.963313
20	1	0	-2.486297	-0.021622	-2.649775
21	6	0	-4.308944	2.834851	-2.367503

22	1	0	-5.150025	3.589345	-0.530330
23	1	0	-3.330459	1.854918	-4.022912
24	1	0	-4.662190	3.670463	-2.966356
25	6	0	-3.008295	-0.247739	1.861018
26	6	0	-2.053684	0.579593	2.467093
27	6	0	-4.155025	-0.627156	2.568796
28	6	0	-2.259565	1.042903	3.764475
29	1	0	-1.140193	0.855578	1.949004
30	6	0	-4.347440	-0.172302	3.873023
31	1	0	-4.892339	-1.276925	2.105431
32	6	0	-3.404559	0.667381	4.468983
33	1	0	-1.512407	1.689668	4.215034
34	1	0	-5.235718	-0.473878	4.422672
35	1	0	-3.559830	1.022245	5.484935
36	6	0	3.118837	-1.048689	0.162197
37	6	0	2.428804	-1.725391	-1.101759
38	6	0	2.038276	0.414245	-1.497046
39	1	0	2.525846	-1.343263	1.034752
40	1	0	3.217764	-1.852676	-1.866364
41	6	0	2.849156	0.452128	-0.070661
42	6	0	3.985940	1.460346	-0.104207
43	1	0	4.384977	1.651415	-1.105533
44	1	0	4.830080	1.165488	0.530904
45	6	0	1.941975	-3.101325	-0.726836
46	7	0	1.392240	-0.842286	-1.525484
47	6	0	4.545719	-1.446358	0.388524
48	6	0	4.931722	-2.022287	1.603453
49	6	0	5.521597	-1.269245	-0.602000
50	6	0	6.252361	-2.411604	1.828133
51	1	0	4.184273	-2.165286	2.381556
52	6	0	6.841903	-1.654841	-0.383437
53	1	0	5.245632	-0.823694	-1.555113
54	6	0	7.213009	-2.229142	0.833900
55	1	0	6.530228	-2.855901	2.780858
56	1	0	7.583526	-1.507327	-1.164795
57	1	0	8.243447	-2.529901	1.005182
58	6	0	1.916582	1.006973	0.959638
59	8	0	1.032551	0.410926	1.536539
60	1	0	2.894598	0.435317	-2.206889
61	6	0	1.219347	1.646815	-1.795760
62	6	0	1.706342	2.573499	-2.723982
63	6	0	0.014882	1.947225	-1.146886
64	6	0	1.014577	3.752486	-3.004024
65	1	0	2.641864	2.364136	-3.239339
66	6	0	-0.687525	3.114751	-1.426447
67	1	0	-0.383205	1.266979	-0.401291
68	6	0	-0.189934	4.025745	-2.357968
69	1	0	1.418502	4.454788	-3.728982
70	1	0	-1.627792	3.304751	-0.915408
71	1	0	-0.736261	4.939916	-2.577624
72	8	0	0.826819	-3.375660	-0.315282
73	8	0	2.913801	-4.014310	-0.842253
74	6	0	2.589057	-5.335054	-0.400068
75	1	0	3.498363	-5.919762	-0.540803

76	1	0	2.298165	-5.322847	0.654016
77	1	0	1.769062	-5.745794	-0.995647
78	6	0	3.404568	2.742817	0.449029
79	7	0	2.179577	2.399599	1.082311
80	8	0	3.904716	3.839084	0.423643
81	6	0	1.215286	3.293447	1.592569
82	8	0	1.363202	4.498019	1.052407
83	8	0	0.356778	2.977980	2.383508
84	6	0	0.396052	5.466010	1.463485
85	1	0	0.685838	6.387332	0.958629
86	1	0	-0.603971	5.152412	1.152078
87	1	0	0.418399	5.594318	2.548931

product (endo)

Center Number	Atomic Number	Atomic Type	Coordinates (Angstroms)		
			X	Y	Z
1	6	0	-1.743291	-0.055442	-0.182394
2	6	0	-1.995778	-1.352555	0.675146
3	6	0	0.060439	-0.590476	1.399233
4	1	0	-1.796754	-0.323084	-1.241764
5	1	0	-2.709644	-1.106828	1.470432
6	6	0	-0.272239	0.315905	0.139016
7	6	0	0.095947	1.778904	0.355008
8	1	0	0.108008	2.092481	1.401750
9	1	0	-0.586453	2.455537	-0.173129
10	6	0	-2.597673	-2.454996	-0.163989
11	7	0	-0.737944	-1.782266	1.248061
12	6	0	-2.730405	1.048814	0.077120
13	6	0	-3.395167	1.657906	-0.990309
14	6	0	-2.976768	1.520054	1.372944
15	6	0	-4.283553	2.711768	-0.774757
16	1	0	-3.215498	1.299082	-2.001613
17	6	0	-3.860485	2.573016	1.594059
18	1	0	-2.471753	1.063580	2.221751
19	6	0	-4.517977	3.173591	0.519032
20	1	0	-4.792400	3.170061	-1.618912
21	1	0	-4.037143	2.925783	2.607033
22	1	0	-5.208960	3.994584	0.690974
23	6	0	0.648652	-0.122990	-0.984547
24	8	0	0.556509	-1.134835	-1.638212
25	1	0	-0.329186	-0.024713	2.257955
26	6	0	1.532374	-0.815209	1.624454
27	6	0	2.245311	0.098614	2.407102
28	6	0	2.231209	-1.858843	1.007333
29	6	0	3.625507	-0.011700	2.559972
30	1	0	1.714556	0.908379	2.903309
31	6	0	3.609882	-1.977596	1.167942
32	1	0	1.712384	-2.579192	0.382057
33	6	0	4.312580	-1.052879	1.939418
34	1	0	4.160732	0.715719	3.164317

35	1	0	4.135487	-2.796179	0.682954
36	1	0	5.388987	-1.145593	2.058566
37	8	0	-2.028953	-3.478231	-0.472270
38	8	0	-3.841676	-2.135139	-0.549478
39	6	0	-4.486461	-3.086672	-1.405397
40	1	0	-5.465597	-2.661482	-1.625395
41	1	0	-3.907932	-3.224165	-2.322713
42	1	0	-4.587926	-4.048076	-0.895190
43	6	0	1.471516	1.945031	-0.252559
44	7	0	1.691788	0.815628	-1.067756
45	8	0	2.221073	2.883170	-0.140434
46	6	0	2.845611	0.608767	-1.873800
47	8	0	3.936415	0.825661	-1.150617
48	8	0	2.798838	0.271486	-3.028141
49	6	0	5.172432	0.711611	-1.865102
50	1	0	5.945639	0.948083	-1.135055
51	1	0	5.293846	-0.305428	-2.246205
52	1	0	5.194266	1.420565	-2.696651
53	1	0	-0.309204	-2.457281	0.617039

INT-E2

Center Number	Atomic Number	Atomic Type	Coordinates (Angstroms)		
			X	Y	Z
1	47	0	-0.968262	0.726948	0.699176
2	15	0	-2.764269	-0.776606	0.351451
3	6	0	-3.074097	-1.896870	1.756772
4	6	0	-3.048718	-1.358536	3.049201
5	6	0	-3.352328	-3.256287	1.577302
6	6	0	-3.320819	-2.167503	4.149495
7	1	0	-2.805414	-0.307602	3.191920
8	6	0	-3.616419	-4.065292	2.682079
9	1	0	-3.348509	-3.682945	0.577746
10	6	0	-3.605181	-3.522257	3.967018
11	1	0	-3.296362	-1.744206	5.150146
12	1	0	-3.825347	-5.122241	2.537819
13	1	0	-3.806689	-4.155721	4.826941
14	6	0	-2.350300	-1.891951	-1.024585
15	6	0	-3.201723	-2.118331	-2.110331
16	6	0	-1.072925	-2.472946	-1.005789
17	6	0	-2.779732	-2.927790	-3.166163
18	1	0	-4.184653	-1.656513	-2.140391
19	6	0	-0.660538	-3.286460	-2.055998
20	1	0	-0.375928	-2.260795	-0.198643
21	6	0	-1.513653	-3.513268	-3.138432
22	1	0	-3.440463	-3.093410	-4.013484
23	1	0	0.340571	-3.704863	-2.028611
24	1	0	-1.185305	-4.134517	-3.967901
25	6	0	-4.404751	-0.078671	-0.022159
26	6	0	-4.500219	1.282565	-0.330934
27	6	0	-5.563193	-0.866220	0.005179

28	6	0	-5.738712	1.846405	-0.635561
29	1	0	-3.602844	1.896335	-0.329278
30	6	0	-6.799112	-0.300597	-0.299000
31	1	0	-5.497295	-1.917633	0.273387
32	6	0	-6.887365	1.055187	-0.623979
33	1	0	-5.806238	2.904943	-0.873028
34	1	0	-7.695088	-0.915590	-0.276515
35	1	0	-7.853467	1.495268	-0.857369
36	6	0	3.405277	-0.399997	0.333758
37	6	0	3.112084	-0.843106	-1.181193
38	6	0	1.706774	0.806420	-1.884526
39	1	0	2.658314	-0.937352	0.926588
40	1	0	3.896654	-0.398354	-1.810465
41	6	0	3.140220	1.044576	0.526041
42	6	0	3.956003	2.226702	0.116270
43	1	0	4.290355	2.243218	-0.932424
44	1	0	4.862186	2.382060	0.722496
45	6	0	3.237415	-2.348371	-1.233459
46	7	0	1.796393	-0.429886	-1.562567
47	6	0	4.779773	-0.879767	0.734455
48	6	0	4.910968	-1.876695	1.706584
49	6	0	5.940375	-0.382574	0.129387
50	6	0	6.166907	-2.361249	2.072530
51	1	0	4.015260	-2.276260	2.176861
52	6	0	7.197353	-0.861021	0.492527
53	1	0	5.863892	0.376325	-0.645157
54	6	0	7.316037	-1.853929	1.466575
55	1	0	6.246534	-3.135724	2.831849
56	1	0	8.086534	-0.461370	0.010682
57	1	0	8.296566	-2.228889	1.749339
58	6	0	1.943465	1.451146	1.051927
59	8	0	1.020975	0.793609	1.614149
60	1	0	2.592880	1.444797	-2.001381
61	6	0	0.427441	1.465624	-2.159362
62	6	0	0.363713	2.865231	-2.191113
63	6	0	-0.740765	0.719164	-2.378384
64	6	0	-0.851432	3.509384	-2.412454
65	1	0	1.267165	3.449221	-2.028146
66	6	0	-1.949604	1.365354	-2.617083
67	1	0	-0.672124	-0.362707	-2.381657
68	6	0	-2.010201	2.761589	-2.625235
69	1	0	-0.892192	4.595537	-2.421697
70	1	0	-2.845919	0.777311	-2.794698
71	1	0	-2.957776	3.263243	-2.806199
72	8	0	2.437938	-3.134659	-0.768814
73	8	0	4.394278	-2.718881	-1.808319
74	6	0	4.702433	-4.112189	-1.731208
75	1	0	5.669602	-4.224746	-2.221821
76	1	0	4.764939	-4.423164	-0.684615
77	1	0	3.938348	-4.705211	-2.241799
78	6	0	3.027096	3.415186	0.320441
79	7	0	1.855816	2.916451	0.931009
80	8	0	3.226695	4.558739	-0.025963
81	6	0	0.677795	3.614762	1.115793

82	8	0	0.894259	4.907245	1.349373
83	8	0	-0.445472	3.126233	1.073644
84	6	0	-0.278109	5.720220	1.430360
85	1	0	0.091352	6.740118	1.538385
86	1	0	-0.876352	5.619574	0.520790
87	1	0	-0.883073	5.434344	2.295159

INT-E3

Center Number	Atomic Number	Atomic Type	Coordinates (Angstroms)		
			X	Y	Z
1	6	0	4.090565	-0.073964	-0.308760
2	6	0	4.210040	1.106545	0.708877
3	6	0	2.170409	2.081574	0.104220
4	1	0	3.709291	0.360538	-1.238574
5	1	0	4.666936	0.743730	1.632734
6	1	0	2.498747	2.124876	-0.937970
7	6	0	3.074659	-1.066246	0.151946
8	6	0	3.210181	-1.957050	1.340271
9	1	0	3.480394	-1.433400	2.269429
10	1	0	3.930464	-2.782507	1.227343
11	6	0	5.138538	2.150165	0.113706
12	7	0	2.900709	1.637212	1.050582
13	6	0	0.814606	2.581900	0.363348
14	6	0	0.122848	3.246703	-0.660693
15	6	0	0.198482	2.418326	1.613117
16	6	0	-1.141308	3.786405	-0.422824
17	1	0	0.598669	3.364341	-1.632331
18	6	0	-1.069440	2.942337	1.840357
19	1	0	0.742954	1.887725	2.389018
20	6	0	-1.732616	3.645570	0.831108
21	1	0	-1.664697	4.316599	-1.213834
22	1	0	-1.546094	2.808870	2.808299
23	1	0	-2.715753	4.065978	1.017278
24	6	0	5.447370	-0.674972	-0.608149
25	6	0	5.921938	-0.700558	-1.923459
26	6	0	6.261586	-1.200238	0.402963
27	6	0	7.171207	-1.241629	-2.226608
28	1	0	5.301445	-0.288814	-2.716468
29	6	0	7.510240	-1.743065	0.106117
30	1	0	5.926506	-1.175415	1.436616
31	6	0	7.970567	-1.766637	-1.211259
32	1	0	7.520166	-1.251150	-3.256546
33	1	0	8.127037	-2.145522	0.906234
34	1	0	8.945233	-2.188862	-1.443221
35	6	0	1.816204	-1.118143	-0.361351
36	8	0	1.267370	-0.431392	-1.292129
37	47	0	-0.763839	0.293544	-1.017466
38	15	0	-3.054451	0.175865	-0.306750
39	6	0	-4.157958	-0.778079	-1.408930
40	6	0	-3.599899	-1.796062	-2.193778

41	6	0	-5.538494	-0.544074	-1.454964
42	6	0	-4.420869	-2.574147	-3.008020
43	1	0	-2.532683	-1.992184	-2.147847
44	6	0	-6.352619	-1.322619	-2.276478
45	1	0	-5.977902	0.248321	-0.855548
46	6	0	-5.795784	-2.339316	-3.053037
47	1	0	-3.980716	-3.362383	-3.613304
48	1	0	-7.422587	-1.133079	-2.308865
49	1	0	-6.431520	-2.943844	-3.694921
50	6	0	-4.058008	1.643088	0.088142
51	6	0	-4.560899	1.883657	1.368962
52	6	0	-4.309863	2.562768	-0.938636
53	6	0	-5.305593	3.036918	1.621728
54	1	0	-4.363327	1.177944	2.170339
55	6	0	-5.060262	3.706761	-0.686935
56	1	0	-3.910894	2.383005	-1.934542
57	6	0	-5.556669	3.948874	0.597228
58	1	0	-5.688267	3.221351	2.622258
59	1	0	-5.252136	4.415063	-1.488719
60	1	0	-6.135369	4.846968	0.796323
61	6	0	-3.010886	-0.803353	1.232233
62	6	0	-1.825541	-0.835882	1.976832
63	6	0	-4.115095	-1.553835	1.656870
64	6	0	-1.734370	-1.623695	3.122462
65	1	0	-0.962513	-0.262262	1.645778
66	6	0	-4.027440	-2.327661	2.812028
67	1	0	-5.032220	-1.548201	1.073696
68	6	0	-2.835828	-2.369668	3.539880
69	1	0	-0.794191	-1.682727	3.662055
70	1	0	-4.884362	-2.913866	3.134260
71	1	0	-2.760635	-2.997181	4.423938
72	8	0	4.884137	2.840461	-0.852319
73	8	0	6.314402	2.182795	0.760033
74	6	0	7.314402	3.021345	0.174271
75	1	0	8.193625	2.913716	0.809945
76	1	0	7.532544	2.688415	-0.844196
77	1	0	6.976854	4.061190	0.151764
78	6	0	1.833897	-2.559392	1.519810
79	8	0	1.465227	-3.259028	2.436945
80	7	0	1.053450	-2.134904	0.414016
81	6	0	-0.121932	-2.716512	-0.014482
82	8	0	-0.722832	-2.391140	-1.029891
83	8	0	-0.546073	-3.686796	0.796964
84	6	0	-1.790919	-4.278832	0.424732
85	1	0	-1.706187	-4.779530	-0.544030
86	1	0	-2.005275	-5.000488	1.213114
87	1	0	-2.575951	-3.520935	0.376568

INT-E4

Center Number	Atomic Number	Atomic Type	Coordinates (Angstroms)		
			X	Y	Z
1	6	0	-4.049137	-0.184418	-0.751949
2	6	0	-4.115448	-0.943974	0.611209
3	6	0	-2.065270	-2.054838	0.364283
4	1	0	-3.554121	-0.864044	-1.453842
5	1	0	-4.573303	-0.294653	1.360646
6	1	0	-2.475688	-2.488326	-0.549884
7	6	0	-3.182685	1.024554	-0.606994
8	6	0	-3.594260	2.314534	0.020285
9	1	0	-4.036019	2.210977	1.021331
10	1	0	-4.293435	2.918626	-0.575496
11	6	0	-4.996208	-2.170308	0.456995
12	7	0	-2.768234	-1.268041	1.089092
13	1	0	-2.401136	0.025928	2.163623
14	6	0	-0.706772	-2.490389	0.688332
15	6	0	-0.102297	-3.421777	-0.171954
16	6	0	-0.003607	-2.042745	1.816930
17	6	0	1.166544	-3.923390	0.106592
18	1	0	-0.643824	-3.758170	-1.053440
19	6	0	1.269074	-2.539264	2.083922
20	1	0	-0.439156	-1.292374	2.467439
21	6	0	1.849180	-3.491523	1.243096
22	1	0	1.623596	-4.650107	-0.559262
23	1	0	1.811324	-2.180330	2.954822
24	1	0	2.837410	-3.883314	1.463127
25	6	0	-5.430430	0.107231	-1.296851
26	6	0	-5.775560	-0.324299	-2.581462
27	6	0	-6.390421	0.796674	-0.546224
28	6	0	-7.040853	-0.069961	-3.109655
29	1	0	-5.040814	-0.868190	-3.171139
30	6	0	-7.656714	1.053616	-1.068428
31	1	0	-6.155607	1.128508	0.461503
32	6	0	-7.987215	0.621797	-2.353614
33	1	0	-7.287780	-0.414977	-4.110858
34	1	0	-8.387632	1.590708	-0.468607
35	1	0	-8.975153	0.821445	-2.761154
36	6	0	-1.840309	0.995533	-0.831639
37	8	0	-1.103335	0.061647	-1.302850
38	47	0	0.959228	-0.347767	-0.883554
39	15	0	3.294639	-0.267375	-0.450237
40	6	0	4.277289	0.475929	-1.797164
41	6	0	3.687909	1.497549	-2.554409
42	6	0	5.599040	0.091788	-2.053901
43	6	0	4.423293	2.130372	-3.554530
44	1	0	2.664010	1.801736	-2.353275
45	6	0	6.325876	0.725224	-3.061584
46	1	0	6.059509	-0.701744	-1.472108
47	6	0	5.740228	1.745378	-3.811718
48	1	0	3.960583	2.921386	-4.138923

49	1	0	7.350490	0.420337	-3.259049
50	1	0	6.307692	2.236513	-4.598097
51	6	0	4.226476	-1.772522	-0.027579
52	6	0	4.907534	-1.911616	1.184205
53	6	0	4.231205	-2.826319	-0.950885
54	6	0	5.583353	-3.098612	1.472373
55	1	0	4.901971	-1.099892	1.905709
56	6	0	4.915495	-4.003603	-0.666609
57	1	0	3.688495	-2.725322	-1.888176
58	6	0	5.589379	-4.144315	0.549933
59	1	0	6.104547	-3.204134	2.420356
60	1	0	4.915880	-4.816641	-1.387981
61	1	0	6.114946	-5.068161	0.776734
62	6	0	3.542960	0.860884	0.956961
63	6	0	2.521971	0.981404	1.906501
64	6	0	4.715027	1.617035	1.094131
65	6	0	2.673224	1.842337	2.991969
66	1	0	1.593878	0.426345	1.803137
67	6	0	4.861112	2.479339	2.178627
68	1	0	5.500614	1.543059	0.346819
69	6	0	3.841926	2.590604	3.128593
70	1	0	1.857162	1.925524	3.702543
71	1	0	5.767865	3.070642	2.278477
72	1	0	3.957025	3.271430	3.968401
73	6	0	-1.407732	1.396447	3.150267
74	6	0	-1.566278	2.786676	3.698585
75	1	0	-2.565925	2.937363	4.113633
76	1	0	-0.803064	2.976932	4.455764
77	1	0	-1.434530	3.500683	2.876985
78	8	0	-2.531016	0.916906	2.633391
79	8	0	-0.349111	0.783444	3.157010
80	8	0	-4.732848	-3.137681	-0.228864
81	8	0	-6.144667	-2.032585	1.135323
82	6	0	-7.112593	-3.065243	0.922348
83	1	0	-7.974407	-2.785507	1.528516
84	1	0	-7.383547	-3.110726	-0.135917
85	1	0	-6.714093	-4.033293	1.237834
86	6	0	-2.303923	3.087535	0.169672
87	8	0	-2.170494	4.212392	0.604722
88	7	0	-1.276705	2.268106	-0.344308
89	6	0	0.037393	2.662359	-0.509316
90	8	0	0.760402	2.283845	-1.420713
91	8	0	0.439492	3.485354	0.458891
92	6	0	1.743530	4.045021	0.283476
93	1	0	1.780560	4.633807	-0.637565
94	1	0	1.897568	4.683375	1.152777
95	1	0	2.500150	3.258990	0.249482

TS-E

Center Number	Atomic Number	Atomic Type	Coordinates (Angstroms)		
			X	Y	Z
1	6	0	-3.806013	0.437504	-0.847098
2	6	0	-4.408085	-0.984906	-0.548836
3	6	0	-2.172413	-1.491344	-0.876897
4	1	0	-3.589828	0.478467	-1.920512
5	1	0	-5.036224	-1.001645	0.341755
6	1	0	-2.267867	-1.046937	-1.864867
7	6	0	-2.495500	0.552030	-0.116563
8	6	0	-2.496008	0.679367	1.375030
9	1	0	-2.305989	-0.277422	1.902654
10	1	0	-3.421143	1.092590	1.791813
11	6	0	-5.230961	-1.420894	-1.749718
12	7	0	-3.314622	-1.903795	-0.312746
13	1	0	-3.320812	-2.313520	0.670262
14	6	0	-0.885398	-2.150097	-0.679661
15	6	0	-0.030387	-2.219374	-1.801750
16	6	0	-0.500939	-2.768248	0.518619
17	6	0	1.178669	-2.916787	-1.726164
18	1	0	-0.370784	-1.812974	-2.753704
19	6	0	0.710328	-3.452811	0.581278
20	1	0	-1.119305	-2.659933	1.409869
21	6	0	1.547814	-3.536746	-0.533453
22	1	0	1.820713	-2.987635	-2.599681
23	1	0	1.007245	-3.916165	1.518386
24	1	0	2.488428	-4.075418	-0.473581
25	6	0	-4.747105	1.585109	-0.545340
26	6	0	-4.657779	2.732898	-1.343898
27	6	0	-5.655710	1.583380	0.518326
28	6	0	-5.448693	3.849770	-1.087703
29	1	0	-3.950699	2.745585	-2.171131
30	6	0	-6.449477	2.701480	0.778871
31	1	0	-5.757687	0.710120	1.156216
32	6	0	-6.349303	3.838184	-0.020962
33	1	0	-5.362734	4.729324	-1.721000
34	1	0	-7.148110	2.679318	1.611458
35	1	0	-6.968954	4.707620	0.182917
36	6	0	-1.345595	1.181391	-0.638713
37	8	0	-0.903645	1.186162	-1.811157
38	47	0	1.215460	0.220160	-1.672738
39	15	0	3.291321	0.012981	-0.410089
40	6	0	4.634137	1.211411	-0.700425
41	6	0	4.319147	2.468237	-1.233646
42	6	0	5.962383	0.908862	-0.372986
43	6	0	5.324426	3.415194	-1.422538
44	1	0	3.288413	2.707020	-1.478199
45	6	0	6.963684	1.858634	-0.568987
46	1	0	6.213119	-0.068186	0.030914
47	6	0	6.646201	3.113014	-1.091860
48	1	0	5.073701	4.388928	-1.835464

49	1	0	7.992318	1.617411	-0.313544
50	1	0	7.428703	3.851484	-1.246242
51	6	0	4.152016	-1.592228	-0.375705
52	6	0	4.397354	-2.277697	0.817440
53	6	0	4.553008	-2.155375	-1.593809
54	6	0	5.036981	-3.517495	0.790368
55	1	0	4.075237	-1.851082	1.762875
56	6	0	5.194914	-3.390176	-1.618320
57	1	0	4.354476	-1.626854	-2.524207
58	6	0	5.434555	-4.075944	-0.424234
59	1	0	5.219011	-4.048953	1.720852
60	1	0	5.501269	-3.822888	-2.567135
61	1	0	5.926819	-5.044677	-0.443395
62	6	0	2.758323	0.278161	1.308589
63	6	0	1.533369	-0.284705	1.692936
64	6	0	3.526309	0.972465	2.249298
65	6	0	1.079660	-0.182498	3.004488
66	1	0	0.930927	-0.816392	0.962694
67	6	0	3.059831	1.098584	3.558515
68	1	0	4.477688	1.412551	1.961526
69	6	0	1.845569	0.522347	3.935005
70	1	0	0.129818	-0.635147	3.282660
71	1	0	3.649032	1.650675	4.286712
72	1	0	1.483477	0.634097	4.953166
73	6	0	-2.966333	-2.430694	3.167355
74	6	0	-3.476044	-2.847453	4.541380
75	1	0	-3.892289	-3.859165	4.503743
76	1	0	-2.682429	-2.789683	5.290800
77	1	0	-4.288600	-2.172714	4.838657
78	8	0	-3.711593	-2.713719	2.179034
79	8	0	-1.864008	-1.822230	3.094106
80	8	0	-4.784928	-1.553263	-2.870228
81	8	0	-6.511676	-1.628070	-1.421571
82	6	0	-7.368944	-2.022940	-2.498935
83	1	0	-8.358770	-2.134322	-2.056302
84	1	0	-7.376104	-1.255272	-3.277482
85	1	0	-7.026959	-2.969169	-2.926447
86	6	0	-1.364279	1.608562	1.697864
87	8	0	-1.083622	2.086195	2.766783
88	7	0	-0.642423	1.812585	0.470746
89	6	0	0.497948	2.589127	0.318606
90	8	0	1.174795	2.616979	-0.700707
91	8	0	0.774212	3.305296	1.398613
92	6	0	1.977004	4.075478	1.329182
93	1	0	1.897532	4.838066	0.549478
94	1	0	2.069935	4.536131	2.312397
95	1	0	2.832032	3.427538	1.126450

INT-E5

Center Number	Atomic Number	Atomic Type	Coordinates (Angstroms)		
			X	Y	Z
1	6	0	-3.753856	0.311091	-0.933586
2	6	0	-4.466836	-1.012037	-0.527002
3	6	0	-2.239805	-1.474498	-0.943934
4	1	0	-3.739178	0.348373	-2.029092
5	1	0	-5.033251	-0.929443	0.401646
6	1	0	-2.390674	-1.426475	-2.029665
7	6	0	-2.293520	0.013917	-0.478794
8	6	0	-2.100656	0.319472	1.003064
9	1	0	-1.449421	-0.401014	1.524789
10	1	0	-3.017115	0.322667	1.589220
11	6	0	-5.397341	-1.467482	-1.638046
12	7	0	-3.434880	-2.047293	-0.351835
13	1	0	-3.310337	-2.182238	0.665805
14	6	0	-0.964169	-2.237902	-0.729587
15	6	0	-0.174858	-2.540291	-1.861998
16	6	0	-0.534889	-2.681930	0.525528
17	6	0	1.031582	-3.251283	-1.728334
18	1	0	-0.550463	-2.287837	-2.853041
19	6	0	0.661981	-3.392461	0.647544
20	1	0	-1.106768	-2.463389	1.428785
21	6	0	1.450792	-3.676371	-0.465084
22	1	0	1.612320	-3.500048	-2.613532
23	1	0	0.978286	-3.717777	1.634974
24	1	0	2.383635	-4.220280	-0.352868
25	6	0	-4.307582	1.613886	-0.425091
26	6	0	-4.040746	2.775462	-1.163103
27	6	0	-5.005080	1.738449	0.781632
28	6	0	-4.441597	4.027738	-0.704717
29	1	0	-3.510803	2.690038	-2.110538
30	6	0	-5.411713	2.990356	1.242064
31	1	0	-5.230186	0.859459	1.379161
32	6	0	-5.127902	4.138927	0.504982
33	1	0	-4.220358	4.915424	-1.292121
34	1	0	-5.946471	3.065463	2.185309
35	1	0	-5.440954	5.113908	0.869375
36	6	0	-1.266147	0.861409	-1.160242
37	8	0	-0.855212	0.720306	-2.307684
38	47	0	1.264783	-0.447425	-1.651964
39	15	0	3.148442	-0.065040	-0.185282
40	6	0	4.512562	1.010439	-0.725178
41	6	0	4.276846	1.984529	-1.702390
42	6	0	5.784464	0.895109	-0.147886
43	6	0	5.305900	2.841356	-2.091926
44	1	0	3.288015	2.081902	-2.139211
45	6	0	6.809216	1.751922	-0.543160
46	1	0	5.970468	0.134490	0.605740
47	6	0	6.570819	2.726160	-1.514795
48	1	0	5.118673	3.595850	-2.851550

49	1	0	7.794198	1.658233	-0.093342
50	1	0	7.372592	3.391720	-1.824080
51	6	0	3.975083	-1.619485	0.287981
52	6	0	3.910320	-2.146850	1.579548
53	6	0	4.632181	-2.336333	-0.721885
54	6	0	4.491416	-3.385648	1.855759
55	1	0	3.398184	-1.601316	2.366295
56	6	0	5.223584	-3.563448	-0.439685
57	1	0	4.677416	-1.932364	-1.731382
58	6	0	5.147198	-4.095123	0.850876
59	1	0	4.428767	-3.794125	2.860951
60	1	0	5.735060	-4.111280	-1.226910
61	1	0	5.597126	-5.059954	1.069356
62	6	0	2.515955	0.657015	1.356006
63	6	0	1.405790	0.045021	1.956882
64	6	0	3.084830	1.792304	1.942302
65	6	0	0.882842	0.539195	3.148133
66	1	0	0.949517	-0.832298	1.503880
67	6	0	2.540026	2.304020	3.121199
68	1	0	3.946047	2.271371	1.484669
69	6	0	1.447816	1.679503	3.722988
70	1	0	0.027712	0.028731	3.588518
71	1	0	2.974494	3.194279	3.569583
72	1	0	1.023036	2.088693	4.635399
73	6	0	-2.626896	-1.773600	3.415072
74	6	0	-3.156103	-1.723191	4.846776
75	1	0	-4.116500	-2.239303	4.930818
76	1	0	-2.429852	-2.152936	5.543870
77	1	0	-3.304173	-0.672809	5.130725
78	8	0	-3.465472	-1.962193	2.490334
79	8	0	-1.384696	-1.582263	3.253075
80	8	0	-5.158889	-1.373115	-2.825641
81	8	0	-6.507478	-2.033365	-1.146205
82	6	0	-7.396906	-2.592826	-2.116812
83	1	0	-8.232105	-2.999757	-1.546149
84	1	0	-7.740923	-1.819942	-2.809891
85	1	0	-6.892618	-3.383059	-2.679789
86	6	0	-1.430670	1.653556	1.049765
87	8	0	-1.338414	2.438773	1.950649
88	7	0	-0.801886	1.822622	-0.253908
89	6	0	0.276688	2.673388	-0.538163
90	8	0	1.137948	2.400125	-1.352034
91	8	0	0.236058	3.772753	0.191928
92	6	0	1.383106	4.623989	0.074492
93	1	0	1.451440	5.028350	-0.938771
94	1	0	1.218240	5.419779	0.799961
95	1	0	2.289756	4.063293	0.312312

product (2,5-trans)

Center Number	Atomic Number	Atomic Type	Coordinates (Angstroms)		
			X	Y	Z
1	6	0	1.627349	-0.245353	-0.298857
2	6	0	2.368541	0.996830	0.236073
3	6	0	0.164652	1.621487	-0.350717
4	1	0	1.729189	-0.228052	-1.390200
5	1	0	2.780353	0.844390	1.236496
6	1	0	0.280297	1.691080	-1.439806
7	6	0	0.150156	0.083962	-0.019596
8	6	0	-0.386135	-0.216048	1.376122
9	1	0	-0.358707	0.627288	2.070151
10	1	0	0.149576	-1.055152	1.837192
11	6	0	3.513624	1.394537	-0.685322
12	7	0	1.392654	2.101371	0.265786
13	1	0	1.237041	2.393411	1.223447
14	6	0	-1.098268	2.338452	0.043346
15	6	0	-2.217729	2.195786	-0.787150
16	6	0	-1.236072	3.063869	1.229995
17	6	0	-3.447675	2.737455	-0.427456
18	1	0	-2.131252	1.643328	-1.719770
19	6	0	-2.465104	3.618680	1.587357
20	1	0	-0.389445	3.218312	1.894657
21	6	0	-3.576441	3.450430	0.764733
22	1	0	-4.304293	2.597830	-1.081016
23	1	0	-2.551103	4.180022	2.514043
24	1	0	-4.535776	3.874645	1.048807
25	6	0	2.092997	-1.591875	0.187427
26	6	0	1.994282	-2.684819	-0.683363
27	6	0	2.566051	-1.816832	1.485567
28	6	0	2.350214	-3.965827	-0.267995
29	1	0	1.631067	-2.521654	-1.695164
30	6	0	2.927039	-3.097609	1.903889
31	1	0	2.660683	-0.991235	2.186773
32	6	0	2.818094	-4.177273	1.029138
33	1	0	2.265729	-4.799301	-0.960643
34	1	0	3.294667	-3.249172	2.915636
35	1	0	3.099992	-5.175244	1.354402
36	6	0	-0.807886	-0.630205	-0.949347
37	8	0	-0.658592	-0.845079	-2.129024
38	8	0	3.516827	1.260793	-1.888566
39	8	0	4.514033	1.956378	0.010536
40	6	0	5.605449	2.452974	-0.774372
41	1	0	6.316664	2.863913	-0.057773
42	1	0	6.059076	1.641347	-1.349137
43	1	0	5.253981	3.228528	-1.459834
44	6	0	-1.816768	-0.654966	1.168768
45	8	0	-2.701579	-0.730153	1.983611
46	7	0	-1.945695	-0.976425	-0.201650
47	6	0	-3.161726	-1.394230	-0.807799
48	8	0	-3.644938	-0.851920	-1.768397

49	8	0	-3.651116	-2.443176	-0.159047
50	6	0	-4.940970	-2.884944	-0.604778
51	1	0	-4.889898	-3.203717	-1.648686
52	1	0	-5.196753	-3.720311	0.045907
53	1	0	-5.668898	-2.076496	-0.501304

3–5. References

1. (a) Burkhard, J. A.; Wagner, B.; Fischer, H.; Schuler, F.; Müller, K.; Carreira, E. M. *Angew. Chem. Int. Ed.* **2010**, *49*, 3524–3527. (b) Carreira, E. M.; Fessard, T. C. *Chem. Rev.* **2014**, *114*, 8257–8322. (c) Hiesinger, K.; Dar'in, D.; Proschak, E.; Krasavin, M. *J. Med. Chem.* **2021**, *64*, 150–183.
2. Selected recent examples: (a) Li, F.; Zhou, Y.; Yang, H.; Liu, D.; Sun, B.; Zhang, F.-L. *Org. Lett.* **2018**, *20*, 146–149. (b) Fominova, K.; Diachuk, T.; Sadkova, I. V.; Mykhailiuk, P. M. *Eur. J. Org. Chem.* **2019**, 3553–3559. (c) Espinosa, M.; Noda, H.; Shibasaki, M. *Org. Lett.* **2019**, *21*, 9296–9299. (d) Lin, S.; Chen, Y.; Li, F.; Shi, C.; Shi, L. *Chem. Sci.* **2020**, *11*, 839–844. (e) Shennan, B. D.; Smith, P. W.; Ogura, Y.; Dixon, D. J. *Chem. Sci.* **2021**, *11*, 10354–10360.
3. Selected recent examples: (a) Chalyk, B. A.; Butko, M. V.; Yanshyna, O. O.; Garvrilenko, K. S.; Druzhenko, T. V.; Mykhailiuk, P. K. *Chem. Eur. J.* **2017**, *23*, 16782–16786. (b) Kirichok, A. A.; Shton, I.; Kliachyna, M.; Pishel, I.; Mykhailiuk, P. K. *Angew. Chem. Int. Ed.* **2017**, *56*, 8865–8869. (c) Kirichok, A. A.; Shton, I. O.; Pishel, I. M.; Zozulya, S. A.; Borysko, P. O.; Kubyshkin, V.; Zaporozhets, O. A.; Tolmachev, A. A.; Mykhailiuk, P. K. *Chem. Eur. J.* **2018**, *24*, 5444–5449.
4. Fang, X.; Wang, C.-J. *Org. Biomol. Chem.* **2018**, *16*, 2591–2601.
5. Adrio, J.; Carretero, J. C. *Chem. Commun.* **2019**, 55, 11979–11991.
6. (a) Antonchick, A. P.; Gerding-Reimers, C.; Catarinella, M.; Schürmann, M.; Preut, H.; Ziegler, S.; Rauh, D.; Waldmann, H. *Nat. Chem.* **2010**, *2*, 735–740. (b) Liu, T.-L.; Xue, Z.-Y.; Tao, H.-Y.; Wang, C.-J. *Org. Biomol. Chem.* **2011**, *9*, 1980–1986. (c) Awata, A.; Arai, T. *Chem. Eur. J.* **2012**, *18*, 8278–8282. (d) Wang, L.; Shi, X.-M.;

- Dong, W.-P.; Zhu, L.-P.; Wang, R. *Chem. Commun.* **2013**, *49*, 3458–3460. (e) Arai, T.; Ogawa, H.; Awata, A.; Sato, M.; Watabe, M.; Yamanaka, M. *Angew. Chem. Int. Ed.* **2015**, *54*, 1595–1599.
7. (a) Liu, T.-L.; He, Z.-L.; Li, Q.-H.; Tao, H.-Y.; Wang, C.-J. *Adv. Synth. Catal.* **2011**, *353*, 1713–1719. (b) Yildirim, O.; Grigalunas, M.; Brieger, L.; Strohmann, C.; Antonchick, A. P.; Waldman, H. *Angew. Chem. Int. Ed.* **2021**, *60*, 20012–20020.
8. Li, Q.-H.; Liu, T.-L.; Wei, L.; Zhou, X.; Tao, H.-Y.; Wang, C.-J. *Chem. Commun.* **2013**, *49*, 9642–9644.
9. (a) Yang, W.-L.; Liu, Y.-Z.; Luo, S.; Yu, X.; Fossey, J. S.; Deng, W.-P. *Chem. Commun.* **2015**, *51*, 9212–9215. (b) Yang, W.-L.; Tang, F.-F.; He, F.-S.; Li, C.-Y.; Yu, X.; Deng, W.-P. *Org. Lett.* **2015**, *17*, 4822–4825. (c) Gan, Z.; Zhi, M.; Han, R.; Li, E.-Q.; Duan, Z.; Mathey, F. *Org. Lett.* **2019**, *21*, 2782–2785.
10. Selected recent examples: (a) Li, J.-L.; Fu, L.; Wu, J.; Yang, K.-C.; Li, Q.-Z.; Gou, X.-J.; Peng, C.; Han, B.; Shen, X.-D. *Chem. Commun.* **2017**, *53*, 6875–6878. (b) Li, Q.; Zhou, L.; Shen, X.-D.; Yang, K.-C.; Zhang, X.; Dai, Q.-S.; Leng, H.-J.; Li, Q.-Z.; Li, J.-L. *Angew. Chem. Int. Ed.* **2018**, *57*, 1913–1917. (c) Wang, Y.; Chen, Y.; Li, X.; Mao, Y.; Chen, W.; Zhan, R.; Huang, H. *Org. Biomol. Chem.* **2019**, *17*, 3945–3950. (d) Lu, X.; Zhang, Y.; Wang, Y.; Chen, Y.; Chen, W.; Zhan, R.; Zhao, J. C.-G.; Huang, H. *Adv. Synth. Catal.* **2019**, *361*, 3234–3238. (e) Zhang, Y.; Wei, Y.; Shi, M. *Chem. Commun.* **2021**, *57*, 3599–3602. (f) Wang, H.; Zeng, T.; Chang, W.; Liu, L.; Li, J. *Org. Lett.* **2021**, *23*, 3573–3577.
11. (a) Zhao, X.; Xiong, J.; An, J.; Yu, J.; Zhu, L.; Feng, X.; Jiang, X. *Org. Chem. Front.* **2019**, *6*, 1989–1995. (b) Liu, X.; Lu, D.; Wu, J.-H.; Tan, J.-P.; Jiang, C.; Gao, G.; Wang, T. *Adv. Synth. Catal.* **2020**, *362*, 1490–1495.
12. Selected examples: (a) Oura, I.; Shimizu, K.; Ogata, K.; Fukuzawa, S.-i. *Org. Lett.* **2010**, *12*, 1752–1755. (b) Harada, M.; Kato, S.; Haraguchi, R.; Fukuzawa, S.-i. *Chem. Eur. J.* **2018**, *24*, 2580–2583. (c) Kato, S.; Suzuki, Y.; Suzuki, K.; Haraguchi, R.; Fukuzawa, S.-i. *J. Org. Chem.* **2018**, *83*, 13965–13972. (d) Suzuki, Y.; Kanemoto, K.; Inoue, A.; Imae, K.; Fukuzawa, S.-i. *J. Org. Chem.* **2021**, *86*, 14586–14596.

13. (a) Arai, T.; Yokoyama, N.; Mishiro, A.; Sato, H. *Angew. Chem. Int. Ed.* **2010**, *122*, 8067–8070. (b) Li, Q.-H.; Wei, L.; Chen, X.; Wang, C.-J. *Chem. Commun.* **2013**, *49*, 6277–6279. (c) Awata, A.; Arai, T. *Angew. Chem. Int. Ed.* **2014**, *53*, 10462–10465. (d) Arai, T.; Tokumitsu, C.; Miyazaki, T.; Kuwano, S.; Awata, A. *Org. Biomol. Chem.* **2016**, *14*, 1831–1839. (e) Wei, L.; Li, Q.-H.; Wang, C.-J. *J. Org. Chem.* **2018**, *83*, 11814–11824.
14. (a) Cheng, F.; Kalita, S. J.; Zhao, Z.-N.; Yang, X.; Zhao, Y.; Schneider, U.; Shibata, N.; Huang, Y.-Y. *Angew. Chem. Int. Ed.* **2019**, *58*, 16637–16643. (b) Kalita, S. J.; Cheng, F.; Fan, Q.-H.; Shibata, N.; Huang, Y.-Y. *J. Org. Chem.* **2021**, *86*, 8695–8705.
15. Selected recent examples of the mechanistic study: (a) Pascual-Escudero, A.; de Cózar, A.; Cossío, F. P.; Adrio, J.; Carretero, J. C. *Angew. Chem. Int. Ed.* **2016**, *55*, 15334–15338. (b) Caleffi, G. S.; Larrañaga, O.; Ferrándiz-Saperas, M.; Costa, P. R. R.; Nájera, C.; de Cózar, A.; Cossío, F. P.; Sansano, J. M. *J. Org. Chem.* **2019**, *84*, 10593–10605. (c) Chang, X.; Yang, Y.; Shen, C.; Xue, K.-S.; Wang, Z.-F.; Cong, H.; Tao, H.-Y.; Chung, L. W.; Wang, C.-J. *J. Am. Chem. Soc.* **2021**, *143*, 3519–3535. (d) Chang, X.; Liu, X.-T.; Li, F.; Yang, Y.; Chung, L. W.; Wang, C.-J. *Chem. Sci.* **2023**, *14*, 5460–5469.
16. Inoue, A.; Hosono, K.; Furuya, S.; Fukuzawa, S.-i. *J. Org. Chem.* **2024**, *89*, 1249–1255.
17. (a) Chen, X.; Zhu, L.; Fang, L.; Yan, S.; Lin, J. *RSC Adv.* **2014**, *4*, 9926–9934. (b) Huang, Y.; Li, Y.; Sun, J.; Li, J.; Zha, Z.; Wang, Z. *J. Org. Chem.* **2018**, *83*, 8464–8472. (c) Wang, H.; Zeng, T.; Li, X.; Wang, S.; Xiao, W.; Liu, L.; Chang, W.; Li, J. *Org. Chem. Front.* **2020**, *7*, 1809–1816.

Chapter 4

Formal Diastereodivergent Synthesis of 2,5-*cis/trans*-Pyrrolidines via Asymmetric (3+2) Cycloaddition

4-1. Introduction

Stereodivergent synthesis that affords several stereoisomers is of interest in drug discovery because stereodivergency can lead to various biological activities of stereoisomeric compounds.¹ Several useful strategies including those controlled by catalysts, additives, and substrates have been proposed by many research groups in recent years and stereodivergent syntheses with high diastereo- and enantioselectivity have been successful.² However, accessing all stereoisomers that exist theoretically is still difficult.³ For example, asymmetric 1,3-DC is one of the most suitable methods for the divergent preparation of chiral pyrrolidines, which are frequently found in biologically active compounds.⁴ Indeed, *endo/exo*-diastereodivergent synthesis has been well developed by metal- and ligand-controlled strategies. Nonetheless, *2,5-cis/trans* diastereodivergent synthesis is limited to a few examples^{5,6} because of the difficulty in accessing *2,5-trans* adducts.^{7,8}

Given this background, the author developed the *exo'*-selective asymmetric (3+2) cycloaddition of imino esters with ylidene-2,3-dioxopyrrolidines.⁹ According to previous work, it was suggested that the unusual *2,5-trans* diastereoselectivity was expressed when spiropyrrolidines were constructed using ylidene-heterocycles.¹⁰ The author envisioned the establishment of a new stereodivergent synthetic methodology using well-designed activated olefins. Initially, *2,5-trans* adducts would be generated by the reaction of imino esters with ylidene-heterocycles which are easy to ring-open, and the subsequent ring-opening reaction could convert spirocyclic compounds to acyclic pyrrolidines with the *2,5-trans* configuration. In contrast to the synthesis of *2,5-trans* pyrrolidines, *2,5-cis* pyrrolidines could be obtained by the common metal complex-catalyzed reaction by using acyclic olefins. Thus, the diastereodivergent *2,5-cis/trans* pyrrolidines could be achieved using different types of activated olefins.

In this work, the author focused on the isoxazolone ring as the heterocycle because it is easy to ring-open.¹¹ The heterocycle smoothly transforms into ketone groups by N–O

bond reduction with decarboxylation.¹² Therefore, the author engaged in the metal complex-catalyzed asymmetric (3+2) cycloaddition using ylidene-isoxazolones which have rarely been employed in the asymmetric (3+2) cycloaddition (Figure 4-1). As a result, the asymmetric (3+2) cycloaddition of imino lactones with ylidene-isoxazolones proceeded with 2,5-*trans* diastereoselectivity. Additionally, the isoxazolone ring could be converted to a ketone group after the construction of the pyrrolidine ring, giving 4-carbonyl group-substituted pyrrolidines in a 2,5-*trans* fashion. The (3+2) cycloaddition using acyclic α,β -unsaturated ketones as the activated olefins afforded the corresponding 2,5-*cis* pyrrolidines with high diastereo- and enantioselectivity.^{13a,14} Thus, the author developed the first diastereodivergent construction of 2,5-*cis/trans*-pyrrolidines by a dipolarophile-controlled strategy. This could become a robust method for the stereodivergent preparation of pyrrolidines in the field of drug discovery because both 2,5-*cis/trans* derivatives are frequently used as biologically active pyrrolidines.¹⁵

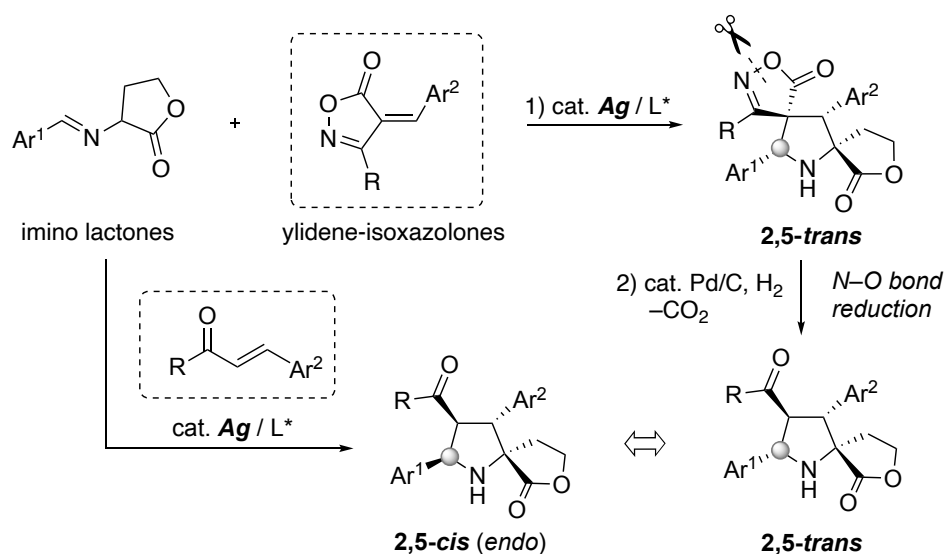


Figure 4-1. This work: dipolarophile-controlled diastereodivergent synthesis of 2,5-*cis/trans* pyrrolidines based on asymmetric (3+2) cycloaddition of imino lactones.

4-2. Results and Discussion

The reaction of imino esters with ylidene-isoxazolones **2a** was initially investigated using common copper and silver catalysts under several conditions.⁴ However, the desired cycloadducts were not obtained and complex mixtures resulted. Thus, the author examined some imino ester derivatives as azomethine ylide precursors. As a result of these initial experiments, the (3+2) cycloaddition of imino lactones **1a** with ylidene-isoxazolones **2a** proceeded efficiently in the presence of AgOAc (5.0 mol%), (*S, S_p*)-*i*Pr-FcPHOX **L1** (5.5 mol%), Et₃N (20 mol%), and 3Å MS (200 mg) in CH₂Cl₂ at room temperature. ¹H NMR analysis of the crude product revealed that a single diastereomer was generated and the corresponding cycloadducts were successfully isolated in 86% yield and 65% ee by column chromatography (Table 4-1, entry 1). X-ray crystallographic analysis disclosed that the desired 2,5-*trans* cycloadducts were obtained, whose carbonyl groups at the 2-position of the pyrrolidine ring were placed *trans* to aryl groups at the 5-position (details of the stereochemistry are described below and in Figure 4-4.).

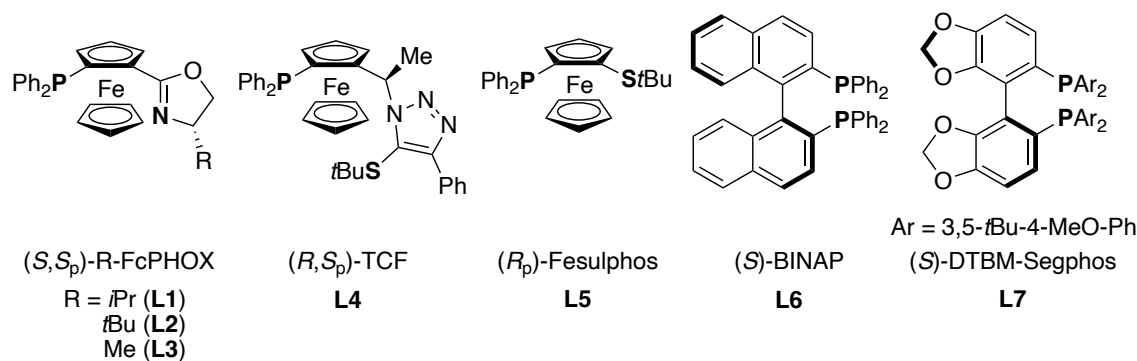


Figure 4-2. Chiral ligands employed in this study.

Screening of chiral copper and silver complexes was next carried out using several ligands (Figure 4-2), and the results are summarized in Table 4-1. Although high enantioselectivity was achieved when *i*Pr-FcPHOX **L1** was applied to the asymmetric (3+2) cycloaddition, other FcPHOX derivatives **L2** and **L3** resulted in moderate enantioselectivity (entries 1-3). When our original ligand TCF **L4** was used under the

Table 4-1. Screening of chiral copper and silver complex^a

Ar¹ = *p*-ClC₆H₄
1a (1.1 equiv.) **2a** (0.20 mmol) **3aa** (2,5-*trans*)

entry	metal / ligand	yield (%) ^b	dr (%) ^c	ee (%) ^d
1	AgOAc / L1	86	>20:1	65
2	AgOAc / L2	76	>20:1	48
3	AgOAc / L3	59	>20:1	47
4	AgOAc / L4	82	>20:1	56
5	AgOAc / L5	71	>20:1	52
6	AgOAc / L6	77	>20:1	27
7	AgOAc / L7	73	6:1	40
8	[Cu(MeCN) ₄]BF ₄ / L1	46	5:1	8
9	[Cu(MeCN) ₄]BF ₄ / L4	54	6:1	7
10	[Cu(MeCN) ₄]BF ₄ / L5	55	5:1	19
11	[Cu(MeCN) ₄]BF ₄ / L6	52	6:1	16
12	[Cu(MeCN) ₄]BF ₄ / L7	48	4:1	3

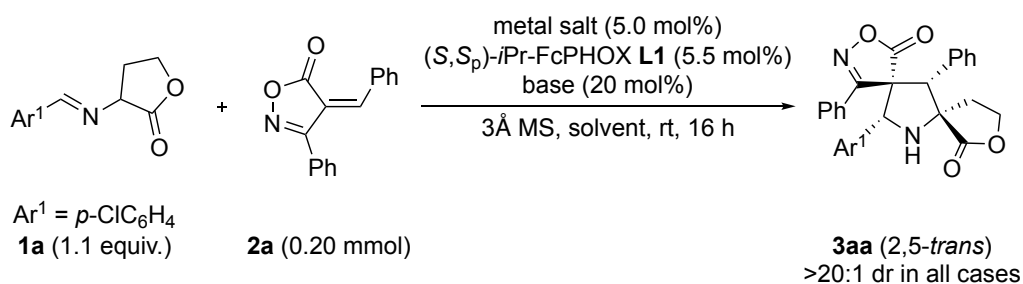
[a] Condition: **1a** (0.22 mmol), **2a** (0.20 mmol), metal salt (5.0 mol%), ligand (5.5 mol%), Et₃N (20 mol%), CH₂Cl₂ (1.0 mL), 3Å MS (200 mg), rt, 16 h. [b] Isolated yield. [c] Determined by crude ¹H NMR. [d] Determined by chiral HPLC (Daicel Chiralpak ID-3).

silver-catalyzed condition, the product was obtained in high yield, but the enantioselectivity was not improved (entry 4). Other chiral ligands such as Fesulphos **L5**, BINAP **L6**, and DTBM-Segphos **L7** were not as effective for the asymmetric reaction, and low enantioselectivity resulted (entries 5-7). In addition, copper complex-catalyzed systems were unsuitable for the reaction of imino lactones **1a** with ylidene-isoxazolones **2a**, with significantly decreased yield and stereoselectivity (entries 8-12). Therefore, the author conducted further examinations to improve the enantioselectivity by using a silver/

*i*Pr-FcPHOX complex catalyst.

The reaction conditions were first optimized (Table 4-2). When several solvents such as THF, Et₂O, toluene, MTBE, and CPME were applied to the reaction, ether-based solvents tended to give higher enantioselectivity (entries 1-5). Et₂O was chosen as the most suitable solvent for the reaction, and the enantioselectivity increased to 80% ee

Table 4-2. Optimization of the reaction conditions.^a



entry	metal salt	base	solvent	yield (%) ^b	ee (%) ^c
1	AgOAc	Et ₃ N	THF	54	65
2	AgOAc	Et ₃ N	Et ₂ O	80	80
3	AgOAc	Et ₃ N	toluene	64	52
4	AgOAc	Et ₃ N	MTBE	73	75
5	AgOAc	Et ₃ N	CPME	76	77
6	AgOAc	DIPEA	Et ₂ O	75	81
7	AgOAc	DBU	Et ₂ O	67	76
8	AgOAc	K ₂ CO ₃	Et ₂ O	77	87
9	AgOAc	none	Et ₂ O	77	88
10	AgOTf	none	Et ₂ O	trace	-
11	AgOCOCF ₃	none	Et ₂ O	82	87
12 ^d	AgOCOCF ₃	none	Et ₂ O	64	89
13 ^e	AgOCOCF ₃	none	Et ₂ O	93	88 (93) ^f

[a] Condition: **1a** (0.22 mmol), **2a** (0.20 mmol), metal salt (5.0 mol%), (*S,S*_p)-FcPHOX **L1** (5.5 mol%), base (20 mol%), solvent (1.0 mL), 3Å MS (200 mg), rt, 16 h. [b] Isolated yield. [c] Determined by chiral HPLC (Daicel Chiralpak ID-3). [d] Conducted at 0°C. [e] 1.5 equiv. of **1a** was used. [f] Determined by using Daicel Chialpak AD-H instead of ID-3.

(entry 2). Screening of additives (entries 6-9) revealed that the reaction smoothly proceeded without the addition of bases, and the enantioselectivity was improved to 88% ee (entry 9). Other silver salts such as AgOTf and AgOCOCF₃ were examined (entries 10, 11), and using AgOCOCF₃ increased the yield to 82% (entry 11). Although the yield decreased when the reaction was carried out at 0 °C (entry 12), the yield was improved to 93% with high enantioselectivity when 1.5 equivalents of imino lactones **1a** were used (entry 13).

The scope of imino lactones **1** was investigated under the optimal conditions (Table 4-2, entry 13), and a variety of substrates was successfully applied to the 2,5-*trans* selective asymmetric (3+2) cycloaddition (Figure 4-3). Imino lactones bearing a halogen atom at *para*- and *meta*-positions reacted with ylidene-isoxazolone **2a**, giving the corresponding products **3ba** and **3ca**, respectively. The reaction using imino lactones bearing no substituent on the aryl groups **1d** also yielded the cycloadducts **3da** with high enantioselectivity. Although the *ortho*-methyl substrate **3ea** was produced in moderate yield, the enantioselectivity remained high. Neither *meta*- nor *para*-methyl substituents had much effect on the yield or stereoselectivity, giving the products **3fa** and **3ga**, respectively. The reaction using strong electron-withdrawing groups such as *para*-CF₃ substituted imino lactones **1h** resulted in good yield and high enantioselectivity. A strong electron-donating substituent such as the *para*-MeO group decreased the yield, but had high enantioselectivity. The cycloadduct substituted 2-thienyl group **3ja** was obtained quantitatively in 86% enantiomeric excess. Therefore, some substituents on the aryl group of imino lactones affected the yield, but in most cases, the diastereo- and enantioselectivity remained high.

The substrate scope of ylidene-isoxazolones **2** was examined under the optimized reaction conditions (Figure 4-4). A *para*-substituent on the aryl group of the isoxazolones **2** did not affect the yield or stereoselectivity, giving the *para*-chloro, -bromo, and -methoxy substituted products **3ab-ad**, respectively. The position of the substituent had

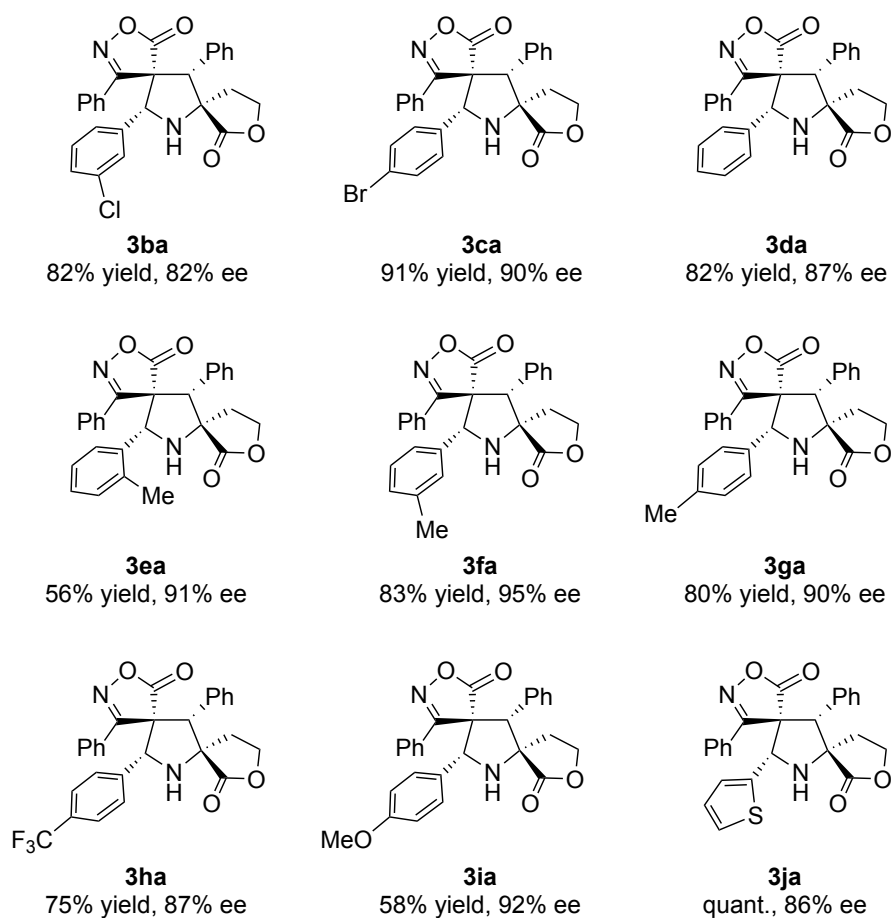
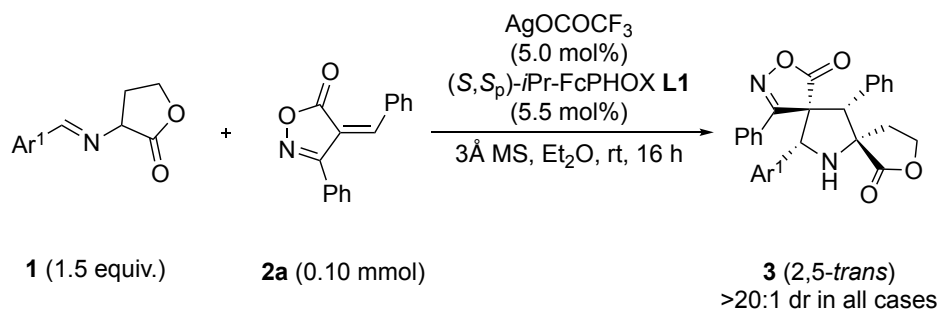
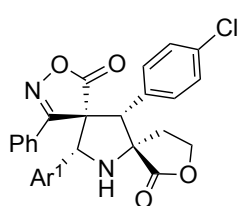
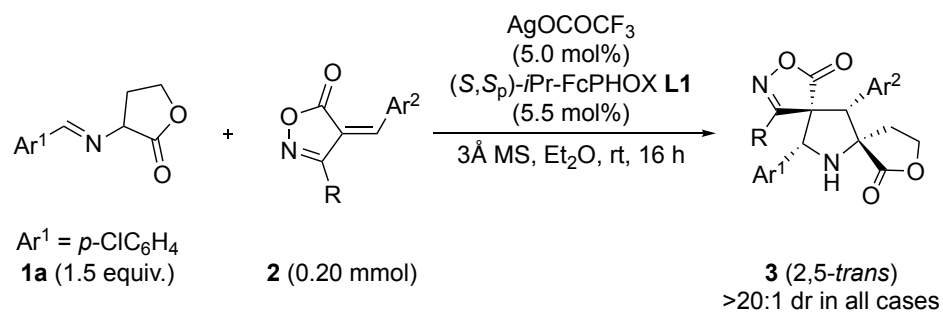


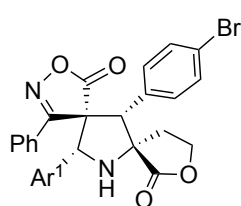
Figure 4-3. Scope of imino lactones **1**.

little impact on the reactivity and stereoselectivity, so the cycloadducts bearing a methyl group at *ortho*-, *meta*-, and *para*-positions **3ae-ag** were obtained efficiently. A 2-thienyl group could be introduced into the 3-position of the pyrrolidine ring with high enantioselectivity. However, a different substituent at the 3-position of the isoxazolone ring affected the enantioselectivity, i.e., *i*Pr-substituted cycloadduct **3ai** was produced in only 59% ee. However, 3-methyl substrates generated the corresponding cycloadducts

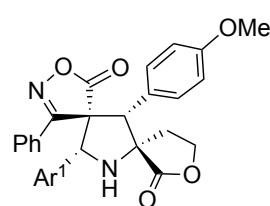
3aj, 3dj, and 3ak with high enantioselectivity.



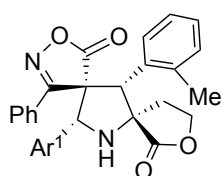
3ab
83% yield, 89% ee



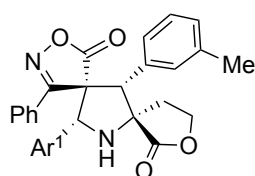
3ac
76% yield, 90% ee



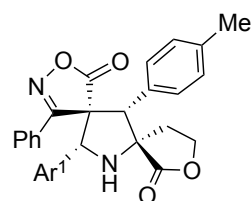
3ad
96% yield, 82% ee



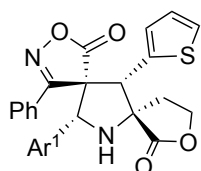
3ae
85% yield, 87% ee



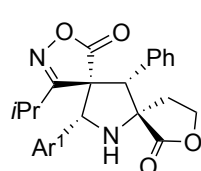
3af
87% yield, 82% ee



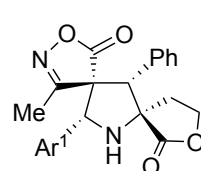
3ag
98% yield, 86% ee



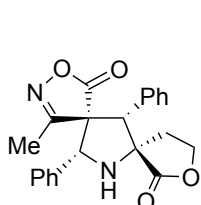
3ah
87% yield, 84% ee



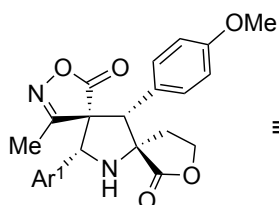
3ai
93% yield, 59% ee



3aj
92% yield, 84% ee



3dj
quant., 86% ee



3ak
quant., 91% ee

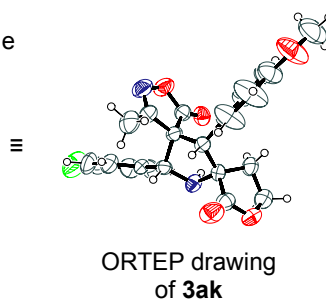


Figure 4-4. Scope of ylidene-isoxazolones **2**.

A single crystal of the product **3ak** was suitable for X-ray crystallographic analysis, in which the stereochemistry could be determined. The stereocenters at the 2- and 5-positions of the pyrrolidine ring were respectively determined as *S* and *R*. The relationship of the carbonyl group at the 2-position and the *para*-chloro phenyl group at the 5-position was *trans*. The stereocenters at the 3- and 4-positions of the pyrrolidine ring, which were derived from the ylidene-isoxazolone **2**, were detected as *S* and *R*, respectively.

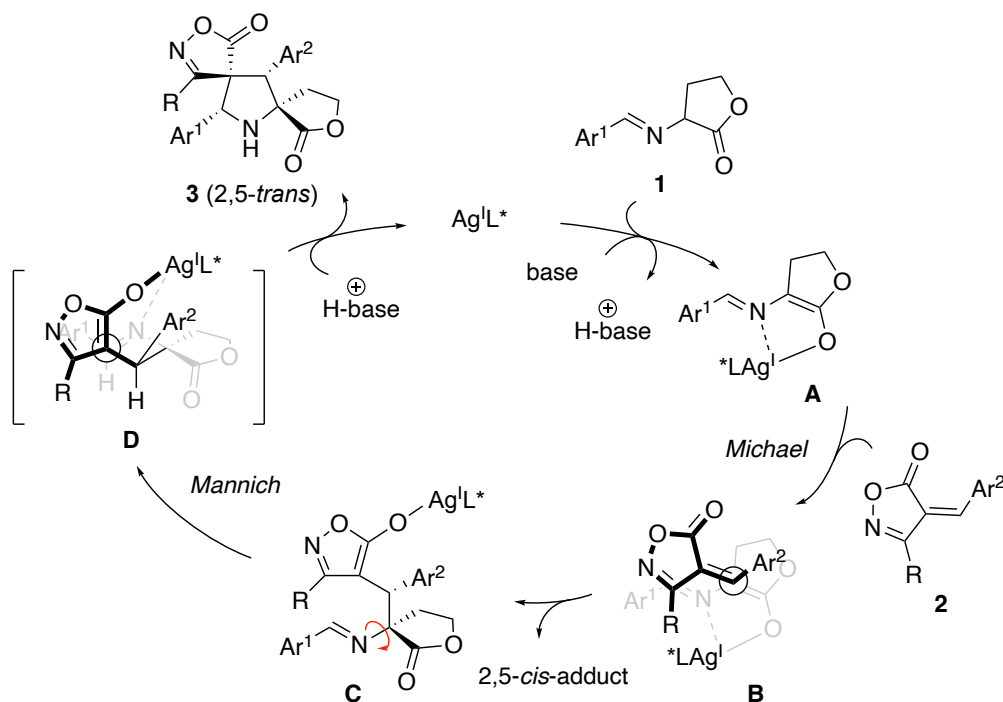


Figure 4-5. Postulated mechanism for asymmetric 2,5-*trans* selective (3+2) cycloaddition of imino lactones **1** with ylidene-isoxazolones **2**.

According to some previous reports,^{5,7,9} the unusual 2,5-*trans* selective (3+2) cycloaddition would proceed via a stepwise Michael addition/Mannich reaction with bond rotation (Figure 4-5). First, azomethine ylides **A** are generated by the action of the silver complex on imino lactones **1**, and azomethine ylides **A** smoothly react with activated olefins **2**. At this time, a suitable transition state **B** is proposed, i.e., the asymmetric Michael addition takes place from the *si*-face of azomethine ylides **A** to the *si*-face of the ylidene-isoxazolones **2**. Simultaneously, the silver complex flips to the isoxazolone moiety, giving the isoxazole intermediate **C** that is stabilized by the formation

of the heteroaromatic ring. After C–N bond rotation, the intramolecular Mannich reaction proceeds via the postulated transition state **D** to afford the 2,5-*trans* products as the major product. If the Mannich reaction immediately took place after the first bond formation, the 2,5-*cis* cycloadducts should be obtained as the major diastereomer. However, the direct cyclization before the C–N bond rotation is unfavorable due to high steric constraints. Therefore, the unusual 2,5-*trans* diastereoselectivity would be guided by ylidene-isoxazolones **2**.

Based on the postulated reaction pathway shown in Figure 4-5, DFT calculations were conducted to gain insight into the mechanism for the 2,5-*trans* selective formation of the pyrrolidine ring (Figure 4-6).¹⁶ Since the 2,5-*trans* diastereoselectivity is also observed when the AgOAc/PPh₃ complex is used, this silver complex was employed in this computational study.

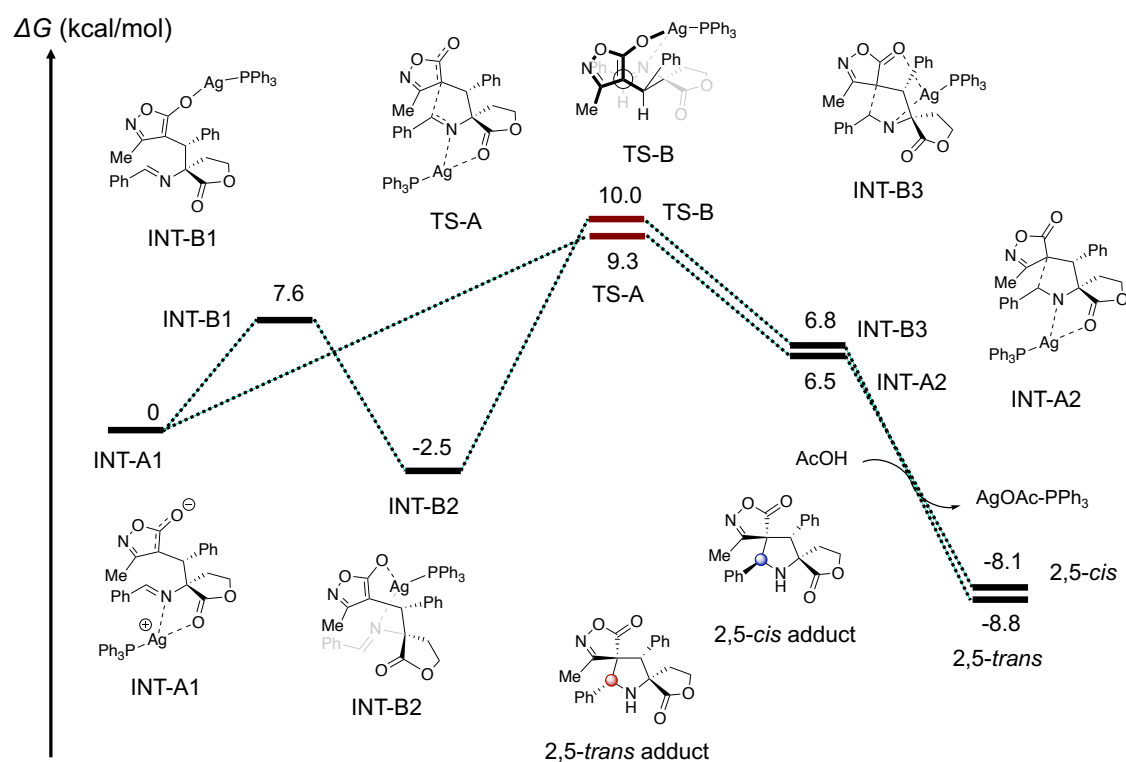


Figure 4-6. The mechanism for the Mannich reaction giving the 2,5-*cis* and 2,5-*trans* adducts under the AgOAc/PPh₃-catalyzed condition (route A and B). The DFT calculations were carried out at B3PW91/LanL2DZ(Ag)+6-31G*(other atoms) with gd3bj level of theory.

The Mannich reaction giving 2,5-*cis* adduct by the direct cyclization from the Michael adduct **INT-A1** was first analyzed (Figure 4-6, route A). As a result, the Gibbs activation energy of the transition state **TS-A** was calculated to be 9.3 kcal/mol. On the other hand, the 2,5-*trans* selective formation would proceed from the intermediate **INT-B2**, which can be formed after the C–N bond rotation of the Michael adduct **INT-A1** (Figure 4-6, route B). The intermediate **INT-B2** has a bidentate coordinate structure to the silver center by its anionic isoxazolone ring moiety and its imine moiety, and the energy was calculated to be $\Delta G = -2.5$ kcal/mol. Thus, the intermediate **INT-B2** has the thermodynamic stability equivalent to the Michael adduct **INT-A1**, and that is much lower than the activation energy of the transition state **TS-A** which affords the 2,5-*cis* adduct. However, the intermediate **INT-B2** may also be formed via the intermediate **INT-B1** in which neither its imine moiety nor its carbonyl group derived from the iminolactone is coordinated, and the energy of this intermediate **INT-B1** was estimated to be $\Delta G = 7.6$ kcal/mol. Also, transition states that should exist between each intermediate were not calculated, because it is considered to be lower than that of Mannich cyclization. The Gibbs activation energy of the transition state **TS-B** which is the Mannich reaction from the intermediate **INT-B2** as the starting material was calculated to be 12.5 kcal/mol, which is comparable to the transition state **TS-A**. These results suggest that the 2,5-*cis* selective process may have a slight kinetic advantage, but the formation of the thermodynamically stable intermediate may have a key role in the 2,5-*trans* selective cycloaddition. However, further calculation studies that consider the actual reaction condition, such as the solvent effect and applying chiral ligand, are necessary to support the origin of the 2,5-*cis/trans* diastereoselectivity enough.

The author next investigated the transformation of the 3-methyl substituted spiropyrrolidines **3aj** to the 4-acetyl substituted pyrrolidines **4aj** by the N–O bond reduction with decarboxylation.¹¹ Examining some conditions,¹² the spiropyrrolidines **3aj** were smoothly transformed to the corresponding 4-acetyl pyrrolidines **4aj** by the action of Pd/C catalyst (10 wt%) in H₂ atmosphere (Figure 4-7). In addition to the reduction proceeding without loss of enantiomeric excess, the retention of the 2,5-*trans* relative

configuration was confirmed by X-ray crystallographic analysis of a single crystal of *rac*-**4aj**. The Pd/C-catalyzed reduction could be applied to several substrates, giving the corresponding 4-acetyl pyrrolidines **4dj** and **4ak** with high yield. On the other hand, 4-benzoyl substrates **4aa** and **4da** could be respectively obtained when MeOH or EtOAc/MeOH was used as the co-solvent because of the low reactivity or solubility of the starting spiropyrrolidines **3aa** and **3da**. Thus, the asymmetric (3+2) cycloaddition of imino lactones **1** with ylidene-isoxazolones **2** and the subsequent N–O bond reduction can access 4-carbonyl pyrrolidines with 2,5-*trans* configuration.

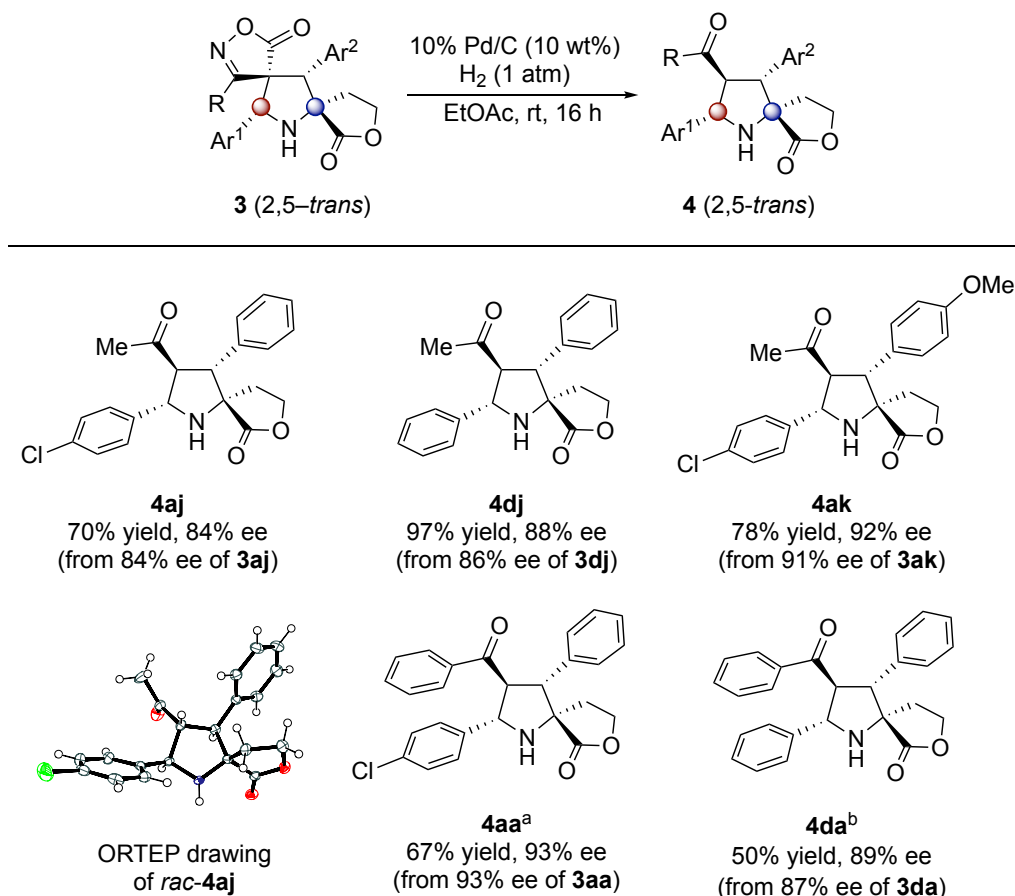


Figure 4-7. Pd/C-catalyzed N–O bond reduction with decarboxylation. [a] MeOH was used as solvent. [b] EtOAc/MeOH was used as co-solvent.

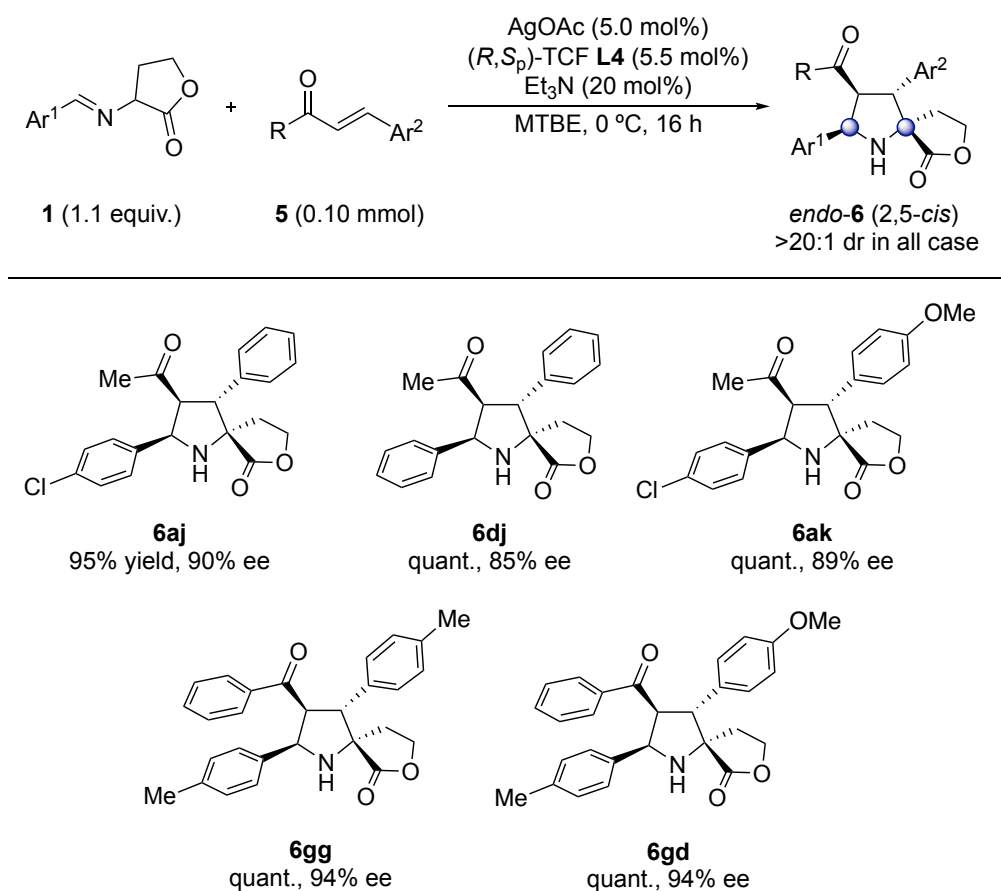


Figure 4-8. 2,5-*cis* Selective synthesis by Ag/TCF-catalyzed 1,3-DC of imino lactones **1** with α,β -unsaturated ketones **5**.

In contrast to the above-described synthesis of 2,5-*trans* pyrrolidines, 2,5-*cis* pyrrolidines were obtained by the reaction using common acyclic-activated olefins.^{4,14} However, the (3+2) cycloaddition of imino lactones **1** with α,β -unsaturated ketones **5** is limited to a copper-catalyzed reaction reported by Wang and co-workers.^{13a} Thus, the author investigated the silver complex-catalyzed (3+2) cycloaddition of imino lactones **1** with α,β -unsaturated ketones **5**. The silver/TCF complex efficiently catalyzed the reaction of imino lactones **1a** with enones **5j**, giving the desired 2,5-*cis* products **6aj** (*endo*-adducts) as a single diastereomer with high enantioselectivity (Figure 4-8). Details of the optimization study are summarized in Table S4-1 (see experimental section). The optimized Ag/TCF-catalyzed reaction condition could be applied to other substrates. For example, both 4-acetyl pyrrolidines **6dj** and **6ak** were quantitatively obtained with high

enantioselectivity from the corresponding starting materials. The *endo*-diastereoselectivity was similar to that in Wang's previous report, and was determined by NMR analysis of the pyrrolidine corresponding to the product **6dj**.^{13a} The absolute configuration was determined by referring to the HPLC analysis of Wang's reported one. Finally, the author investigated whether chalcones could be used in this silver-catalyzed reaction. 4-Benzoyl substituted pyrrolidines with 2,5-*cis* configuration **6gg** and **6gd** were successfully obtained with high enantioselectivity.

4-3. Conclusion

In conclusion, the author has developed a diastereodivergent synthetic method for 2,5-*cis/trans* pyrrolidines using different types of activated olefins. Chiral 2,5-*trans* spiropyrrolidines were obtained by the silver/*i*Pr-FcPHOX-catalyzed asymmetric (3+2) cycloaddition of imino lactones **1** with ylidene-isoxazolones **2**. The subsequent reduction of isoxazolone rings proceeded using a Pd/C catalyst, giving the 4-carbonyl pyrrolidines with 2,5-*trans* stereoretention. In contrast, chiral 2,5-*cis* pyrrolidines were synthesized by the silver/TCF-catalyzed asymmetric (3+2) cycloaddition of imino lactones **1** with α,β -unsaturated ketones **5**. This is the first example of the formal diastereodivergent synthesis of 2,5-*cis/trans* pyrrolidines based on a dipolarophile-controlled strategy in the metal-catalyzed asymmetric (3+2) cycloaddition of imino esters.

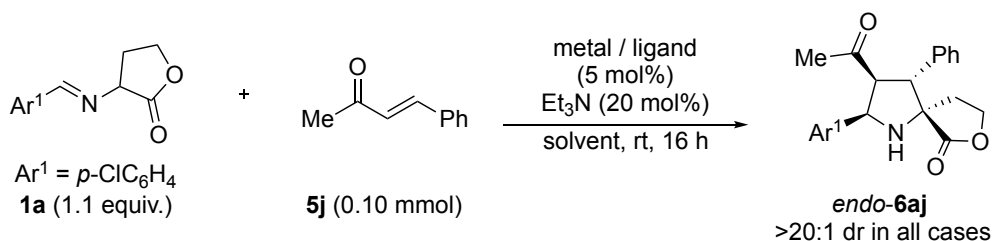
4-4. Experimental Section

The general information was described in the Experimental Section of Chapter 2.

Unless otherwise stated, all reactions were carried out with oven-dried glassware under the atmosphere of nitrogen. Starting materials, imino lactones **1**,^{12,17} ylidene-isoxazolones **2**,¹⁸ and α,β -unsaturated ketones **5**^{14,19} were prepared and identified by reported methods. Racemic products of **3**, **4**, and **6** were prepared using PPh₃ (5.5 mol%) as the ligand. All other chemical reagents used commercial grade and used as received.

Optimization study of the reaction of imino lactone **1a with enones **5j**.**

Table S4-1. Results of the screening of the catalyst and the optimization study^a



entry	metal / ligand	solvent	yield (%) ^b	ee (%) ^c
1	AgOAc/(<i>S</i> , <i>S_p</i>)- <i>i</i> Pr-FcPHOX L1	CH ₂ Cl ₂	n. r.	-
2	AgOAc/(<i>R</i> , <i>S_p</i>)-TCF L4	CH ₂ Cl ₂	quant.	80
3	AgOAc/(<i>S_p</i>)-Fesulphos L5	CH ₂ Cl ₂	95	-26
4	AgOAc/(<i>S</i>)-DTBM-Segphos L7	CH ₂ Cl ₂	65	0
5	[Cu(MeCN) ₄]BF ₄ /(<i>S</i> , <i>S_p</i>)- <i>i</i> Pr-FcPHOX L1	CH ₂ Cl ₂	trace	-
6	[Cu(MeCN) ₄]BF ₄ /(<i>S_p</i>)-Fesulphos L5	CH ₂ Cl ₂	trace	-
7	[Cu(MeCN) ₄]BF ₄ /(<i>S</i>)-DTBM-Segphos L7	CH ₂ Cl ₂	trace	-
8	AgOAc/(<i>R</i> , <i>S_p</i>)-TCF L4	THF	quant.	64
9	AgOAc/(<i>R</i> , <i>S_p</i>)-TCF L4	toluene	quant.	74
10	AgOAc/(<i>R</i> , <i>S_p</i>)-TCF L4	Et ₂ O	quant.	82
11	AgOAc/(<i>R</i> , <i>S_p</i>)-TCF L4	MTBE	quant.	86
12 ^d	AgOAc/(<i>R</i> , <i>S_p</i>)-TCF L4	MTBE	95	90
13 ^e	AgOAc/(<i>R</i> , <i>S_p</i>)-TCF L4	MTBE	89	90
14 ^{d,f}	AgOAc/(<i>R</i> , <i>S_p</i>)-TCF L4	MTBE	quant.	87
15 ^d	AgOCOCF ₃ /(<i>R</i> , <i>S_p</i>)-TCF L4	MTBE	91	81

[a] Conditions: **1a** (0.11 mmol), **5j** (0.10 mmol), metal salt (5.0 mol%), ligand (5.5 mol%), Et₃N (20 mol%), solvent (1.0 mL), 16 h, rt. [b] Isolated yield. [c] Determined by chiral HPLC analysis. [d] Conducted at 0 °C. [e] Conducted at -20 °C. [f] Without Et₃N.

Silver-Catalyzed Asymmetric (3+2) Cycloaddition of Imino Lactones 1 with Ylidene-Isoxazolones 2. A mixture of AgOCOCF₃ (2.2 mg, 10 μmol, 5.0 mol%) and (*S*, *S*_p)-*i*Pr-FcPHOX **L1** (5.3 mg, 11 μmol, 5.5 mol%) was dissolved in dry Et₂O (1.0 mL) at room temperature. To the mixture was added 3 Å MS (200 mg), and the mixture was stirred for 30 minutes at the same temperature. After that, imino lactones **1a** (67.1 mg, 0.30 mmol, 1.50 equiv.) and ylidene-isoxazolones **2a** (49.9 mg, 0.20 mmol, 1.00 equiv.). After stirring for 16 h at room temperature, EtOAc (30 mL) was added to the mixture. Then, the mixture was filtered through a short Celite pad and concentrated under reduced pressure. ¹H NMR analysis of the crude product showed that the corresponding cycloadduct was the sole product. The residue was purified by column chromatography (20 g, *n*-hexane/EtOAc = 2/1) to afford (*5R*, *6S*, *7S*, *13R*)-13-(4-chlorophenyl)-4,6-diphenyl-2,9-dioxa-3,12-diazadispiro[4.1.4⁷.2⁵]tridec-3-ene-1,8-dione (**3aa**) (88.1 mg, 0.186 mmol, 93.1%, >20:1 dr, 93% ee) as a white solid.

2 mmol Scale Experiment of the Asymmetric (3+2) cycloaddition of Imino Lactones 1a with Ylidene-isoxazolones 2a. A mixture of AgOCOCF₃ (22.1 mg, 0.100 mmol, 5.0 mol%) and (*S*, *S*_p)-*i*Pr-FcPHOX **L1** (52.9 mg, 0.110 mmol, 5.5 mol%) was dissolved in dry Et₂O (10.0 mL) at room temperature. To the mixture was added 3 Å MS (2.00 g), and the mixture was stirred for 30 minutes at the same temperature. After that, imino lactones **1a** (671 mg, 3.00 mmol, 1.50 equiv.) and ylidene-isoxazolones **2a** (499 mg, 2.00 mmol, 1.00 equiv.). After stirring for 16 h at room temperature, EtOAc (60 mL) was added to the mixture. Then, the mixture was filtered through a short Celite pad and concentrated under reduced pressure. ¹H NMR analysis of the crude product showed that the corresponding cycloadduct was the sole product. The residue was purified by silica gel column chromatography (50 g, *n*-hexane/EtOAc = 2/1) to afford (*5R*, *6S*, *7S*, *13R*)-13-(4-chlorophenyl)-4,6-diphenyl-2,9-dioxa-3,12-diazadispiro[4.1.4⁷.2⁵]tridec-3-ene-1,8-dione (**3aa**) (868 mg, 1.84 mmol, 91.8%, >20:1 dr, 93% ee) as a white solid.

(*5R*, *6S*, *7S*, *13R*)-13-(4-chlorophenyl)-4,6-diphenyl-2,9-dioxa-3,12-diazadispiro[4.1.4⁷.2⁵]tridec-3-ene-1,8-dione (3aa**).** (88.1 mg, 0.186 mmol, 93.1%,

>20:1 dr, 93% ee); white solid; mp 79–83 °C; ¹H NMR (400 MHz, CDCl₃): δ 7.96–7.94 (m, 2H), 7.65–7.57 (m, 3H), 7.30–7.24 (m, 5H), 7.13 (d, 2H, *J* = 8.4 Hz), 7.07–7.05 (m, 2H), 5.40 (s, 1H), 5.00 (s, 1H), 4.47 (ddd, 1H, *J* = 12.1, 9.2, 6.3 Hz), 4.12 (ddd, 1H, *J* = 14.7, 8.6, 2.6 Hz), 3.72 (brs, 1H), 2.65–2.59 (m, 1H), 2.48–2.40 (m, 1H); ¹³C NMR (101 MHz, CDCl₃): δ 179.1, 177.3, 164.9, 135.1, 132.33, 132.28, 131.6, 129.8, 129.6, 129.5, 129.2, 129.1, 127.8, 127.4, 127.2, 68.1, 67.4, 66.9, 66.5, 58.7, 34.9; HPLC (Daicel Chiralpak AD-H, *n*-hexane/2-propanol = 90/10, 1.0 mL/min, 254 nm); *t*_R = 21.8 min (minor), 39.1 min (major); [α]_D²⁵ 79.04 (*c* 0.06, CHCl₃); HRMS (ESI) *m/z*: [M+Na]⁺ Calcd for C₂₇H₂₁³⁵ClN₂NaO₄⁺, 495.1082; found 495.1071.

(5R, 6S, 7S, 13R)-13-(3-chlorophenyl)-4,6-diphenyl-2,9-dioxa-3,12-diazadispiro[4.1.4⁷.2⁵]tridec-3-ene-1,8-dione (3ba). (38.9 mg, 82.3%, >20:1 dr, 82% ee); white solid; mp 151–154 °C; ¹H NMR (400 MHz, CDCl₃): δ 7.96–7.93 (m, 2H), 7.65–7.57 (m, 3H), 7.33–7.21 (m, 6H), 7.08–7.03, 5.39 (s, 1H), 4.99 (s, 1H), 4.48 (ddd, 1H, *J* = 12.2, 9.4, 5.9 Hz), 4.13 (ddd, 1H, *J* = 14.8, 8.7, 2.5 Hz), 3.72 (brs, 1H), 2.65–2.60 (m, 1H), 2.48–2.40 (m, 1H); ¹³C NMR (101 MHz, CDCl₃): δ 179.0, 177.2, 165.0, 135.3, 135.1, 132.3, 132.2, 130.3, 129.9, 129.7, 129.5, 129.4, 129.1, 127.5, 127.1, 126.8, 124.5, 67.8, 67.3, 66.7, 66.5, 58.8, 34.9; HPLC (Daicel Chiralpak AD-H, *n*-hexane/2-propanol = 90/10, 1.0 mL/min, 220 nm); *t*_R = 19.7 min (minor), 24.3 min (major); [α]_D²⁵ 67.37 (*c* 0.04, CHCl₃); HRMS (ESI) *m/z*: [M+Na]⁺ Calcd for C₂₇H₂₁³⁵ClN₂NaO₄⁺, 495.1082; found 495.1075.

(5R, 6S, 7S, 13R)-13-(4-bromophenyl)-4,6-diphenyl-2,9-dioxa-3,12-diazadispiro[4.1.4⁷.2⁵]tridec-3-ene-1,8-dione (3ca). (47.2 mg, 91%, >20:1 dr, 90% ee); white solid; mp 89–93 °C; ¹H NMR (400 MHz, CDCl₃): δ 7.96–7.94 (m, 2H), 7.63–7.57 (m, 3H), 7.45 (d, 2H, *J* = 8.6 Hz), 7.30–7.24 (m, 3H), 7.08–7.05 (m, 4H), 5.38 (s, 1H), 5.00 (s, 1H), 4.47 (ddd, 1H, *J* = 12.1, 9.4, 6.8 Hz), 4.13 (ddd, 1H, *J* = 14.7, 8.5, 2.6 Hz), 2.65–2.59 (m, 1H), 2.48–2.40 (m, 1H); ¹³C NMR (101 MHz, CDCl₃): δ 179.1, 177.3, 164.9, 132.30, 132.29, 132.2, 132.1, 129.8, 129.6, 129.5, 129.1, 128.1, 127.4, 127.1, 123.3, 68.0, 67.4, 66.9, 66.5, 58.7, 34.9; HPLC (Daicel Chiralpak AD-H, *n*-hexane/2-

propanol = 90/10, 1.0 mL/min, 250 nm); t_R = 23.6 min (minor), 42.0 min (major); $[\alpha]_D^{25}$ 73.00 (c 0.04, CHCl_3); HRMS (ESI) m/z : $[\text{M}+\text{Na}]^+$ Calcd for $\text{C}_{27}\text{H}_{21}^{79}\text{BrN}_2\text{NaO}_4^+$, 539.0577; found 539.0588.

(5R, 6S, 7S, 13R)-4,6,13-triphenyl-2,9-dioxa-3,12-diazadispiro[4.1.4⁷.2⁵]tridec-3-ene-1,8-dione (3da). (36.1 mg, 82.3%, >20:1 dr, 87% ee); white solid; mp 119–121 °C; ^1H NMR (400 MHz, CDCl_3): δ 7.97–7.95 (m, 2H), 7.62–7.56 (m, 3H), 7.30–7.24 (m, 6H), 7.20–7.18 (m, 2H), 7.20–7.18 (m, 2H), 7.08–7.06 (m, 2H), 5.43 (s, 1H), 5.02 (s, 1H), 4.49 (ddd, 1H, J = 12.4, 9.6, 6.2 Hz), 4.15 (ddd, 1H, J = 15.0, 8.6, 2.4 Hz), 2.66–2.60 (m, 1H), 2.47–2.39 (m, 1H); ^{13}C NMR (101 MHz, CDCl_3): δ 179.0, 177.5, 165.1, 132.9, 132.6, 132.1, 129.8, 129.7, 129.4, 129.2, 129.02, 128.98, 127.5, 127.3, 126.3, 68.3, 67.7, 67.4, 66.4, 58.7, 35.0; HPLC (Daicel Chiralpak AD-H, n -hexane/2-propanol = 90/10, 1.0 mL/min, 254 nm); t_R = 22.5 min (minor), 31.5 min (major); $[\alpha]_D^{25}$ 58.73 (c 0.05, CHCl_3); HRMS (ESI) m/z : $[\text{M}+\text{Na}]^+$ Calcd for $\text{C}_{27}\text{H}_{22}\text{N}_2\text{NaO}_4^+$, 461.1472; found 461.1451.

(5R, 6S, 7S, 13R)-4,6-diphenyl-13-(*o*-tolyl)-2,9-dioxa-3,12-diazadispiro[4.1.4⁷.2⁵]tridec-3-ene-1,8-dione (3ea). (25.2 mg, 55.7%, >20:1 dr, 91% ee); white solid; mp 75–78 °C; ^1H NMR (400 MHz, CDCl_3): δ 7.81–7.78 (m, 2H), 7.56–7.49 (m, 3H), 7.34–7.26 (m, 4H), 7.23–7.16 (m, 2H), 7.13–7.11 (m, 3H), 5.46 (s, 1H), 5.03 (s, 1H), 4.43 (ddd, 1H, J = 12.8, 9.1, 6.1 Hz), 4.18–4.14 (m, 1H), 2.66–2.62 (m, 1H), 2.49–2.41 (m, 1H), 2.15 (s, 3H); ^{13}C NMR (101 MHz, CDCl_3): δ 179.0, 178.4, 165.4, 138.0, 132.3, 132.0, 131.5, 131.1, 130.0, 129.6, 129.4, 129.2, 129.0, 127.5, 127.3, 126.7, 125.4, 67.2, 66.7, 66.4, 65.2, 58.8, 34.9, 20.1; HPLC (Daicel Chiralpak AD-H, n -hexane/2-propanol = 90/10, 1.0 mL/min, 254 nm); t_R = 16.1 min (minor), 24.5 min (major); $[\alpha]_D^{25}$ 31.33 (c 0.04, CHCl_3); HRMS (ESI) m/z : $[\text{M}+\text{Na}]^+$ Calcd for $\text{C}_{28}\text{H}_{24}\text{N}_2\text{NaO}_4^+$, 475.1628; found 475.1654.

(5R, 6S, 7S, 13R)-4,6-diphenyl-13-(*m*-tolyl)-2,9-dioxa-3,12-diazadispiro[4.1.4⁷.2⁵]tridec-3-ene-1,8-dione (3fa). (37.5 mg, 82.9%, >20:1 dr, 95% ee); white solid; mp 164–166 °C; ^1H NMR (400 MHz, CDCl_3): δ 7.95–7.93 (m, 2H), 7.62–7.57 (m, 3H), 7.29–7.26 (m, 3H), 7.19 (t, 1H, J = 7.6 Hz), 7.12 (d, 1H, J = 7.5 Hz), 7.08–

7.05 (m, 2H), 7.01 (s, 1H), 6.96 (d, 1H, $J = 7.5$ Hz), 5.38 (s, 1H), 5.00 (s, 1H), 4.50 (ddd, 1H, $J = 12.5, 9.7, 6.2$ Hz), 4.18–4.14 (m, 1H), 2.65–2.61 (m, 1H), 2.46–2.37 (m, 1H), 2.30 (s, 3H); ^{13}C NMR (101 MHz, CDCl_3): δ 179.0, 177.7, 165.3, 138.7, 132.8, 132.1, 129.9, 129.74, 129.68, 129.4, 128.95, 128.86, 127.5, 127.4, 126.9, 123.4, 68.2, 67.7, 67.4, 66.4, 58.7, 35.0, 21.6; HPLC (Daicel Chiralpak AD-H, *n*-hexane/2-propanol = 90/10, 1.0 mL/min, 254 nm); $t_{\text{R}} = 18.2$ min (minor), 27.1 min (major); $[\alpha]_{\text{D}}^{25}$ 64.34 (*c* 0.04, CHCl_3); HRMS (ESI) m/z : $[\text{M}+\text{Na}]^+$ Calcd for $\text{C}_{28}\text{H}_{24}\text{N}_2\text{NaO}_4^+$, 475.1628; found 475.1615.

(5R, 6S, 7S, 13R)-4,6-diphenyl-13-(*p*-tolyl)-2,9-dioxa-3,12-diazadispiro[4.1.4⁷.2⁵]tridec-3-ene-1,8-dione (3ga). (36.1 mg, 79.8%, >20:1 dr, 90% ee); white solid; mp 84–87 °C; ^1H NMR (400 MHz, CDCl_3): δ 7.95–7.93 (m, 2H), 7.62–7.56 (m, 3H), 7.28–7.26 (m, 3H), 7.11 (d, 2H, $J = 8.2$ Hz), 7.07–7.05 (m, 4H), 5.39 (s, 1H), 5.01 (s, 1H), 4.49 (ddd, 1H, $J = 12.5, 9.6, 6.2$ Hz), 4.17–4.12 (m, 1H), 2.65–2.60 (m, 1H), 2.46–2.40 (m, 1H), 2.31 (s, 3H); ^{13}C NMR (101 MHz, CDCl_3): δ 179.1, 177.6, 165.2, 139.1, 132.7, 132.1, 129.75, 129.73, 129.69, 129.65, 129.4, 128.9, 127.5, 127.4, 126.2, 68.4, 67.8, 67.4, 66.4, 58.6, 35.0, 21.3; HPLC (Daicel Chiralpak AD-H, *n*-hexane/2-propanol = 90/10, 1.0 mL/min, 254 nm); $t_{\text{R}} = 20.9$ min (minor), 36.9 min (major); $[\alpha]_{\text{D}}^{25}$ 55.74 (*c* 0.05, CHCl_3); HRMS (ESI) m/z : $[\text{M}+\text{Na}]^+$ Calcd for $\text{C}_{28}\text{H}_{24}\text{N}_2\text{NaO}_4^+$, 475.1628; found 475.1645.

(5R, 6S, 7S, 13R)-4,6-diphenyl-13-(4-(trifluoromethyl)phenyl)-2,9-dioxa-3,12-diazadispiro[4.1.4⁷.2⁵]tridec-3-ene-1,8-dione (3ha). (38.0 mg, 75.0%, >20:1 dr, 87% ee); white solid; mp 157–159 °C; ^1H NMR (400 MHz, CDCl_3): δ 7.99–7.97 (m, 2H), 7.64–7.57 (m, 5H), 7.34–7.28 (m, 5H), 7.08–7.06 (m, 2H), 5.49 (s, 1H), 5.03 (s, 1H), 4.49 (ddd, 1H, $J = 9.3, 6.3$ Hz), 4.16–4.11 (m, 1H), 2.66–2.61 (m, 1H), 2.51–2.43 (m, 1H); ^{13}C NMR (101 MHz, CDCl_3): δ 179.0, 177.2, 164.8, 137.3 (q, $J_{\text{C-F}} = 1.1$ Hz), 132.4, 132.1, 131.3 (q, $J_{\text{C-F}} = 32.8$ Hz), 129.9, 129.7, 129.5, 129.2, 127.4, 127.1, 126.9, 126.0 (q, $J_{\text{C-F}} = 3.8$ Hz), 123.8 (q, $J_{\text{C-F}} = 272.4$ Hz), 68.0, 67.4, 66.8, 66.5, 58.9, 34.9; HPLC (Daicel Chiralpak AD-H, *n*-hexane/2-propanol = 90/10, 1.0 mL/min, 254 nm); $t_{\text{R}} = 19.8$ min (minor), 25.4

min (major); $[\alpha]_{\text{D}}^{25}$ 51.94 (*c* 0.05, CHCl_3); HRMS (ESI) *m/z*: $[\text{M}+\text{Na}]^+$ Calcd for $\text{C}_{28}\text{H}_{21}\text{N}_2\text{NaO}_4\text{F}_3^+$, 529.1346; found 529.1369.

(5R, 6S, 7S, 13R)-13-(4-methoxyphenyl)-4,6-diphenyl-2,9-dioxa-3,12-diazadispiro[4.1.4⁷.2⁵]tridec-3-ene-1,8-dione (3ia). (27.1 mg, 57.8%, >20:1 dr, 92% ee); pale yellow solid; mp 151–154 °C; ^1H NMR (400 MHz, CDCl_3): δ 7.94–7.92 (m, 2H), 7.61–7.55 (m, 3H), 7.28–7.23 (m, 3H), 7.11 (d, 2H, *J* = 8.7 Hz), 7.08–7.06 (m, 2H), 6.82 (d, *J* = 8.8 Hz), 5.36 (s, 1H), 5.00 (s, 1H), 4.47 (ddd, 1H, *J* = 12.3, 9.3, 6.2 Hz), 4.12 (ddd, 1H, *J* = 15.0, 8.6, 2.3 Hz), 3.77 (s, 3H), 2.65–2.59 (m, 1H), 2.46–2.38 (m, 1H); ^{13}C NMR (101 MHz, CDCl_3): δ 179.1, 177.6, 165.2, 160.1, 132.7, 132.1, 129.7, 129.6, 129.4, 128.9, 127.6, 127.5, 127.4, 124.7, 114.4, 68.4, 67.7, 67.4, 66.4, 58.4, 55.4, 34.9; HPLC (Daicel Chiralpak AD-H, *n*-hexane/2-propanol = 90/10, 1.0 mL/min, 220 nm); t_{R} = 36.1 min (minor), 67.1 min (major); $[\alpha]_{\text{D}}^{25}$ 77.92 (*c* 0.04, CHCl_3); HRMS (ESI) *m/z*: $[\text{M}+\text{H}]^+$ Calcd for $\text{C}_{28}\text{H}_{25}\text{N}_2\text{O}_5^+$, 469.1758; found 469.1748.

(5R, 6S, 7S, 13R)-4,6-diphenyl-13-(thiophen-2-yl)-2,9-dioxa-3,12-diazadispiro[4.1.4⁷.2⁵]tridec-3-ene-1,8-dione (3ja). (44.8 mg, quant., >20:1% dr, 86% ee); pale yellow solid; mp 144–146 °C; ^1H NMR (400 MHz, CDCl_3): δ 7.82–7.80 (m, 2H), 7.62–7.53 (m, 3H), 7.32–7.26 (m, 4H), 7.11–7.08 (m, 2H), 6.99–6.97 (m, 2H), 5.48 (s, 1H), 4.90 (s, 1H), 4.46 (ddd, 1H, *J* = 12.4, 9.6, 6.2 Hz), 4.11 (ddd, 1H, *J* = 15.0, 8.7, 2.4 Hz), 2.63–2.57 (m, 1H), 2.44–2.36 (m, 1H); ^{13}C NMR (101 MHz, CDCl_3): δ 178.7, 177.6, 165.5, 135.6, 132.2, 132.1, 129.7, 129.6, 129.5, 129.1, 127.52, 127.48, 127.0, 126.1, 125.3, 68.0, 67.6, 66.3, 64.1, 58.8, 34.8; HPLC (Daicel Chiralpak AD-H, *n*-hexane/2-propanol = 90/10, 1.0 mL/min, 254 nm); t_{R} = 24.7 min (minor), 32.9 min (major); $[\alpha]_{\text{D}}^{25}$ 31.73 (*c* 0.05, CHCl_3); HRMS (ESI) *m/z*: $[\text{M}+\text{Na}]^+$ Calcd for $\text{C}_{25}\text{H}_{20}\text{N}_2\text{NaO}_4\text{S}^+$, 467.1036; found 467.1025.

(5R, 6S, 7S, 13R)-6,3-bis(4-chlorophenyl)-4-phenyl-2,9-dioxa-3,12-diazadispiro[4.1.4⁷.2⁵]tridec-3-ene-1,8-dione (3ab). (42.3 mg, 83.4%, >20:1 dr, 89% ee); white solid; mp 95–98 °C; ^1H NMR (400 MHz, CDCl_3): δ 7.99–7.96 (m, 2H), 7.66–7.58 (m, 3H), 7.28 (d, 2H, *J* = 8.6 Hz), 7.24 (d, 2H, *J* = 8.6 Hz), 7.11 (d, 2H, *J* = 8.4 Hz), 6.99

(d, 2H, $J = 8.5$ Hz), 5.40 (s, 1H), 4.98 (s, 1H), 4.50 (ddd, 1H, $J = 12.8, 9.7, 6.0$ Hz), 4.20 (ddd, 1H, $J = 15.4, 8.7, 2.1$ Hz), 3.75 (brs, 1H), 2.65–2.60 (m, 1H), 2.41–2.33 (m, 1H); ^{13}C NMR (101 MHz, CDCl_3): δ 178.7, 177.2, 164.7, 135.3, 135.2, 132.4, 131.4, 131.1, 130.9, 129.9, 129.7, 129.3, 127.7, 127.3, 127.0, 68.3, 67.3, 66.8, 66.5, 57.9, 34.9; HPLC (Daicel Chiralpak AD-H, *n*-hexane/2-propanol = 90/10, 1.0 mL/min, 254 nm); $t_{\text{R}} = 21.3$ min (minor), 33.0 min (major); $[\alpha]_{\text{D}}^{25}$ 41.00 (*c* 0.04, CHCl_3); HRMS (ESI) m/z : $[\text{M}+\text{H}]^+$ Calcd for $\text{C}_{27}\text{H}_{20}^{35}\text{Cl}_2\text{N}_2\text{NaO}_4^+$, 507.0873; found 507.0870.

(5R, 6S, 7S, 13R)-6-(4-bromophenyl)-13-(4-chlorophenyl)-4-phenyl-2,9-dioxa-3,12-diazadispiro[4.1.4⁷.2⁵]tridec-3-ene-1,8-dione (3ac). (42.1 mg, 76.3%, >20:1% dr, 90% ee); white solid; mp 87–91 °C; ^1H NMR (400 MHz, CDCl_3): δ 7.98–7.96 (m, 2H), 7.64–7.58 (m, 3H), 7.40 (d, 2H, $J = 8.6$ Hz), 7.28 (d, 2H, $J = 8.6$ Hz), 7.11 (d, 2H, $J = 8.5$ Hz), 6.93 (d, 2H, $J = 8.5$ Hz), 5.40 (s, 1H), 4.97 (s, 1H), 4.50 (ddd, 1H, $J = 12.8, 9.7, 6.1$ Hz), 4.21 (ddd, 1H, $J = 15.4, 8.7, 2.1$ Hz), 3.74 (brs, 1H), 2.65–2.59 (m, 1H), 2.41–2.33 (m, 1H); ^{13}C NMR (101 MHz, CDCl_3): δ 178.7, 177.2, 164.6, 135.3, 132.7, 132.5, 132.5, 131.4, 131.3, 130.0, 129.3, 127.7, 127.3, 127.0, 123.5, 68.3, 67.3, 66.9, 66.5, 58.0, 34.9; HPLC (Daicel Chiralpak AD-H, *n*-hexane/2-propanol = 90/10, 1.0 mL/min, 254 nm); $t_{\text{R}} = 23.4$ min (minor), 34.7 min (major); $[\alpha]_{\text{D}}^{25}$ 31.15 (*c* 0.04, CHCl_3); HRMS (ESI) m/z : $[\text{M}+\text{H}]^+$ Calcd for $\text{C}_{27}\text{H}_{20}^{79}\text{Br}^{35}\text{ClN}_2\text{NaO}_4^+$, 551.0368; found 551.0366.

(5R, 6S, 7S, 13R)-13-(4-chlorophenyl)-6-(4-methoxyphenyl)-4-phenyl-2,9-dioxa-3,12-diazadispiro[4.1.4⁷.2⁵]tridec-3-ene-1,8-dione (3ad). (48.5 mg, 96.4%, >20:1 dr, 82% ee); white solid; mp 89–93 °C; ^1H NMR (400 MHz, CDCl_3): δ 7.97–7.95 (m, 2H), 7.64–7.56 (m, 3H), 7.27 (d, 2H, $J = 8.6$ Hz), 7.13 (d, 2H, $J = 8.5$ Hz), 6.99 (d, 2H, $J = 8.8$ Hz), 6.78 (d, 2H, $J = 8.8$ Hz), 5.39 (s, 1H), 4.94 (s, 1H), 4.45 (ddd, 1H, $J = 11.9, 9.1, 6.4$ Hz), 4.10 (ddd, 1H, $J = 14.5, 8.6, 2.7$ Hz), 3.74 (s, 3H), 3.72 (brs, 1H), 2.63–2.57 (m, 1H), 2.50–2.42 (m, 1H); ^{13}C NMR (101 MHz, CDCl_3): δ 179.2, 177.3, 165.0, 160.0, 135.0, 132.2, 131.8, 130.9, 129.8, 129.2, 127.8, 127.4, 127.2, 123.9, 114.8, 68.2, 67.3, 66.6, 66.4, 58.2, 34.9; HPLC (Daicel Chiralpak AD-H, *n*-hexane/2-propanol = 90/10, 1.0 mL/min, 254 nm); $t_{\text{R}} = 32.7$ min (minor), 52.9 min (major); $[\alpha]_{\text{D}}^{25}$ 48.79 (*c* 0.05, CHCl_3); HRMS (ESI)

m/z : $[M+Na]^+$ Calcd for $C_{28}H_{23}^{35}ClN_2NaO_5^+$, 525.1188; found 525.1201.

(5R, 6S, 7S, 13R)-13-(4-chlorophenyl)-4-phenyl-6-(*o*-tolyl)-2,9-dioxa-3,12-diazadispiro[4.1.4⁷.2⁵]tridec-3-ene-1,8-dione (3ae). (41.5 mg, 85.2%, >20:1 dr, 87% ee); white solid; mp 95–98 °C; ¹H NMR (400 MHz, CDCl₃): δ 8.01–7.99 (m, 2H), 7.64–7.56 (m, 3H), 7.41–7.39 (m, 1H), 7.28 (d, 2H, $J = 8.6$ Hz), 7.17–7.12 (m, 4H), 7.02–7.00 (m, 1H), 5.58 (s, 1H), 5.35 (s, 1H), 4.46 (ddd, 1H, $J = 12.0, 9.1, 6.3$ Hz), 4.06 (ddd, 1H, $J = 14.4, 8.5, 2.7$ Hz), 3.89 (brs, 1H), 2.57–2.51 (m, 1H), 2.37–2.29 (m, 1H), 1.71 (s, 3H); ¹³C NMR (101 MHz, CDCl₃): δ 179.2, 177.8, 164.8, 138.3, 135.0, 132.4, 131.6, 131.6, 130.8, 129.9, 129.2, 128.9, 128.7, 127.7, 127.43, 127.37, 126.9, 68.8, 67.0, 66.9, 66.5, 53.4, 35.1, 19.7; HPLC (Daicel Chiralpak AD-H, *n*-hexane/2-propanol = 90/10, 1.0 mL/min, 220 nm); $t_R = 17.2$ min (minor), 27.6 min (major); $[\alpha]_D^{25}$ 101.35 (c 0.04, CHCl₃); HRMS (ESI) m/z : $[M+H]^+$ Calcd for $C_{28}H_{24}^{35}ClN_2NaO_4^+$, 487.1419; found 487.1398.

(5R, 6S, 7S, 13R)-13-(4-chlorophenyl)-4-phenyl-6-(*m*-tolyl)-2,9-dioxa-3,12-diazadispiro[4.1.4⁷.2⁵]tridec-3-ene-1,8-dione (3af). (42.4 mg, 87.1%, >20:1 dr, 82% ee); white solid; mp 80–83 °C; ¹H NMR (400 MHz, CDCl₃): δ 7.94–7.92 (m, 2H), 7.62–7.56 (m, 3H), 7.28 (d, 2H, $J = 8.6$ Hz), 7.18–7.08 (m, 4H), 6.89 (d, 1H, $J = 7.7$ Hz), 6.81 (s, 1H), 5.37 (s, 1H), 4.96 (s, 1H), 4.45 (ddd, 1H, $J = 11.9, 9.1, 6.4$ Hz), 4.10 (ddd, 1H, $J = 14.6, 8.6, 2.8$ Hz), 3.71 (brs, 1H), 2.63–2.57 (m, 1H), 2.48–2.40 (m, 1H), 2.25 (s, 3H); ¹³C NMR (101 MHz, CDCl₃): δ 179.2, 177.3, 165.0, 139.2, 135.1, 132.2, 132.2, 131.7, 130.3, 129.84, 129.80, 129.3, 129.2, 127.8, 127.4, 127.2, 126.4, 67.9, 67.3, 67.0, 66.5, 58.6, 34.9, 21.5; HPLC (Daicel Chiralpak AD-H, *n*-hexane/2-propanol = 90/10, 1.0 mL/min, 254 nm); $t_R = 16.2$ min (minor), 33.6 min (major); $[\alpha]_D^{25}$ 61.03 (c 0.04, CHCl₃); HRMS (ESI) m/z : $[M+Na]^+$ Calcd for $C_{28}H_{23}^{35}ClN_2NaO_4^+$, 509.1239; found 509.1225.

(5R, 6S, 7S, 13R)-13-(4-chlorophenyl)-4-phenyl-6-(*p*-tolyl)-2,9-dioxa-3,12-diazadispiro[4.1.4⁷.2⁵]tridec-3-ene-1,8-dione (3ag). (47.6 mg, 97.8%, >20:1 dr, 86% ee); white solid; mp 85–87 °C; ¹H NMR (400 MHz, CDCl₃): δ 7.96–7.93 (m, 2H), 7.64–7.56 (m, 3H), 7.28 (d, 2H, $J = 8.6$ Hz), 7.13 (d, 2H, $J = 8.5$ Hz), 7.06 (d, 2H, $J = 7.9$ Hz), 6.95 (d, 2H, $J = 8.2$ Hz), 5.38 (s, 1H), 4.96 (s, 1H), 4.45 (ddd, 1H, $J = 11.9, 9.2, 6.4$ Hz),

4.09 (ddd, 1H, $J = 14.5, 8.6, 2.7$ Hz), 3.71 (brs, 1H), 2.63–2.57 (m, 1H), 2.50–2.42 (m, 1H), 2.28 (s, 3H); ^{13}C NMR (101 MHz, CDCl_3): δ 179.2, 177.3, 165.0, 139.0, 135.1, 132.2, 131.7, 130.1, 129.8, 129.5, 129.2, 129.1, 127.8, 127.4, 127.2, 68.1, 67.3, 66.8, 66.5, 58.4, 34.9, 21.1; HPLC (Daicel Chiralpak AD-H, *n*-hexane/2-propanol = 90/10, 1.0 mL/min, 254 nm); $t_{\text{R}} = 20.5$ min (minor), 34.3 min (major); $[\alpha]_{\text{D}}^{25}$ 61.20 (*c* 0.04, CHCl_3); HRMS (ESI) m/z : $[\text{M}+\text{Na}]^+$ Calcd for $\text{C}_{28}\text{H}_{23}^{35}\text{ClN}_2\text{NaO}_4^+$, 509.1239; found 509.1242.

(5R, 6S, 7S, 13R)-13-(4-chlorophenyl)-4-phenyl-6-(thiophen-2-yl)-2,9-dioxo-3,12-diazadispiro[4.1.4⁷.2⁵]tridec-3-ene-1,8-dione (3ah). (41.9 mg, 87.4%, >20:1% dr, 84% ee); pale yellow solid; mp 90–93 °C; ^1H NMR (400 MHz, CDCl_3): δ 7.97–7.95 (m, 2H), 7.65–7.57 (m, 3H), 7.28 (d, 2H, $J = 8.6$ Hz), 7.22 (dd, 1H, $J = 5.1, 0.7$ Hz), 7.11 (d, 2H, $J = 8.4$ Hz), 6.94 (dd, 1H, $J = 5.1, 3.6$ Hz), 6.89–6.88 (m, 1H), 5.36 (s, 1H), 5.26 (s, 1H), 4.47 (ddd, 1H, $J = 11.2, 8.9, 6.6$ Hz), 4.15 (ddd, 1H, $J = 13.3, 8.0, 3.4$ Hz), 3.71 (brs, 1H), 2.65–2.52 (m, 2H); ^{13}C NMR (101 MHz, CDCl_3): δ 178.8, 177.0, 164.5, 135.2, 133.5, 132.4, 131.5, 129.9, 129.3, 128.6, 128.0, 127.7, 127.3, 126.9, 126.8, 68.7, 67.7, 66.64, 66.58, 53.5, 35.0; HPLC (Daicel Chiralpak AD-H, *n*-hexane/2-propanol = 90/10, 1.0 mL/min, 254 nm); $t_{\text{R}} = 27.3$ min (minor), 48.4 min (major); $[\alpha]_{\text{D}}^{25}$ 90.98 (*c* 0.04, CHCl_3); HRMS (ESI) m/z : $[\text{M}+\text{Na}]^+$ Calcd for $\text{C}_{25}\text{H}_{19}^{35}\text{ClN}_2\text{NaO}_4\text{S}^+$, 501.0646; found 501.0646.

(5R, 6S, 7S, 13R)-13-(4-chlorophenyl)-4-isopropyl-6-phenyl-2,9-dioxo-3,12-diazadispiro[4.1.4⁷.2⁵]tridec-3-ene-1,8-dione (3ai). (40.9 mg, 93.2%, >20:1 dr, 59% ee); pale yellow solid; mp 169–172 °C; ^1H NMR (400 MHz, CDCl_3): δ 7.34–7.32 (m, 5H), 7.22 (d, 2H, $J = 8.4$ Hz), 7.17–7.15 (m, 2H), 4.93 (s, 1H), 4.61 (s, 1H), 4.35 (ddd, 1H, $J = 10.6, 8.6, 6.8$ Hz), 3.91 (ddd, 1H, $J = 13.4, 8.4, 3.8$ Hz), 2.98–2.91 (m, 1H), 2.54–2.47 (m, 1H), 2.40–2.33 (m, 1H), 1.35 (d, 3H, $J = 6.9$ Hz), 1.10 (d, 3H, $J = 6.8$ Hz); ^{13}C NMR (101 MHz, CDCl_3): δ 179.5, 177.5, 173.0, 135.3, 132.5, 131.9, 129.7, 129.3, 129.1, 128.8, 128.3, 67.43, 67.40, 66.3, 66.1, 58.0, 34.5, 27.3, 21.4, 20.9; HPLC (Daicel Chiralpak AD-H, *n*-hexane/2-propanol = 90/10, 1.0 mL/min, 220 nm); $t_{\text{R}} = 15.4$ min (minor), 22.4 min (major); $[\alpha]_{\text{D}}^{25}$ 52.20 (*c* 0.05, CHCl_3); HRMS (ESI) m/z : $[\text{M}+\text{Na}]^+$ Calcd for $\text{C}_{24}\text{H}_{23}^{35}\text{ClN}_2\text{NaO}_4^+$, 461.1239; found 461.1222.

(5R, 6S, 7S, 13R)-13-(4-chlorophenyl)-4-methyl-6-phenyl-2,9-dioxo-3,12-diazadispiro[4.1.4⁷.2⁵]tridec-3-ene-1,8-dione (3aj). (37.8 mg, 92.0%, >20:1 dr, 84% ee); pale yellow solid; mp 114–117 °C; ¹H NMR (400 MHz, CDCl₃): δ 7.35–7.32 (m, 5H), 7.21–7.17 (m, 4H), 4.99 (s, 1H), 4.49 (s, 1H), 4.36 (ddd, 1H, *J* = 10.6, 8.7, 6.8 Hz), 3.92 (ddd, 1H, *J* = 13.4, 8.4, 3.4 Hz), 3.33 (brs, 1H), 2.61–2.55 (m, 1H), 2.50–2.42 (m, 1H), 2.26 (s, 3H); ¹³C NMR (101 MHz, CDCl₃): δ 179.3, 176.8, 165.4, 135.3, 131.9, 131.6, 129.7, 129.31, 129.30, 129.2, 127.8, 67.1, 66.7, 66.6, 66.3, 58.1, 34.7, 12.2; HPLC (Daicel Chiralpak IC-3, *n*-hexane/EtOAc = 85/15, 1.0 mL/min, 254 nm); *t*_R = 9.5 min (minor), 15.7 min (major); [α]_D²⁵ 53.06 (*c* 0.04, CHCl₃); HRMS (ESI) *m/z*: [M+Na]⁺ Calcd for C₂₂H₂₀³⁵ClN₂O₄⁺, 411.1106; found 411.1126.

(5R, 6S, 7S, 13R)-4-methyl-6,13-diphenyl-2,9-dioxo-3,12-diazadispiro[4.1.4⁷.2⁵]tridec-3-ene-1,8-dione (3dj). (76.5 mg, quant., >20:1 dr, 86% ee); white solid; mp 145–147 °C; ¹H NMR (400 MHz, CDCl₃): δ 7.37–7.32 (m, 6H), 7.23–7.20 (m, 4H), 4.91 (s, 1H), 4.53 (s, 1H), 4.39 (ddd, 1H, *J* = 11.3, 9.0, 6.6 Hz), 3.98 (ddd, 1H, *J* = 13.9, 8.5, 3.4 Hz), 3.45 (brs, 1H), 2.63–2.57 (m, 1H), 2.47–2.39 (m, 1H), 2.78 (s, 3H); ¹³C NMR (101 MHz, CDCl₃): δ 179.2, 177.1, 165.7, 132.8, 132.2, 129.7, 129.4, 129.4, 129.21, 129.18, 129.08, 126.4, 67.5, 67.1, 67.9, 66.2, 58.2, 34.7, 12.2; HPLC (Daicel Chiralpak AD-H, *n*-hexane/2-propanol = 90/10, 1.0 mL/min, 220 nm); *t*_R = 24.3 min (minor), 47.1 min (major); [α]_D²⁵ 75.65 (*c* 0.05, CHCl₃); HRMS (ESI) *m/z*: [M+Na]⁺ Calcd for C₂₂H₂₀N₂NaO₄⁺, 399.1315; found 399.1329.

(5R, 6S, 7S, 13R)-13-(4-chlorophenyl)-6-(4-methoxyphenyl)-4-methyl-2,9-dioxo-3,12-diazadispiro[4.1.4⁷.2⁵]tridec-3-ene-1,8-dione (3ak). (89.3 mg, quant., >20:1 dr, 91% ee); yellow solid; mp 171–173 °C; ¹H NMR (400 MHz, CDCl₃): δ 7.33 (d, 2H, *J* = 8.6 Hz), 7.18–7.13 (m, 4H), 6.85 (d, 2H, *J* = 8.9 Hz), 4.88 (s, 1H), 4.43 (s, 1H), 4.35 (ddd, 1H, *J* = 10.3, 8.3, 6.9 Hz), 3.93–3.88 (m, 1H), 3.78 (s, 3H), 2.60–2.46 (m, 2H), 2.23 (s, 3H); ¹³C NMR (101 MHz, CDCl₃): δ 179.4, 176.8, 165.5, 160.2, 135.2, 131.8, 130.5, 129.3, 127.8, 123.5, 115.0, 67.0, 66.9, 66.4, 66.3, 57.6, 55.4, 34.7, 12.2; HPLC (Daicel Chiralpak IC-3, *n*-hexane/2-propanol = 90/10, 1.0 mL/min, 220 nm); *t*_R = 32.8 min (major), 40.7

min (minor); $[\alpha]_{\text{D}}^{25}$ 77.86 (c 0.05, CHCl_3); HRMS (ESI) m/z : $[\text{M}+\text{Na}]^+$ Calcd for $\text{C}_{23}\text{H}_{21}^{35}\text{ClN}_2\text{NaO}_5^+$, 463.1031; found 463.1021. CCDC 2278098.

Typical Procedure for the Preparation of 4-Carbonyl Substituted Pyrrolidines 4 by the Pd/C-catalyzed Decarboxylation of the 2,5-trans Spiropyrrolidines 3. To a solution of the spiropyrrolidines **3aj** (41.1 mg, 0.10 mmol, 1.00 equiv.) in EtOAc (3 mL) was added 10% Pd/C (4.1 mg, 10 wt%) at room temperature, and the mixture was stirred under H_2 (1 atm) atmosphere. After stirring for 16 h at the same temperature, the mixture was diluted with 30 mL EtOAc, filtered through a short Celite pad, and concentrated under reduced pressure. The residue was purified by column chromatography (silica gel, 20 g, n -hexane/EtOAc = 2/1) to afford (2*S*, 3*S*, 4*R*, 5*S*)-3-acetyl-2-(4-chlorophenyl)-4-phenyl-7-oxa-1-azaspiro[4.4]nonan-6-one (**4aj**) (25.8 mg, 0.0698 mmol, 69.8%, 85% ee) as a white solid.

(2*S*, 3*S*, 4*R*, 5*S*)-3-acetyl-2-(4-chlorophenyl)-4-phenyl-7-oxa-1-azaspiro[4.4]nonan-6-one (4aj). White solid; mp 138–142 °C; ^1H NMR (400 MHz, CDCl_3): δ 7.42–7.30 (m, 9H), 4.88 (d, 1H, J = 9.4 Hz), 4.07–4.01 (m, 1H), 3.99 (d, 1H, J = 11.1 Hz), 3.43 (dd, 1H, J = 11.0, 9.4 Hz), 3.26–3.20 (m, 1H), 2.23–2.18 (m, 2H), 1.88 (s, 3H); ^{13}C NMR (101 MHz, CDCl_3): δ 206.4, 180.1, 140.5, 136.6, 133.7, 129.2, 129.0, 128.5, 128.4, 128.2, 67.9, 65.5, 65.3, 63.0, 56.0, 35.0, 31.3; HPLC (Daicel Chiralpak AD-H, n -hexane/2-propanol = 90/10, 1.0 mL/min, 220 nm); t_{R} = 20.1 min (minor), 26.1 min (major); $[\alpha]_{\text{D}}^{25}$ 11.17 (c 0.05, CHCl_3); HRMS (ESI) m/z : $[\text{M}+\text{Na}]^+$ Calcd for $\text{C}_{21}\text{H}_{20}^{35}\text{ClNNaO}_3^+$, 392.1024; found 392.1040. CCDC 2278099 (racemate of **4aj**).

(2*S*, 3*S*, 4*R*, 5*S*)-3-acetyl-2,4-diphenyl-7-oxa-1-azaspiro[4.4]nonan-6-one (4dj). (32.6 mg, 97%, 88% ee); white solid; mp 127–130 °C; ^1H NMR (400 MHz, CDCl_3): δ 7.45 (d, 2H, J = 7.1 Hz), 7.39–7.31 (m, 8H), 4.87 (d, 1H, J = 9.4 Hz), 4.67–4.01 (m, 2H), 3.55–3.49 (m, 1H), 3.26–3.20 (m, 1H), 2.25–2.21 (m, 2H), 1.88 (s, 3H); ^{13}C NMR (101 MHz, CDCl_3): δ 206.6, 180.2, 141.8, 136.7, 129.1, 128.8, 128.5, 128.3, 128.1, 126.9, 67.9, 65.5, 65.3, 63.9, 55.9, 35.1, 31.2; HPLC (Daicel Chiralpak IC-3, n -hexane/2-propanol = 70/30, 1.0 mL/min, 220 nm); t_{R} = 20.3 min (major), 72.5 min (minor); $[\alpha]_{\text{D}}^{25}$ 4.76 (c 0.05,

CHCl₃); HRMS (ESI) *m/z*: [M+Na]⁺ Calcd for C₂₁H₂₁NNaO₃⁺, 358.1414; found 358.1429.

(2*S*, 3*S*, 4*R*, 5*S*)-3-acetyl-2-(4-chlorophenyl)-4-(4-methoxyphenyl)-7-oxa-1-azaspiro[4.4]nonan-6-one (4ak). (31.3 mg, 78%, 92% ee); White solid; mp 146–150 °C; ¹H NMR (400 MHz, CDCl₃): δ 7.39 (d, 2H, *J* = 8.4 Hz), 7.32 (d, 2H, *J* = 8.6 Hz), 7.23 (d, 2H, *J* = 8.7 Hz), 6.89 (d, 2H, *J* = 8.8 Hz), 4.87 (d, 1H, *J* = 9.4 Hz), 4.04 (dt, 1H, *J* = 8.2, 4.1 Hz), 3.93 (d, 1H, *J* = 11.3 Hz), 3.81 (s, 3H), 3.37 (dd, 1H, *J* = 11.3, 9.4 Hz), 3.22 (ddd, 1H, *J* = 10.4, 8.3, 6.8 Hz), 2.26–2.18 (m, 1H), 1.88 (s, 3H); ¹³C NMR (101 MHz, CDCl₃): δ 206.5, 180.3, 159.6, 140.6, 133.6, 129.5, 128.9, 128.2, 128.1, 114.5, 67.9, 65.5, 65.4, 62.9, 55.7, 55.4, 35.0, 31.3; HPLC (Daicel Chiralpak IC-3, *n*-hexane/2-propanol = 70/30, 1.0 mL/min, 220 nm); *t*_R = 20.2 min (major), 37.5 min (minor); [α]_D²⁵ 10.84 (*c* 0.05, CHCl₃); HRMS (ESI) *m/z*: [M+Na]⁺ Calcd for C₂₂H₂₂³⁵ClNNaO₄⁺, 422.1130; found 422.1114.

(2*S*, 3*S*, 4*R*, 5*S*)-3-benzoyl-2-(4-chlorophenyl)-4-phenyl-7-oxa-1-azaspiro[4.4]nonan-6-one (4aa). (29.1 mg, 67%, 93% ee); white solid; mp 167–171 °C; ¹H NMR (400 MHz, CDCl₃): δ 7.45–7.40 (m, 3H), 7.36 (d, 2H, *J* = 8.4 Hz), 7.25–7.17 (m, 9H), 5.04 (d, 1H, *J* = 8.3 Hz), 4.27–4.23 (m, 2H), 4.09–4.03 (m, 1H), 3.28–3.21 (m, 1H), 2.31–2.28 (m, 2H); ¹³C NMR (101 MHz, CDCl₃): δ 198.7, 180.2, 140.4, 137.2, 136.7, 133.5, 133.4, 129.0, 128.8, 128.5, 128.4, 128.2, 128.1, 67.9, 65.5, 64.5, 59.5, 56.8, 35.4; HPLC (Daicel Chiralpak IC-3, *n*-hexane/2-propanol = 70/30, 1.0 mL/min, 254 nm); *t*_R = 17.4 min (major), 79.4 min (minor); [α]_D²⁵ 84.31 (*c* 0.04, CHCl₃); HRMS (ESI) *m/z*: [M+Na]⁺ Calcd for C₂₆H₂₂³⁵ClNNaO₃⁺, 454.1180; found 454.1171.

(2*S*, 3*S*, 4*R*, 5*S*)-3-benzoyl-2,4-diphenyl-7-oxa-1-azaspiro[4.4]nonan-6-one (4da). (19.9 mg, 50%, 89% ee); white solid; mp 159–163 °C; ¹H NMR (400 MHz, CDCl₃): δ 7.45–7.37 (m, 6H), 7.26–7.22 (m, 7H), 7.20–7.16 (m, 2H), 5.06 (d, 1H, *J* = 9.4 Hz), 4.40–4.37 (m, 1H), 4.29 (d, 1H, *J* = 10.6 Hz), 4.07–4.04 (m, 1H), 3.27–3.21 (m, 1H), 2.37–2.30 (m, 1H); ¹³C NMR (101 MHz, CDCl₃): δ 198.9, 180.3, 141.9, 137.4, 133.2, 128.9, 128.7, 128.5, 128.4, 128.3, 128.1, 127.9, 126.8, 68.0, 65.5 (two peaks overlapped), 59.6, 56.9, 35.5; HPLC (Daicel Chiralpak AD-H, *n*-hexane/2-propanol = 70/30, 1.0 mL/min,

220 nm); t_R = 10.8 min (minor), 18.4 min (major); $[\alpha]_D^{25}$ 76.74 (c 0.05, CHCl_3); HRMS (ESI) m/z : $[\text{M}+\text{Na}]^+$ Calcd for $\text{C}_{26}\text{H}_{23}\text{NNaO}_3^+$, 420.1570; found 422.1590.

Typical Procedure for the Preparation of 4-Carbonyl Substituted Pyrrolidines 6 by the Silver-Catalyzed endo-Selective Asymmetric (3+2) Cycloaddition of Imino Lactones 1 with α,β -Unsaturated Ketones 5. A mixture of AgOAc (0.83 mg, 5 μmol , 5.0 mol%) and (R, S_p)-ThioClickFerrophos **L4** (3.5 mg, 5.5 μmol , 5.5 mol%) was dissolved in dry MTBE (1.0 mL) at room temperature. After stirring for 30 minutes at the same temperature, to the mixture were added imino lactones **1a** (24.6 mg, 0.11 mmol, 1.10 equiv.), dry Et_3N (2.7 μL , 20 μmol , 20 mol %), and enones **5j** (24.9 mg, 0.10 mmol, 1.00 equiv.) at 0 °C. After stirring for 16 h at the same temperature, the mixture was diluted with 30 mL EtOAc , filtered through a pad of Celite, and concentrated under reduced pressure. ^1H NMR analysis of the crude product showed that the *endo*-adduct was the sole product. The residue was purified by column chromatography (silica gel, 20 g, *n*-hexane/ EtOAc = 2/1) to afford ($2R, 3S, 4R, 5S$)-3-acetyl-2-(4-chlorophenyl)-4-phenyl-7-oxa-1-azaspiro[4.4]nonan-6-one (*endo*-**6aj**) (39.2 mg, 0.0954 mmol, 95.4%, >20:1 dr, 90% ee) as a white solid.

($2R, 3S, 4R, 5S$)-3-acetyl-2-(4-chlorophenyl)-4-phenyl-7-oxa-1-azaspiro[4.4]nonan-6-one (*endo*-6aj**).** White solid; mp 68–71 °C; ^1H NMR (400 MHz, CDCl_3): δ 7.49 (d, 2H, J = 8.4), 7.37–7.30 (m, 5H), 7.27–7.25 (m, 2H), 4.87 (d, 1H, J = 9.5 Hz), 4.26 (d, 1H, J = 12.4 Hz), 4.07–3.99 (m, 2H), 2.94 (ddd, 1H, J = 10.4, 8.8, 7.3 Hz), 2.37–2.31 (m, 1H), 2.21–2.13 (m, 1H), 1.59 (s, 3H); ^{13}C NMR (101 MHz, CDCl_3): δ 206.2, 179.7, 139.0, 135.2, 134.6, 129.55, 129.50, 129.4, 128.7, 128.1, 69.3, 65.8, 63.1, 60.8, 53.8, 33.8, 30.9; HPLC (Daicel Chiralpak IC-3, *n*-hexane/2-propanol = 70/30, 1.0 mL/min, 220 nm); t_R = 9.7 min (major), 11.8 min (minor); $[\alpha]_D^{25}$ –6.23 (c 0.05, CHCl_3); HRMS (ESI) m/z : $[\text{M}+\text{Na}]^+$ Calcd for $\text{C}_{21}\text{H}_{20}^{35}\text{ClINaO}_3^+$, 392.1024; found 392.1040.

($2R, 3S, 4R, 5S$)-3-acetyl-2,4-diphenyl-7-oxa-1-azaspiro[4.4]nonan-6-one (*endo*-6dj**).** (36.3 mg, quant., >20:1 dr, 85% ee); white solid; mp 117–120 °C; ^1H NMR (400 MHz, CDCl_3): δ 7.53–7.51 (m, 2H), 7.40–7.28 (m, 8H), 4.89 (d, 1H, J = 9.6 Hz), 4.31 (d, 1H, J

= 12.4 Hz), 4.08–4.00 (m, 2H), 3.00–2.93 (m, 1H), 2.37–2.31 (m, 1H), 2.26–2.18 (m, 1H), 1.54 (s, 3H); ¹³C NMR (101 MHz, CDCl₃): δ 206.2, 179.4, 139.8, 135.2, 129.2, 129.0, 128.5, 128.3, 127.84, 127.76, 69.1, 65.6, 63.6, 60.8, 53.8, 33.3, 30.4; HPLC (Daicel Chiralpak IC-3, *n*-hexane/2-propanol = 90/10, 1.0 mL/min, 220 nm); *t*_R = 12.2 min (major), 16.5 min (minor); [α]_D²⁵ 3.78 (*c* 0.04, CHCl₃); HRMS (ESI) *m/z*: [M+Na]⁺ Calcd for C₂₁H₂₁NNaO₃⁺, 358.1414; found 358.1423.

(2R, 3S, 4R, 5S)-3-acetyl-2-(4-chlorophenyl)-4-(4-methoxyphenyl)-7-oxa-1-azaspiro[4.4]nonan-6-one (endo-6ak). (42.7 mg, quant., >20:1 dr, 89% ee); white solid; mp 79–82 °C; ¹H NMR (400 MHz, CDCl₃): δ 7.50 (d, 2H, *J* = 8.4 Hz), 7.36 (d, 2H, *J* = 8.6 Hz), 7.18 (d, 2H, *J* = 8.6 Hz), 6.86 (d, 2H, *J* = 8.8 Hz), 4.85 (d, 1H, *J* = 9.6 Hz), 4.19 (d, 1H, *J* = 12.5 Hz), 4.05 (ddd, 1H, *J* = 14.4, 9.0, 3.4 Hz), 3.94 (dd, 1H, *J* = 12.5, 9.6 Hz), 3.79 (s, 3H), 3.02–2.96 (m, 1H), 2.37–2.32 (m, 1H), 2.21–2.13 (m, 1H), 1.56 (s, 3H); ¹³C NMR (101 MHz, CDCl₃): δ 206.1, 179.6, 159.6, 138.8, 134.2, 129.2, 129.1, 128.9, 126.6, 114.6, 68.9, 65.5, 62.6, 60.7, 55.4, 52.8, 33.6, 30.5; HPLC (Daicel Chiralpak IC-3, *n*-hexane/2-propanol = 70/30, 1.0 mL/min, 220 nm); *t*_R = 12.6 min (major), 16.5 min (minor); [α]_D²⁵ –5.43 (*c* 0.05, CHCl₃); HRMS (ESI) *m/z*: [M+Na]⁺ Calcd for C₂₂H₂₂³⁵ClNNaO₄⁺, 422.1130; found 422.1130.

(2R, 3S, 4R, 5S)-3-benzoyl-2,4-di-*p*-tolyl-7-oxa-1-azaspiro[4.4]nonan-6-one (endo-6gg). (45.2 mg, quant., >20:1 dr, 94% ee); yellow wish solid; mp 194–196 °C; ¹H NMR (400 MHz, DMSO-*d*₆): δ 7.89–7.87 (m, 2H), 7.61–7.58 (m, 1H), 7.49–7.45 (m, 2H), 7.16 (d, 2H, *J* = 8.2 Hz), 7.08 (d, 1H, *J* = 8.0 Hz), 7.04 (d, 1H, *J* = 8.1 Hz), 6.85 (d, 1H, *J* = 7.8 Hz), 5.20 (dd, 1H, *J* = 12.2, 9.9 Hz), 5.04 (d, 2H, *J* = 9.7 Hz), 4.25 (d, 1H, *J* = 12.2 Hz), 4.14–4.08 (m, 1H), 3.67 (brs, 1H), 3.15–3.09 (m, 1H), 2.30–2.25 (m, 1H), 2.22 (s, 3H), 2.14 (s, 3H); ¹³C NMR (101 MHz, DMSO-*d*₆): δ 197.0, 179.5, 139.1, 137.2, 136.6, 135.8, 133.4, 133.2, 129.1, 128.6, 128.3, 127.9, 127.74, 127.70, 67.6, 64.9, 61.6, 53.6, 51.2, 32.1, 20.61, 20.59; HPLC (Daicel Chiralpak IC-3, *n*-hexane/2-propanol = 70/30, 1.0 mL/min, 220 nm); *t*_R = 13.4 min (major), 30.9 min (minor); [α]_D²⁵ –36.14 (*c* 0.04, CHCl₃); HRMS (ESI) *m/z*: [M+Na]⁺ Calcd for C₂₈H₂₇NNaO₃⁺, 448.1883; found 448.1896.

(**2R**, **3S**, **4R**, **5S**)-3-benzoyl-4-(4-methoxyphenyl)-2-(*p*-tol)-7-oxa-1-azaspiro[4.4]nonan-6-one (*endo-6gd*). (45.9 mg, quant., >20:1 dr, 94% ee); yellow wisk solid; mp 190–193 °C; ¹H NMR (400 MHz, DMSO-*d*₆): δ 7.89–7.87 (m, 2H), 7.61–7.57 (m, 1H), 7.48–7.44 (d, 2H), 7.20 (d, 2H, *J* = 8.8 Hz), 7.05 (d, 2H, *J* = 8.1 Hz), 6.86–6.83 (m, 4H), 5.18 (dd, 1H, *J* = 12.2, 9.9 Hz), 5.03 (d, 1H, *J* = 9.7 Hz), 4.24 (d, 1H, *J* = 12.2 Hz), 4.15–4.09 (m, 1H), 3.68 (s, 3H), 3.65 (brs, 1H), 3.16–3.10 (m, 1H), 2.36–2.22 (m, 2H), 2.14 (s, 3H); ¹³C NMR (101 MHz, DMSO-*d*₆): δ 197.0, 179.6, 158.5, 139.1, 137.2, 135.8, 133.2, 128.9, 128.6, 128.3, 128.2, 128.0, 127.7, 114.0, 67.6, 64.9, 61.7, 55.0, 53.7, 51.0, 32.1, 20.6; HPLC (Daicel Chiralpak IC-3, *n*-hexane/2-propanol = 70/30, 1.0 mL/min, 220 nm); *t*_R = 17.3 min (major), 29.2 min (minor); [*α*]_D²⁵ –28.99 (*c* 0.04, CHCl₃); HRMS (ESI) *m/z*: [M+Na]⁺ Calcd for C₂₈H₂₇NNaO₄⁺, 464.1832; found 464.1847.

X-ray Crystallographic Analysis. The crystallographic data of **3ak** and *rac*-**4aj** were summarized in Table S4-2. Single crystals of **3ak** and *rac*-**4aj** were prepared from CHCl₃ and EtOAc by vapor diffusion technique using *n*-hexane as an anti-solvent, respectively. A suitable single crystal was respectively selected and mounted on the glass fiber and transferred to the goniometer of a Rigaku VariMax Saturn CCD diffractometer with graphite-monochromated MoK α radiation (λ = 71.073 pm). Yadokari-XG 2009 program was used as a graphical interface. The structure was solved and refined by SIR-2004 by SHELX-97 programs. The refinement was performed anisotropically for all non-hydrogen atoms. Hydrogen atoms were placed using AFIX instructions.

In the case of **3ak**, *CrystalStructure* crystallographic software package was used as a graphical interface. The structure was solved and refined by SHELXS Version 2014/5 and SHELXL Version 2016/6. The difference Fourier maps has suggested that the voids of each crystal were occupied by *n*-hexane molecules, which could not be appropriate because of heavy disorders. The electron density associated with the solvent molecule was removed by SQUEEZE routine of PLATON.

Table S4-2. Crystal data and structure refinements for **3ak** and *rac*-**4aj**.

Compound	3ak	<i>rac</i> - 4aj
CCDC	2278098	2278099
Empirical formula	C ₂₃ H ₂₁ ClN ₂ O ₅	C ₂₁ H ₂₀ ClNO ₃
Formula weight	440.88	369.83
Crystal system	hexagonal	triclinic
Space group	P 61	-P 1
a, Å	19.662(4)	5.897(3)
b, Å	19.662(4)	11.468(6)
c, Å	10.308(2)	13.965(7)
α, °	90	96.04(10)
β, °	90	92.04(7)
γ, °	120	96.39(10)
Volume, Å ³	3451.2(12)	932.3(8)
Z	6	2
Temperature, K	93(2)	93
2θ range for data collection, °	6.330 to 54.918	6.542 to 54.922
σ _{calcd} , g cm ⁻³	1.273	1.317
μ, mm ⁻¹	0.201	0.225
F(000)	1380	388
Crystal size, mm ³	0.363 × 0.083 × 0.058	0.440 × 0.120 × 0.030
Crystal color, habit	colorless, block	colorless, prism
Radiation	MoKα	MoKα
Reflections collected	27879	7698
Independent	5118	4180
Index ranges	-25 ≤ h ≤ 25, -25 ≤ k ≤ 24, -12 ≤ l ≤ 13	-7 ≤ h ≤ 6, -14 ≤ k ≤ 14, -17 ≤ l ≤ 18
Flack	-0.11(11)	-
Absolute configuration	ad	-
Data/restraints/parameters	5118/1/286	4180/0/235
Final R indexes [<i>I</i> > 2σ(<i>I</i>)]	R1 = 0.042, wR2 = 0.1044	R1 = 0.0627, wR2 = 0.1525
Final R indexes [all data]	R1 = 0.1084, wR2 = 0.1203	R1 = 0.1107, wR2 = 0.1742
Goodness-of-fit on <i>F</i> ²	1.000	1.084
Largest peak/deepest hole, e Å ⁻³	0.124/-0.149	0.534/-0.489

Computational Study.

The computational study was carried out under the same conditions described in the Experimental Section of Chapter 3.

Table S4-3. Total electronic energies (E, in a.u.), thermal correction to Gibbs free energy (TCGFE, in a.u.), and number of imaginary frequencies (NIMAG) in the Mannich reaction of the Michael adduct formed by the (3+2) cycloaddition of ylidene-isoxazolone with azomethine ylide derived from imino lactone **1** and AgOAc/PPh₃ complex. ^a

Structure	E (a.u.)	TCGFE (a.u.)	NIMAG (ν) ^b
INT-A1	-2441.79251043	0.572015	0
TS-A	-2441.77851592	0.572855	1 (-303.64)
INT-A2	-2441.78231991	0.572208	0
2,5- <i>cis</i> adduct	-1260.43509867	0.334772	0
INT-B1	-2441.77687105	0.568419	0
INT-B2	-2441.79339468	0.568962	0
TS-B	-2441.77477391	0.570153	1 (-307.01)
INT-B3	-2441.77935614	0.569731	0
2,5- <i>trans</i> adduct	-1260.43204906	0.332923	0

^[a] Computed at B3PW91/LanL2DZ(Ag)+6-31G*(other atoms) with gd3bj level of theory. ^[b] The number in parentheses shows the imaginary frequency ν (cm⁻¹).

INT-A1

Center Number	Atomic Number	Atomic Type	Coordinates (Angstroms)		
			X	Y	Z
1	47	0	0.258184	0.679139	-0.896999
2	15	0	2.434195	0.774077	0.062889
3	6	0	3.108638	2.412808	0.468774
4	6	0	2.219141	3.404008	0.901721
5	6	0	4.478202	2.691446	0.394925
6	6	0	2.697733	4.657681	1.275103
7	1	0	1.152325	3.193522	0.941686
8	6	0	4.952291	3.950589	0.760342
9	1	0	5.169483	1.927711	0.048815
10	6	0	4.064678	4.931915	1.203834
11	1	0	2.003065	5.422739	1.611005
12	1	0	6.015952	4.165114	0.697761
13	1	0	4.436880	5.912980	1.486832

14	6	0	3.678210	0.001854	-1.020384
15	6	0	4.641227	-0.880547	-0.521497
16	6	0	3.638760	0.284750	-2.391366
17	6	0	5.560494	-1.470612	-1.388722
18	1	0	4.658191	-1.120142	0.537866
19	6	0	4.559952	-0.303031	-3.254499
20	1	0	2.879640	0.959290	-2.783216
21	6	0	5.521240	-1.184495	-2.753545
22	1	0	6.302728	-2.161409	-0.997239
23	1	0	4.521882	-0.083015	-4.318044
24	1	0	6.233265	-1.652048	-3.428495
25	6	0	2.510777	-0.182526	1.605385
26	6	0	1.796431	-1.385610	1.658664
27	6	0	3.240767	0.247756	2.719288
28	6	0	1.816068	-2.160413	2.813313
29	1	0	1.194244	-1.703366	0.813904
30	6	0	3.256960	-0.532289	3.875415
31	1	0	3.782520	1.189035	2.688894
32	6	0	2.547741	-1.734091	3.922596
33	1	0	1.213982	-3.061994	2.855854
34	1	0	3.816012	-0.193921	4.744111
35	1	0	2.546667	-2.328186	4.832655
36	6	0	-2.965107	0.292349	0.316022
37	6	0	-1.461406	-1.884183	-1.205335
38	1	0	-2.200977	1.037831	0.578113
39	6	0	-2.672715	-0.916499	1.123458
40	7	0	-1.479754	-0.612338	-1.418783
41	6	0	-4.309545	0.948417	0.547350
42	6	0	-4.419093	2.341346	0.469034
43	6	0	-5.459793	0.190778	0.800702
44	6	0	-5.656391	2.970078	0.609800
45	1	0	-3.528509	2.940636	0.288328
46	6	0	-6.696167	0.818593	0.938723
47	1	0	-5.381590	-0.890615	0.873123
48	6	0	-6.801830	2.208011	0.837561
49	1	0	-5.723076	4.053170	0.542445
50	1	0	-7.582049	0.217807	1.129748
51	1	0	-7.768739	2.692999	0.946270
52	1	0	-2.392718	-2.446402	-1.089678
53	6	0	-0.209054	-2.638159	-1.133489
54	6	0	-0.142896	-3.728581	-0.254031
55	6	0	0.929334	-2.264145	-1.865009
56	6	0	1.063985	-4.403637	-0.079259
57	1	0	-1.020726	-4.002738	0.325457
58	6	0	2.126012	-2.952177	-1.698311
59	1	0	0.864177	-1.447966	-2.580441
60	6	0	2.197621	-4.014879	-0.794289
61	1	0	1.118825	-5.229423	0.624879
62	1	0	3.002002	-2.658503	-2.268594
63	1	0	3.137860	-4.541344	-0.652007
64	6	0	-2.738553	0.062647	-1.264826
65	6	0	-3.943957	-0.531919	-2.000690
66	6	0	-4.667897	0.703141	-2.534557
67	1	0	-4.566208	-1.155591	-1.355978

68	1	0	-3.581467	-1.151221	-2.829461
69	1	0	-5.071427	0.580106	-3.541058
70	1	0	-5.448354	1.062748	-1.861468
71	6	0	-2.587750	1.431792	-1.916791
72	8	0	-3.662998	1.754312	-2.623987
73	8	0	-1.612759	2.159090	-1.817655
74	6	0	-1.694184	-0.996312	2.143432
75	6	0	-0.872742	0.126596	2.685411
76	1	0	-0.264850	0.598293	1.901493
77	1	0	-1.519391	0.904258	3.110463
78	1	0	-0.196102	-0.233661	3.463577
79	7	0	-1.601692	-2.198696	2.671271
80	8	0	-2.551882	-2.981948	1.983801
81	6	0	-3.231580	-2.213948	1.048112
82	8	0	-4.089183	-2.736602	0.314889

TS-A

Center Number	Atomic Number	Atomic Type	Coordinates (Angstroms)		
			X	Y	Z
1	47	0	-0.351524	-0.687240	-0.763262
2	15	0	-2.557017	-0.703972	0.107593
3	6	0	-3.354656	-2.298740	0.457080
4	6	0	-2.546980	-3.434654	0.582719
5	6	0	-4.741261	-2.406440	0.623700
6	6	0	-3.120853	-4.668294	0.889655
7	1	0	-1.472488	-3.352639	0.431322
8	6	0	-5.311125	-3.640746	0.924953
9	1	0	-5.370777	-1.527299	0.512478
10	6	0	-4.501195	-4.771076	1.060991
11	1	0	-2.490277	-5.548148	0.984295
12	1	0	-6.387570	-3.722902	1.050805
13	1	0	-4.949081	-5.733681	1.293579
14	6	0	-3.688830	0.176031	-1.018273
15	6	0	-4.659197	1.072032	-0.558745
16	6	0	-3.545834	-0.044005	-2.394063
17	6	0	-5.477663	1.740633	-1.468565
18	1	0	-4.759749	1.264846	0.505550
19	6	0	-4.369758	0.618328	-3.300167
20	1	0	-2.777411	-0.725118	-2.754864
21	6	0	-5.334721	1.515974	-2.837949
22	1	0	-6.223325	2.443421	-1.105940
23	1	0	-4.248970	0.446531	-4.366400
24	1	0	-5.968349	2.044508	-3.545312
25	6	0	-2.638329	0.238448	1.662805
26	6	0	-2.207891	1.573205	1.636042
27	6	0	-3.021871	-0.344625	2.874031
28	6	0	-2.182426	2.321147	2.807383
29	1	0	-1.882212	2.023699	0.703681

30	6	0	-2.983057	0.408594	4.049090
31	1	0	-3.346085	-1.381083	2.903410
32	6	0	-2.567806	1.739600	4.017760
33	1	0	-1.836126	3.350143	2.773196
34	1	0	-3.277469	-0.049242	4.989946
35	1	0	-2.533460	2.320576	4.935628
36	6	0	2.967744	-0.265444	0.174749
37	6	0	1.649854	1.565306	-1.081514
38	1	0	2.170474	-0.849585	0.650987
39	6	0	2.665443	1.171535	0.551001
40	7	0	1.423817	0.301205	-1.531025
41	6	0	4.264336	-0.906108	0.603837
42	6	0	4.219974	-2.248973	1.004529
43	6	0	5.511688	-0.270807	0.542781
44	6	0	5.383830	-2.947795	1.319267
45	1	0	3.258441	-2.756505	1.056122
46	6	0	6.675824	-0.966830	0.865643
47	1	0	5.578750	0.766511	0.234750
48	6	0	6.620577	-2.307482	1.248935
49	1	0	5.322413	-3.990785	1.619740
50	1	0	7.633124	-0.453782	0.814746
51	1	0	7.532144	-2.846014	1.495275
52	1	0	2.516163	2.085645	-1.516039
53	6	0	0.465305	2.466054	-0.953161
54	6	0	0.485044	3.596948	-0.128372
55	6	0	-0.681058	2.220271	-1.726508
56	6	0	-0.629231	4.432140	-0.046117
57	1	0	1.367070	3.831652	0.455964
58	6	0	-1.790821	3.059672	-1.651977
59	1	0	-0.683180	1.382381	-2.417408
60	6	0	-1.772736	4.165159	-0.800505
61	1	0	-0.597270	5.298479	0.609994
62	1	0	-2.667883	2.845928	-2.256594
63	1	0	-2.639815	4.817402	-0.732289
64	6	0	2.632151	-0.437968	-1.370841
65	6	0	3.805040	-0.103336	-2.306358
66	6	0	4.451411	-1.464389	-2.551421
67	1	0	4.504849	0.620150	-1.882878
68	1	0	3.395899	0.309410	-3.235114
69	1	0	4.805075	-1.614448	-3.573151
70	1	0	5.255378	-1.683892	-1.845253
71	6	0	2.387855	-1.914249	-1.663110
72	8	0	3.407056	-2.452414	-2.329514
73	8	0	1.405923	-2.554918	-1.335148
74	6	0	1.936147	1.409116	1.788419
75	6	0	0.914430	0.515003	2.392410
76	1	0	0.159679	0.236778	1.647067
77	1	0	1.374981	-0.411623	2.756691
78	1	0	0.413532	1.010773	3.226428
79	7	0	2.270126	2.513513	2.381208
80	8	0	3.296092	3.105102	1.595853
81	6	0	3.618981	2.285788	0.541670
82	8	0	4.475029	2.603555	-0.266576

INT-A2

Center Number	Atomic Number	Atomic Type	Coordinates (Angstroms)		
			X	Y	Z
1	47	0	0.392549	0.655182	-0.683460
2	15	0	2.618435	0.660459	0.118641
3	6	0	3.443052	2.249255	0.432385
4	6	0	2.651485	3.398615	0.537839
5	6	0	4.832253	2.341487	0.586808
6	6	0	3.244963	4.630876	0.812618
7	1	0	1.574901	3.327969	0.395307
8	6	0	5.421236	3.573917	0.856666
9	1	0	5.448946	1.451470	0.490792
10	6	0	4.627622	4.718237	0.972487
11	1	0	2.627085	5.521261	0.891374
12	1	0	6.499594	3.644077	0.973413
13	1	0	5.090405	5.679481	1.180455
14	6	0	3.699298	-0.238861	-1.042810
15	6	0	4.692703	-1.126684	-0.617432
16	6	0	3.488124	-0.042940	-2.413551
17	6	0	5.464724	-1.811760	-1.555131
18	1	0	4.847763	-1.300704	0.443641
19	6	0	4.266919	-0.720252	-3.348093
20	1	0	2.700388	0.629876	-2.747018
21	6	0	5.253748	-1.610499	-2.919442
22	1	0	6.228136	-2.508283	-1.218108
23	1	0	4.092652	-0.566740	-4.409725
24	1	0	5.851578	-2.151497	-3.648262
25	6	0	2.751676	-0.275111	1.675288
26	6	0	2.354303	-1.620417	1.661982
27	6	0	3.137423	0.322880	2.878638
28	6	0	2.361608	-2.361656	2.838310
29	1	0	2.032425	-2.086106	0.734743
30	6	0	3.132324	-0.423777	4.058450
31	1	0	3.438711	1.366525	2.897504
32	6	0	2.748015	-1.764293	4.040657
33	1	0	2.046578	-3.401275	2.813617
34	1	0	3.429891	0.046176	4.992341
35	1	0	2.742647	-2.341160	4.961822
36	6	0	-3.013720	0.290536	0.122781
37	6	0	-1.743994	-1.479261	-1.018841
38	1	0	-2.244700	0.818421	0.696477
39	6	0	-2.659542	-1.209590	0.313247
40	7	0	-1.392046	-0.195090	-1.521956
41	6	0	-4.331174	0.857524	0.583015
42	6	0	-4.291702	2.087319	1.256538
43	6	0	-5.586246	0.299430	0.301614
44	6	0	-5.459679	2.747771	1.631258
45	1	0	-3.326151	2.539534	1.475405
46	6	0	-6.756003	0.953520	0.685362
47	1	0	-5.660859	-0.646996	-0.220049
48	6	0	-6.701164	2.180584	1.346689

49	1	0	-5.397997	3.703326	2.145903
50	1	0	-7.717271	0.497449	0.461622
51	1	0	-7.616851	2.687864	1.639460
52	1	0	-2.482933	-1.974365	-1.679009
53	6	0	-0.573208	-2.425734	-0.884893
54	6	0	-0.599991	-3.546253	-0.046993
55	6	0	0.561971	-2.224401	-1.685176
56	6	0	0.492745	-4.411552	0.024587
57	1	0	-1.474406	-3.763307	0.556577
58	6	0	1.653376	-3.089844	-1.620257
59	1	0	0.567554	-1.393186	-2.383230
60	6	0	1.627462	-4.183897	-0.754824
61	1	0	0.449665	-5.270106	0.690469
62	1	0	2.524657	-2.902598	-2.242261
63	1	0	2.479575	-4.856434	-0.694616
64	6	0	-2.573011	0.585899	-1.363872
65	6	0	-3.689836	0.386516	-2.406730
66	6	0	-4.297605	1.778414	-2.541349
67	1	0	-4.428890	-0.364852	-2.121409
68	1	0	-3.216691	0.070573	-3.342655
69	1	0	-4.587083	2.045745	-3.559575
70	1	0	-5.139378	1.941491	-1.864092
71	6	0	-2.279679	2.078973	-1.491969
72	8	0	-3.250718	2.709897	-2.154083
73	8	0	-1.309815	2.662955	-1.047339
74	6	0	-2.062300	-1.456381	1.655902
75	6	0	-0.904668	-0.739001	2.246327
76	1	0	-0.079818	-0.709286	1.526417
77	1	0	-1.161680	0.296777	2.496728
78	1	0	-0.564331	-1.244477	3.152854
79	7	0	-2.659192	-2.376824	2.330038
80	8	0	-3.715406	-2.893428	1.524629
81	6	0	-3.768655	-2.226924	0.336739
82	8	0	-4.552925	-2.534382	-0.531885

2,5-*cis* adduct

Center Number	Atomic Number	Atomic Type	Coordinates (Angstroms)		
			X	Y	Z
1	6	0	-0.503353	0.114212	0.115159
2	6	0	1.477831	0.039303	-1.231636
3	1	0	0.097979	0.577243	0.909283
4	6	0	0.446781	-0.919249	-0.509004
5	6	0	-1.789918	-0.343244	0.743325
6	6	0	-2.246513	0.351095	1.871471
7	6	0	-2.575573	-1.380986	0.231499
8	6	0	-3.467948	0.034556	2.460821
9	1	0	-1.641509	1.157441	2.281169
10	6	0	-3.794067	-1.706050	0.825904

11	1	0	-2.255280	-1.944598	-0.638375
12	6	0	-4.247758	-0.996536	1.937124
13	1	0	-3.807567	0.591271	3.330137
14	1	0	-4.388442	-2.518375	0.416180
15	1	0	-5.199304	-1.250614	2.396432
16	1	0	1.855219	-0.464799	-2.128198
17	6	0	2.663470	0.368957	-0.356145
18	6	0	3.734656	-0.530116	-0.316976
19	6	0	2.689505	1.507102	0.450787
20	6	0	4.808740	-0.312664	0.542337
21	1	0	3.720871	-1.414024	-0.952839
22	6	0	3.764933	1.722247	1.314061
23	1	0	1.872993	2.221419	0.396125
24	6	0	4.821566	0.813352	1.368131
25	1	0	5.634943	-1.018612	0.566414
26	1	0	3.775757	2.608523	1.943539
27	1	0	5.657504	0.985799	2.041262
28	6	0	-0.631504	1.209213	-0.978675
29	6	0	-1.838635	1.098796	-1.916300
30	6	0	-2.900197	1.959324	-1.243394
31	1	0	-2.165876	0.074273	-2.086785
32	1	0	-1.566944	1.526098	-2.889323
33	1	0	-3.534469	2.507580	-1.942544
34	1	0	-3.526837	1.386997	-0.553858
35	6	0	-0.908289	2.548037	-0.257007
36	8	0	-2.177007	2.940265	-0.469218
37	8	0	-0.145969	3.169307	0.440672
38	6	0	0.954648	-1.916052	0.484860
39	6	0	1.408935	-1.631028	1.872399
40	1	0	2.186208	-0.863328	1.892450
41	1	0	0.559805	-1.268855	2.465817
42	1	0	1.786502	-2.547709	2.331692
43	7	0	0.844675	-3.131143	0.082916
44	8	0	0.268884	-3.124330	-1.223337
45	6	0	-0.061986	-1.856015	-1.587522
46	8	0	-0.577708	-1.610012	-2.650963
47	7	0	0.668155	1.185150	-1.632148
48	1	0	0.571085	1.228854	-2.638510

INT-B1

Center Number	Atomic Number	Atomic Type	Coordinates (Angstroms)		
			X	Y	Z
1	6	0	-4.046248	0.217139	0.500389
2	6	0	-1.510795	1.538247	-0.558505
3	1	0	-4.591377	1.083567	0.891186
4	1	0	-1.140155	0.503674	-0.527360
5	7	0	-2.725389	1.815054	-0.819908
6	6	0	-0.493613	2.560885	-0.278382

7	6	0	0.463463	2.294182	0.708919
8	6	0	-0.441042	3.766570	-0.987850
9	6	0	1.470691	3.216353	0.978903
10	1	0	0.392618	1.377957	1.289028
11	6	0	0.582035	4.677112	-0.732537
12	1	0	-1.200517	3.967669	-1.738362
13	6	0	1.540904	4.401546	0.246356
14	1	0	2.199486	3.006820	1.755193
15	1	0	0.631857	5.605825	-1.295839
16	1	0	2.338550	5.114152	0.441128
17	6	0	-5.030900	-0.934903	0.424821
18	6	0	-6.393824	-0.661720	0.256136
19	6	0	-4.615621	-2.271269	0.474328
20	6	0	-7.318388	-1.695573	0.112626
21	1	0	-6.732215	0.371022	0.223775
22	6	0	-5.539334	-3.305599	0.332295
23	1	0	-3.565147	-2.505509	0.613927
24	6	0	-6.893407	-3.023338	0.144499
25	1	0	-8.370973	-1.460420	-0.023777
26	1	0	-5.197716	-4.337359	0.370965
27	1	0	-7.611835	-3.831674	0.032594
28	6	0	3.361851	0.306097	1.280676
29	6	0	2.606125	0.167129	2.451044
30	6	0	4.449505	1.187869	1.251493
31	6	0	2.940442	0.901152	3.587747
32	1	0	1.736507	-0.486475	2.473316
33	6	0	4.785162	1.913031	2.392482
34	1	0	5.019098	1.319094	0.335352
35	6	0	4.031852	1.770224	3.560304
36	1	0	2.332245	0.805620	4.482527
37	1	0	5.626787	2.600236	2.366342
38	1	0	4.286599	2.349054	4.444186
39	6	0	3.363249	0.377014	-1.606454
40	6	0	4.593843	0.229198	-2.257389
41	6	0	2.478441	1.386580	-2.006140
42	6	0	4.935929	1.092579	-3.297883
43	1	0	5.279480	-0.558104	-1.956179
44	6	0	2.830456	2.252077	-3.037869
45	1	0	1.525004	1.511157	-1.502338
46	6	0	4.058214	2.105691	-3.685873
47	1	0	5.890357	0.973057	-3.804019
48	1	0	2.140723	3.038420	-3.330702
49	1	0	4.329476	2.778337	-4.495358
50	6	0	4.061450	-2.066579	-0.237817
51	6	0	3.867752	-3.043783	-1.224453
52	6	0	5.118142	-2.195872	0.668200
53	6	0	4.734481	-4.128763	-1.313445
54	1	0	3.039935	-2.951482	-1.924848
55	6	0	5.978441	-3.291426	0.581878
56	1	0	5.267264	-1.446954	1.440370
57	6	0	5.791214	-4.254718	-0.408123
58	1	0	4.581228	-4.880875	-2.082660
59	1	0	6.795307	-3.389864	1.291910
60	1	0	6.462468	-5.106899	-0.472415

61	6	0	-3.619935	0.685830	-0.959595
62	6	0	-3.143176	-0.455145	-1.874399
63	6	0	-4.391706	-0.824455	-2.672660
64	1	0	-2.730803	-1.302644	-1.325520
65	1	0	-2.366551	-0.066469	-2.544014
66	1	0	-4.186656	-1.064104	-3.718795
67	1	0	-4.951983	-1.643322	-2.213460
68	6	0	-4.891544	1.184300	-1.670831
69	8	0	-5.236609	0.341873	-2.666118
70	8	0	-5.529649	2.170181	-1.403899
71	6	0	-2.883388	-0.000691	1.417425
72	6	0	-2.593376	0.791340	2.567846
73	7	0	-1.467553	0.452319	3.157682
74	6	0	-3.393189	1.931555	3.098984
75	1	0	-4.404137	1.610611	3.375913
76	1	0	-2.903369	2.351818	3.981657
77	1	0	-3.488358	2.717377	2.340103
78	8	0	-0.957405	-0.606866	2.378006
79	6	0	-1.799695	-0.861328	1.329556
80	8	0	-1.411977	-1.730974	0.462039
81	15	0	2.901876	-0.663731	-0.186981
82	47	0	0.642715	-1.340296	-0.005403

INT-B2

Center Number	Atomic Number	Atomic Type	Coordinates (Angstroms)		
			X	Y	Z
1	6	0	3.648996	-0.399486	0.134502
2	6	0	1.488338	-1.997914	-1.171895
3	1	0	4.029733	-1.408567	-0.076281
4	1	0	2.359805	-2.575356	-1.490927
5	7	0	1.544921	-0.722523	-1.080957
6	6	0	0.258110	-2.714873	-0.811277
7	6	0	-0.271910	-3.711710	-1.641470
8	6	0	-0.370742	-2.417504	0.408450
9	6	0	-1.452194	-4.358560	-1.282279
10	1	0	0.228795	-3.958734	-2.574794
11	6	0	-1.539905	-3.081880	0.771374
12	1	0	0.092040	-1.715511	1.097306
13	6	0	-2.089480	-4.039218	-0.080116
14	1	0	-1.874624	-5.115342	-1.938283
15	1	0	-2.013013	-2.850418	1.720046
16	1	0	-3.009475	-4.546916	0.197152
17	6	0	4.851593	0.512768	0.267690
18	6	0	6.033627	0.217165	-0.420334
19	6	0	4.785649	1.684470	1.029441
20	6	0	7.121518	1.088760	-0.373741
21	1	0	6.100308	-0.699073	-1.003737
22	6	0	5.868685	2.560223	1.071902

23	1	0	3.880438	1.903229	1.589142
24	6	0	7.038140	2.268755	0.365797
25	1	0	8.032561	0.845107	-0.914546
26	1	0	5.801885	3.470168	1.663234
27	1	0	7.883375	2.951438	0.402410
28	6	0	-2.931962	-0.061939	1.489943
29	6	0	-1.943087	0.020987	2.479919
30	6	0	-4.091186	-0.811616	1.719500
31	6	0	-2.107696	-0.654320	3.687094
32	1	0	-1.028227	0.584879	2.304907
33	6	0	-4.256895	-1.475185	2.934672
34	1	0	-4.848483	-0.896411	0.944947
35	6	0	-3.264592	-1.402139	3.915331
36	1	0	-1.314711	-0.611872	4.427854
37	1	0	-5.154813	-2.062736	3.109630
38	1	0	-3.387561	-1.939451	4.852273
39	6	0	-3.666819	-0.110323	-1.299054
40	6	0	-4.975174	0.308854	-1.567843
41	6	0	-3.159848	-1.254504	-1.926548
42	6	0	-5.770688	-0.418479	-2.452549
43	1	0	-5.367138	1.203350	-1.090768
44	6	0	-3.961589	-1.984244	-2.800245
45	1	0	-2.140061	-1.572985	-1.727439
46	6	0	-5.266870	-1.566786	-3.065902
47	1	0	-6.784649	-0.087722	-2.662642
48	1	0	-3.561210	-2.874516	-3.277521
49	1	0	-5.889185	-2.131642	-3.755295
50	6	0	-3.313121	2.417407	0.030536
51	6	0	-3.074891	3.326332	-1.009154
52	6	0	-4.088188	2.806981	1.127060
53	6	0	-3.621376	4.605439	-0.959585
54	1	0	-2.460921	3.029127	-1.857019
55	6	0	-4.625451	4.093771	1.178456
56	1	0	-4.266173	2.108432	1.939761
57	6	0	-4.396924	4.991528	0.136409
58	1	0	-3.434933	5.305066	-1.770146
59	1	0	-5.222284	4.393319	2.036045
60	1	0	-4.815522	5.993600	0.179585
61	6	0	2.824572	-0.025365	-1.163754
62	6	0	2.608204	1.472246	-1.394165
63	6	0	3.736279	1.868318	-2.337882
64	1	0	2.587280	2.045963	-0.467435
65	1	0	1.639221	1.602521	-1.895768
66	1	0	3.445719	2.603644	-3.090844
67	1	0	4.626848	2.215500	-1.808831
68	6	0	3.649118	-0.427463	-2.400552
69	8	0	4.090665	0.660082	-3.047925
70	8	0	3.898665	-1.551383	-2.773059
71	6	0	2.799672	-0.502621	1.361572
72	6	0	2.882086	-1.527771	2.337355
73	7	0	2.001207	-1.383299	3.306213
74	6	0	3.819080	-2.689285	2.358245
75	1	0	4.863127	-2.354060	2.372013
76	1	0	3.634955	-3.300421	3.246379

77	1	0	3.686877	-3.321185	1.470344
78	8	0	1.283117	-0.217331	2.975561
79	6	0	1.757200	0.317376	1.799020
80	8	0	1.177118	1.339391	1.321785
81	15	0	-2.595120	0.750504	-0.105132
82	47	0	-0.242432	0.507139	-0.396532

TS-B

Center Number	Atomic Number	Atomic Type	Coordinates (Angstroms)		
			X	Y	Z
1	6	0	3.670668	-0.252735	-0.199486
2	6	0	1.723206	-1.584948	-0.856699
3	1	0	4.275885	-0.987744	-0.744920
4	1	0	2.571265	-2.131096	-1.287763
5	7	0	1.498867	-0.338746	-1.333609
6	6	0	0.541095	-2.476209	-0.668658
7	6	0	0.261635	-3.407800	-1.677812
8	6	0	-0.331292	-2.383232	0.421062
9	6	0	-0.875054	-4.211549	-1.606844
10	1	0	0.931837	-3.481693	-2.531317
11	6	0	-1.461758	-3.196176	0.501003
12	1	0	-0.127174	-1.699543	1.234152
13	6	0	-1.740392	-4.107615	-0.515058
14	1	0	-1.083713	-4.921164	-2.403819
15	1	0	-2.121619	-3.104810	1.358711
16	1	0	-2.626089	-4.735211	-0.458382
17	6	0	4.651354	0.701817	0.431524
18	6	0	5.938553	0.781360	-0.116057
19	6	0	4.326702	1.548520	1.499118
20	6	0	6.874664	1.691833	0.372532
21	1	0	6.204372	0.127189	-0.944565
22	6	0	5.262153	2.456753	1.991579
23	1	0	3.337629	1.506666	1.943056
24	6	0	6.537372	2.536868	1.429219
25	1	0	7.866044	1.737599	-0.071217
26	1	0	4.991529	3.104986	2.821476
27	1	0	7.263428	3.246946	1.816753
28	6	0	-2.915572	-0.203242	1.578778
29	6	0	-1.905378	-0.205070	2.549844
30	6	0	-4.089121	-0.936612	1.789382
31	6	0	-2.069158	-0.942539	3.720835
32	1	0	-0.973148	0.330403	2.376969
33	6	0	-4.250129	-1.666446	2.966167
34	1	0	-4.863612	-0.955652	1.027625
35	6	0	-3.239829	-1.673399	3.930124
36	1	0	-1.267768	-0.962613	4.454031
37	1	0	-5.159214	-2.241387	3.123719
38	1	0	-3.359766	-2.258965	4.838005

39	6	0	-3.711241	-0.082634	-1.186024
40	6	0	-5.026479	0.342804	-1.405393
41	6	0	-3.208969	-1.186248	-1.887872
42	6	0	-5.835229	-0.338289	-2.314698
43	1	0	-5.414042	1.206684	-0.871510
44	6	0	-4.024545	-1.870075	-2.785537
45	1	0	-2.183811	-1.512226	-1.730239
46	6	0	-5.337249	-1.446879	-3.001240
47	1	0	-6.854548	-0.002141	-2.486879
48	1	0	-3.627808	-2.728124	-3.321244
49	1	0	-5.969757	-1.975803	-3.709582
50	6	0	-3.349098	2.362730	0.295003
51	6	0	-3.134867	3.339495	-0.687033
52	6	0	-4.114770	2.671257	1.423549
53	6	0	-3.695611	4.605902	-0.548407
54	1	0	-2.529845	3.103765	-1.560326
55	6	0	-4.665802	3.945550	1.564532
56	1	0	-4.276304	1.919181	2.190675
57	6	0	-4.461107	4.911179	0.579721
58	1	0	-3.528976	5.357845	-1.315235
59	1	0	-5.256009	4.181686	2.446197
60	1	0	-4.891532	5.902835	0.691936
61	6	0	2.731068	0.412204	-1.310077
62	6	0	2.485909	1.913629	-1.190287
63	6	0	3.591483	2.536772	-2.033476
64	1	0	2.476376	2.270258	-0.159729
65	1	0	1.506022	2.122608	-1.639783
66	1	0	3.284453	3.434257	-2.574823
67	1	0	4.491010	2.751960	-1.449920
68	6	0	3.508985	0.317530	-2.635291
69	8	0	3.929549	1.541028	-3.022550
70	8	0	3.752807	-0.681760	-3.266785
71	6	0	2.783415	-1.075956	0.704820
72	6	0	3.243292	-2.256086	1.409063
73	7	0	2.618852	-2.454819	2.532050
74	6	0	4.270329	-3.222370	0.934881
75	1	0	5.250584	-2.737580	0.853628
76	1	0	4.347998	-4.062026	1.630438
77	1	0	4.010369	-3.608663	-0.058793
78	8	0	1.731613	-1.356729	2.700807
79	6	0	1.858060	-0.488956	1.653200
80	8	0	1.183352	0.542549	1.604162
81	15	0	-2.619773	0.715747	0.034488
82	47	0	-0.338379	0.491337	-0.579547

INT-B3

Center Number	Atomic Number	Atomic Type	Coordinates (Angstroms)		
			X	Y	Z
1	6	0	3.623040	-0.290325	-0.307767
2	6	0	1.769742	-1.626894	-0.793884
3	1	0	4.220741	-1.010424	-0.879704
4	1	0	2.491528	-2.250861	-1.356663
5	7	0	1.493517	-0.395670	-1.452920
6	6	0	0.518496	-2.450896	-0.615841
7	6	0	-0.045683	-2.971768	-1.791567
8	6	0	-0.145976	-2.662396	0.594493
9	6	0	-1.247895	-3.671915	-1.756421
10	1	0	0.464620	-2.797140	-2.735510
11	6	0	-1.358199	-3.355664	0.629922
12	1	0	0.256368	-2.289134	1.528059
13	6	0	-1.914868	-3.858370	-0.541938
14	1	0	-1.669590	-4.066763	-2.677996
15	1	0	-1.868671	-3.483937	1.579987
16	1	0	-2.862901	-4.389602	-0.512811
17	6	0	4.605039	0.593412	0.409204
18	6	0	5.917794	0.629239	-0.082659
19	6	0	4.278480	1.428862	1.485860
20	6	0	6.874561	1.478849	0.469133
21	1	0	6.185600	-0.009869	-0.922020
22	6	0	5.236410	2.272753	2.045798
23	1	0	3.273129	1.437824	1.890944
24	6	0	6.535876	2.306326	1.539243
25	1	0	7.883154	1.491331	0.063863
26	1	0	4.961388	2.909269	2.883169
27	1	0	7.278174	2.968383	1.977529
28	6	0	-2.875538	-0.379811	1.488508
29	6	0	-1.873183	-0.394622	2.467889
30	6	0	-4.019805	-1.166995	1.649506
31	6	0	-2.021593	-1.187976	3.602394
32	1	0	-0.964166	0.186217	2.330143
33	6	0	-4.161639	-1.962307	2.787012
34	1	0	-4.791025	-1.170858	0.884564
35	6	0	-3.165062	-1.973942	3.763481
36	1	0	-1.232513	-1.204965	4.349387
37	1	0	-5.049717	-2.578033	2.905656
38	1	0	-3.274158	-2.601308	4.644517
39	6	0	-3.924650	0.156992	-1.137410
40	6	0	-5.168644	0.795907	-1.177513
41	6	0	-3.674184	-0.936258	-1.976381
42	6	0	-6.157303	0.337665	-2.048035
43	1	0	-5.362094	1.649736	-0.533746
44	6	0	-4.668870	-1.397659	-2.834884
45	1	0	-2.704060	-1.426853	-1.950330
46	6	0	-5.910795	-0.760651	-2.873056
47	1	0	-7.121045	0.839379	-2.081072
48	1	0	-4.469875	-2.248524	-3.481220

49	1	0	-6.683300	-1.115272	-3.550542
50	6	0	-3.049884	2.338794	0.536699
51	6	0	-2.625554	3.411927	-0.256997
52	6	0	-3.816253	2.583750	1.681336
53	6	0	-2.978583	4.715902	0.081555
54	1	0	-2.015319	3.222377	-1.137776
55	6	0	-4.159540	3.891515	2.023205
56	1	0	-4.135825	1.754203	2.306208
57	6	0	-3.745275	4.956950	1.223439
58	1	0	-2.646710	5.544414	-0.538587
59	1	0	-4.750048	4.077265	2.916677
60	1	0	-4.012483	5.975336	1.493292
61	6	0	2.688386	0.403238	-1.385661
62	6	0	2.418349	1.896204	-1.205165
63	6	0	3.533444	2.573318	-1.990022
64	1	0	2.374938	2.208336	-0.160976
65	1	0	1.445419	2.105540	-1.668930
66	1	0	3.233598	3.501129	-2.482528
67	1	0	4.421340	2.758311	-1.377323
68	6	0	3.501771	0.387012	-2.698400
69	8	0	3.895242	1.639297	-3.028966
70	8	0	3.791504	-0.575598	-3.366616
71	6	0	2.647926	-1.185894	0.483695
72	6	0	3.262875	-2.294229	1.253122
73	7	0	2.889052	-2.342228	2.485375
74	6	0	4.204921	-3.308452	0.712078
75	1	0	5.137996	-2.833090	0.387426
76	1	0	4.435642	-4.054101	1.477012
77	1	0	3.769339	-3.809988	-0.160246
78	8	0	2.002390	-1.244490	2.707571
79	6	0	1.849485	-0.522148	1.562568
80	8	0	1.140013	0.465205	1.539767
81	15	0	-2.604195	0.653638	0.012195
82	47	0	-0.404541	0.319158	-0.802848

2,5-*trans* adduct

Center Number	Atomic Number	Atomic Type	Coordinates (Angstroms)		
			X	Y	Z
1	6	0	-0.921253	0.094133	0.484860
2	6	0	1.393874	0.555333	0.537133
3	1	0	-0.943069	0.269856	1.567505
4	1	0	1.290359	0.795198	1.605152
5	6	0	2.855473	0.370582	0.209319
6	6	0	3.604206	1.474701	-0.216331
7	6	0	3.500690	-0.860208	0.364467
8	6	0	4.962845	1.344533	-0.496453
9	1	0	3.116305	2.439468	-0.316491
10	6	0	4.859336	-0.990180	0.081445

11	1	0	2.954053	-1.734146	0.702457
12	6	0	5.595602	0.110515	-0.352395
13	1	0	5.527501	2.212170	-0.828133
14	1	0	5.338881	-1.958629	0.197129
15	1	0	6.654179	0.007485	-0.576056
16	6	0	-2.221760	-0.573710	0.135922
17	6	0	-3.280915	-0.438322	1.043802
18	6	0	-2.451463	-1.269863	-1.057088
19	6	0	-4.538902	-0.968772	0.767287
20	1	0	-3.117230	0.102930	1.973877
21	6	0	-3.707013	-1.809179	-1.331657
22	1	0	-1.660748	-1.395143	-1.788543
23	6	0	-4.755746	-1.658176	-0.425060
24	1	0	-5.346066	-0.845973	1.484592
25	1	0	-3.862558	-2.350951	-2.260848
26	1	0	-5.733249	-2.079244	-0.644478
27	6	0	-0.653604	1.508559	-0.149524
28	6	0	-1.354419	1.829295	-1.464999
29	6	0	-2.655756	2.487866	-1.018255
30	1	0	-1.516167	0.958018	-2.100225
31	1	0	-0.738045	2.548036	-2.017715
32	1	0	-2.994993	3.288885	-1.677547
33	1	0	-3.462253	1.761996	-0.879414
34	6	0	-1.266007	2.539247	0.812810
35	8	0	-2.371059	3.084493	0.265319
36	8	0	-0.876648	2.811074	1.919878
37	6	0	0.417519	-0.647653	0.270214
38	6	0	0.521601	-1.884346	1.093020
39	7	0	0.725402	-2.944440	0.395220
40	6	0	0.372228	-1.962152	2.569377
41	1	0	-0.644647	-1.681787	2.868382
42	1	0	0.569930	-2.979917	2.913909
43	1	0	1.065807	-1.273002	3.065185
44	8	0	0.824858	-2.564887	-0.976283
45	6	0	0.649021	-1.221677	-1.108796
46	8	0	0.700109	-0.663923	-2.178504
47	7	0	0.797350	1.642009	-0.227391
48	1	0	1.071336	1.514563	-1.201398

4–5. References

1. (a) Brooks, W. H.; Guida, W. C.; Daniel, K. G. *Curr. Top. Med. Chem.* **2011**, *11*, 760–770. (b) Gandhi, K.; Shah, U.; Patel, S. *Curr. Drug. Discovery Technol.* **2020**, *17*, 565–573.
2. Selected recent review: (a) Lin, L.; Feng, X. *Chem. Eur. J.* **2017**, *23*, 6464–6428. (b) Beletskaya, I. P.; Nájera, C.; Yus, M. *Chem. Rev.* **2018**, *118*, 5080–5200. (c) Nájera, C.; Foubelo, F.; Sansano, J. M.; Yus, M. *Org. Biomol. Chem.* **2020**, *18*, 1232–1278. (d) Huo, X.; Li, G.; Wang, X.; Zhang, W. *Angew. Chem. Int. Ed.* **2022**, *61*, e202210086.
3. Selected recent example: (a) Xun, L.; Zhang, Z.; Zhou, Y.; Qin, S.; Fu, S.; Liu, B. *J. Org. Chem.* **2023**, *88*, 3987–3991. (b) Ma, Z.-C.; Wei, L.-W.; Huang, Y. *Org. Lett.* **2023**, *25*, 1661–1666. (c) Jung, Y.; Yoo, S. Y.; Jin, Y.; You, J.; Han, S.; Yu, J.; Park, Y.; Cho, S. H. *Angew. Chem. Int. Ed.* **2023**, *62*, e202218794. (d) Hu, Y.; Huang, J.-Y.; Yan, R.-J.; Chen, Z.-C.; Quyang, Q.; Du, W.; Chen, Y.-C. *Chem. Sci.* **2023**, *14*, 1896–1901.
4. (a) Adrio, J.; Carretero, J. C. *Chem. Commun.* **2019**, *55*, 11979–11991. (b) Wei, L.; Chang, X.; Wang, C. J. *Acc. Chem. Res.* **2020**, *53*, 1084–1100. (c) Kumar, S. V.; Guiry, P. J. *Chem. Eur. J.* **2023**, *29*, e202300296.
5. Examples of a nickel complex-controlled strategy: (a) Arai, T.; Yokoyama, N.; Mishiro, A.; Sato, H. *Angew. Chem. Int. Ed.* **2010**, *122*, 8067–8070. (b) Awata, A.; Arai, T. *Chem. Eur. J.* **2012**, *18*, 8278–8282. (c) Arai, T.; Tokumitsu, C.; Miyazaki, T.; Kuwano, S.; Awata, A. *Org. Biomol. Chem.* **2016**, *14*, 1831–1839.
6. Examples of an epimerization strategy: (a) Cheng, F.; Kalita, S. J.; Zhao, Z.-N.; Yang, X.; Zhao, Y.; Schneider, U.; Shibata, N.; Huang, Y.-Y. *Angew. Chem. Int. Ed.* **2019**, *58*, 16637–16643. (b) Kalita, S. J.; Cheng, F.; Fan, Q.-H.; Shibata, N.; Huang, Y.-Y. *J. Org. Chem.* **2021**, *86*, 8695–8705.
7. Other examples of 2,5-*trans* selective asymmetric (3+2) cycloaddition: (a) Li, Q.-H.; Wei, L.; Chen, X.; Wang, C.-J. *Chem. Commun.* **2013**, *49*, 6277–6279. (b) Awata, A.;

- Arai, T. *Angew. Chem. Int. Ed.* **2014**, *53*, 10462–10465. (c) Wei, L.; Li, Q.-H.; Wang, C.-J. *J. Org. Chem.* **2018**, *83*, 11814–11824.
8. Selected recent example by the thermal reaction: (a) Selva, V.; Selva, E.; Merino, P.; Nájera, C.; Sansano, J. M. *Org. Lett.* **2018**, *20*, 3522–3526. (b) Taha, A. G.; Elboray, E. E.; Kobayashi, Y.; Furuta, T.; Abbas-Temirek, H. H.; Aly, M. F. *J. Org. Chem.* **2021**, *86*, 547–558. (c) Belabbes, A.; Retamosa, M. G.; Foubelo, F.; Sirvent, A.; Nájera, C. Yus, M.; Sansano, J. M. *Org. Biomol. Chem.* **2023**, *21*, 1927–1936. (d) Radwan, M.; Elboray, E. E.; Dardeer, H. M.; Kobayashi, Y.; Furuta, T.; Hamada, S.; Dohi, T.; Aly, M. F. *Chem. Asian J.* **2023**, *18*, e202300215.
9. Furuya, S.; Kanemoto, K.; Fukuzawa, S.-i. *Chem. Asian J.* **2022**, *17*, e202200239.
10. Torán, R.; Miguélez, R.; Sanz-Marco, A.; Vila, C.; Pedro, J. R.; Blay, G. *Adv. Synth. Catal.* **2021**, *363*, 5196–5234.
11. Silva, A. F.; Fernandes, A. A. G.; Thurow, S.; Stivanin, M. L.; Jurberg, I. D. *Synthesis*, **2018**, *50*, 2473–2458.
12. (a) Capreti, N. M. R.; Jurberg, I. D. *Org. Lett.* **2015**, *17*, 2490–2493. (b) Rieckhoff, S.; Hellmuth, T.; Peters, R. *J. Org. Chem.* **2015**, *80*, 6822–6830. (c) Christodoulou, M. S.; Giofrè, S.; Beccalli, E. M.; Foschi, F.; Broggin, G. *Org. Lett.* **2020**, *22*, 2735–2739. (d) Wang, Y.; Du, D.-M. *J. Org. Chem.* **2020**, *85*, 15325–15336.
13. (a) Liu, T.-L.; He, Z.-L.; Tao, H.-Y.; Wang, C.-J. *Chem. Eur. J.* **2012**, *18*, 8042–8046. (b) Li, Q.-H.; Liu, T.-L.; Wei, L.; Zhou, X.; Tao, H.-Y.; Wang, C.-J. *Chem. Commun.* **2013**, *49*, 9642–9644. (c) Cayuelas, A.; Ortiz, R.; Nájera, C.; Sansano, J. M.; Larraña, O.; de Cózar, A.; Cossío, F. P.; *Org. Lett.* **2016**, *18*, 2926–2929.
14. (a) Hernández-Toribio, J.; Arrayás, R. G.; Martín-Matute, B.; Carretero, J. C. *Org. Lett.* **2009**, *11*, 393–396. (b) Oura, I.; Shimizu, K.; Ogata, K.; Fukuzawa, S.-i. *Org. Lett.* **2010**, *12*, 1752–1755.
15. Selected examples of the biologically active 2,5-*trans* pyrrolidines: (a) Maring, C. J.; Stoll, V. S.; Zhao, C.; Sun, M.; Krueger, A. C. Stewart, K. D.; Madigan, D. L.; Kati, W. M.; Xu, Y.; Carrick, R. J.; Montgomery, D. A.; Kempf-Grote, A.; Marsh, K. C.; Molla, A.; Steffy, K. R.; Sham, H. L.; Laver, W. G.; Gu, Y.-g.; Kempf, D. J.;

- Kohlbrenner, W. E. *J. Med. Chem.* **2005**, *48*, 3980–3990. (b) Ding, Q.; Zhang, Z.; Liu, J.-J.; Jiang, N.; Zhang, J.; Ross, T. M.; Chu, X. J.; Bartkovitz, D.; Podlaski, F.; Janson, C.; Tovar, C.; Filipovic, Z. M.; Higgins, B.; Glenn, K.; Packman, K.; Vassilev, L. T.; Graves, B. *J. Med. Chem.* **2013**, *56*, 5979–5983.
16. Selected recent examples of the mechanistic study: (a) Pascual-Escudero, A.; de Cózar, A.; Cossío, F. P.; Adrio, J.; Carretero, J. C. *Angew. Chem. Int. Ed.* **2016**, *55*, 15334–15338. (b) Caleffi, G. S.; Larrañaga, O.; Ferrándiz-Saperas, M.; Costa, P. R. R.; Nájera, C.; de Cózar, A.; Cossío, F. P.; Sansano, J. M. *J. Org. Chem.* **2019**, *84*, 10593–10605. (c) Chang, X.; Yang, Y.; Shen, C.; Xue, K.-S.; Wang, Z.-F.; Cong, H.; Tao, H.-Y.; Chung, L. W.; Wang, C.-J. *J. Am. Chem. Soc.* **2021**, *143*, 3519–3535. (d) Chang, X.; Liu, X.-T.; Li, F.; Yang, Y.; Chung, L. W.; Wang, C.-J. *Chem. Sci.* **2023**, *14*, 5460–5469.
17. Wu, Y.; Liu, H.; Zhang, L.; Sun, Z.; Xiao, Y.; Huang, J.; Wang, M.; Guo, H. *RSC Adv.* **2016**, *6*, 73547–73550.
18. (a) Capreti, N. M. R.; Jurberg, I. D. *Org. Lett.* **2015**, *17*, 2490–2493. (b) Martínez-Pardo, P.; Laviós, A.; Sanz-Marco, A.; Vila, C.; Pedro, J. R.; Blay, G. *Adv. Synth. Catal.* **2020**, *362*, 3564–3569.
19. Liu, Y.-W.; Li, L.-J.; Xu, H.; Dai, H.-X. *J. Org. Chem.* **2022**, *87*, 6807–6811.

Chapter 5

Copper-Catalyzed Asymmetric (3+2)

Cycloaddition of Imino Lactones

with Ylidene-pyrazolones

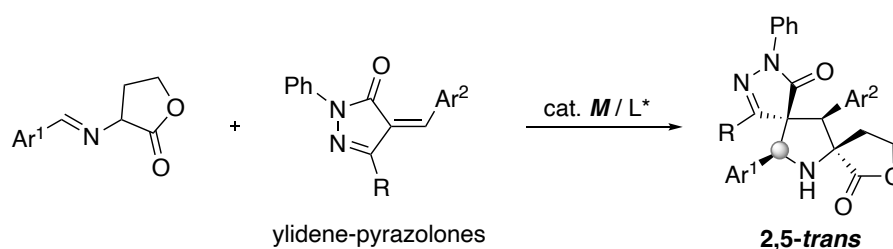
5-1. Introduction

The metal complex-catalyzed 1,3-DC of imino esters with activated olefins is a robust method for stereodivergent preparation of pyrrolidines.¹ Indeed, chiral copper and silver complexes have been developed by many research groups, enabling access to *endo/exo*-diastereomers stereodivergently. However, the *2,5-trans* configuration in *endo/exo'*-adducts is still difficult because the generated azomethine ylides are in the *cis*-conformation. To address this issue, a nickel catalyst-controlled strategy that enables access to *exo'*-adducts via stepwise addition/cyclization with bond rotation was proposed by Arai and co-workers.² Huang and co-workers also developed an epimerization strategy; the common *2,5-cis* selective formation of a pyrrolidine ring and subsequent base-promoted epimerization enabled access to the *2,5-trans* adducts.³ However, useful methods have rarely been reported except for these pioneering works, and a new methodology is desired for preparing *2,5-trans* pyrrolidines.^{4,5}

Our research group has engaged in the development of metal complex-catalyzed asymmetric (3+2) cycloaddition of imino esters with activated olefins bearing heterocyclic moieties.⁶ This process revealed that the (3+2) cycloaddition proceeds with *2,5-trans* diastereoselectivity when ylidene-heterocycles⁷ were employed.⁸ For example, the reaction of imino lactones with ylidene-isoxazolones to afford the *2,5-trans* pyrrolidines as a single diastereomer was previously accomplished by the author and co-workers, and a chiral silver complex was efficient for the enantioselective synthesis (Chapter 4).^{8b}

The author here focused on pyrazolone rings⁹ which are frequently found in biologically active compounds¹⁰ and whose structure is similar to isoxazolones. Currently, ylidene-pyrazolones are frequently used as suitable Michael acceptors in the asymmetric cycloaddition for constructing spiropyrazolone scaffolds.¹¹ For example, Cai and co-workers previously reported the organocatalytic reaction of imino lactones with ylidene-pyrazolones.¹² Interestingly, it was shown that the rare *2,5-trans* cycloadducts were

formed, not the common *2,5-cis* adducts. In this work, the author engaged in the asymmetric (3+2) cycloaddition using ylidene-pyrazolones as the dipolarophiles, which was catalyzed by a metal complex catalyst (Scheme 5-1). As a result, the reaction proceeded with high *2,5-trans* diastereoselectivity when imino lactones were employed as the azomethine ylide precursors. In addition, a copper/Fesulphos catalyst was shown to be the most suitable for the enantioselective synthesis. These results suggest that the rare *2,5-trans* diastereoselectivity depended on the heterocyclic structure, not the catalyst used.



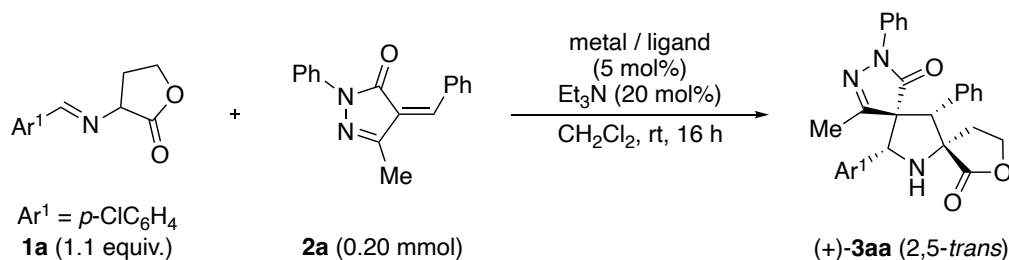
Scheme 5-1. This work: metal-catalyzed *2,5-trans* selective (3+2) cycloaddition using ylidene-pyrazolones.

5-2. Results and Discussion

The author carried out the asymmetric (3+2) cycloaddition of imino lactones **1a** with ylidene-pyrazolones **2a** in the presence of $[\text{Cu}(\text{MeCN})_4]\text{BF}_4$ (5.0 mol%), PPh_3 (5.5 mol%), and Et_3N (20 mol%) in CH_2Cl_2 at room temperature as an initial experiment. The reaction smoothly gave the corresponding cycloadducts as an almost single diastereomer with a high yield. To reveal the diastereoselectivity, 2-thienyl-substituted spiropyrrolidines *rac*-**3ja** were prepared by the reaction using imino lactones **1j** under the same conditions, and the ^1H NMR spectrum of the product *rac*-**3ja** was compared to the previous report.¹² It was revealed that the same *2,5-trans* adducts were obtained under the copper complex-catalyzed condition. On the other hand, low diastereoselectivity resulted when acyclic imino esters derived from glycine or alanine were applied to the reaction as the azomethine ylide precursors. Based on these initial experiments, the author decided

to investigate the 2,5-*trans* selective asymmetric reaction of imino lactones with ylidene-pyrazolones by using the chiral metal complex catalyst.

Table 5-1. Screening of several metal complex catalyst.^a



entry	metal / ligand	yield (%) ^b	dr (%) ^c	ee (%) ^d
1	[Cu(MeCN) ₄]BF ₄ / L1	quant.	15:1	80
2	[Cu(MeCN) ₄]BF ₄ / L2	quant.	13:1	30
3	[Cu(MeCN) ₄]BF ₄ / L3	97	15:1	18
4	[Cu(MeCN) ₄]BF ₄ / L4	quant.	15:1	74
5	AgOAc / L1	97	17:1	40
6	AgOAc / L2	94	15:1	50
7	AgOAc / L3	95	14:1	48
8	AgOAc / L4	99	18:1	68
9 ^e	[Cu(MeCN) ₄]BF ₄ / L1	93	15:1	-83

[a] Condition: **1a** (0.22 mmol), **2a** (0.20 mmol), metal salt (5.0 mol%), ligand (5.5 mol%), Et₃N (20 mol%), CH₂Cl₂ (1.0 mL), rt, 16 h. [b] Combined yield. [c] Determined by crude ¹H NMR. [d] Determined by chiral HPLC. [e] (*S*_p)-**L1** was used instead of (*R*_p)-**L1**.

Screening of several chiral metal complexes was carried out next. The results are summarized in Table 5-1 and the ligands adopted in this investigation are shown in Figure 5-1. The copper/Fesulphos complex was shown to be the most effective for the enantioselective cycloaddition to give the desired spiropyrazolones (+)-**3aa** with 15:1 dr and 80% ee (Table 5-1, entry 1). When TCF **L2** and FcPHOX **L3** were used under the copper-catalyzed condition, the enantioselectivity was significantly decreased (entries 2, 3). The use of DTBM-Segphos **L4** resulted in good enantioselectivity, but it was not

superior to Fesulphos **L1**. Although the silver complex-catalyzed conditions were also investigated, the enantioselectivity was not increased (entries 5-8). Also, when (*S_p*)-Fesulphos, the enantiomer of (*R_p*)-Fesulphos **L1**, was used under the copper-catalyzed condition, the corresponding enantiomers (–)-**3aa** were smoothly formed with almost the same enantioselectivity (entry 9).

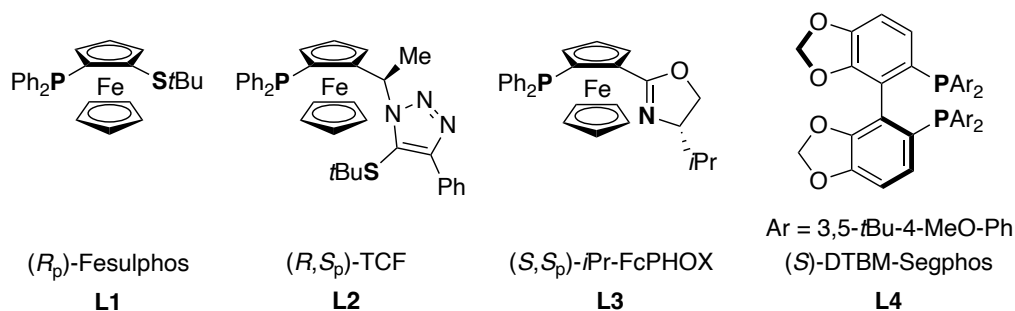
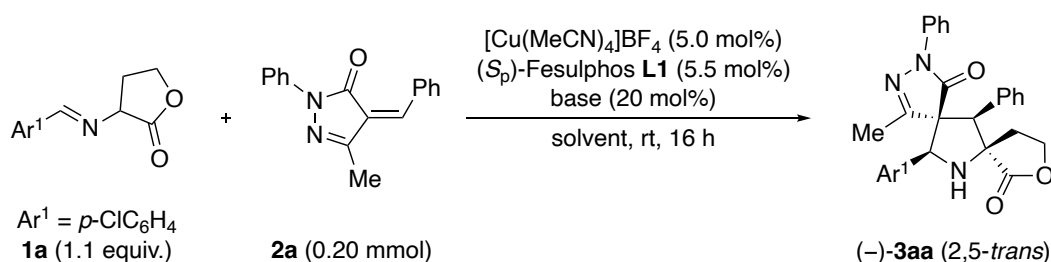


Figure 5-1. Chiral ligands employed in this study.

The optimization study was performed after screening metal complex catalysts, and Table 5-2 summarizes the results. Although several solvents such as THF, Et₂O, MTBE, and toluene were first screened (entries 1-5), CH₂Cl₂ was shown to be the most suitable for the asymmetric reaction (entry 1). Furthermore, screening of additives (bases) revealed that the addition of base affected the enantioselectivity (entries 6-9). For example, the use of DBU largely decreased the enantioselectivity (entry 7). While the reaction without the addition of base improved the enantioselectivity, the cycloadducts (–)-**3aa** were afforded with 94% ee (entry 9). The reaction temperature also had an impact on the enantioselectivity; it increased to 99% ee when the reaction was conducted at 0 °C (entry 10).

Table 5-2. Optimization of the reaction conditions.^a

entry	solvent	base	yield (%) ^b	dr ^c	ee (%) ^d
1	CH ₂ Cl ₂	Et ₃ N	93	15:1	83
2	THF	Et ₃ N	91	12:1	50
3	Et ₂ O	Et ₃ N	90	10:1	77
4	MTBE	Et ₃ N	quant.	18:1	75
5	toluene	Et ₃ N	96	15:1	65
6	CH ₂ Cl ₂	DIPEA	89	>20:1	67
7	CH ₂ Cl ₂	DBU	80	17:1	13
8	CH ₂ Cl ₂	K ₂ CO ₃	89	17:1	61
9	CH ₂ Cl ₂	none	97	>20:1	94
10 ^e	CH ₂ Cl ₂	none	98	>20:1	99

[a] Condition: **1a** (0.22 mmol), **2a** (0.20 mmol), [Cu(MeCN)₄]BF₄ (5.0 mol%), (S_p)-**L1** (5.5 mol%), base (20 mol%), solvent (1.0 mL), rt, 16 h. [b] Combined yield. [c] Determined by crude ¹H NMR. [d] Determined by chiral HPLC. [e] Conducted at 0°C.

The substrate scope was investigated under the optimal conditions, and various imino lactones **1** could be applied to the copper complex-catalyzed asymmetric (3+2) cycloaddition (Figure 5-2). Imino lactones bearing phenyl, *para*-bromophenyl, and *meta*-chlorophenyl groups gave nearly single 2,5-*trans* diastereomers **3ba**, **3ca**, and **3da** with high enantioselectivity, respectively. However, the methyl group on the phenyl group of imino lactones **1** affected the diastereoselectivity. Although the *meta*- and *para*-methyl substituted cycloadducts **3ea** and **3fa** were produced with excellent stereoselectivity, the *ortho*-methyl substituted one was produced as a mixture of multiple diastereomers and

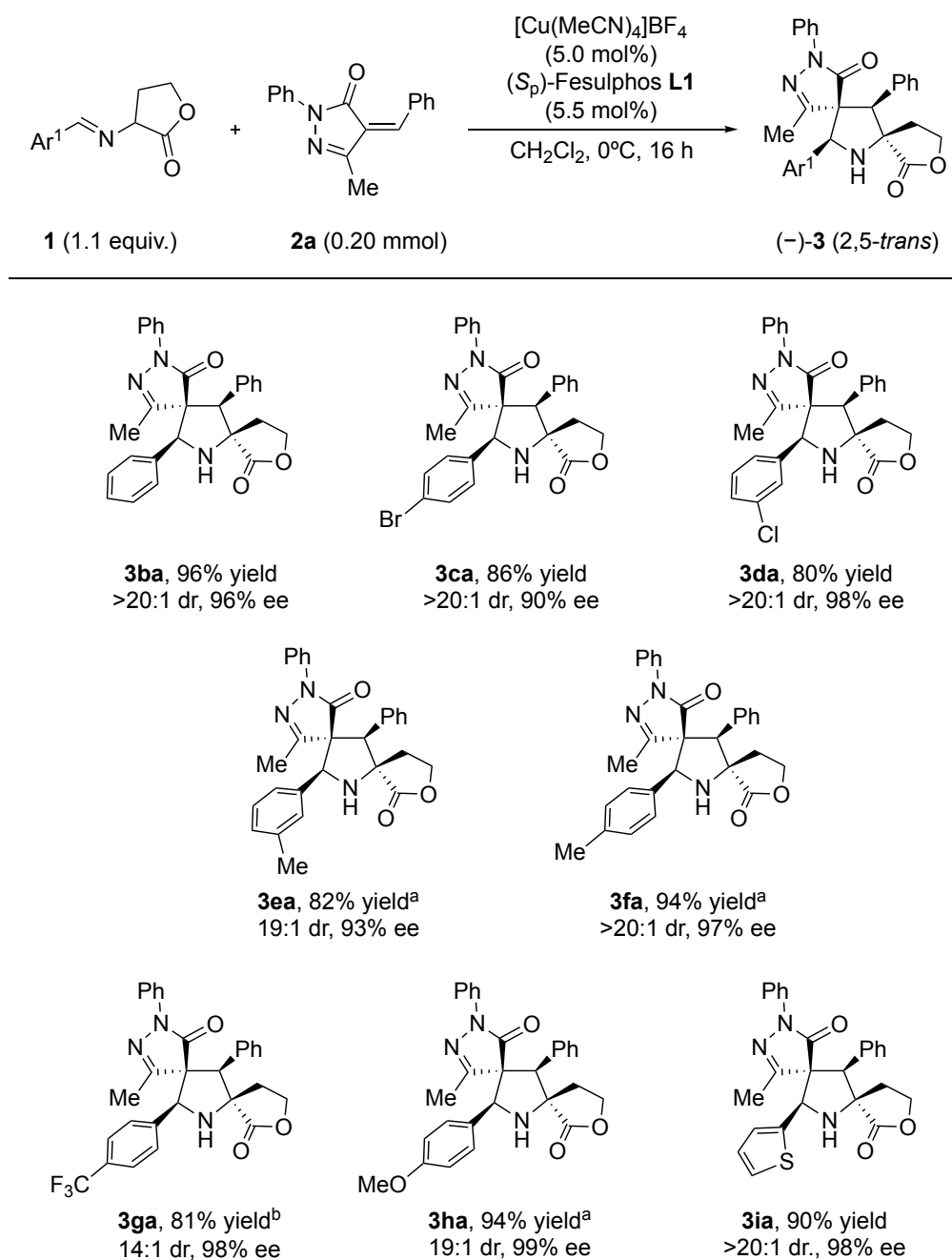


Figure 5-1. Scope of imino lactones **1**. [a] 3Å MS (100 mg) was added. [b] 1.5 equiv. of imino lactones **1h** was used.

could not be isolated. Although a *para*-CF₃ phenyl group of the imino lactones slightly decreased the reactivity, the enantioselectivity maintained an excellent value of 98% ee. The electron-donating *para*-MeO substituent could also be used in the reaction to give the spiropyrrolidines **3ha** with excellent enantioselectivity. The 2-thienyl substituted

pyrrolidines **3ia** were successfully obtained under this metal-catalyzed condition as well as under the previous organocatalytic condition.¹²

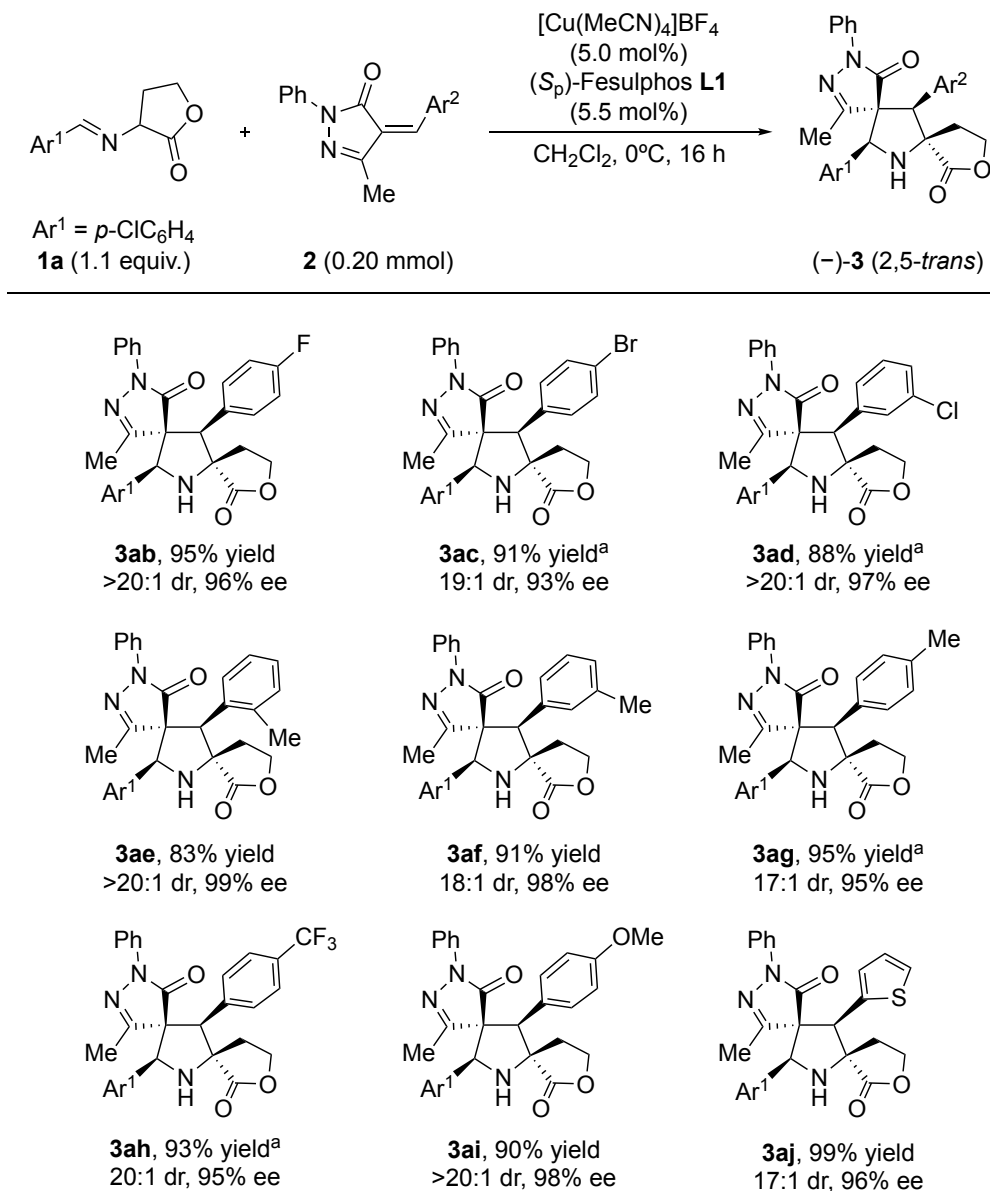


Figure 5-2. Scope of ylidene-pyrazolones **2**. [a] 3 Å MS (100 mg) was added.

The scope of ylidene-pyrazolones **2** was investigated under the optimal conditions, and a wide range of substrates was successfully applied to the stereoselective reaction (Figure 5-3). The reaction of ylidene-pyrazolones bearing the *para*-fluoro, -bromo, and *meta*-chloro substituents on the phenyl group gave the corresponding products **3ab**, **3ac**, and **3ad** with excellent enantioselectivity, respectively. The position of the substituents

had little impact on the yield and stereoselectivity compared to imino lactones **1**, and the *ortho*-, *meta*-, and *para*-methyl substituted products **3ae**, **3af**, and **3ag** were obtained with excellent %ee values. The electronic nature of the substituents had little effect on the results with *para*-CF₃ and *para*-MeO phenyl substituted products **3ah** and **3ai**, which were obtained with excellent stereoselectivities. In addition, the 2-thiophene group could be introduced under the optimized reaction conditions, affording the product **3aj** with 96% ee.

5-3. Conclusion

In conclusion, the author developed a copper complex-catalyzed asymmetric (3+2) cycloaddition of imino lactones with ylidene-pyrazolones. The reaction catalyzed by a copper/Fesulphos catalyst proceeded with high 2,5-*trans* diastereoselectivity and excellent enantioselectivity. Furthermore, a wide range of substrates was successfully applied to the reaction, and the spiro-pyrazolones bearing various substituents could be obtained under the optimal reaction conditions. The rare 2,5-*trans* diastereoselectivity exhibited a similar trend to the previous organocatalyzed reaction reported by Cai and co-workers,¹² and our previous silver-catalyzed reaction of ylidene-isoxazolones^{8b} also showed the same results. Therefore, the diastereoselectivity is thought to largely depend on the ylidene-heterocycles which are the reaction substrates, not the catalyst.

5-4. Experimental Section

The general information was described in the Experimental Section of Chapter 2.

Unless otherwise stated, all reactions were carried out with oven-dried glassware under atmosphere of nitrogen. with oven-dried glassware. Starting materials, ylidene-pyrazolones **2** were prepared and identified by reported methods.¹³ Racemic products of **3** were prepared using PPh₃ (5.5 mol%) as the ligand. All other chemical reagents used commercial grade and used as received.

Copper-Catalyzed Asymmetric (3+2) Cycloaddition of Imino Lactones 1 with Ylidene-Pyrazolones 2. A mixture of $[\text{Cu}(\text{MeCN})_4]\text{BF}_4$ (3.2 mg, 10 μmol , 5.0 mol%) and (*S_p*)-*Fesulphos* L1 (5.0 mg, 11 μmol , 5.5 mol%) was dissolved in dry CH_2Cl_2 (1.0 mL) and 3Å MS (100 mg) was added to the mixture at room temperature. After stirring for 30 minutes, the mixture was cooled to 0°C. Then, imino lactones **1a** (49.2 mg, 0.22 mmol, 1.10 equiv.) and ylidene-pyrazolones **2a** (52.5 mg, 0.20 mmol, 1.00 equiv.). After stirring for 16 h at the same temperature, EtOAc (30 mL) was added to the mixture. Then, the mixture was filtered through a short Celite pad and concentrated under reduced pressure. ^1H NMR analysis of the crude product showed that the corresponding cycloadduct was the sole product. The residue was purified by silica gel column chromatography (20 g, *n*-hexane/EtOAc = 2/1) to afford (*5S,6R,7R,13S*)-13-(4-chlorophenyl)-4-methyl-2,6-diphenyl-9-oxa-2,3,12-triazadispiro[4.1.4⁷.2⁵]tridec-3-ene-1,8-dione (**3aa**) (96.2 mg, 0.198 mmol, 98.4%, >20:1 dr, 99% ee) as a white solid.

(5S,6R,7R,13S)-13-(4-chlorophenyl)-4-methyl-2,6-diphenyl-9-oxa-2,3,12-triazadispiro[4.1.4⁷.2⁵]tridec-3-ene-1,8-dione (3aa). (96.2 mg, 0.198 mmol, 98.4%, >20:1 dr, 99% ee); white solid; mp 82–85 °C; ^1H NMR (400 MHz, CDCl_3): δ 7.42–7.40 (m, 2H), 7.32–7.24 (m, 9H), 7.19–7.14 (m, 3H), 4.88 (br s, 1H), 4.58 (s, 1H), 4.40 (dt, 1H, $J = 8.9, 6.5$ Hz), 3.97 (dt, 1H, $J = 8.5, 3.3$ Hz), 2.63 (ddd, 1H, $J = 14.0, 6.5, 3.4$ Hz), 2.47–2.40 (m, 1H), 2.33 (s, 3H); ^{13}C NMR (101 MHz, CDCl_3): δ 179.5, 171.8, 158.6, 137.0, 134.6, 133.2, 132.4, 129.5, 129.3, 128.9, 128.8, 128.7, 127.7, 126.0, 119.9, 70.7, 67.4, 67.2, 66.2, 58.5, 34.7, 14.0; HPLC (Daicel Chiralpak IC-3, *n*-hexane/EtOAc = 90/10, 1.0 mL/min, 254 nm); $t_{\text{R}} = 17.8$ min (major), 60.3 min (minor); $[\alpha]_{\text{D}}^{25} -117.54$ (c 0.05, CHCl_3); HRMS (ESI) m/z : $[\text{M}+\text{Na}]^+$ Calcd for $\text{C}_{28}\text{H}_{24}^{35}\text{ClN}_3\text{NaO}_3^+$, 508.1398; found 508.1420.

(5S,6R,7R,13S)-4-methyl-2,6,13-triphenyl-9-oxa-2,3,12-triazadispiro[4.1.4⁷.2⁵]tridec-3-ene-1,8-dione (3ba). (87.4 mg, 0.194 mmol, 95.5%, >20:1 dr, 96% ee); white solid; mp 91–93 °C; ^1H NMR (400 MHz, CDCl_3): δ 7.39–7.36 (m, 2H), 7.29–7.22 (m, 12H), 7.15–7.11 (m, 1H), 4.90 (s, 1H), 4.61 (s, 1H), 4.42 (dt, 1H, $J = 9.0, 6.5$ Hz), 4.00 (dt, 1H, $J =$

8.6, 3.0 Hz), 2.65 (ddd, 1H, $J = 14.0, 6.5, 3.1$ Hz), 2.45–2.37 (m, 1H), 2.34 (s, 3H); ^{13}C NMR (101 MHz, CDCl_3): δ 179.5, 172.0, 158.8, 137.1, 133.50, 133.45, 129.5, 129.3, 128.8 (two peaks overlapped), 128.6, (two peaks overlapped), 126.2, 125.8, 120.0 (two peaks overlapped), 71.1, 68.1, 67.4, 66.2, 58.4, 34.8, 14.1; HPLC (Daicel Chiralpak IC-3, *n*-hexane/2-propanol = 80/20, 1.0 mL/min, 254 nm); $t_{\text{R}} = 12.6$ min (major), 18.2 min (minor); $[\alpha]_{\text{D}}^{25} -120.27$ (c 0.05, CHCl_3); HRMS (ESI) m/z : $[\text{M}+\text{Na}]^+$ Calcd for $\text{C}_{28}\text{H}_{25}\text{N}_3\text{NaO}_3^+$, 474.1788; found 474.1798.

(5S,6R,7R,13S)-13-(4-bromophenyl)-4-methyl-2,6-diphenyl-9-oxa-2,3,12-triazadispiro[4.1.4⁷.2⁵]tridec-3-ene-1,8-dione (3ca). (92.0 mg, 0.173 mmol, 86.4%, >20:1 dr, 90% ee); white solid; mp 86–90 °C; ^1H NMR (400 MHz, CDCl_3): δ 7.42–7.39 (m, 4H), 7.32–7.22 (m, 7H), 7.18–7.11 (m, 3H), 4.86 (s, 1H), 4.57 (s, 1H), 4.40 (dt, 1H, $J = 8.9, 6.6$ Hz), 3.97 (dt, 1H, $J = 8.5, 3.2$ Hz), 2.63 (ddd, 1H, $J = 14.0, 6.5, 3.3$ Hz), 2.47–2.39 (m, 1H), 2.33 (s 3H); ^{13}C NMR (101 MHz, CDCl_3): 179.5, 171.8, 158.6, 137.0, 133.2, 132.9, 131.8, 129.5, 129.3, 128.9, 128.7, 128.0, 126.0, 122.8, 119.9, 70.7, 67.4, 67.2, 66.2, 58.5, 34.7, 14.0; HPLC (Daicel Chiralpak IC-3, *n*-hexane/EtOAc = 90/10, 1.0 mL/min, 254 nm); $t_{\text{R}} = 22.5$ min (major), 84.7 min (minor); $[\alpha]_{\text{D}}^{25} -107.16$ (c 0.05, CHCl_3); HRMS (ESI) m/z : $[\text{M}+\text{Na}]^+$ Calcd for $\text{C}_{28}\text{H}_{24}^{79}\text{BrN}_3\text{NaO}_3^+$, 552.0893; found 552.0899.

(5S,6R,7R,13S)-13-(3-chlorophenyl)-4-methyl-2,6-diphenyl-9-oxa-2,3,12-triazadispiro[4.1.4⁷.2⁵]tridec-3-ene-1,8-dione (3da). (78.0 mg, 0.161 mmol, 80.4%, >20:1 dr, 98% ee); white solid; mp 78–82 °C; ^1H NMR (400 MHz, CDCl_3): δ 7.43–7.40 (m, 2H), 7.32–7.22 (m, 9H), 7.21–7.08 (m, 3H), 4.87 (s, 1H), 4.57 (s, 1H), 4.41 (dt, 1H, $J = 8.9, 6.5$ Hz), 3.98 (dt, 1H, $J = 8.5, 3.2$ Hz), 2.64 (ddd, 1H, 14.0, 6.5, 3.2 Hz), 2.47–2.39 (m, 1H), 2.34 (s, 3H); ^{13}C NMR (101 MHz, CDCl_3): δ 179.5, 171.8, 158.6, 137.0, 136.0, 134.6, 133.2, 129.9, 129.5, 129.3, 129.0, 128.9, 128.7, 126.6, 126.0, 124.5, 119.9, 70.7, 67.4, 67.1, 66.2, 58.4, 34.8, 14.0; HPLC (Daicel Chiralpak IC-3, *n*-hexane/EtOAc = 90/10, 1.0 mL/min, 250 nm); $t_{\text{R}} = 18.6$ min (major), 50.7 min (minor); $[\alpha]_{\text{D}}^{25} -137.31$ (c 0.05, CHCl_3); HRMS (ESI) m/z : $[\text{M}+\text{Na}]^+$ Calcd for $\text{C}_{28}\text{H}_{24}^{35}\text{ClN}_3\text{NaO}_3^+$, 508.1398; found 508.1413.

(5S,6R,7R,13S)-4-methyl-2,6-diphenyl-13-(*m*-tolyl)-9-oxa-2,3,12-triazadispiro[4.1.4⁷.2⁵]tridec-3-ene-1,8-dione (3ea). (76.4 mg, 0.164 mmol, 81.6%, 19:1 dr, 93% ee); white solid; mp 78–80 °C; ¹H NMR (400 MHz, CDCl₃): δ 7.42–7.39 (m, 2H), 7.30–7.26 (m, 7H), 7.14 (t, 2H, *J* = 7.4 Hz), 7.06–7.00 (m, 3H), 4.85 (s, 1H), 4.60 (s, 1H), 4.42 (dt, 1H, *J* = 9.0, 6.4 Hz), 4.02 (dt, 1H, *J* = 8.6, 2.8 Hz), 2.65 (ddd, 1H, *J* = 14.0, 6.3, 2.9 Hz), 2.44–2.38 (m, 1H), 2.33 (s, 3H), 2.26 (s, 3H); ¹³C NMR (101 MHz, CDCl₃): δ 179.5, 172.1, 158.9, 138.3, 137.1, 133.6, 133.4, 129.6, 129.5, 129.3, 128.8, 128.6, 128.5, 126.9, 125.8, 123.4, 120.0, 71.0, 68.2, 67.4, 66.1, 58.3, 34.8, 21.5, 14.1; HPLC (Daicel Chiralpak IC-3, *n*-hexane/2-propanol = 80/20, 1.0 mL/min, 210 nm); *t*_R = 10.5 min (major), 13.9 min (minor); [α]_D²⁵ -118.22 (*c* 0.05, CHCl₃); HRMS (ESI) *m/z*: [M+Na]⁺ Calcd for C₂₉H₂₇N₃NaO₃⁺, 488.1945; found 488.1935.

(5S,6R,7R,13S)-4-methyl-2,6-diphenyl-13-(*p*-tolyl)-9-oxa-2,3,12-triazadispiro[4.1.4⁷.2⁵]tridec-3-ene-1,8-dione (3fa). (86.8 mg, 0.186 mmol, 94.1%, >20:1 dr, 97% ee); white solid; mp 85–88 °C; ¹H NMR (400 MHz, CDCl₃): δ 7.43–7.40 (m, 2H), 7.33–7.25 (m, 7H), 7.16–7.10 (m, 3H), 7.03 (d, 2H, *J* = 8.1 Hz), 4.86 (s, 1H), 4.60 (s, 1H), 4.41 (dt, 1H, *J* = 9.0, 6.4 Hz), 4.01 (dt, 1H, *J* = 8.6, 2.8 Hz), 2.64 (ddd, 1H, *J* = 13.9, 6.3, 2.9 Hz), 2.45–2.38 (m, 1H), 2.32 (s, 3H), 2.24 (s, 3H); ¹³C NMR (101 MHz, CDCl₃): δ 179.5, 172.1, 158.9, 138.6, 137.2, 133.6, 130.4, 129.5, 129.28, 129.26, 128.8, 128.5, 126.1, 125.8, 120.0, 71.1, 68.1, 67.4, 66.1, 58.4, 34.8, 21.1, 14.0; HPLC (Daicel Chiralpak IC-3, *n*-hexane/EtAOc = 90/10, 1.0 mL/min, 254 nm); *t*_R = 18.7 min (major), 45.6 min (minor); [α]_D²⁵ -107.05 (*c* 0.05, CHCl₃); HRMS (ESI) *m/z*: [M+Na]⁺ Calcd for C₂₉H₂₇N₃NaO₃⁺, 488.1945; found 488.1943.

(5S,6R,7R,13S)-4-methyl-2,6-diphenyl-13-(4-(trifluoromethyl)phenyl)-9-oxa-2,3,12-triazadispiro[4.1.4⁷.2⁵]tridec-3-ene-1,8-dione (3ga). (85.4 mg, 0.164 mmol, 80.7%, 14:1 dr, 98% ee); white solid; mp 78–81 °C; ¹H NMR (400 MHz, CDCl₃): δ 7.53 (d, 2H, *J* = 8.2 Hz), 7.37 (d, 2H, *J* = 8.4 Hz), 7.34–7.32 (m, 2H), 7.30–7.25 (m, 7H), 7.17–7.12 (m, 1H), 4.96 (s, 1H), 4.59 (s, 1H), 4.41 (dt, 1H, *J* = 8.5, 6.6 Hz), 3.97 (dt, 1H, *J* = 8.6, 3.4 Hz), 2.64 (ddd, 1H, *J* = 14.0, 6.5, 3.4 Hz), 2.50–2.43 (m, 1H), 2.36 (s, 3H); ¹³C NMR (101

MHz, CDCl₃): δ 179.5, 171.7, 158.5, 138.0, 136.9, 133.0, 130.9 (q, J_{C-F} = 32.6 Hz), 129.5, 129.4, 128.9, 128.8, 126.8, 126.1, 125.6 (q, J_{C-F} = 3.6 Hz), 123.8 (q, J_{C-F} = 272 Hz), 120.0, 70.7, 67.4, 67.1, 66.2, 58.5, 34.8, 14.1; HPLC (Daicel Chiralpak IC-3, *n*-hexane/EtOAc = 90/10, 1.0 mL/min, 254 nm); t_R = 11.3 min (major), 49.4 min (minor); $[\alpha]_D^{25}$ -105.15 (*c* 0.05, CHCl₃); HRMS (ESI) m/z : $[M+Na]^+$ Calcd for C₂₉H₂₄N₃NaO₃F₃⁺, 542.1662; found 542.1646.

(5*S*,6*R*,7*R*,13*S*)-13-(4-methoxyphenyl)-4-methyl-2,6-diphenyl-9-oxa-2,3,12-triazadispiro[4.1.4⁷.2⁵]tridec-3-ene-1,8-dione (3ha). (89.8 mg, 0.187 mmol, 93.9%, 19:1 dr, 99% ee); white solid; mp 87-90 °C; ¹H NMR (400 MHz, CDCl₃): δ 7.45–7.42 (m, 2H), 7.31–7.25 (m, 7H), 7.18–7.12 (m, 3H), 6.79 (d, 2H, J = 8.8 Hz), 4.84 (s, 1H), 4.59 (s, 1H), 4.41 (dt, 1H, J = 9.0, 6.4 Hz), 4.00 (dt, 1H, J = 8.6, 2.9 Hz), 3.72 (s, 3H), 2.64 (ddd, 1H, J = 14.0, 6.4, 3.0 Hz), 2.44–2.36 (m, 1H), 2.31 (s, 3H); ¹³C NMR (101 MHz, CDCl₃): δ 179.5, 172.2, 159.8, 158.9, 137.2, 133.6, 129.5, 129.3, 128.8, 128.5, 127.5, 125.8, 125.5, 119.9, 114.0, 71.1, 67.9, 67.4, 66.1, 58.3, 55.3, 34.8, 14.0; HPLC (Daicel Chiralpak IC-3, *n*-hexane/EtOAc = 90/10, 1.0 mL/min, 254 nm); t_R = 43.9 min (major), 76.3 min (minor); $[\alpha]_D^{25}$ -108.74 (*c* 0.05, CHCl₃); HRMS (ESI) m/z : $[M+Na]^+$ Calcd for C₂₉H₂₇N₃NaO₄⁺, 504.1894; found 504.1906.

(5*S*,6*R*,7*R*,13*S*)-4-methyl-2,6-diphenyl-13-(thiophen-2-yl)-9-oxa-2,3,12-triazadispiro[4.1.4⁷.2⁵]tridec-3-ene-1,8-dione (3ia). (82.5 mg, 0.180 mmol, 90.2%, >20:1 dr, 98% ee); white solid; mp 176–178 °C; ¹H NMR (400 MHz, CDCl₃): δ 7.57–7.55 (m, 2H), 7.35–7.31 (m, 2H), 7.28–7.23 (m, 5H), 7.19–7.15 (m, 2H), 6.96 (d, 1H, J = 3.5 Hz), 6.89 (dd, 1H, J = 5.0, 3.6 Hz), 5.06 (s, 1H), 4.58 (s, 1H), 4.41 (dt, 1H, J = 9.1, 6.3 Hz), 4.02 (dt, 1H, J = 8.6, 2.7 Hz), 3.88 (br s, 1H), 2.63 (ddd, 1H, J = 14.0, 6.3, 2.7 Hz), 2.41–2.33 (m, 1H), 2.29 (s, 3H); ¹³C NMR (101 MHz, CDCl₃): δ 179.2, 172.1, 158.7, 137.3, 136.2, 133.2, 129.5, 129.3, 128.9, 128.7, 127.1, 125.9, 125.5, 125.1, 119.8, 70.7, 67.6, 66.1, 64.4, 58.5, 34.6, 13.8; HPLC (Daicel Chiralpak IC-3, *n*-hexane/EtOAc = 90/10, 1.0 mL/min, 254 nm); t_R = 19.7 min (major), 36.4 min (minor); $[\alpha]_D^{25}$ -133.08 (*c* 0.05, CHCl₃); HRMS (ESI) m/z : $[M+Na]^+$ Calcd for C₂₆H₂₃N₃NaO₃S⁺, 480.1352; found

480.1365.

(5S,6R,7R,13S)-13-(4-chlorophenyl)-6-(4-fluorophenyl)-4-methyl-2-phenyl-9-oxa-2,3,12-triazadispiro[4.1.4⁷.2⁵]tridec-3-ene-1,8-dione (3ab). (94.1 mg, 0.187 mmol, 94.7%, >20:1 dr, 96% ee); white solid; mp 93–95 °C; ¹H NMR (400 MHz, CDCl₃): δ 7.41–7.39 (m, 2H), 7.31 (t, 2H, *J* = 7.4 Hz), 7.26–7.22 (m, 4H), 7.19–7.14 (m, 3H), 6.96 (t, 2H, *J* = 8.6 Hz), 4.85 (s, 1H), 4.57 (s, 1H), 4.46–4.40 (m, 1H), 4.05 (dt, 1H, *J* = 8.5, 2.6 Hz), 2.64 (ddd, 1H, *J* = 13.9, 6.2, 2.8 Hz), 2.41–2.35 (m, 1H), 2.33 (s, 3H); ¹³C NMR (101 MHz, CDCl₃): δ 179.2, 171.7, 162.8 (d, *J*_{C-F} = 249 Hz), 158.5, 136.9, 134.7, 132.3, 131.4 (d, *J*_{C-F} = 8.0 Hz), 129.0 (d, *J*_{C-F} = 3.2 Hz), 128.93, 128.85, 127.7, 126.1, 119.8, 116.3 (d, *J*_{C-F} = 21.4 Hz), 71.0, 67.3, 67.0, 66.2, 57.5, 34.8, 14.0; HPLC (Daicel Chiralpak IH-3, *n*-hexane/EtOAc = 90/10, 1.0 mL/min, 254 nm); *t*_R = 41.3 min (minor), 53.5 min (major); [α]_D²⁵ -101.20 (*c* 0.05, CHCl₃); HRMS (ESI) *m/z*: [M+Na]⁺ Calcd for C₂₈H₂₃³⁵ClN₃NaO₃F⁺, 526.1304; found 526.1336.

(5S,6R,7R,13S)-6-(4-fluorophenyl)-13-(4-chlorophenyl)-4-methyl-2-phenyl-9-oxa-2,3,12-triazadispiro[4.1.4⁷.2⁵]tridec-3-ene-1,8-dione (3ac). (102.7 mg, 0.182 mmol, 90.8%, 19:1 dr, 93% ee); white solid; mp 108–110 °C; ¹H NMR (400 MHz, CDCl₃): δ 7.42–7.39 (m, 4H), 7.33–7.29 (m, 2H), 7.26–7.22 (m, 2H), 7.18–7.12 (m, 5H), 4.84 (s, 1H), 4.54 (s, 1H), 4.43 (dt, 1H, *J* = 9.2, 6.3 Hz), 4.08 (dt, 1H, *J* = 8.6, 2.3 Hz), 3.74 (br s, 1H), 2.64 (ddd, 1H, *J* = 14.0, 6.3, 2.7 Hz), 2.38–2.29 (m, 1H), 2.33 (s, 3H); ¹³C NMR (101 MHz, CDCl₃): δ 179.1, 171.6, 158.4, 136.9, 134.7, 132.5, 132.3, 132.1, 131.2, 128.9, 128.9, 127.7, 126.1, 123.0, 119.8, 70.9, 67.3, 67.2, 66.2, 57.6, 34.8, 14.0; HPLC (Daicel Chiralpak IC-3, *n*-hexane/EtOAc = 90/10, 1.0 mL/min, 250 nm); *t*_R = 18.5 min (major), 58.9 min (minor); [α]_D²⁵ -100.73 (*c* 0.05, CHCl₃); HRMS (ESI) *m/z*: [M+Na]⁺ Calcd for C₂₈H₂₃⁷⁹Br³⁵ClN₃NaO₃⁺, 586.0504; found 586.0535.

(5S,6R,7R,13S)-6-(3-chlorophenyl)-13-(4-chlorophenyl)-4-methyl-2-phenyl-9-oxa-2,3,12-triazadispiro[4.1.4⁷.2⁵]tridec-3-ene-1,8-dione (3ad). (92.0 mg, 0.177 mmol, 88.1%, >20:1 dr, 97% ee); white solid; mp 95–98 °C; ¹H NMR (400 MHz, CDCl₃): δ 7.41–7.37 (m, 2H), 7.33–7.29 (m, 2H), 7.26–7.14 (m, 9H), 4.84 (s, 1H), 4.55 (s, 1H), 4.45

(dt, 1H, $J = 9.3, 6.2$ Hz), 4.13 (dt, 1H, $J = 8.7, 2.4$ Hz), 2.65 (ddd, 1H, $J = 14.0, 6.1, 2.5$ Hz), 2.38–2.30 (m, 1H), 2.34 (s, 3H); ^{13}C NMR (101 MHz, CDCl_3): δ 179.0, 171.6, 158.4, 158.4, 136.8, 135.4, 135.2, 134.7, 132.1, 130.6, 129.8, 129.0, 128.94, 128.89, 127.7, 127.6, 126.1, 120.0, 70.8, 67.3, 67.1, 66.2, 57.7, 34.8, 14.0; HPLC (Daicel Chiralpak IC-3, *n*-hexane/EtOAc = 90/10, 1.0 mL/min, 254 nm); $t_{\text{R}} = 16.1$ min (major), 60.2 min (minor); $[\alpha]_{\text{D}}^{25} -114.67$ (c 0.05, CHCl_3); HRMS (ESI) m/z : $[\text{M}+\text{Na}]^+$ Calcd for $\text{C}_{28}\text{H}_{23}^{35}\text{Cl}_2\text{N}_3\text{NaO}_3^+$, 542.1009; found 542.1031.

(5S,6R,7R,13S)-13-(4-chlorophenyl)-4-methyl-2-phenyl-6-(*o*-tolyl)-9-oxa-2,3,12-triazadispiro[4.1.4⁷.2⁵]tridec-3-ene-1,8-dione (3ae). (81.3 mg, 0.163 mmol, 83.4%, >20:1 dr, 99% ee); white solid; mp 154–157 °C; ^1H NMR (400 MHz, CDCl_3): δ 7.49 (d, 1H, $J = 7.8$ Hz), 7.40 (d, 2H, $J = 8.3$ Hz), 7.30 (t, 2H, $J = 7.6$ Hz), 7.26–7.24 (m, 2H), 7.19–7.11 (m, 5H), 7.08–7.04 (m, 1H), 4.99 (s, 1H), 4.91 (s, 1H), 4.37 (dt, 1H, $J = 8.6, 6.7$ Hz), 3.89 (dt, 1H, $J = 8.5, 3.8$ Hz), 2.57 (ddd, 1H, $J = 13.9, 6.6, 3.8$ Hz), 2.46–2.36 (m, 1H), 2.42 (s, 3H), 2.34 (s, 3H); ^{13}C NMR (101 MHz, CDCl_3): δ 179.8, 172.2, 158.6, 137.4, 137.0, 134.5, 132.3, 131.65, 131.61, 129.1, 128.9, 128.8, 128.4, 127.8, 126.7, 126.0, 120.0, 71.4, 67.2, 66.7, 66.3, 52.9, 34.8, 20.4, 14.2; HPLC (Daicel Chiralpak IC-3, *n*-hexane/EtOAc = 90/10, 1.0 mL/min, 254 nm); $t_{\text{R}} = 14.3$ min (major), 66.1 min (minor); $[\alpha]_{\text{D}}^{25} -158.84$ (c 0.05, CHCl_3); HRMS (ESI) m/z : $[\text{M}+\text{Na}]^+$ Calcd for $\text{C}_{29}\text{H}_{26}^{35}\text{ClN}_3\text{NaO}_3^+$, 522.1555; found 522.1571.

(5S,6R,7R,13S)-13-(4-chlorophenyl)-4-methyl-2-phenyl-6-(*m*-tolyl)-9-oxa-2,3,12-triazadispiro[4.1.4⁷.2⁵]tridec-3-ene-1,8-dione (3af). (91.0 mg, 0.182 mmol, 91.2%, 18:1 dr, 98% ee); white solid; mp 92–95 °C; ^1H NMR (400 MHz, CDCl_3): δ 7.43–7.40 (m, 2H), 7.33–7.28 (m, 2H), 7.26–7.23 (m, 2H), 7.19–7.15 (m, 3H), 7.13 (d, 1H, $J = 7.2$ Hz), 7.06 (t, 2H, $J = 7.1$ Hz), 7.01 (s, 1H), 4.86 (s, 1H), 4.53 (s, 1H), 4.39 (dt, 1H, $J = 8.9, 6.6$ Hz), 3.97 (dt, 1H, $J = 8.5, 3.3$ Hz), 3.73 (br s, 1H), 2.61 (ddd, 1H, $J = 14.0, 6.6, 3.3$ Hz), 2.47–2.40 (m, 1H), 2.32 (s, 3H), 2.24 (s, 3H); ^{13}C NMR (101 MHz, CDCl_3): δ 179.6, 171.9, 158.7, 139.0, 137.0, 134.6, 133.1, 132.5, 130.2, 129.4, 129.2, 128.9, 128.8, 127.7, 126.2, 125.9, 119.9, 70.6, 67.3, 67.1, 66.2, 58.6, 34.7, 21.5, 14.0; HPLC (Daicel Chiralpak IC-

3, *n*-hexane/EtOAc = 90/10, 1.0 mL/min, 254 nm); t_R = 19.5 min (major), 84.0 min (minor); $[\alpha]_D^{25}$ -127.76 (*c* 0.05, CHCl₃); HRMS (ESI) *m/z*: [M+Na]⁺ Calcd for C₂₉H₂₆³⁵ClN₃NaO₃⁺, 522.1555; found 522.1565.

(5*S*,6*R*,7*R*,13*S*)-13-(4-chlorophenyl)-4-methyl-2-phenyl-6-(*p*-tolyl)-9-oxa-2,3,12-triazadispiro[4.1.4⁷.2⁵]tridec-3-ene-1,8-dione (3ag). (95.9 mg, 0.192 mmol, 95.0%, 17:1 dr, 95% ee); white solid; mp 101–103 °C; ¹H NMR (400 MHz, CDCl₃): δ 7.43–7.41 (m, 2H), 7.32–7.28 (m, 2H), 7.25–7.22 (m, 2H), 7.19–7.15 (m, 3H), 7.12 (d, 2H, *J* = 8.2 Hz), 7.06 (d, 2H, *J* = 8.1 Hz), 4.86 (s, 1H), 4.53 (s, 1H), 4.38 (dt, 1H, *J* = 8.8, 6.6 Hz), 3.94 (dt, 1H, *J* = 8.5, 3.5 Hz), 2.61 (ddd, 1H, *J* = 14.0, 6.6, 3.5 Hz), 2.50–2.42 (m, 1H), 2.31 (s, 3H), 2.27 (s, 3H); ¹³C NMR (101 MHz, CDCl₃): δ 179.7, 171.9, 158.6, 138.6, 137.1, 134.6, 132.5, 130.0, 129.3, 129.1, 128.9, 128.8, 127.7, 125.9, 119.8, 70.7, 67.3, 67.1, 66.2, 58.3, 34.7, 21.1, 14.0; HPLC (Daicel Chiralpak IC-3, *n*-hexane/EtOAc = 90/10, 1.0 mL/min, 254 nm); t_R = 19.4 min (major), 64.1 min (minor); $[\alpha]_D^{25}$ -101.36 (*c* 0.05, CHCl₃); HRMS (ESI) *m/z*: [M+Na]⁺ Calcd for C₂₉H₂₆³⁵ClN₃NaO₃⁺, 522.1555; found 522.1596.

(5*S*,6*R*,7*R*,13*S*)-13-(4-chlorophenyl)-4-methyl-2-phenyl-6-(4-(trifluoromethyl)phenyl)-9-oxa-2,3,12-triazadispiro[4.1.4⁷.2⁵]tridec-3-ene-1,8-dione (3ah). (105.1 mg, 0.190 mmol, 93.3%, 20:1 dr, 95% ee); white solid; mp 100–102 °C; ¹H NMR (400 MHz, CDCl₃): δ 7.54 (d, 2H, *J* = 8.2 Hz), 7.41–7.37 (m, 4H), 7.33–7.29 (m, 2H), 7.25–7.23 (m, 2H), 7.19–7.15 (m, 3H), 4.86 (s, 1H), 4.67 (s, 1H), 4.46 (dt, 1H, *J* = 9.5, 6.1 Hz), 4.12 (dt, 1H, *J* = 8.7, 2.3 Hz), 3.79 (br s, 1H), 2.67 (ddd, 1H, *J* = 13.9, 6.1, 2.3 Hz), 2.34 (s, 3H), 2.32–2.24 (m, 1H); ¹³C NMR (101 MHz, CDCl₃): δ 178.8, 171.5, 158.2, 137.6 (q, *J*_{C-F} = 1.1 Hz), 136.8, 134.8, 131.8, 130.8 (q, *J*_{C-F} = 32.8 Hz), 130.0, 128.9, 128.8, 127.6, 126.2 (q, *J*_{C-F} = 3.8 Hz), 126.1, 123.7, 119.7 (q, *J*_{C-F} = 272 Hz), 70.9, 67.4, 67.3, 66.2, 57.6, 34.7, 14.0; HPLC (Daicel Chiralpak IC-3, *n*-hexane/EtOAc = 90/10, 1.0 mL/min, 250 nm); t_R = 12.7 min (major), 39.2 min (minor); $[\alpha]_D^{25}$ -106.90 (*c* 0.05, CHCl₃); HRMS (ESI) *m/z*: [M+Na]⁺ Calcd for C₂₉H₂₃³⁵ClN₃NaO₃F₃⁺, 576.1272; found 576.1278.

(5*S*,6*R*,7*R*,13*S*)-13-(4-chlorophenyl)-6-(4-methoxyphenyl)-4-methyl-2-phenyl-9-oxa-2,3,12-triazadispiro[4.1.4⁷.2⁵]tridec-3-ene-1,8-dione (3ai). (93.8 mg, 0.182 mmol, 90.4%, >20:1 dr, 98% ee); white solid; mp 96–99 °C; ¹H NMR (400 MHz, CDCl₃): δ 7.43–7.41 (m, 2H), 7.32–7.28 (m, 2H), 7.25–7.23 (m, 2H), 7.19–7.14 (m, 5H), 6.78 (d, 2H, *J* = 8.9 Hz), 4.86 (s, 1H), 4.52 (s, 1H), 4.39 (dt, 1H, *J* = 8.8, 6.6 Hz), 3.95 (dt, 1H, *J* = 8.5, 3.4 Hz), 3.74 (s, 3H), 2.61 (ddd, 1H, *J* = 14.0, 6.6, 3.5 Hz), 2.51–2.43 (m, 1H), 2.32 (s, 3H); ¹³C NMR (101 MHz, CDCl₃): δ 179.7, 171.9, 159.7, 158.7, 137.0, 134.5, 132.6, 130.7, 128.9, 128.8, 127.7, 125.9, 124.9, 119.8, 114.6, 70.9, 67.3, 67.0, 66.2, 57.9, 55.3, 34.7, 14.0; HPLC (Daicel Chiralpak IC-3, *n*-hexane/2-propanol = 80/20, 1.0 mL/min, 250 nm); *t*_R = 14.3 min (major), 29.6 min (minor); [α]_D²⁵ -112.88 (*c* 0.05, CHCl₃); HRMS (ESI) *m/z*: [M+Na]⁺ Calcd for C₂₉H₂₆³⁵ClN₃NaO₄⁺, 538.1504; found 538.1523.

(5*S*,6*R*,7*R*,13*S*)-13-(4-chlorophenyl)-4-methyl-2-phenyl-6-(thiophen-2-yl)-9-oxa-2,3,12-triazadispiro[4.1.4⁷.2⁵]tridec-3-ene-1,8-dione (3aj). (99.2 mg, 0.202 mmol, 99.3%, 17:1 dr, 96% ee); white solid; mp 98–100 °C; ¹H NMR (400 MHz, CDCl₃): δ 7.49–7.46 (m, 2H), 7.33–7.30 (m, 2H), 7.26–7.24 (m, 2H), 7.19–7.14 (m, 4H), 6.96 (dd, 1H, *J* = 3.5, 1.0 Hz), 6.92 (dd, 1H, *J* = 5.1, 3.6 Hz), 4.854–4.847 (m, 2H), 4.44–3.38 (m, 1H), 4.03 (dt, 1H, *J* = 8.1, 3.8 Hz), 2.66–2.52 (m, 1H), 2.33 (s, 3H); ¹³C NMR (101 MHz, CDCl₃): δ 179.3, 171.5, 158.2, 137.1, 134.7, 134.5, 132.4, 128.92, 128.90, 128.3, 127.7, 127.6, 126.6, 125.9, 119.7, 71.1, 67.7, 66.8, 66.3, 53.4, 34.8, 13.9; HPLC (Daicel Chiralpak IC-3, *n*-hexane/2-propanol = 90/10, 1.0 mL/min, 254 nm); *t*_R = 24.5 min (major), 45.5 min (minor); [α]_D²⁵ -104.91 (*c* 0.05, CHCl₃); HRMS (ESI) *m/z*: [M+Na]⁺ Calcd for C₂₆H₂₃³⁵ClN₃O₃S⁺, 514.0963; found 514.0995.

5-5. References

1. (a) Adrio, J.; Carretero, J. C. *Chem. Commun.* **2019**, *55*, 11979–11991. (b) Wei, L.; Chang, X.; Wang, C. J. *Acc. Chem. Res.* **2020**, *53*, 1084–1100. (c) Kumar, S. V.; Guiry, P. J. *Chem. Eur. J.* **2023**, *29*, e202300296.
2. (a) Arai, T.; Yokoyama, N.; Mishiro, A.; Sato, H. *Angew. Chem. Int. Ed.* **2010**, *122*, 8067–8070. (b) Awata, A.; Arai, T. *Chem. Eur. J.* **2012**, *18*, 8278–8282. (c) Arai, T.; Tokumitsu, C.; Miyazaki, T.; Kuwano, S.; Awata, A. *Org. Biomol. Chem.* **2016**, *14*, 1831–1839.
3. (a) Cheng, F.; Kalita, S. J.; Zhao, Z.-N.; Yang, X.; Zhao, Y.; Schneider, U.; Shibata, N.; Huang, Y.-Y. *Angew. Chem. Int. Ed.* **2019**, *58*, 16637–16643. (b) Kalita, S. J.; Cheng, F.; Fan, Q.-H.; Shibata, N.; Huang, Y.-Y. *J. Org. Chem.* **2021**, *86*, 8695–8705.
4. Other examples of 2,5-*trans* selective asymmetric (3+2) cycloaddition: (a) Li, Q.-H.; Wei, L.; Chen, X.; Wang, C.-J. *Chem. Commun.* **2013**, *49*, 6277–6279. (b) Awata, A.; Arai, T. *Angew. Chem. Int. Ed.* **2014**, *53*, 10462–10465. (c) Wei, L.; Li, Q.-H.; Wang, C.-J. *J. Org. Chem.* **2018**, *83*, 11814–11824.
5. Other examples of 2,5-*trans* diastereoselective (3+2) cycloaddition (not asymmetric synthesis): (a) Taha, A. G.; Elboray, E. E.; Kobayashi, Y.; Furuta, T.; Abbas-Temirek, H. H.; Aly, M. F. *J. Org. Chem.* **2021**, *86*, 547–558. (b) Radwan, M.; Elboray, E. E.; Dardeer, H. M.; Kobayashi, Y.; Furuta, T.; Hamada, S.; Dohi, T.; Aly, M. F. *Chem. Asian J.* **2023**, *18*, e202300215.
6. (a) Harada, M.; Kato, S.; Haraguchi, R.; Fukuzawa, S.-i. *Chem. Eur. J.* **2018**, *24*, 2580–2583. (b) Kato, S.; Suzuki, Y.; Suzuki, K.; Haraguchi, R.; Fukuzawa, S.-i. *J. Org. Chem.* **2018**, *83*, 13965–13972. (c) Furuya, S.; Kanemoto, K.; Fukuzawa, S.-i. *J. Org. Chem.* **2020**, *85*, 8142–8148.
7. Torán, R.; Miguélez, R.; Sanz-Marco, A.; Vila, C.; Pedro, J. R.; Blay, G. *Adv. Synth. Catal.* **2021**, *363*, 5196–5234.
8. (a) Furuya, S.; Kanemoto, K.; Fukuzawa, S.-i. *Chem. Asian J.* **2022**, *17*, e202200239. (b) Furuya, S.; Muroi, K.; Kanemoto, K.; Fukuzawa, S.-i. *Chem. Eur. J.* **2023**, *29*,

e202302609.

9. Selected review: (a) Chauhan, P.; Mahajan, S.; Enders, D. *Chem. Commun.* **2015**, *51*, 12890–12907. (b) Liu, S.; Bao, X.; Wang, B. *Chem. Commun.* **2018**, *54*, 11515–11529.
10. (a) Chande, M. S.; Barve, P. A.; Suryanarayan, V. *J. Heterocycl. Chem.* **2007**, *44*, 49–53. (b) Amata, E.; Bland, N. D.; Campbell, R.; Pollastri, M. *Tetrahedron Lett.* **2015**, *56*, 2832–2835. (c) Wang, L.; Yang, Z.; Ni, T.; Shi, W.; Guo, Y.; Li, K.; Shi, A.; Wu, S.; Sheng, C. *Bioorg. Med. Chem. Lett.* **2020**, *30*, 126662–126666.
11. Recent examples of asymmetric cycloaddition: (a) Deng, Y.; Dong, Z.; Gao, F.; Guo, Y.; Sun, M.; Li, Y.; Wang, Y.; Chen, Q.; Wang, K.; Yan, W. *J. Org. Chem.* **2021**, *86*, 13011–13024. (b) Wang, Y.; Li, E.-Q.; Duan, Z. *Chem. Sci.* **2022**, *13*, 8131–8136. (c) Prasad, M. S.; Sivaprakash, M. *Org. Biomol. Chem.* **2023**, *21*, 339–344. (d) Li, G.; Zhang, H.; Zhang, G.; Wei, B.; Liu, B.; Song, H.; Li, Q.; Ban, S. *J. Org. Chem.* **2023**, *88*, 4809–4813. (e) Bania, N.; Barman, D.; Pan, S. C. *Synlett.* **2023**, *34*, 663–666.
12. Chen, N.; Zhu, L.; Gan, L.; Liu, Z.; Wang, R.; Cai, X.; Jiang, X. *Eur. J. Org. Chem.* **2018**, 2939–2943.
13. (a) Zhao, C.; Shi, K.; He, G.; Gu, Q.; Ru, Z.; Yang, L.; Zhong, G. *Org. Lett.* **2019**, *21*, 7943–7947. (b) Awasthi, A.; Yadav, P.; Kumar, V.; Tiwari, D. K. *Adv. Synth. Catal.* **2020**, *362*, 4378–4383.

Chapter 6

Conclusion and Perspective

The metal-catalyzed asymmetric 1,3-dipolar cycloaddition of imino esters with activated olefins is useful for preparing chiral pyrrolidines in one step. Recently, several methods for diastereodivergent synthesis have been developed by many research groups. Indeed, metal- and ligand-controlled strategies have been frequently reported, and the *endo/exo*-diastereodivergent synthesis of chiral pyrrolidine derivatives has been achieved. Nevertheless, *2,5-cis/trans* diastereodivergent synthesis has remained challenging because it requires stepwise addition/cyclization with a bond rotation pathway that is usually mechanistically unfavorable. Given this background, the author investigated the asymmetric 1,3-dipolar cycloaddition of imino esters with activated olefins containing heterocyclic moieties, which have rarely been employed in the reaction.

In Chapter 2, the author developed the asymmetric (3+2) cycloaddition using α,β -unsaturated cyclic sulfonic acid esters (sultones) for the asymmetric synthesis of sultone-fused pyrrolidines. A chiral copper catalyst was shown to be efficient for the asymmetric synthesis to afford the desired fused pyrrolidines with high enantioselectivity. In addition, it was revealed that the (3+2) cycloaddition gave *exo*-adducts as a single diastereomer, but in the *2,5-trans* configuration.

In Chapter 3, the author developed the asymmetric synthesis of spiropyrrolidines by the asymmetric (3+2) cycloaddition of imino esters with ylidene-2,3-dioxopyrrolidines. The reaction was efficiently catalyzed by our original silver/TCF catalyst to give the rare *exo'*-diastereomers with excellent enantioselectivity. Several control experiments suggested that the reaction proceeded via a stepwise addition/cyclization with bond rotation, not via an epimerization pathway after the common *2,5-cis* selective (3+2) cycloaddition.

In Chapter 4, the author described a new *2,5-cis/trans*-diastereodivergent synthetic method using ylidene-isoxazolones as ketone equivalents. The reaction of imino lactones with ylidene-isoxazolones was catalyzed by the silver/FcPHOX catalyst to afford the corresponding spiropyrrolidines with high *2,5-trans* diastereo- and enantioselectivity. The subsequent N–O bond reduction of the isoxazolone ring smoothly gave the 4-carbonyl

pyrrolidines with 2,5-*trans* stereoretention. In contrast, the corresponding 4-carbonyl pyrrolidines were obtained as 2,5-*cis* diastereomers by the common 1,3-dipolar cycloaddition using α,β -unsaturated ketones.

In Chapter 5, the author developed the asymmetric (3+2) cycloaddition of imino lactones with ylidene-pyrazolones with structures similar to the ylidene-isoxazolones. The reaction also proceeded with 2,5-*trans* diastereoselectivities as did the reaction using ylidene-isoxazolones described in Chapter 4. In addition, the enantioselective synthesis was achieved by using the copper/Fesulphos catalyst.

The present study indicated that 2,5-*trans* configured pyrrolidines whose formation is mechanistically unfavorable could be obtained by the catalytic asymmetric (3+2) cycloaddition using ylidene-heterocycles. In addition, 2,5-*cis/trans* diastereodivergent preparation was shown to be achieved by a dipolarophile-controlled strategy, which uses different types of activated olefins. Both 2,5-*cis/trans* substituted pyrrolidines have potential as bioactive compounds. Thus, the author hopes for further studies for applications in drug discovery. Compared to the catalyst-controlled strategy for stereodivergent synthesis, the substrate-controlled strategy has not been well considered. However, this study has shown the potential to gain access to other stereoisomers that are not usually obtained in the cycloaddition reaction. Therefore, further studies into divergent synthesis by the substrate-controlled strategy in other types of cycloadditions and new reagents for easy access to 2,5-*trans* adducts are expected to develop. Also, this study indicated that *endo/exo*-diastereodivergent synthesis by the catalytic asymmetric cycloaddition of imino esters with activated olefins remains one of the challenging tasks. Although this would be possible if the reaction face of ylidene-heterocycles could be controlled in the first Michael addition step, few examples have been reported to switch the stereoselectivity in the reaction using this type of olefins. Thus, the methods for switching the diastereoselectivity which can be applied to the asymmetric (3+2) cycloaddition using ylidene-heterocycles are desired to develop.

Publication List

Original Papers

- (1) "Copper-Catalyzed Regio- and Diastereoselective 1,3-Dipolar Cycloaddition Reactions of Glycine Imino Esters with 1-Propene-1,3-sultone"
Shohei Furuya, Shuma Kato, Kazuya Kanemoto, Shin-ichi Fukuzawa
European Journal of Organic Chemistry, **2019**, 4561–4565.
(Chapter 2)
- (2) "Copper-Catalyzed Asymmetric 1,3-Dipolar Cycloaddition of Imino Esters to Unsaturated Sultones"
Shohei Furuya, Kazuya Kanemoto, Shin-ichi Fukuzawa
The Journal of Organic Chemistry, **2020**, 85, 8142–8148.
(Chapter 2)
- (3) "*exo'*-Selective Construction of Spirobipyrrolidines by the Silver-catalyzed Asymmetric [3+2] Cycloaddition of Imino Esters with 4-Benzylidene-2,3-dioxopyrrolidines"
Shohei Furuya, Kazuya Kanemoto, Shin-ichi Fukuzawa
Chemistry An Asian Journal, **2022**, 17, e202200239.
(Chapter 3)
- (4) "Dipolarophile-Steered Formal Stereodivergent Synthesis of 2,5-*cis/trans*-Pyrrolidines Based on Asymmetric 1,3-Dipolar Cycloaddition of Imino Lactones"
Shohei Furuya, Kenji Muroi, Kazuya Kanemoto, Shin-ichi Fukuzawa
Chemistry A European Journal, **2023**, 29, e202302609.
(Chapter 4)
- (5) "Copper-Catalyzed Asymmetric (3+2) Cycloaddition of Imino Lactones with Benzylidene-pyrazolones"
Kenji Muroi, Shohei Furuya, Shin-ichi Fukuzawa
manuscript in preparation.
(Chapter 5)

The following publications are not included in the dissertation.

- (6) "Chiral Silver Complex-Catalyzed Asymmetric Conjugate Addition of 1-Pyrroline-5-Carbonitrile to α -Enones"
Haruna Araki, Shohei Furuya, Kazuya Kanemoto, Shin-ichi Fukuzawa
The Journal of Organic Chemistry, **2023**, 88, 924–932.
- (7) "Synthesis of Spirocyclic Pyrrolidine Compounds via Silver-catalyzed Asymmetric [3+2] Cycloaddition Reaction of Imino Esters with α -Alkylidene Succinimides"
Ayana Inoue, Kenya Hosono, Shohei Furuya, Shin-ichi Fukuzawa
The Journal of Organic Chemistry, **2024**, 89, 1249–1255.
- (8) "Construction of Diverse Pyrrolidine-Based Skeletons through Ag-Catalyzed Stereoselective Addition-Elimination Reaction of Azomethine Ylides with Nitroallyl Acetates"
Itsuki Ohno, Kazuya Kanemoto, Shohei Furuya, Yuko Suzuki, Shin-ichi Fukuzawa
manuscript in preparation.

Acknowledgment

The studies described in this dissertation have been conducted under the guidance of Professor Shin-ichi Fukuzawa of Chuo University at the Department of Applied Chemistry, Institution of Science and Engineering from April 2018 to March 2024. The author would like to express his best gratitude to Professor Shin-ichi Fukuzawa, who has frequently encouraged the author in addition to having stimulating discussions.

The author greatly appreciates Assistant Professor Kazuya Kanemoto for their guidance for the studies, experimental techniques, and valuable suggestions. Associate Professor Ryosuke Haraguchi is also appreciated for the fundamentals of the studies.

The author deeply thanks Project Lecturer Yoshiaki Tanabe of the University of Tokyo at the Department of Applied Chemistry, School of Engineering for his helpfulness in the X-ray crystallographic analysis.

The computation was performed using Research Center for Computational Science, Okazaki, Japan. The author greatly thanks Professor Hirotohi Mori for teaching him computational chemistry and its techniques.

His laboratory member, Kenji Muroi, is particularly appreciated for helping him with the experiments of this work. The laboratory seniors, Shuma Kato and Tatsuro Yamazaki, and his compeers, Koki Torita, Kodai Furuhashi, Yuko Suzuki, Kota Suzuki, Satoshi Kenmochi, and junior members who conducted related studies, Itsuki Ohno, Ayana Inoue, Haruna Araki, Nana Kogai, Kenya Hosono, Yuki Sakuma, are also appreciated for their valuable contributions. The author would like to thank all the other members for their friendship.

Financial support is acknowledged from JSPS as a Grant-in-Aid for JSPS Fellow during his Ph.D. program.

Finally, the author expresses gratitude to his family, particularly to his father Kazutoshi Furuya, and his mother, Mieko, for their encouragement and kind support.

March, 2024

Shohei Furuya